

The complete next-to-leading order potential for $B^{(*)}\bar{B}^{(*)} \rightarrow B^{(*)}\bar{B}^{(*)}$ scattering

Masterarbeit in Physik

von Simon León Krug

angefertigt am Institute for Advanced Simulation
des Forschungszentrums Jülich

vorgelegt der Mathematisch-Naturwissenschaftlichen Fakultät
der Universität Bonn

August 2020

1. Gutachter: Prof. Dr. Christoph Hanhart
2. Gutachter: PD Dr. Bastian Kubis

I hereby declare that the work presented here was formulated by myself and that no sources or tools other than those cited were used.

Bonn, 25.08.2020

Abstract

Motivation for a next-to-leading order potential of a $B^{(*)}-\bar{B}^{(*)}$ system is given. Full calculations of $B^{(*)}\bar{B}^{(*)} \rightarrow B^{(*)}\bar{B}^{(*)}$ scattering are presented. Starting with Heavy Meson Chiral Perturbation Theory, Feynman rules are derived and effective potentials up to next-to-leading order obtained. These are subsequently partial wave projected for $J^{PC} = 0^{++}, 1^{++}, 1^{+-}$ and 2^{++} .

Acronyms

1PE One-Pion-Exchange

2PE Two-Pion-Exchange

2PR Two-Particle Reducible

χ **PT** Chiral Perturbation Theory

C1PE Corrected One-Pion-Exchange

CI Contact Interaction

CCI Corrected Contact Interaction

EFT Effective Field Theory

HM χ PT Heavy Meson Chiral Perturbation Theory

HQET Heavy Quark Effective Theory

HQFS Heavy Quark Flavor Symmetry

HQSS Heavy Quark Spin Symmetry

LO Leading Order

LSE Lippmann-Schwinger Equation

NLO Next-to-Leading Order

QCD Quantum Chromodynamics

SSB Spontaneous Symmetry Breaking

Table of Contents

Acronyms	ii
Table of Contents	iii
1 Motivation	1
2 Effective field theory	7
2.1 Chiral perturbation theory	7
2.2 Inclusion of heavy mesons	10
2.3 Power counting and the chiral dimension	13
2.4 Vertices	16
2.5 Propagators	21
3 The Lippmann-Schwinger equation	23
4 Leading order diagrams	25
4.1 Contact interaction (CI)	25
4.2 One-pion-exchange (1PE)	27
5 Next-to-leading order diagrams	30
5.1 Two-pion-exchange (2PE)	30
5.1.1 The triangle diagrams	30
5.1.2 The football diagrams	38
5.1.3 The box diagrams	39
5.2 Corrections to leading order (CCI & C1PE)	55
5.2.1 Non-contributing diagrams	56
5.2.2 Renormalization of m_π, m_B, g	57
5.2.3 The remaining diagrams	66
6 The effective potentials	86
7 Partial wave decomposition	90
7.1 $J^{PC} = 0^{++}$	94
7.2 $J^{PC} = 1^{++}$	96
7.3 $J^{PC} = 1^{+-}$	98
7.4 $J^{PC} = 2^{++}$	101
7.5 External comparison	104

8	Summary and discussion	105
9	Acknowledgments	106
A	Relations	107
B	Integrals of dimensional regularization	109
B.1	The triangle integral	109
B.2	The football integral	111
B.3	The box integrals	112
B.4	Integrals from CCI or C1PE	117
C	Diagrams of 2PE	124
D	Diagrams of CCI and C1PE	126
E	Integrals of partial wave decomposition	134
	Bibliography	139
	List of Figures	142

1 Motivation

Starting with the discovery of the $X(3872)$ by the Belle collaboration in 2003¹ and an experimental validation from different experiments (e.g. CDF²) in the following years, many new exotic multiquark states beyond the simple, yet successful quark model were found.^{3,4} Examples are the charged states $Z_b^\pm(10610)$ and $Z_b^\pm(10650)$,⁵ $Z_c^\pm(3900)$,⁶ and $Z_c^\pm(4020)$.⁷ Their decays into charmonium (or bottomium) states *and* a pion exclude a simple $Q\bar{Q}$ -meson, with Q (\bar{Q}) denoting a heavy (anti-)quark. Thus, they must have at least a four quark content.⁸

All those exotic states share that they are located above the first open heavy quark open-flavor threshold $D\bar{D}$ for charmonium-like states (fig. 1.1⁹) or $B\bar{B}$ for bottomium-like states (fig. 1.2¹⁰). Moreover, many have masses in close proximity to meson-meson thresholds. These narrow systems at those thresholds, when assumed to be in S -wave, often share their quantum numbers with the exotic states, which makes them candidates for hadronic molecules, composite systems built out of hadrons.¹¹ The most prominent hadronic molecule is built of a proton and a neutron – the deuteron. Both constituents neither carry netto-color nor are they bound by charge, yet their binding energy is 2.2 MeV.¹² Naturally, the question arises if the XYZ-states are simply heavier cousins to the deuteron.

Especially in the $c\bar{c}$ -sector, an abundance of states with exotic properties is found. In the $b\bar{b}$ -sector only two so far: $Z_b^\pm(10610)$ and $Z_b^\pm(10650)$, with quantum numbers $J^{PC} = 1^{+-}$,¹³

¹Choi et al. “Observation of a Narrow Charmoniumlike State in Exclusive $B^\pm \rightarrow K^\pm \pi^+ \pi^- J/\psi$ Decays”

²Acosta et al. “Observation of the Narrow State $X(3872) \rightarrow J/\psi \pi^+ \pi^-$ in $\bar{p}p$ Collisions at $\sqrt{s} = 1.96$ TeV”

³Q. Wang et al. “The line shapes of the $Z_b(10610)$ and $Z_b(10650)$ in the elastic and inelastic channels revisited”. In: *Phys. Rev. D* 98 (7 Oct. 2018), p. 074023. DOI: 10.1103/PhysRevD.98.074023. URL: <https://link.aps.org/doi/10.1103/PhysRevD.98.074023>, p.1.

⁴Zhan-Wei Liu, Bo Wang, and Xiang Liu. “ $\bar{B}^{(*)}\bar{B}^{(*)}$ interactions in chiral effective field theory”. In: *Physical Review D* 99.3 (Feb. 2019). ISSN: 2470-0029. DOI: 10.1103/physrevd.99.036007. URL: <http://dx.doi.org/10.1103/PhysRevD.99.036007>, p.1.

⁵Bondar et al. “Observation of Two Charged Bottomoniumlike Resonances in $\Upsilon(5S)$ Decays”

⁶Ablikim et al. “Observation of a Charged Charmoniumlike Structure in $e^+e^- \rightarrow \pi^+\pi^- J/\psi$ at $\sqrt{s}=4.26$ GeV”

⁷Ablikim et al. “Observation of a Charged Charmoniumlike Structure $Z_c(4020)$ and Search for the $Z_c(3900)$ in $e^+e^- \rightarrow \pi^+\pi^- h_c$ ”

⁸Wang et al., loc. cit.

⁹Nora Brambilla et al. *The XYZ states: experimental and theoretical status and perspectives*. 2019. arXiv: 1907.07583 [hep-ex], p.4.

¹⁰Ibid., p.5.

¹¹C. Hanhart. *Theory of hadronic molecules applied to the XYZ states*. 2017. arXiv: 1709.09920 [hep-ph], p.1.

¹²R. Machleidt and D.R. Entem. “Chiral effective field theory and nuclear forces”. In: *Physics Reports* 503.1 (2011), pp. 1–75. ISSN: 0370-1573. DOI: <https://doi.org/10.1016/j.physrep.2011.02.001>. URL: <http://www.sciencedirect.com/science/article/pii/S0370157311000457>, p.49; value taken from Tab. 9.

¹³We assume an odd C -combination of $B^*\bar{B}$ and $B\bar{B}^*$.

which are of special interest in this thesis.¹⁴ However, Heavy Quark Flavor Symmetry (HQFS) suggests a similar abundance in the $b\bar{b}$ -sector.

This expectation is substantiated by Heavy Quark Spin Symmetry (HQSS). It states that in the limit of an infinitely massive heavy quark $m_Q \rightarrow \infty$, the spin of heavy quarks Q inside hadrons is conserved by strong interactions. Since deviations scale with $\Lambda_{QCD}/m_b \sim 0.04$, one expects exotic states similar to $Z_b^\pm(10610)$ and $Z_b^\pm(10650)$ but with different quantum numbers J^{++} ($J = 0, 1, 2$). These particles are their respective spin partners W_{bJ} . Furthermore, HQSS allows any hadronic interaction to be reduced to a "cloud" of light quarks surrounding Q , which we exploit in sec. 2.2.

Discovered by the Belle collaboration, the dipion transitions of the bottomium-like $\Upsilon(10860)$ in the subsystem $\Upsilon(nS)\pi^\pm$ with $n = 1, 2, 3$ and $h_b(mP)\pi^\pm$ with $m = 1, 2$ revealed two peaks at around 10.61 GeV and 10.65 GeV, respectively. These isovector particles were named $Z_b^\pm(10610)$ and $Z_b^\pm(10650)$.¹⁵ Their masses are remarkably close to the $B\bar{B}^*$ and $B^*\bar{B}^*$ thresholds:¹⁶

$$(10, 607.8 \pm 2.0) \text{ MeV} \approx m_B + m_{B^*} \approx 10, 603 \text{ MeV}$$

$$(10, 652.2 \pm 1.5) \text{ MeV} \approx 2m_{B^*} \approx 10, 648 \text{ MeV}$$

In 2016, they were found in elastic $B\bar{B}^*$ - and $B^*\bar{B}^*$ -channels as well,¹⁷ which are also their main decay channels. Together with their narrow widths of $\Gamma(Z_b^\pm(10610)) = (18.4 \pm 2.4) \text{ MeV}$ and $\Gamma(Z_b^\pm(10650)) = (11.5 \pm 2.2) \text{ MeV}$,¹⁸ this strongly hints towards both particles being hadronic molecules consisting of $B\bar{B}^* + c.c.$ and $B^*\bar{B}^*$, respectively.¹⁹ However, it is to mention that a tetraquark interpretation of these states is compatible with the available data, too.²⁰

This thesis will continue the work done in the papers by Wang et al.²¹ and Nefediev et al.²² in investigating the line shapes of the Z_b^\pm 's and their still to be discovered spin partners. There, Heavy Meson Chiral Perturbation Theory (HM χ PT) was employed to calculate effective potentials at Leading Order (LO) and an incomplete Next-to-Leading Order (NLO).²³ This effective potential was subsequently partial wave projected to the quantum numbers $J^{PC} = 1^{+-}$ and given as input for the coupled-channel Lippmann-Schwinger Equation (LSE), as described in

¹⁴Brambilla et al., op. cit., p.4.

¹⁵A. Bondar et al. "Observation of Two Charged Bottomoniumlike Resonances in $\Upsilon(5S)$ Decays". In: *Phys. Rev. Lett.* 108 (12 Mar. 2012), p. 122001. doi: 10.1103/PhysRevLett.108.122001. URL: <https://link.aps.org/doi/10.1103/PhysRevLett.108.122001>.

¹⁶Tanabashi et al. "Review of Particle Physics", pp.70,109

¹⁷A. Garmash et al. "Observation of $Z_b(10610)$ and $Z_b(10650)$ Decaying to B Mesons". In: *Phys. Rev. Lett.* 116 (21 May 2016), p. 212001. doi: 10.1103/PhysRevLett.116.212001. URL: <https://link.aps.org/doi/10.1103/PhysRevLett.116.212001>.

¹⁸Bondar et al., op. cit.

¹⁹Wang et al., loc. cit.

²⁰Ahmed Ali, Christian Hambrock, and Wei Wang. "Tetraquark interpretation of the charged bottomonium-like states $Z_b^\pm(10610)$ and $Z_b^\pm(10650)$ and implications". In: *Phys. Rev. D* 85 (5 Mar. 2012), p. 054011. doi: 10.1103/PhysRevD.85.054011. URL: <https://link.aps.org/doi/10.1103/PhysRevD.85.054011>.

²¹Wang et al., op. cit.

²²A. V. Nefediev et al. "Spin partners W_{bJ} from the line shapes of the $Z_b(10610)$ and $Z_b(10650)$ ". In: *Physical Review D* 99.9 (May 2019). ISSN: 2470-0029. doi: 10.1103/physrevd.99.094013. URL: <http://dx.doi.org/10.1103/PhysRevD.99.094013>.

²³When talking about leading or next-to-leading order, we always mean the order of χ .

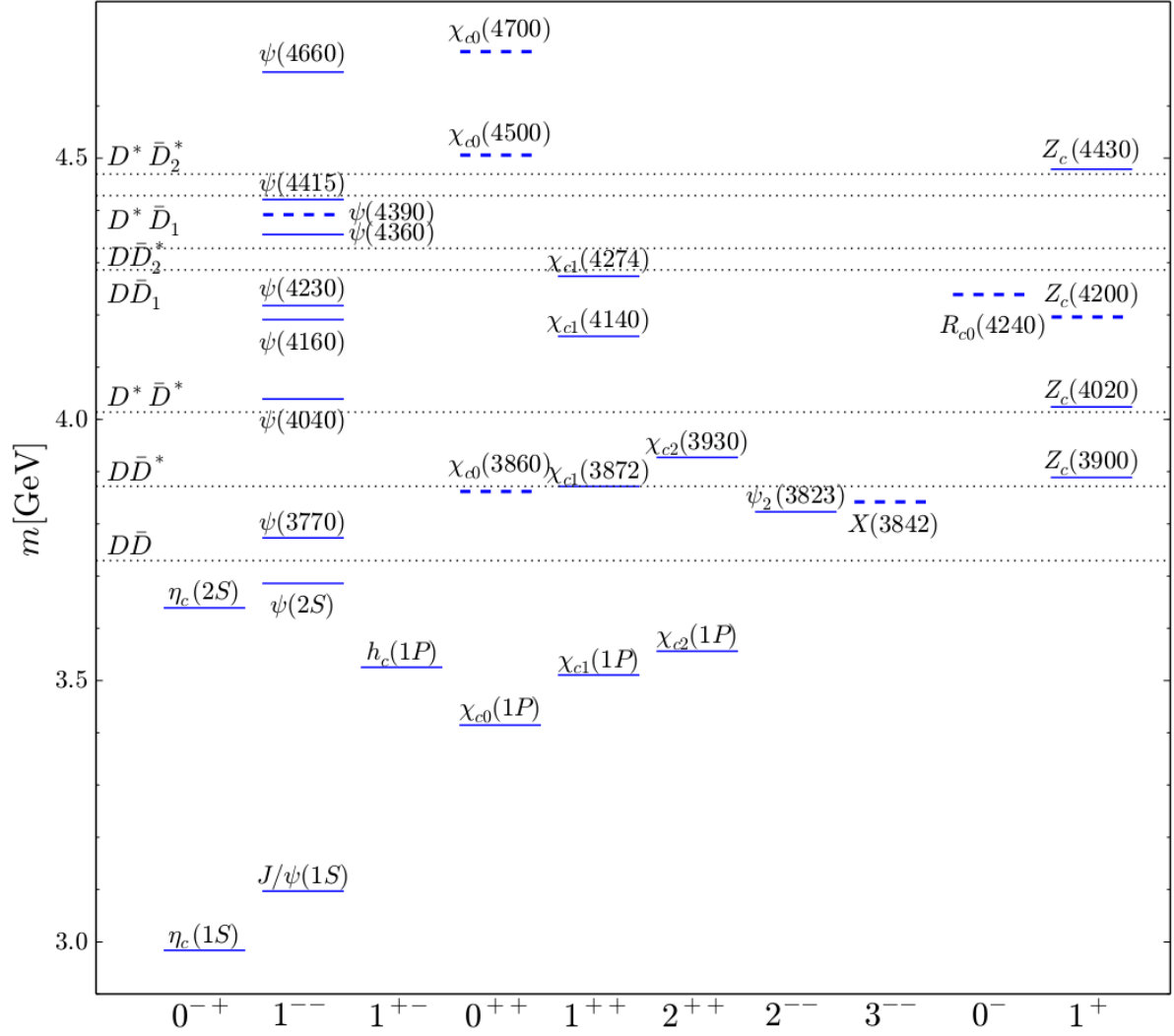


Fig. 1.1: Charmonium-like states with completely determined quantum numbers and without hidden strangeness (as of July 2019). Established states are depicted with solid lines, not (yet) established ones with dashed lines. $D_1 \equiv D_1(2420)$, $D_2^* \equiv D_2^*(2460)$. Details in the paper.

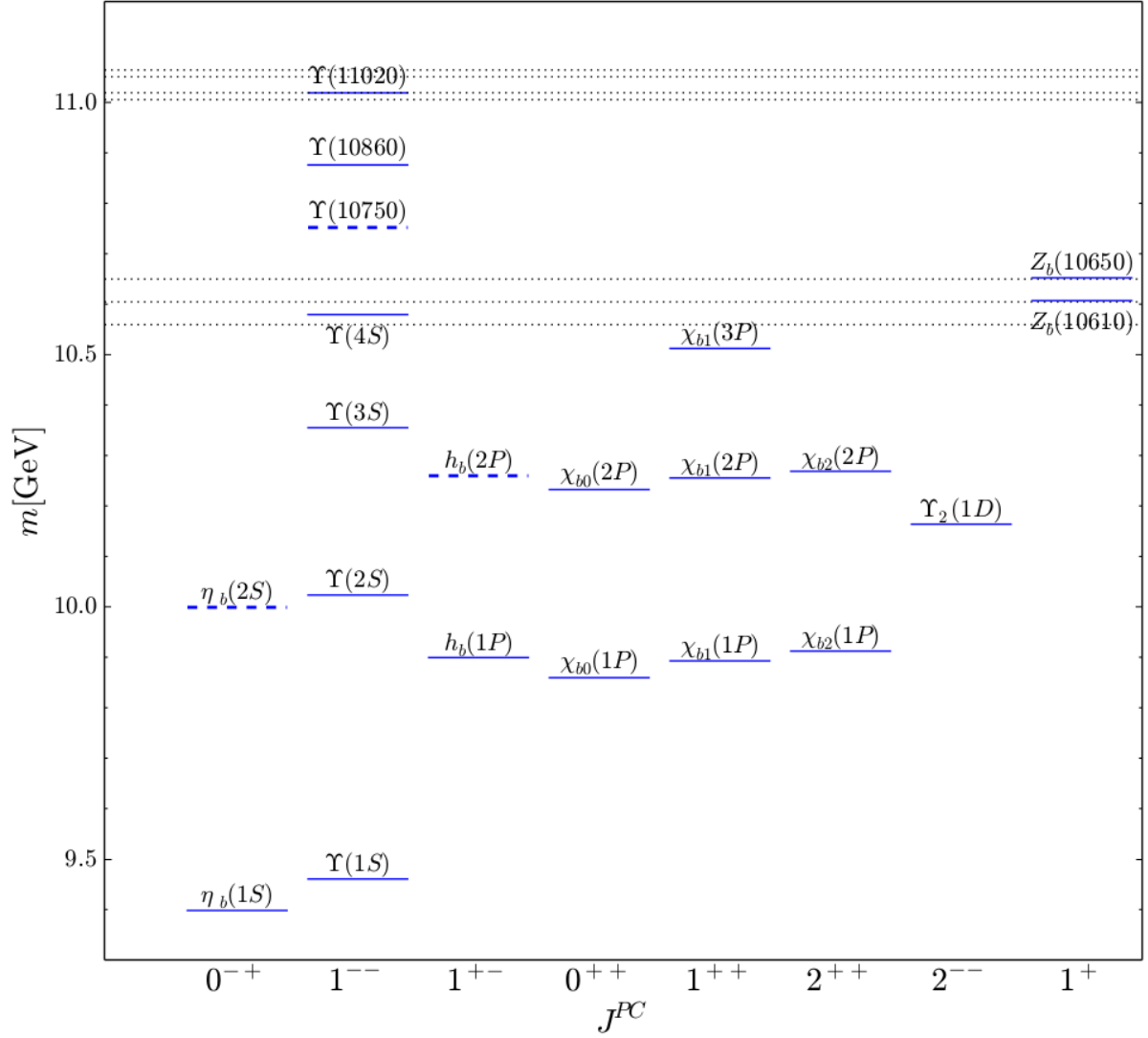


Fig. 1.2: Bottomium-like states with completely determined quantum numbers and without hidden strangeness (as of July 2019). Established states are depicted with solid lines, not (yet) established ones with dashed lines. The fine dots depict open-bottom thresholds from lowest to highest: $B\bar{B}$, $B^*\bar{B}$, $B^*\bar{B}^*$, $\bar{B}B_1(5721)$, $\bar{B}B_2^*(5747)$, $\bar{B}^*B_1(5721)$, $\bar{B}^*B(5747)$. Details in the paper.

sec. 3. The parameters were fixed by fitting line shapes in the elastic $B^{(*)}\bar{B}^*$ -channels (fig. 1.3²⁴) and the inelastic $h_b(mP)$ channels with $m = 1, 2$. In doing so, they encountered some challenges:

- They found that the One-Pion-Exchange (1PE) in S - to D -wave transitions at typical momenta around a few hundred MeV is of greater importance than naively expected; however, the experimental data does not indicate such importance.
- A study of the regulator dependence revealed that the S - to D -wave Contact Interaction (CI), stemming from the NLO Lagrangian $\mathcal{L}_{4H}^{(2)}$ (cf. sec. 2.2), needs to be promoted to LO for a proper renormalization of the theory. To further diminish the regulator dependence, additional S - to S -wave counter terms had to be introduced.
- Treating binding momenta and the pion mass as soft ($p_{typ} \sim 500$ MeV), the hadronic scale at which chiral symmetry breaks down ($\Lambda_h \sim 1$ GeV) as hard, the expansion parameter χ of HM χ PT grants only a relatively slow convergence of $\chi = p_{typ}/\Lambda_h \sim 0.5$.

Thus, a complete NLO calculation is required. This thesis presents such a potential decomposed into its partial waves beyond $J^{PC} = 1^{+-}$ in anticipation of the still to be discovered spin partners. When being used in the LSE, the convergence of the theory can be tested and the impact of contributions at NLO examined. This will prepare ground for further investigations.

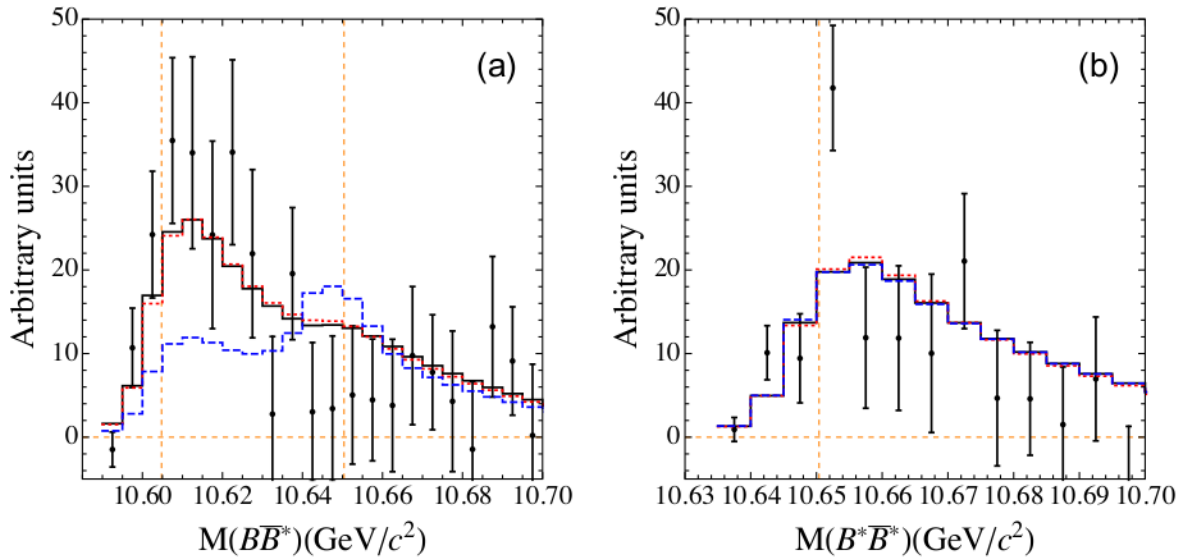


Fig. 1.3: Line shapes for the invariant mass distribution at $\sqrt{s} \sim M(B\bar{B}^*)$ (a) and $\sqrt{s} \sim M(B^*\bar{B}^*)$ (b) in three different schemes. Blue dashed = LO potential; red dotted = LO + S - to D -wave CI of NLO; solid black = LO + S - to D -wave CI of NLO + S - to S -wave CI of NLO. Orange vertical lines display the $B\bar{B}^*$ and $B^*\bar{B}^*$ thresholds. The error bars of the data points represent the 1σ -environment. Details in the paper.

²⁴Wang et al., op. cit., p.9, Fig. 3a,b.

The structure of this thesis is as follows: in secs. 2.1 and 2.2, we explain the theoretical frameworks of Chiral Perturbation Theory (χ PT) and $\text{HM}\chi$ PT. The resulting Feynman rules can be found in secs. 2.4 and 2.5 while the accuracy of the Effective Field Theory (EFT) is discussed in sec. 2.3. In sec. 3, we outline the LSE for coupled channels because it is the basis of this calculation. There, we also investigate which effective potentials need to be calculated. Secs. 4 and 5 are devoted to the enumeration and computation of the relevant diagrams; additional diagrams are collected in the appendices C and D. The one-loop corrections to diagrams of LO are discussed in sec. 5.2. The pertinent integrals from all one-loop diagrams are solved in appendix B. Finally, the complete effective potentials are presented in sec. 6 and partial wave decomposed thereafter in sec. 7. The results can be viewed in secs. 7.1 to 7.4. Sec. 8 concludes this thesis and provides a short discussion of the findings.

2 Effective field theory

2.1 Chiral perturbation theory

This section gives a brief summary of χ PT. For a general outline, especially in the context of nucleons, we recommend the review by Bernard, Kaiser & Meißner;²⁵ for an educational introduction with many details, we recommend the script by Scherer & Schindler.²⁶ Both references form the basis of this synopsis.

The strong interactions are described by the Lagrangian of Quantum Chromodynamics (QCD) which comprises the behavior of quarks and gluons. However, a perturbative treatment of QCD only works at high energies stemming from the running of the theory's coupling constant α_s : it leads to the asymptotic freedom of quarks, i.e. they interact weakly at high energies. Since many quark composites (= hadrons) and related processes emerge predominantly from quark-gluon dynamics at small momentum transfers, one needs to resort to an effective description of the strong interactions. Here, one can work in the desired kinematic regime employing the relevant degrees of freedom and expand the new theory in powers of a low-energy scale where "low" is defined in comparison to some other "high" scale at which the theory breaks down. In doing so, one loses renormalizability at all scales and the theory must not be considered fundamental anymore. However, it allows for a perturbative treatment that enables quantitative predictions.

The basis for χ PT is the global $U(N)_L \times U(N)_R$ flavor symmetry of QCD (eq. (2.1)) in the massless limit of the N lightest quarks. All quarks with masses below $\Lambda_{QCD} \sim 200$ MeV can be considered "light" i.e. u, d ($N = 2$) and s ($N = 3$).

$$m_u, m_d \ll \Lambda_{QCD} \quad m_s \lesssim \Lambda_{QCD}$$

Recall the Lagrangian of QCD:

$$\mathcal{L}_{QCD} = \sum_f \bar{q}_f (i \not{D} - m_f) q_f - \frac{1}{4} \mathcal{G}_{\mu\nu,a} \mathcal{G}_a^{\mu\nu} + \Theta \frac{\alpha_s}{8\pi} \epsilon^{\mu\nu\rho\sigma} \mathcal{G}_{\mu\nu}^a \mathcal{G}_{\rho\sigma}^a \quad (2.1)$$

The quark flavor fields q_f themselves are color triplets (red, green, blue), \not{D} is the covariant derivative of QCD, $\mathcal{G}_a^{\mu\nu}$ the non-Abelian field-strength tensor for a SU(3) color symmetry and the term proportional to Θ is responsible for the explicit P - and CP -violation in QCD. Since

²⁵V. Bernard, N. Kaiser, and Ulf-G. Meißner. "Chiral Dynamics in Nucleons and Nuclei". In: *International Journal of Modern Physics E* 04.02 (June 1995), pp. 193–344. issn: 1793-6608. doi: 10.1142/s0218301395000092. URL: <http://dx.doi.org/10.1142/s0218301395000092>.

²⁶Stefan Scherer and Matthias R. Schindler. *A Chiral Perturbation Theory Primer*. 2005. arXiv: hep-ph/0505265 [hep-ph].

$\Theta < 10^{-10}$, we can safely drop it here.²⁷ Furthermore, the light quark fields can be rewritten in their left- and right-handed components with $q_f = q_{f,L} + q_{f,R}$. Assume $N = 3$, in the limit of $m_u, m_d, m_s \rightarrow 0$, one obtains

$$\begin{aligned}\hat{\mathcal{L}}_{\text{QCD}} &= \sum_{f=u,d,s} i\bar{q}_f \not{D} q_f + \text{heavy quarks } c, b, t + \text{gluons} \\ &= \sum_{f=u,d,s} i\left(\bar{q}_{L,f} \not{D} q_{L,f} + \bar{q}_{R,f} \not{D} q_{R,f}\right) + \text{heavy quarks } c, b, t + \text{gluons}.\end{aligned}\quad (2.2)$$

In the massless limit, left- and right-handed components of the light quark fields decouple such that the Lagrangian exhibits a $U(3)_L \times U(3)_R$ flavor symmetry as can be seen from eq. (2.2).

Instead of working with left- and right-handed fields, we express them as vectorial and axial fields with corresponding symmetry:

$$U(3)_L \times U(3)_R \equiv SU(3)_V \times SU(3)_A \times U(1)_V \times U(1)_A \quad (2.3)$$

$U(1)_A$ corresponds to the so-called axial anomaly, $U(1)_V$ to the baryon number conservation. Both will be omitted from now on.

The ground state of QCD does not have the full $SU(3)_V \times SU(3)_A$ chiral symmetry. If it had so, one would observe parity doubling, i.e. two particle multiplets with equal masses but opposite parity. This would be the so-called Wigner-Weyl mode of the symmetry. The other possibility is the Nambu-Goldstone mode, where one observes Spontaneous Symmetry Breaking (SSB) of the chiral symmetry. SSB states that "the Lagrangian is invariant under the symmetry but the ground state of the theory is not."²⁸ In case of QCD, one finds

$$SU(3)_V \times SU(3)_A \xrightarrow{\text{SSB}} SU(3)_V. \quad (2.4)$$

By Goldstone's theorem, a spontaneously broken continuous symmetry necessitates the existence of massless scalar particles. For every broken generator of the symmetry, there is one Goldstone boson with matching quantum numbers. In case of *massless* light quarks, one thus expects $N^2 - 1$ massless pseudoscalars ($J^P = 0^-$) from the spontaneously broken symmetry $SU(N)_A$. These pseudoscalars are the three pions for $N = 2$ or three pions, four kaons and the eta for $N = 3$.

Since u - and d -quark are one order of magnitude lighter than even the s -quark, one expects the chiral symmetry to be much better conserved for the $SU(2)$ subgroup. From here on after, this thesis works within this $SU(2)$ isospin subgroup of χPT because, firstly, the strange-sector of the Goldstone bosons plays a subordinate role due to the higher s -quark mass; secondly, an expansion in terms of the Goldstone bosons should converge much faster in $SU(2)$ χPT than in $SU(3)$ χPT .

²⁷Matthew D. Schwartz. *Quantum Field Theory and the Standard Model*. Cambridge University Press, 2014. ISBN: 1107034736, 9781107034730. URL: <http://www.cambridge.org/us/academic/subjects/physics/theoretical-physics-and-mathematical-physics/quantum-field-theory-and-standard-model>, pp.613f.

²⁸Ibid., p.561.

As shown by Weinberg,²⁹ the parameter of this so-called chiral expansion is p_{typ}/Λ_h , where $\Lambda_h \sim 1$ GeV denotes the hadronic scale, where χ PT breaks down, and p_{typ} the typical momentum of the pions (sec. 2.3). An expansion in p_{typ} is equivalent to an expansion in derivatives of the Goldstone boson fields such that we can write an effective Lagrangian as

$$\mathcal{L}^{\text{eff}} = \mathcal{L}^{(2)} + \mathcal{L}^{(4)} + \dots \quad (2.5)$$

The superscript in parentheses, the chiral dimension, denotes the Lagrangian's number of derivatives or insertions of pion mass. The lowest order Lagrangian $\mathcal{L}^{(2)}$ will suffice in this thesis because $\mathcal{L}^{(4)}$ is already of order $\mathcal{O}(\chi^4 = p_{typ}^4/\Lambda_h^4)$ and thus beyond NLO, $\mathcal{O}(\chi^2)$. The presence of heavy meson fields (cf. sec. 2.2) allows for odd orders in χ , therefore exposing the first subleading terms to be of order $\mathcal{O}(\chi^3)$ (cf. sec. 8). Still, $\mathcal{L}^{(4)}$ can be used to absorb the infinities from loop calculations as the theory is renormalizable order by order.

It is convenient to formulate the theory in terms of the Goldstone bosons, which are collected in a unitary matrix U :

$$U = \exp\left(\frac{i\phi}{f_\pi}\right) = \exp\left(\frac{i}{f_\pi} \begin{pmatrix} \pi^0 & \sqrt{2}\pi^+ \\ \sqrt{2}\pi^- & -\pi^0 \end{pmatrix}\right) \quad (2.6)$$

The parameter f_π measures the coupling strength of the matrix element of an axial current between a pion and the vacuum. It is the so-called pion decay constant with $f_\pi = 92.4$ MeV.

We represent ϕ in the following manner:

$$\phi = \begin{pmatrix} \pi^0 & \sqrt{2}\pi^+ \\ \sqrt{2}\pi^- & -\pi^0 \end{pmatrix} = \begin{pmatrix} \pi_3 & \pi_1 - i\pi_2 \\ \pi_1 + i\pi_2 & -\pi_3 \end{pmatrix} = \vec{\tau} \cdot \vec{\pi} \quad (2.7)$$

Here, $\vec{\tau}$ and $\vec{\pi}$ are 3-dimensional vectors holding the Pauli matrices and the Cartesian representation of the pions, respectively.

Combining U and the expansion of \mathcal{L}^{eff} in orders of derivatives, we can constitute the lowest order Lagrangian that satisfies Lorentz invariance and chiral symmetry:

$$\mathcal{L}^{(2)} = \frac{f_\pi^2}{4} \text{Tr}[\partial_\mu U \partial^\mu U^\dagger] \quad (2.8)$$

The trace acts on the flavor indices of U , U^\dagger .

Since the chiral symmetry is only approximately conserved ($m_u, m_d \neq 0$) and consequently the pions massive, one adds a term to account for m_π . This yields the famous χ PT Lagrangian at lowest order by Gasser & Leutwyler:³⁰

$$\mathcal{L}^{(2)} = \frac{f_\pi^2}{4} \text{Tr}[\partial_\mu U \partial^\mu U^\dagger + m_\pi^2(U + U^\dagger)] \quad (2.9)$$

²⁹Steven Weinberg. “Effective chiral lagrangians for nucleon-pion interactions and nuclear forces”. In: *Nuclear Physics B* 363.1 (1991), pp. 3–18. issn: 0550-3213. doi: [https://doi.org/10.1016/0550-3213\(91\)90231-L](https://doi.org/10.1016/0550-3213(91)90231-L). url: <http://www.sciencedirect.com/science/article/pii/055032139190231L>.

³⁰J. Gasser and H. Leutwyler. “Chiral Perturbation Theory to One Loop”. In: *Annals Phys.* 158 (1984), p. 142. doi: 10.1016/0003-4916(84)90242-2.

We now traded the fundamental theory of strong interactions, QCD, for an effective theory, χ PT. Instead of gluons (gauge bosons) mediating color charge between the quarks (matter fields), we now have the light pseudoscalars mediating isospin between e.g. heavy hadrons. Since f_π and m_π are fixed, there is no free parameter in $\mathcal{L}^{(2)}$.

Expanding eq. (2.9) in powers of $\vec{\pi}$ gives

$$\mathcal{L}_{\pi\pi}^{(2)} = \frac{1}{2} \left(\partial_\mu \vec{\pi} \cdot \partial^\mu \vec{\pi} - m_\pi^2 \vec{\pi}^2 \right) + \frac{1}{6f_\pi^2} \left((\vec{\pi} \cdot \partial_\mu \vec{\pi})(\vec{\pi} \cdot \partial^\mu \vec{\pi}) - \vec{\pi}^2 \partial_\mu \vec{\pi} \partial^\mu \vec{\pi} \right) + \frac{m_\pi^2}{24f_\pi^2} \vec{\pi}^4 + \mathcal{O}(\vec{\pi}^6), \quad (2.10)$$

where the constant term $f_\pi^2 m_\pi^2$ was dropped because it does not contribute to the dynamics. This Lagrangian produces the pion propagator (eq. (2.33)) and the contact term of four pions (eq. (2.18)).

2.2 Inclusion of heavy mesons

For the low-energy interaction between two heavy, quasi-stable mesons, we employ an effective Lagrangian that is composed of three essential parts: the interaction of the pions among themselves is found in $\mathcal{L}_{\pi\pi}$, the Contact Interaction (CI) of four heavy meson fields is in \mathcal{L}_{4H} and the interaction of heavy mesons with axial and vector sources is described via $\mathcal{L}_{\pi HH}$, which also holds the kinetic terms of the heavy mesons. With these Lagrangians, we cover the $B^{(*)}-\bar{B}^{(*)}$ interactions at LO with the 1PE and the CI, at NLO with the Two-Pion-Exchange (2PE) and the one-loop corrections to 1PE and CI.

The leading heavy meson effective Lagrangian density is given by^{31,32}

$$\begin{aligned} \mathcal{L}_{\pi HH}^{(1)} = & -i \text{Tr}[\bar{H}_a v_\mu \partial^\mu H_a] \\ & + \frac{i}{4} \text{Tr}[\bar{H}_a H_b] v^\mu (u^\dagger \partial_\mu u + u \partial_\mu u^\dagger)_{ba} \\ & + \frac{i}{4} g \text{Tr}[\bar{H}_a H_b \gamma_\rho \gamma_5] (u^\dagger \partial^\rho u - u \partial^\rho u^\dagger)_{ba} \\ & + h.c., \end{aligned} \quad (2.11)$$

with $u = \sqrt{U}$. The first line comprises the kinetic term of a heavy meson, represented by a superfield H_a , with velocity v_μ . The second and third line describe the vertices of the heavy meson with the Goldstone bosons of SU(2) isospin. Here, the second line represents the vertices with an even number of Goldstone bosons and the third line those vertices with an odd number. The latter also includes a factor of g denoting the coupling strength of the heavy mesons to the axial-vector field $i(u^\dagger \partial^\rho u - u \partial^\rho u^\dagger)$. The last line accounts for the Hermitian

³¹Mark B. Wise. “Chiral perturbation theory for hadrons containing a heavy quark”. In: *Phys. Rev. D* 45 (7 Apr. 1992), R2188–R2191. DOI: 10.1103/PhysRevD.45.R2188. URL: <https://link.aps.org/doi/10.1103/PhysRevD.45.R2188>.

³²Aneesh V. Manohar and Mark B. Wise. *Heavy Quark Physics*. Cambridge Monographs on Particle Physics, Nuclear Physics and Cosmology. Cambridge University Press, 2000. DOI: 10.1017/CB09780511529351.006, pp.131ff. Caution: A different convention for the heavy meson superfields \bar{H} and H is introduced when compared to the paper by Wise!

conjugate, which will be omitted from now on. The trace acts on the Dirac indices of the gamma matrices.

Expanding u and u^\dagger in eq. (2.11) gives:³³

$$i(u^\dagger \partial_\mu u + u \partial_\mu u^\dagger)_{ba} = -\frac{\vec{\tau}_{ba}}{2f_\pi^2} \cdot (\vec{\pi} \times \partial_\mu \vec{\pi}) + O(\vec{\pi}^4) \quad (2.12)$$

$$i(u^\dagger \partial^\mu u - u \partial^\mu u^\dagger)_{ba} = -\frac{\vec{\tau}_{ba}}{f_\pi} \cdot \partial^\mu \vec{\pi} - \frac{\vec{\tau}_{ba}}{6f_\pi^3} \cdot (\vec{\pi} (\vec{\pi} \cdot \partial^\mu \vec{\pi}) - \partial^\mu \vec{\pi} (\vec{\pi} \cdot \vec{\pi})) + O(\vec{\pi}^5) \quad (2.13)$$

The Pauli matrices' entries are denoted $a, b = \{1, 2\}$.

\bar{H}_a and H_b are superfields that incorporate both the pseudoscalar (anti-)field P_b (P_a^\dagger) and the vector (anti-)field $P_b^{*\mu}$ ($P_a^{*\mu}$):

$$\begin{aligned} \bar{H}_a &= \gamma_0 H_a^\dagger \gamma_0 = (P_a^{*\mu} \gamma_\mu + P_a^\dagger \gamma_5) \frac{1 + \not{v}'}{2} \\ H_b &= \frac{1 + \not{v}''}{2} (P_b^{*\mu} \gamma_\mu - P_b \gamma_5) \end{aligned} \quad (2.14)$$

\bar{H}_a creates a superfield with velocity v' and H_b annihilates one with velocity v'' . P_a transforms as a spin singlet, whereas $P_a^{*\mu}$ is a spin triplet and thus carries a spin λ .

To manage heavy mesons H containing one heavy quark Q ($m_Q \approx m_H > \Lambda_{QCD}$) and one light quark q ($m_q \ll \Lambda_{QCD} < m_Q$), we employ Heavy Quark Effective Theory (HQET): since the heavy quark accounts almost for the total mass of the meson, we regard the limit of $m_Q \rightarrow \infty$ and $m_q \rightarrow 0$. p_{typ} is the largest scale kept dynamically such that we can assume the momentum of the light quarks to be of the same order. This enables us to expand the heavy meson fields in p_{typ}/m_Q , already neglecting terms of the first order $O(p_{typ}/m_Q)$ and use a non-relativistic treatment of Q . Thus, we can rewrite the momenta of the heavy mesons as $p^\mu = m_Q v^\mu + l^\mu$ with a small residual momentum l^μ . Only through this residual momentum do the heavy mesons contribute when we later deal with e.g. loop integrals. Since Q is in the infinite-mass frame, $v^\mu = (1, \vec{0})^T$. This treatment implies $l^0 = E_p - m_Q = 0 + \vec{l}^2/2m_Q + \dots$, allowing us to drop the 0-th component of the heavy meson fields as all contributions are subleading. Since now only the light quarks $q = \{u, d\}$ are the relevant degrees of freedom, this expansion yields a SU(2) isospin symmetry, allowing us to interpret the heavy meson system similar to the deuteron as indicated in sec. 1. Furthermore, this yields a HQSS at order $O(1)$ such that P and P^* are degenerate and their interactions related. As this symmetry is only broken at next-to-leading order in p_{typ}/m_Q ,³⁴ we are allowed to set $m_P \approx m_{P^*} \approx m_B = (m_P + m_{P^*})/2$.

P_a and $P_a^{*\mu}$ from eq. (2.14) contain the physical fields B, B^* and factors of $\sqrt{m_P} \approx \sqrt{m_{P^*}} \approx \sqrt{m_B}$ such that the Lagrangian is independent of a heavy mass, e.g. $P = \sqrt{m_B} \cdot (B^-, \vec{B}^0)^T$ or $P^* = \sqrt{m_B} \cdot (B^{*-}, \vec{B}^{*0})^T$. These factors stem from the normalization of the fields.

The relativistic normalization condition for hadronic states reads³⁵

$$\langle H(p') | H(p) \rangle = 2E_p (2\pi)^3 \delta(\vec{p}' - \vec{p}),$$

³³Machleidt and Entem, op. cit., p.12.

³⁴Additionally to the expansion in p_{typ}/m_Q , an explicit mass breaking term in the Lagrangian is not introduced until $\mathcal{L}_{\pi HH}^{(2)}$ and hence subleading in χ , too.

³⁵Manohar and Wise, op. cit., p.60f.

with $E_p = \sqrt{\vec{p}^2 + m_H^2}$. This differs from the normalization convention of HQET:

$$\langle H(v', l') | H(v, l) \rangle = 2v^0 \delta_{vv'} (2\pi)^3 \delta(\vec{p}' - \vec{p})$$

Employing the well-known expansion of E_p and comparing both conventions gives

$$|H(p)\rangle = \sqrt{m_H} |H(v)\rangle \left(1 + O\left(\frac{|\vec{p}|}{m_H}\right) \right).$$

The polarization vectors of the heavy vector meson fields follow the convention $\epsilon_\mu^*(\lambda) \epsilon^\mu(\lambda) = -1$ for a given spin λ , where ϵ describes the polarization of an incoming particle and ϵ^* of an outgoing one. Since the heavy mesons are treated as static and the contribution of the 0-th component is of order $O(\vec{l}^2/m_H)$, the polarization vectors can be broken down to $\vec{\epsilon}^*(\lambda) \cdot \vec{\epsilon}(\lambda) = +1$. When summing over all possible spins (e.g. for internal heavy mesons), we obtain:

$$\begin{aligned} \sum_\lambda \epsilon_\mu^*(\lambda) \epsilon_\nu(\lambda) &= -g_{\mu\nu} + \frac{p_\mu p_\nu}{m_H^2} = \begin{pmatrix} 0 & & & \\ & 1 & & \\ & & 1 & \\ & & & 1 \end{pmatrix} + O\left(\frac{\vec{l}^2}{m_H^2}\right) \\ \Rightarrow \sum_\lambda \epsilon_i^*(\lambda) \epsilon_j(\lambda) &= \delta_{ij} \end{aligned} \quad (2.15)$$

We will label the polarization vectors in the following manner: the particle will be denoted 1 when incoming and 1' when outgoing. The anti-particle will be denoted 2 when incoming and 2' when outgoing. This will be of special importance in sec. 7. The Pauli matrices, which carry the SU(2) isospin, will be denoted $\vec{\tau}_1$ for the particle and $\vec{\tau}_2$ for the anti-particle, although it ought to be $\vec{\tau}_2^c$, where the superscript c denotes a charge conjugation. This has already been accounted for in eqs. (A.1) to (A.5) and allows us to use the total isospin I .

Expanding eq. (2.11) with all these constraints gives³⁶

$$\begin{aligned} \mathcal{L}_{\pi HH}^{(1)} &= 2i \left(\vec{P}_a^{*\dagger} \cdot \partial^0 \vec{P}_b^* + P_a^\dagger \partial^0 P_b \right) \\ &\quad - \frac{1}{4f_\pi^2} \left(\vec{P}_a^{*\dagger} \cdot \vec{P}_b^* + P_a^\dagger P_b \right) \left(\vec{\tau}_{ba} \cdot (\vec{\pi} \times \partial_0 \vec{\pi}) \right) \\ &\quad - i \frac{g}{2f_\pi} \left(\vec{P}_a^{*\dagger} \times \vec{P}_b^* \right) \left(\vec{\tau}_{ba} \cdot \vec{\nabla} \vec{\pi} \right) - \frac{g}{2f_\pi} \left(\vec{P}_a^{*\dagger} P_b + P_a^\dagger \vec{P}_b^* \right) \left(\vec{\tau}_{ba} \cdot \vec{\nabla} \vec{\pi} \right) \\ &\quad - i \frac{g}{12f_\pi^3} \left(\vec{P}_a^{*\dagger} \times \vec{P}_b^* \right) \vec{\tau}_{ba} \cdot \left(\vec{\pi} \left(\vec{\pi} \cdot \vec{\nabla} \vec{\pi} \right) - \vec{\nabla} \vec{\pi} \left(\vec{\pi} \cdot \vec{\pi} \right) \right) \\ &\quad - \frac{g}{12f_\pi^3} \left(\vec{P}_a^{*\dagger} P_b + P_a^\dagger \vec{P}_b^* \right) \vec{\tau}_{ba} \cdot \left(\vec{\pi} \left(\vec{\pi} \cdot \vec{\nabla} \vec{\pi} \right) - \vec{\nabla} \vec{\pi} \left(\vec{\pi} \cdot \vec{\pi} \right) \right). \end{aligned} \quad (2.16)$$

The dagger indicates the incoming particles.

³⁶M. Pavón Valderrama. “Power counting and perturbative one pion exchange in heavy meson molecules”. In: *Physical Review D* 85.11 (June 2012). ISSN: 1550-2368. DOI: 10.1103/physrevd.85.114037. URL: <http://dx.doi.org/10.1103/PhysRevD.85.114037>.

The heavy meson contact Lagrangian at LO, $\mathcal{L}_{4H}^{(0)}$, reads³⁷

$$\begin{aligned}\mathcal{L}_{4H}^{(0)}(C \text{ even}) = & D_1 \text{Tr}[\bar{H}H\gamma_\mu] \text{Tr}[H\bar{H}\gamma^\mu] \\ & + D_2 \text{Tr}[\bar{H}H\gamma_\mu\gamma_5] \text{Tr}[H\bar{H}\gamma^\mu\gamma_5] \\ & + E_1 \text{Tr}[\bar{H}(\tau_1)_e H\gamma_\mu] \text{Tr}[H\bar{H}(\tau_2)_e \gamma^\mu] \\ & + E_2 \text{Tr}[\bar{H}(\tau_1)_e H\gamma_\mu\gamma_5] \text{Tr}[H\bar{H}(\tau_2)_e \gamma^\mu\gamma_5].\end{aligned}$$

However, the paper³⁸ uses a C -even parity such that the relative sign in eq. (3.3) would have to change. To compensate for this, we ascribe a minus sign to D_2 , E_2 . In this way, we are consistent with the chosen C -parity.³⁹ The Lagrangian $\mathcal{L}_{4H}^{(0)}$ can then be written as

$$\begin{aligned}\mathcal{L}_{4H}^{(0)}(C \text{ odd}) = & -C_1(P^\dagger P + \vec{P}^{*\dagger} \vec{P}^*)(\bar{P}\bar{P}^\dagger + \vec{P}^* \vec{P}^{*\dagger}) \\ & -C_2(\vec{P}^* P^\dagger + P \vec{P}^{*\dagger})(\vec{P}^* \bar{P}^\dagger + \bar{P} \vec{P}^{*\dagger}) \\ & + iC_2 \left[(\vec{P}^* P^\dagger + P \vec{P}^{*\dagger})(\vec{P}^{*\dagger} \times \vec{P}^*) \right. \\ & \quad \left. - (\vec{P}^{*\dagger} \times \vec{P}^*)(\vec{P}^* \bar{P}^\dagger + \bar{P} \vec{P}^{*\dagger}) \right] \\ & -C_2(\vec{P}^{*\dagger} \times \vec{P}^*)(\vec{P}^{*\dagger} \times \vec{P}^*),\end{aligned}\tag{2.17}$$

where $C_i = D_i + (\vec{\tau}_1 \cdot \vec{\tau}_2)E_i$.

The heavy meson contact Lagrangian at NLO, $\mathcal{L}_{4H}^{(2)}$, will not be treated in this thesis although it is necessary for a complete NLO potential. Together with the already partial wave projected potential, $\mathcal{L}_{4H}^{(2)}$ can be found in a paper by Nefediev.⁴⁰

2.3 Power counting and the chiral dimension

The great merit of EFT over a phenomenological model is power counting allowing one to estimate the accuracy of a given calculation. A field theory needs to provide an organizational scheme in which contributions and operators can be ordered by importance. Therefore, when expanding the theory in a parameter χ , the uncertainty of the amplitudes at maximum order ν_{\max} is expected to be of order $\mathcal{O}(\chi^{\nu_{\max}+1})$. For this to work, one needs to identify a parameter $\chi < 1$ such that the sum of all contributions converges sufficiently fast. Like Wang et al., we use $\chi = p_{\text{typ}}/\Lambda_h$ to rank the diagrams in importance. Here, p_{typ} is a typical momentum and Λ_h the hadronic scale (~ 1 GeV) at which χ PT breaks down. As shown in sec. 8, this lets us estimate that a NLO potential at order $\mathcal{O}(\chi^2)$ is afflicted with an error at order $\mathcal{O}(\chi^3)$. Similarly, expanding the hadronic superfield $|H(p)\rangle$ in orders of p_{typ}/m_H to order $\mathcal{O}(1)$ due to non-relativistic treatment lets us expect an error of order $\mathcal{O}(p_{\text{typ}}/m_H)$.^{41,42}

³⁷Ibid.

³⁸Ibid.

³⁹Nefediev et al., op. cit., We use the same C -odd convention.

⁴⁰Ibid.

⁴¹Wang et al., op. cit., pp.1f.

⁴²Pavón Valderrama, op. cit., pp.1ff.

To identify the order of a given diagram, we introduce Weinberg's power counting scheme, originally established to classify nucleon-nucleon interactions.⁴³ It provides a way of determining the order ν of the expansion parameter p_{typ}/Λ_h for a diagram. From his article, we extract

$$\nu = 2 - \frac{E_n}{2} + 2L + \sum_i V_i \left(d_i + \frac{n_i}{2} - 2 \right),$$

E_n = Number of external nucleon fields,

L = Number of loops,

V_i = Number of vertices of type i ,

d_i = Number of derivatives in an interaction of type i ,

n_i = Number of nucleon fields in an interaction of type i .

Due to HQET, we may interpret the heavy mesons analogous to the constituents of a deuteron such that the above formula facilitates a convenient way to justify predictions.

However, this power counting argument cannot be true for processes of more than one nucleon, or in our case heavy meson, because it forbids bound states. Bound states are non-perturbative; they can only exist if contributions from diagrams do *not* decrease with an increasing number of loops, which is clearly the opposite statement of what was just argued for. Because of that, Weinberg proposed to expand the *potential* and not the full scattering amplitude. Then, summing up the potential non-perturbatively via the LSE (cf. sec. 3) allows the use of naive power counting and yields a non-perturbative result. However, for this to work, the potential has to be completely irreducible.

When talking about reducible or irreducible contributions to the effective potentials, we mean 2PR or non-2PR diagrams. This is more easily seen when returning to time-ordered perturbation theory and placing a vertical cut (time slice) in the diagrams (e.g. in fig. 2.1). Depending on whether there exists a placement of the time slice which only cuts two heavy meson lines, the contribution is considered reducible. For the box diagram: if the first pion has not yet been absorbed before the second one is ejected, the diagram cannot be reducible. Often, single diagrams in covariant perturbation theory consist of both reducible and irreducible diagrams in time-ordered perturbation theory as both diagrams in fig. 2.2 do.

As can be shown in secs. B.3 and B.4, the diagram's reducible pieces are enhanced by a factor of m_B/p_{typ} compared to the irreducible ones. Since the reducible pieces will be reproduced by summation using the coupled-channel LSE (cf. sec. 3), we explicitly omit them to avoid double counting and thereby drop all parts that break naive power counting.

To determine the chiral dimension of the diagrams consistent with Weinberg's power counting scheme, we avail ourselves of the rules outlined in appendix E of a work by Hanhart.⁴⁴ These expressions were derived by assuming all momenta to be of a typical size. The respective orders are given with the vertex rules and propagators in secs. 2.4 and 2.5. The integral's

⁴³Weinberg, op. cit., pp.4-8.

⁴⁴Christoph Hanhart. "Meson production in nucleon-nucleon collisions close to the threshold". In: *Physics Reports* 397.3-4 (July 2004), pp. 155–256. ISSN: 0370-1573. DOI: 10.1016/j.physrep.2004.03.007. URL: <http://dx.doi.org/10.1016/j.physrep.2004.03.007>, pp.139ff.

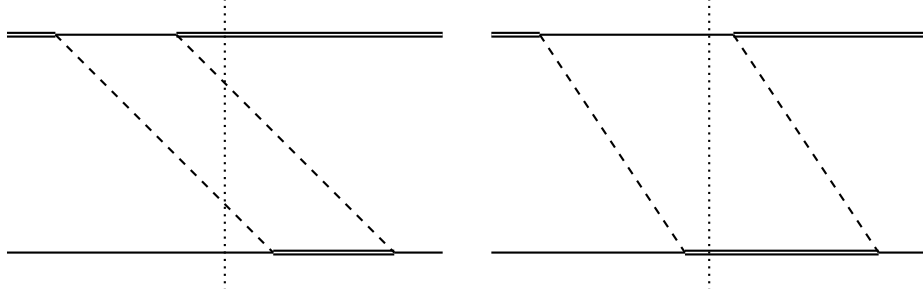


Fig. 2.1: Box diagrams of $P^*\bar{P} \rightarrow P^*\bar{P}$ at NLO in time-ordered perturbation theory. Both contribute to the box diagram in covariant perturbation theory, but the first one is completely irreducible and thus considered in the LSE, while the other one is completely reducible and thus omitted. Dashed lines denote pions, plain lines heavy mesons with spin 0, P , and double lines heavy mesons with spin 1, P^* . Particles are always on top, anti-particles always on the bottom. Time moves from left to right. The dotted lines denote the time slices.

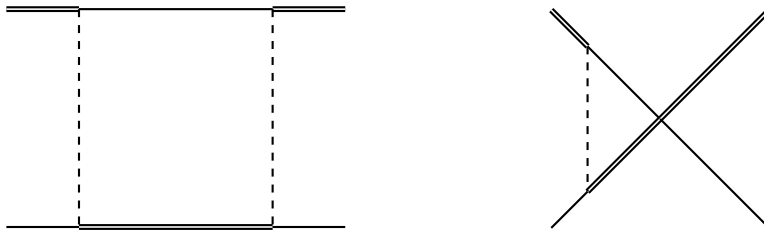


Fig. 2.2: Exemplary diagrams of $P^*\bar{P} \rightarrow P^*\bar{P}$ at NLO which violate naive power counting.

measure, which appears for one-loop contributions, scales as

$$\int \frac{d^4 l}{(2\pi)^4} \sim O\left(\frac{p_0 p_{typ}^3}{(4\pi)^2}\right).$$

Furthermore, $4\pi f_\pi \approx \Lambda_h$ and the constant contact terms scale as $O(1/f_\pi^2)$.

However, the orders may differ when considering reducible or irreducible diagrams, which manifests in evaluating p_0 :

$$p_0 \sim \begin{cases} p_{typ} & \text{if irreducible,} \\ p_{typ}^2/m_B & \text{if reducible.} \end{cases}$$

In secs. B.3 and B.4, it is shown how the reducible parts of a given diagram can be removed.

As can be checked, the contributions of the effective potentials in this thesis scale as follows:

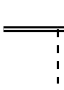
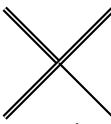
$$\begin{aligned} \text{CI} &\sim O(1) \\ \text{1PE} &\sim O(1) \\ \text{CCI \& C1PE} &\sim O\left(\frac{p_{typ}^2}{\Lambda_h^2}\right) \\ \text{2PE} &\sim O\left(\frac{p_{typ}^2}{\Lambda_h^2}\right) \end{aligned}$$

The ordering explicitly comprises the expansion parameter of $\text{HM}\chi\text{PT}$, $\chi = p_{typ}/\Lambda_h$. Since every $1/(4\pi)^2$ from one integration measure is combined with a factor of $1/f_\pi^2$ per loop to the hadronic scale $1/\Lambda_h^2$, the "remaining" order of $O(1/f_\pi^2)$ is omitted due to dimensional reasons.

The factors of $\sqrt{m_H}$ or rather $\sqrt{m_B}$ due to normalization of the superfields H are not included in the ordering as they are mere normalization factors in front of *every* effective potential. The order of the non-relativistic approximation of the superfields is $O(1)$.

2.4 Vertices

Generally, pions are shown with dashed lines, a P with a plain line and a P^* with a doubled one. The heavy mesons $P^{(*)}$ are always on top of the diagram, the heavy anti-mesons $\bar{P}^{(*)}$ on the bottom. Time runs from left to right.

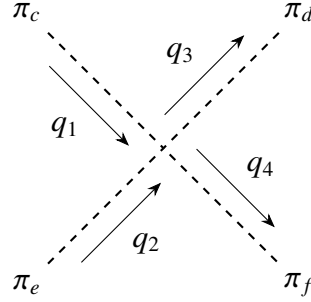
There are two Feynman rules that demand some caution:  and ,

comprise exactly *one* cross product of two polarization vectors resulting in a minus sign after conversion (*h.c.*) in the corresponding anti-vertex ($\vec{\epsilon}$ and $\vec{\epsilon}^*$ are interchanged and hence the order of polarization indices in the Levi-Civita tensor). Defining a composite, Hermitian vector like $\vec{A} = \frac{i}{\sqrt{2}}(\vec{\epsilon} \times \vec{\epsilon}^*)$ ⁴⁵ handles this minus sign with another one through the factor of i , which

⁴⁵Nefediev et al., op. cit.

also changes sign under conversion. However, up to and including sec. 5, the polarization vectors and their components will be kept explicit for perspicuity. This leads to some Feynman rules appearing with different signs depending on the participating (anti-)particles (e.g. the Feynman rules in eqs. (2.21) and (2.25)). Only from sec. 7 on after, we will make use of \vec{A} when projecting the effective potential onto partial waves.

From $\mathcal{L}_{\pi\pi}^{(2)}$, the four-pion vertex is found to be (in accordance with Scherer⁴⁶):



$$= \frac{i}{f_\pi^2} \left[\delta_{ce} \delta_{df} (s - m_\pi^2) + \delta_{cd} \delta_{ef} (t - m_\pi^2) + \delta_{cf} \delta_{de} (u - m_\pi^2) \right] \sim \mathcal{O} \left(\frac{p_{typ}^2}{f_\pi^2} \right), \quad (2.18)$$

with the Mandelstam variables s, t, u .

From $\mathcal{L}_{\pi HH}^{(1)}$, the 3-vertices are found to be the following (in accordance with Pavón Valderrama,⁴⁷ Casalbuoni et al.⁴⁸ or Machleidt & Entem⁴⁹):

$= -\frac{g}{2f_\pi} m_B (\vec{\epsilon}^* \cdot \vec{q}) (\tau)_c \sim \mathcal{O} \left(\frac{p_{typ}}{f_\pi} \right) \quad (2.19)$

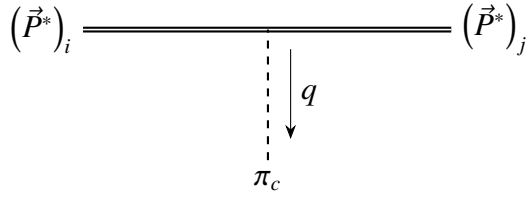
$= -\frac{g}{2f_\pi} m_B (\vec{\epsilon} \cdot \vec{q}) (\tau)_c \sim \mathcal{O} \left(\frac{p_{typ}}{f_\pi} \right) \quad (2.20)$

⁴⁶Scherer and Schindler, op. cit., p.89.

⁴⁷Pavón Valderrama, op. cit.

⁴⁸R. Casalbuoni et al. “Phenomenology of heavy meson chiral lagrangians”. In: *Physics Reports* 281.3 (Mar. 1997), pp. 145–238. ISSN: 0370-1573. DOI: 10.1016/S0370-1573(96)00027-0. URL: [http://dx.doi.org/10.1016/S0370-1573\(96\)00027-0](http://dx.doi.org/10.1016/S0370-1573(96)00027-0), p.79f.

⁴⁹Machleidt and Entem, op. cit., p.62.

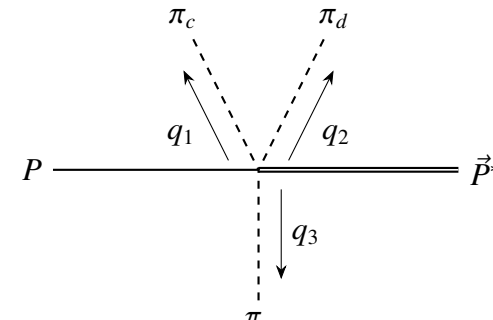


$$(\vec{P}^*)_i \text{---} \text{---} (\vec{P}^*)_j \quad \begin{array}{c} \downarrow q \\ \pi_c \end{array} = \mp i \frac{g}{2f_\pi} m_B \varepsilon_{ijk} \epsilon_i \epsilon_j^* q_k(\tau)_c \sim O\left(\frac{p_{typ}}{f_\pi}\right) \quad (2.21)$$

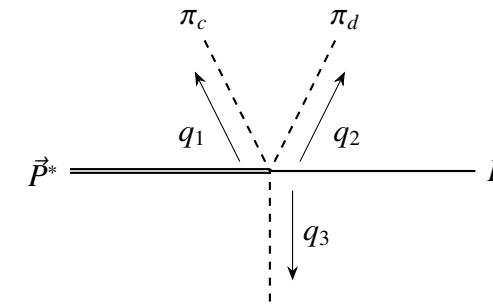
The plus sign in eq. (2.21) denotes the corresponding anti-particle vertex. These vertices are still gauge-independent. The Feynman rules of the 3-Vertices enable us to determine g by experiment.⁵⁰ However, the mass difference between B^* and B is less than the pion mass ($\Delta = m_{B^*} - m_B \approx 45 \text{ MeV}$), so a decay involving a pion does not occur. But due to HQFS, the matrix elements for the decays $B^* \rightarrow B\pi$ and $D^* \rightarrow D\pi$ are equal at leading order.

$$\Gamma(D^{*+} \rightarrow D^0 \pi^+) = \frac{g^2 |\vec{p}_\pi|^3}{6\pi f_\pi^2} \quad (2.22)$$

The vertex from $\mathcal{L}_{\pi HH}^{(1)}$ with three pions is the first gauge-dependent one. Using exponential gauge, we find:

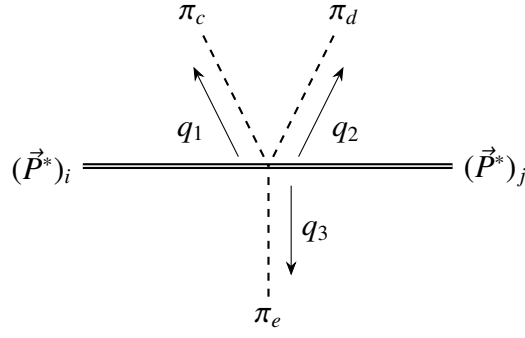


$$= - \frac{g}{12f_\pi^3} m_B \vec{\epsilon}^* \cdot \left[(\vec{q}_3 - \vec{q}_1)(\tau)_c \delta_{de} + (\vec{q}_1 - \vec{q}_2)(\tau)_d \delta_{ce} + (\vec{q}_2 - \vec{q}_3)(\tau)_e \delta_{cd} \right] \sim O\left(\frac{p_{typ}}{f_\pi^3}\right) \quad (2.23)$$

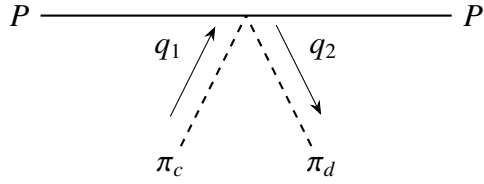


$$= - \frac{g}{12f_\pi^3} m_B \vec{\epsilon} \cdot \left[(\vec{q}_3 - \vec{q}_1)(\tau)_c \delta_{de} + (\vec{q}_1 - \vec{q}_2)(\tau)_d \delta_{ce} + (\vec{q}_2 - \vec{q}_3)(\tau)_e \delta_{cd} \right] \sim O\left(\frac{p_{typ}}{f_\pi^3}\right) \quad (2.24)$$

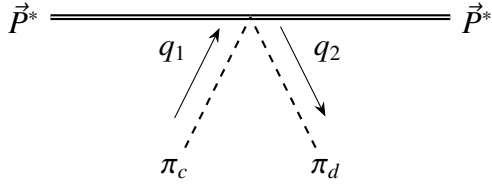
⁵⁰Manohar and Wise, op. cit., p.135.



$$= \mp i \frac{g}{12f_\pi^3} m_B \varepsilon_{ijk} \epsilon_i \epsilon_j \left[(q_3 - q_1)_k (\tau)_c \delta_{de} + (q_1 - q_2)_k (\tau)_d \delta_{ce} + (q_2 - q_3)_k (\tau)_e \delta_{cd} \right] \sim \mathcal{O}\left(\frac{p_{typ}}{f_\pi^3}\right) \quad (2.25)$$

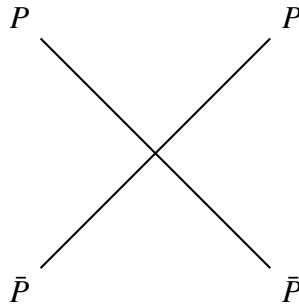


$$= \frac{1}{4f_\pi^2} m_B (q_1^0 + q_2^0) \varepsilon_{cde} (\tau)_e \sim \mathcal{O}\left(\frac{p_{typ}}{f_\pi^2}\right) \quad (2.26)$$



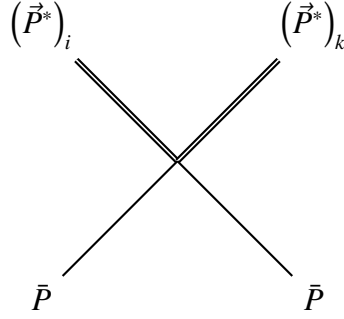
$$= \frac{1}{4f_\pi^2} m_B (\vec{\epsilon}^* \cdot \vec{\epsilon}) (q_1^0 + q_2^0) \varepsilon_{cde} (\tau)_e \sim \mathcal{O}\left(\frac{p_{typ}}{f_\pi^2}\right) \quad (2.27)$$

From $\mathcal{L}_{4H}^{(0)}$, we draw the vertices:

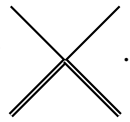


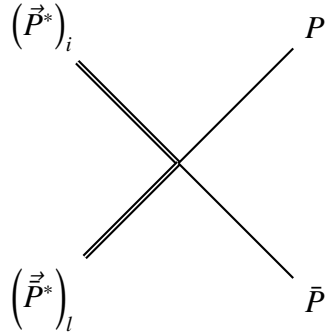
$$= -iC_1 m_B^2 \sim \mathcal{O}(1) \quad (2.28)$$

From here on after, we will use a fixed notation for the polarization indices of external legs: i corresponds to the incoming meson (1), k to the outgoing one (1'), l to the incoming anti-meson (2) and n to the outgoing one (2').


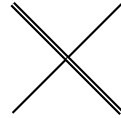
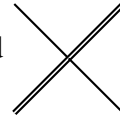


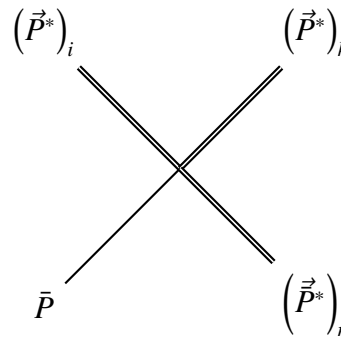
$$= -iC_1 m_B^2 (\vec{\epsilon}^* \cdot \vec{\epsilon}) = -iC_1 m_B^2 \delta_{ik} \epsilon_i \epsilon_k^* \sim \mathcal{O}(1) \quad (2.29)$$

The same holds for .



$$= -iC_2 m_B^2 (\vec{\epsilon}^* \cdot \vec{\epsilon}) = -iC_2 m_B^2 \delta_{il} \epsilon_i \epsilon_l^* \sim \mathcal{O}(1) \quad (2.30)$$

The same holds for , , and .



$$= \pm C_2 \varepsilon_{ikn} \epsilon_i \epsilon_k^* \epsilon_n m_B^2 \sim \mathcal{O}(1) \quad (2.31)$$

Again, the lower sign denotes the corresponding anti-particle vertex with two \bar{P}^* -mesons and indices l, k, n instead of i, k, n , respectively.

$$\begin{array}{ccc}
 (\vec{P}^*)_i & & (\vec{P}^*)_k \\
 & \diagdown \quad \diagup & \\
 & \text{X} & \\
 & \diagup \quad \diagdown & \\
 (\vec{P}^*)_l & & (\vec{P}^*)_n
 \end{array}$$

$$\begin{aligned}
 &= -i \left(C_1 (\vec{\epsilon}_1 \cdot \vec{\epsilon}_1^*) (\vec{\epsilon}_2^* \cdot \vec{\epsilon}_2) + C_2 (\vec{\epsilon}_1 \times \vec{\epsilon}_1^*) (\vec{\epsilon}_2^* \times \vec{\epsilon}_2) \right) m_B^2 \\
 &= -i \left(C_1 \delta_{ik} \delta_{ln} + C_2 \varepsilon_{ikj} \varepsilon_{lnj} \right) \epsilon_i \epsilon_k^* \epsilon_l^* \epsilon_n m_B^2 \sim \mathcal{O}(1)
 \end{aligned} \tag{2.32}$$

2.5 Propagators

The propagator for pions derived from eq. (2.9) matches the relativistic one for spin 0 particles:⁵¹

$$\pi_c \xrightarrow{q} \pi_d = \frac{i\delta_{cd}}{q^2 - m_\pi^2 + i\epsilon} \sim \mathcal{O}\left(\frac{1}{p_{typ}^2}\right) \tag{2.33}$$

In the non-relativistic propagator, the heavy mesons only appear through their residual momentum l :⁵²

$$\begin{aligned}
 P_a &\xrightarrow{l^0} P_b = \frac{i\delta_{ab}}{2l^0 + i\epsilon} \\
 (\vec{P}_a)_i &\xrightarrow{l^0} (\vec{P}_b)_k = \frac{i\delta_{ab}\delta_{ik}}{2l^0 + i\epsilon}
 \end{aligned}$$

The Kronecker deltas match the polarization indices i, k and the SU(2) isospin indices a, b . The latter are treated implicitly with the Pauli matrices τ from next chapter on after. When encountering intermediate spin 1 particles, the polarization indices have always been matched implicitly using eq. (2.15).

However, we need to include the correct mass normalization. This can be obtained by either canceling the factors of $\sqrt{m_B}$ with the intermediate heavy meson mass or by explicitly inserting $p^\mu = m_B v^\mu + l^\mu$ into the propagator's denominator:

$$(p^2 - m_B^2)^{-1} = (m_B \cdot 2vl + \mathcal{O}(l^2))^{-1}$$

⁵¹Schwartz, op. cit., p.76f.

⁵²Wise, op. cit.

This yields

$$P_a \xrightarrow{l^0} P_b = m_B^{-1} \frac{i\delta_{ab}}{2l^0 + i\epsilon} \sim O\left(\frac{1}{p^0}\right), \quad (2.34)$$

$$(\vec{P}_a^*)_i \xrightarrow{l^0} (\vec{P}_b^*)_k = m_B^{-1} \frac{i\delta_{ab}\delta_{ik}}{2l^0 + i\epsilon} \sim O\left(\frac{1}{p^0}\right). \quad (2.35)$$

3 The Lippmann-Schwinger equation

With the methods of EFT, we calculate the potential V^{eff} of $B^{(*)}\bar{B}^{(*)} \rightarrow B^{(*)}\bar{B}^{(*)}$ scattering. For the quantum numbers $J^{PC} = 0^{++}, 1^{++}, 1^{+-}, 2^{++}$, the potentials are then partial wave projected in a coupled-channel formalism. These pairs of $B^{(*)}$ and $\bar{B}^{(*)}$ form a basis in the LSE, which is the central tool in the calculation of the T -matrix.⁵³

The LSE for a partial wave projected coupled channel between a meson (denoted with 1) and an anti-meson (denoted with 2) from initial state β (non-primed) to final state α (primed) reads

$$T_{\alpha\beta}(M, \vec{p}, \vec{p}') = V_{\alpha\beta}^{\text{eff}}(\vec{p}, \vec{p}') - \sum_{\gamma} \int \frac{d^3\vec{q}}{(2\pi)^3} V_{\alpha\gamma}^{\text{eff}}(\vec{p}, \vec{q}) G_{\gamma}(M, \vec{q}) T_{\gamma\beta}(M, \vec{q}, \vec{p}') . \quad (3.1)$$

M is the total energy, T the scattering amplitude and G the coupled-channel propagator:

$$T_{\alpha\beta}(M, \vec{p}, \vec{p}') = - \frac{\mathcal{M}_{\alpha\beta}(M, \vec{p}, \vec{p}')}{\sqrt{(2m_{1,\alpha})(2m_{2,\alpha})(2m_{1,\beta})(2m_{2,\beta})}} ,$$

$$G_{\gamma}(M, \vec{q}) = \frac{1}{\frac{\vec{q}^2}{2\mu_{\gamma}} + m_{1,\gamma} + m_{2,\gamma} - M - i\epsilon} ,$$

with the reduced mass $\mu_{\gamma} = m_{1,\gamma} m_{2,\gamma} / (m_{1,\gamma} + m_{2,\gamma})$.⁵⁴ The common normalization factor of $(2\pi)^4$, relating $T_{\alpha\beta}$ to the full matrix element $\mathcal{M}_{\alpha\beta}$, is dropped and the $\delta^{(4)}(\vec{p}_1 + \vec{p}_1 - \vec{p}'_1 - \vec{p}'_2)$ is omitted because we enforce momentum conservation explicitly.⁵⁵ T is associated with the S -matrix via^{56,57}

$$\langle \alpha | S | \beta \rangle = \mathbb{1} + iT . \quad (3.2)$$

This fixes the irreducible potential to be treated as $V^{\text{eff}} = i\mathcal{M}$.

As stated in sec. 2.3, bound states cannot be obtained perturbatively to desired order because diagrams of all orders contribute. However, summing irreducible diagrams of LO and NLO yields a non-perturbative result. This is why we use the LSE.

⁵³Nefediev et al., op. cit.

⁵⁴Ibid.

⁵⁵M. Tanabashi et al. “Review of Particle Physics”. In: *Phys. Rev. D* 98 (3 Aug. 2018), p. 030001. doi: 10.1103/PhysRevD.98.030001. URL: <https://link.aps.org/doi/10.1103/PhysRevD.98.030001>, p.236f.

⁵⁶Machleidt and Entem, op. cit., p.61.

⁵⁷Schwartz, op. cit., p.60, eq. (5.17).

The potential's decomposition $V_{\alpha\beta}^{\text{eff}}$ is obtained with⁵⁸

$$V_{\alpha\beta}^{\text{eff}}(J^{PC}) = \frac{1}{2J+1} \int \frac{d\Omega_n}{4\pi} \frac{d\Omega_{n'}}{4\pi} \text{Tr} \left[P^\dagger(\alpha, \vec{n}') V^{\text{eff}} P(\beta, \vec{n}) \right].$$

$P^\dagger(\alpha, \vec{n}')$, $P(\beta, \vec{n})$ are the partial wave projectors. They are to be found in sec. 7 together with details on the calculation of $V_{\alpha\beta}^{\text{eff}}$. The coupled-channel basis is given as:

$$\begin{aligned} 0^{++} : \quad \alpha, \beta &= \{ B\bar{B}(^1S_0), B^* \bar{B}^*(^1S_0), B^* \bar{B}^*(^5D_0) \} \\ 1^{++} : \quad \alpha, \beta &= \{ B\bar{B}^*(^3S_1, +), B\bar{B}^*(^3D_1, +), B^* \bar{B}^*(^5D_1) \} \\ 1^{+-} : \quad \alpha, \beta &= \{ B\bar{B}^*(^3S_1, -), B\bar{B}^*(^3D_1, -), B^* \bar{B}^*(^3S_1), B^* \bar{B}^*(^3D_1) \} \\ 2^{++} : \quad \alpha, \beta &= \{ B\bar{B}(^1D_2), B\bar{B}^*(^3D_2), B^* \bar{B}^*(^5S_2), B^* \bar{B}^*(^1D_2), B^* \bar{B}^*(^5D_2), B^* \bar{B}^*(^5G_2) \} \end{aligned}$$

The partial waves are denoted $^{2S+1}L_J$ with the total spin S , the angular momentum L and the total momentum J of the two-meson system. The sign in parentheses after the partial wave denotes the symmetry under the C -conjugation:

$$|B\bar{B}^*, \pm\rangle = \frac{1}{\sqrt{2}} (|B\bar{B}^*\rangle \pm |B^* \bar{B}\rangle) \quad (3.3)$$

This is consistent with the C -parity transformation $\hat{C}|M\rangle = |\bar{M}\rangle$ between a meson state $|M\rangle$ and an anti-meson state $|\bar{M}\rangle$.⁵⁹

The central part of this thesis is the calculation of the matrix elements V^{eff} of $B^{(*)} \bar{B}^{(*)} \rightarrow B^{(*)} \bar{B}^{(*)}$ scattering. Technically, there are 16 different possibilities but thanks to CPT -invariance, we only need to consider the seven matrix elements listed below, which differ from one another. These invariances stem from QCD and are therefore also respected by χ PT. Hence, the following contributions to the potential need to be calculated:

- $V^{\text{eff}}(B\bar{B} \rightarrow B\bar{B})$
- $V^{\text{eff}}(B^* \bar{B} \rightarrow B^* \bar{B}) \Leftrightarrow V^{\text{eff}}(B\bar{B}^* \rightarrow B\bar{B}^*)$
- $V^{\text{eff}}(B^* \bar{B} \rightarrow B\bar{B}^*) \Leftrightarrow V^{\text{eff}}(B\bar{B}^* \rightarrow B^* \bar{B})$
- $V^{\text{eff}}(B^* \bar{B}^* \rightarrow B^* \bar{B}^*)$
- $V^{\text{eff}}(B^* \bar{B}^* \rightarrow B\bar{B}) \Leftrightarrow V^{\text{eff}}(B\bar{B} \rightarrow B^* \bar{B}^*)$
- $V^{\text{eff}}(B^* \bar{B} \rightarrow B\bar{B}) \Leftrightarrow V^{\text{eff}}(B\bar{B}^* \rightarrow B\bar{B}) \Leftrightarrow V^{\text{eff}}(B\bar{B} \rightarrow B^* \bar{B}) \Leftrightarrow V^{\text{eff}}(B\bar{B} \rightarrow B\bar{B}^*)$
- $V^{\text{eff}}(B\bar{B}^* \rightarrow B^* \bar{B}^*) \Leftrightarrow V^{\text{eff}}(B^* \bar{B} \rightarrow B^* \bar{B}^*) \Leftrightarrow V^{\text{eff}}(B^* \bar{B}^* \rightarrow B\bar{B}^*) \Leftrightarrow V^{\text{eff}}(B^* \bar{B}^* \rightarrow B^* \bar{B})$

⁵⁸Nefediev et al., op. cit., p.8.

⁵⁹V. Baru et al. "Spin partners of the $Z_b(10610)$ and $Z_b(10650)$ revisited". In: *JHEP* 06 (2017), p. 158. doi: 10.1007/JHEP06(2017)158. arXiv: 1704.07332 [hep-ph], p.5.

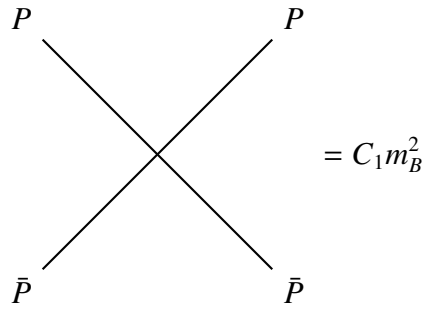
4 Leading order diagrams

The LO splits into the momentum-independent CI and the momentum-dependent 1PE. The external polarization vectors are excluded. They will be reintroduced in sec. 7.

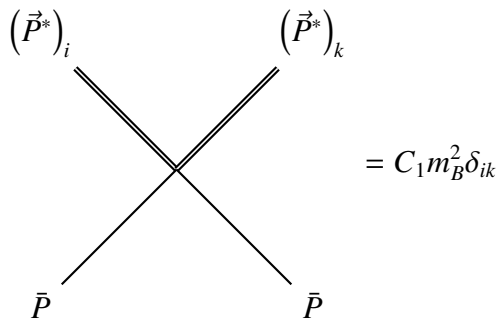
4.1 Contact interaction (CI)

The CI contribution stems from the Feynman rules in eqs. (2.28), (2.29), (2.30), (2.31) and (2.32).

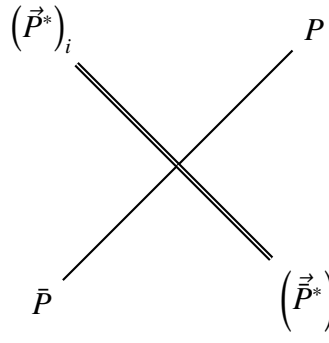
$\mathbf{P}\bar{\mathbf{P}} \rightarrow \mathbf{P}\bar{\mathbf{P}}$



$\mathbf{P}^*\bar{\mathbf{P}} \rightarrow \mathbf{P}^*\bar{\mathbf{P}}$

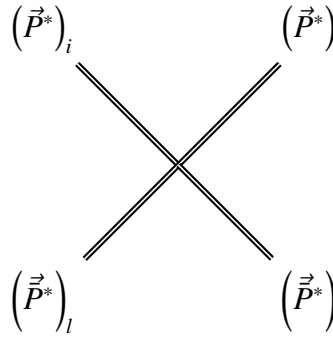


$$\mathbf{P}^* \bar{\mathbf{P}} \rightarrow \mathbf{P} \bar{\mathbf{P}}^*$$



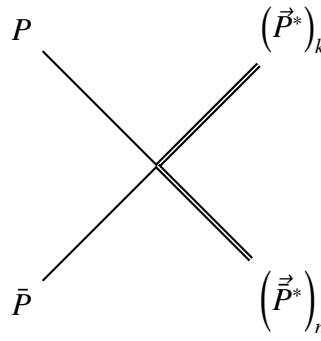
$$= C_2 m_B^2 \delta_{in}$$

$$\mathbf{P}^* \bar{\mathbf{P}}^* \rightarrow \mathbf{P}^* \bar{\mathbf{P}}^*$$



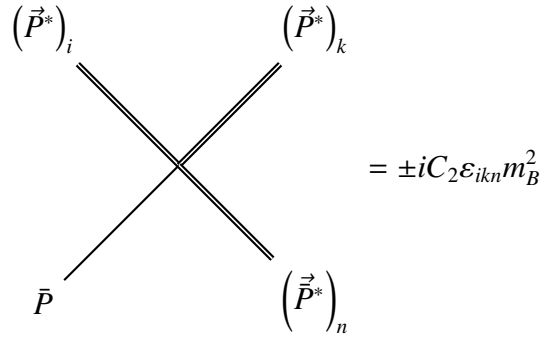
$$= (C_1 \delta_{ik} \delta_{ln} + C_2 \delta_{il} \delta_{kn} - C_2 \delta_{in} \delta_{kl}) m_B^2$$

$$\mathbf{P} \bar{\mathbf{P}} \rightarrow \mathbf{P}^* \bar{\mathbf{P}}^*$$



$$= C_2 m_B^2 \delta_{kn}$$

$$\mathbf{P}^* \bar{\mathbf{P}} \rightarrow \mathbf{P}^* \bar{\mathbf{P}}^*$$

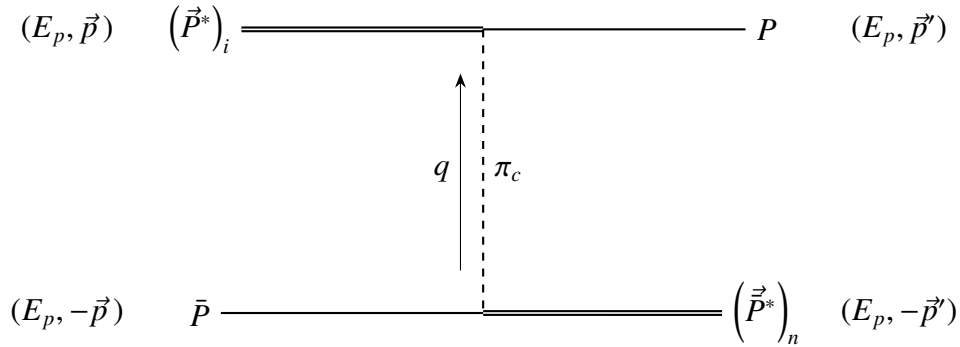


The lower sign denotes the corresponding anti-vertex with two \bar{P}^* -mesons and indices l, k, n instead of i, k, n .

4.2 One-pion-exchange (1PE)

In the 1PE, we do not find $P\bar{P} \rightarrow P\bar{P}$ or $P^*\bar{P} \rightarrow P^*\bar{P}$ since no 3-vertex includes two P s. However, we encounter $P^*\bar{P} \rightarrow P\bar{P}^*$ (mind the change of the spin 1 particle), $P^*\bar{P} \rightarrow P^*\bar{P}^*$, $P^*\bar{P}^* \rightarrow P^*\bar{P}^*$ and $P\bar{P} \rightarrow P^*\bar{P}^*$. We regularly use $q^0 = E_p - E_p = 0$ because P and P^* are degenerate at leading order in p_{typ}/m_H .

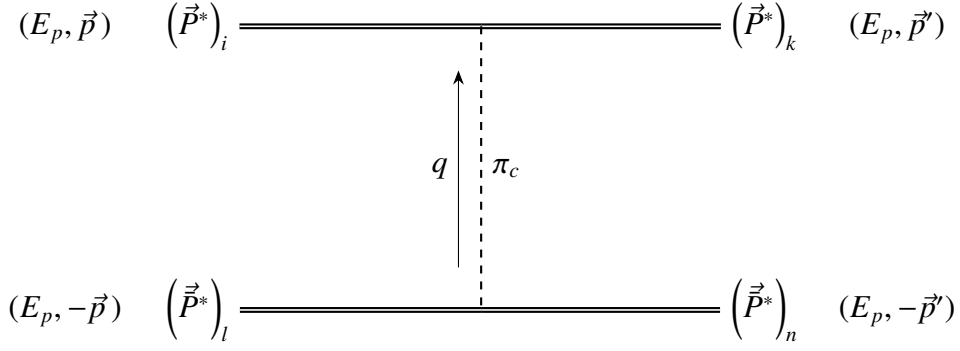
$$\mathbf{P}^* \bar{\mathbf{P}} \rightarrow \mathbf{P} \bar{\mathbf{P}}^*$$



$$\begin{aligned} &= i \left(-\frac{g}{2f_\pi} m_B \right)^2 (-q_i)(\tau_1)_c \frac{i}{q^2 - m_\pi^2 + i\epsilon} q_n (\tau_2)_c \\ &= -\frac{g^2 m_B^2}{4f_\pi^2} (\vec{\tau}_1 \cdot \vec{\tau}_2) \frac{q_i q_n}{\vec{q}^2 + m_\pi^2}, \end{aligned}$$

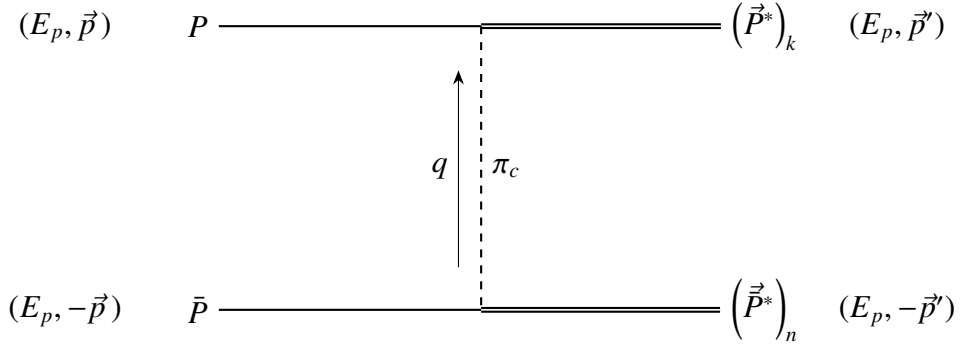
where we used $q^0 = E_p - E_p = 0$ and $\vec{q} = \vec{p}' - \vec{p}$ and the index c has been summed over.

$$\mathbf{P}^* \bar{\mathbf{P}}^* \rightarrow \mathbf{P}^* \bar{\mathbf{P}}^*$$



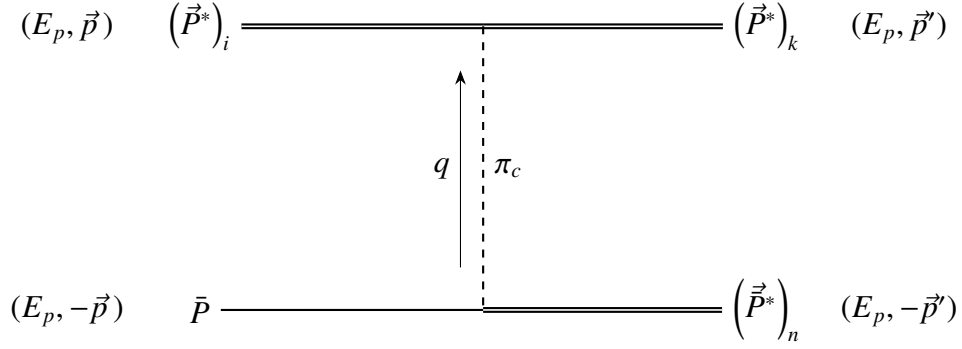
$$\begin{aligned}
 &= i \left(-i \frac{g}{2f_\pi} m_B \right) \left(i \frac{g}{2f_\pi} m_B \right) \varepsilon_{ikr} (-q_r) (\tau_1)_c \frac{i}{q^2 - m_\pi^2 + i\epsilon} \varepsilon_{lns} q_s (\tau_2)_c \\
 &= -\frac{g^2 m_B^2}{4f_\pi^2} (\vec{\tau}_1 \cdot \vec{\tau}_2) \varepsilon_{ikr} \varepsilon_{lns} \frac{q_r q_s}{\vec{q}^2 + m_\pi^2}
 \end{aligned}$$

$$\mathbf{P} \bar{\mathbf{P}} \rightarrow \mathbf{P}^* \bar{\mathbf{P}}^*$$



$$\begin{aligned}
 &= i \left(-\frac{g}{2f_\pi} m_B \right)^2 (-q_k) (\tau_1)_c \frac{i}{q^2 - m_\pi^2 + i\epsilon} q_n (\tau_2)_c \\
 &= -\frac{g^2 m_B^2}{4f_\pi^2} (\vec{\tau}_1 \cdot \vec{\tau}_2) \frac{q_k q_n}{\vec{q}^2 + m_\pi^2}
 \end{aligned}$$

$\mathbf{P}^* \bar{\mathbf{P}} \rightarrow \mathbf{P}^* \bar{\mathbf{P}}^*$



$$\begin{aligned}
 &= i \left(-i \frac{g}{2f_\pi} m_B \right) \left(-\frac{g}{2f_\pi} m_B \right) \varepsilon_{ikr} (-q_r) (\tau_1)_c \frac{i}{q^2 - m_\pi^2 + i\epsilon} q_n (\tau_2)_c \\
 &= -i \frac{g^2 m_B^2}{4f_\pi^2} (\vec{\tau}_1 \cdot \vec{\tau}_2) \frac{\varepsilon_{ikr} q_r q_n}{\vec{q}^2 + m_\pi^2}
 \end{aligned}$$

For the corresponding anti-vertex of $P \bar{P}^* \rightarrow P^* \bar{P}$ scattering, we obtain a sign flip due to the Feynman rule in eq. (2.21) and use indices l, k, n instead of i, k, n , respectively.

5 Next-to-leading order diagrams

We can split the NLO diagrams into the 2PE (sec. 5.1), the Corrected One-Pion-Exchange (C1PE) and the Corrected Contact Interaction (CCI). Although both the explicit calculations to the C1PE and the CCI can be evaded by renormalizing the parameters of the theory, namely m_π , m_B , g and the constants of the contact terms, we treat them differently: the C1PE will be managed via renormalization (sec. 5.2.2), the CCI via explicit calculation (sec. 5.2.3). However, the equivalence of these treatments becomes apparent from the effective potentials of the CCI in sec. 6.

The 2PE holds the interesting long-range behavior at NLO and will be calculated in any case. It is the only contribution that cannot be treated as renormalization of physical parameters and hence improves the accuracy of the prediction of the effective potential beyond LO.

Throughout this chapter, $q_0 = 0$ and the relations concerning the Pauli matrices (eqs. (A.1) to (A.4)) will be used regularly. To avoid double counting (cf. sec. 2.3), we exclusively consider irreducible diagrams in the potential. To organize the plenty calculations at NLO, each new part starts with an angle \lrcorner .

5.1 Two-pion-exchange (2PE)

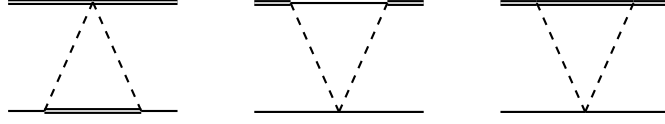
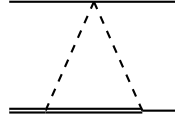
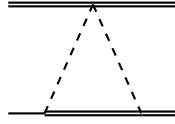
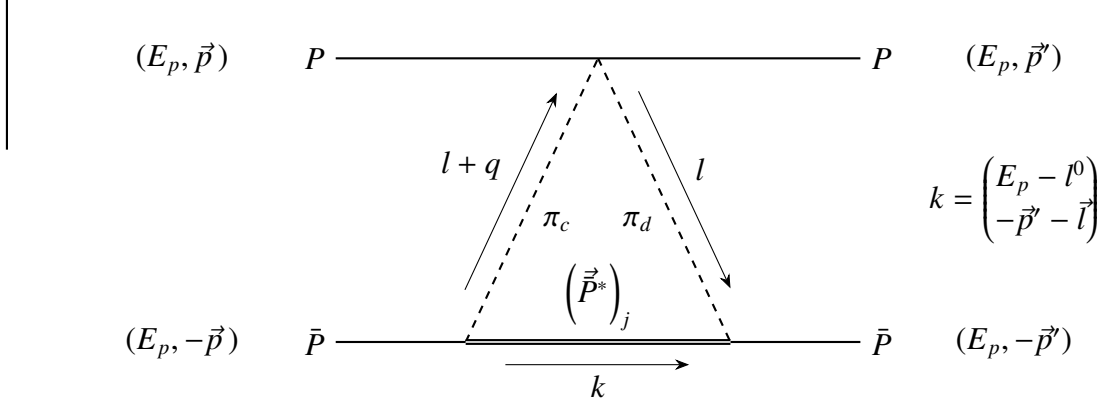
Within the 2PE, we encounter three different types of diagrams: triangle-like, football-like and box-like. This section follows closely the appendix of Machleidt & Entem⁶⁰ in the construction of the Feynman diagrams. The pertinent integrals can be found in appendix B. A complete collection of the respective diagrams is provided in appendix C.

5.1.1 The triangle diagrams



Fig. 5.1: Triangle-like diagrams for $P\bar{P} \rightarrow P\bar{P}$

⁶⁰Machleidt and Entem, op. cit., pp.62-77.

Fig. 5.2: Triangle-like diagrams for $P^* \bar{P} \rightarrow P^* \bar{P}$ Fig. 5.3: Triangle-like diagrams for $P^* \bar{P}^* \rightarrow P^* \bar{P}^*$ Fig. 5.4: Triangle-like diagram for $P \bar{P}^* \rightarrow P \bar{P}$ Fig. 5.5: Triangle-like diagram for $P^* \bar{P} \rightarrow P^* \bar{P}^*$ **$P \bar{P} \rightarrow P \bar{P}$** 

$$\begin{aligned}
 &= i \left(-\frac{g}{2f_\pi} m_B \right)^2 \left(\frac{1}{4f_\pi^2} m_B \right) \int \frac{d^4 l}{(2\pi)^4} (2l^0 + q^0) \varepsilon_{cdh} (\tau_1)_h \frac{i}{(l+q)^2 - m_\pi^2 + i\epsilon} \\
 &\quad \times (\tau_2)_d (-l_j) (\tau_2)_c (l+q)_j \frac{i}{l^2 - m_\pi^2 + i\epsilon} m_B^{-1} \frac{i}{-2l^0 + i\epsilon}
 \end{aligned}$$

We used $q^0 = 0$.

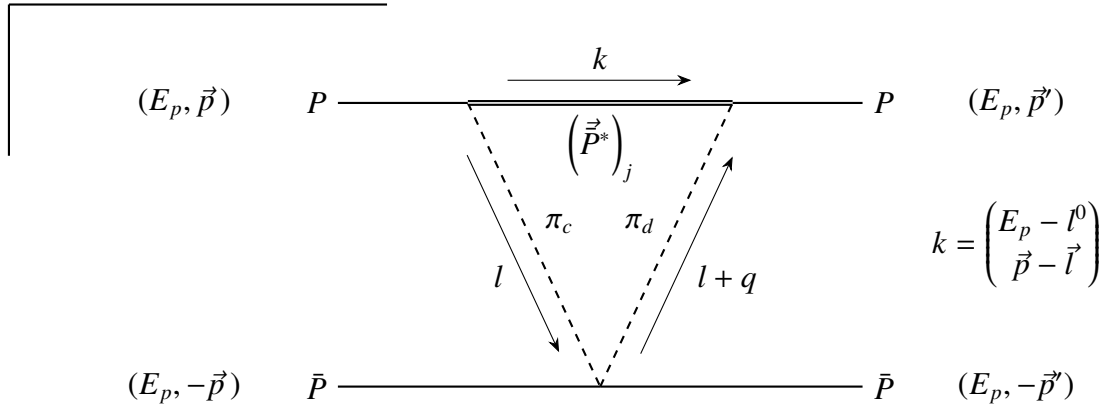
$$= \frac{g^2 m_B^2}{16 f_\pi^4} (\tau_1)_h (\tau_2)_d (\tau_2)_c \varepsilon_{cdh} \underbrace{\int \frac{d^4 l}{(2\pi)^4} \frac{l^0}{l^0 - i\epsilon} \frac{(\vec{l} + \vec{q}) \cdot \vec{l}}{[(l+q)^2 - m_\pi^2 + i\epsilon][l^2 - m_\pi^2 + i\epsilon]}}_{=I_{\text{tr}}}$$

Abbreviating the integral and applying eq. (A.1): $(\tau_1)_h (\tau_2)_d (\tau_2)_c \varepsilon_{cdh} = -2i(\vec{\tau}_1 \cdot \vec{\tau}_2)$ finally gives:

$$= -i \frac{m_B^2}{8 f_\pi^4} (\vec{\tau}_1 \cdot \vec{\tau}_2) g^2 I_{\text{tr}}$$

The calculation of I_{tr} has been transferred to sec. B.1.

Turning towards the second diagram, we get:



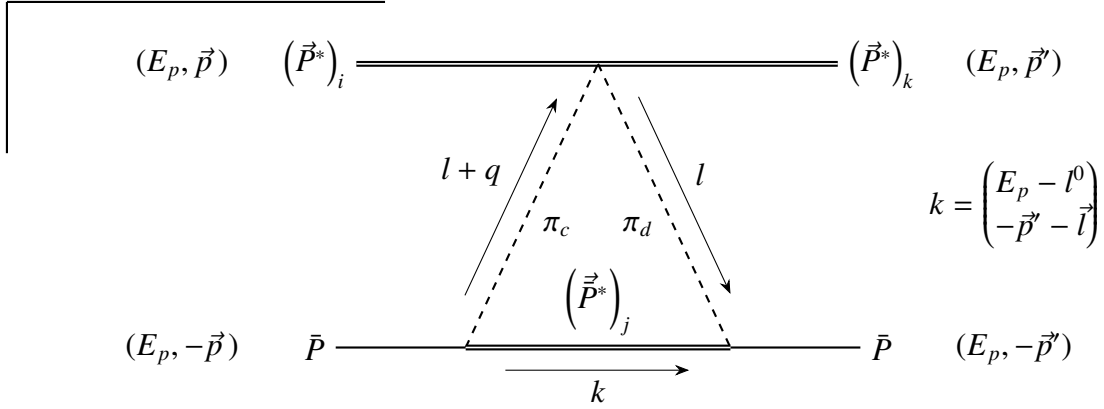
$$= i \left(-\frac{g}{2f_\pi} m_B \right)^2 \left(\frac{1}{4f_\pi^2} m_B \right) \int \frac{d^4 l}{(2\pi)^4} \frac{i}{l^2 - m_\pi^2 + i\epsilon} (2l^0 + q^0) \varepsilon_{cdh} (\tau_2)_h \\ \times \frac{i}{(l+q)^2 - m_\pi^2 + i\epsilon} (\tau_1)_d (-l-q)_j m_B^{-1} \frac{i}{-2l^0 + i\epsilon} (\tau_1)_c l_j$$

Using eq. (A.1) and $q^0 = 0$ gives:

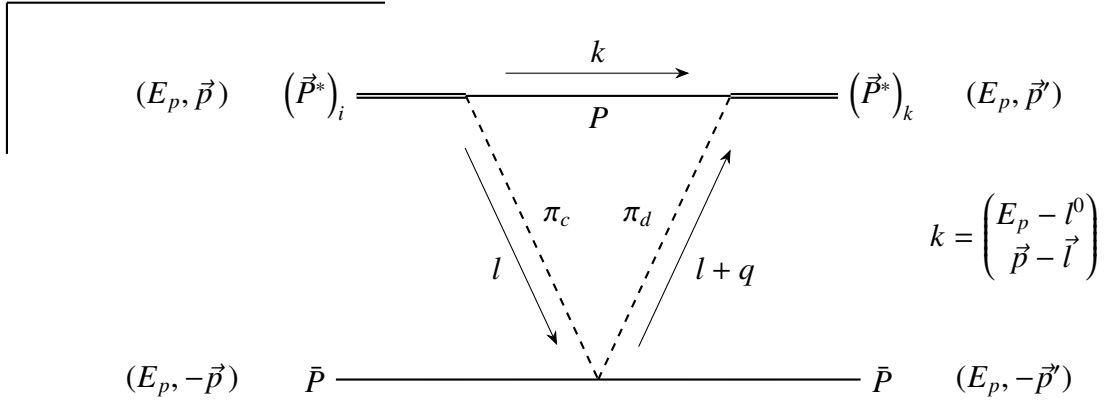
$$= -i \frac{m_B^2}{8 f_\pi^4} (\vec{\tau}_1 \cdot \vec{\tau}_2) g^2 I_{\text{tr}}$$

Thus, summing up both diagrams gives:

$$\boxed{V_{\text{tr}}^{\text{eff}}(P\bar{P} \rightarrow P\bar{P}) = -i \frac{m_B^2}{4 f_\pi^4} (\vec{\tau}_1 \cdot \vec{\tau}_2) (g^2 I_{\text{tr}})} \quad (5.1)$$

$\mathbf{P}^* \bar{\mathbf{P}} \rightarrow \mathbf{P}^* \bar{\mathbf{P}}$ 

$$\begin{aligned}
&= i \left(-\frac{g}{2f_\pi} m_B \right)^2 \left(\frac{1}{4f_\pi^2} m_B \right) \int \frac{d^4 l}{(2\pi)^4} \frac{i}{(l+q)^2 - m_\pi^2 + i\epsilon} \\
&\quad \times \delta_{ik} (2l^0 + q^0) \varepsilon_{cdh} (\tau_1)_h \frac{i}{l^2 - m_\pi^2 + i\epsilon} (\tau_2)_d (-l_j) m_B^{-1} \frac{i}{-2l^0 + i\epsilon} (\tau_2)_c (l+q)_j \\
&= -i \frac{m_B^2}{8f_\pi^4} (\vec{\tau}_1 \cdot \vec{\tau}_2) g^2 \delta_{ik} \mathcal{I}_{\text{tr}}
\end{aligned}$$



$$\begin{aligned}
&= i \left(-\frac{g}{2f_\pi} m_B \right)^2 \left(\frac{1}{4f_\pi^2} m_B \right) \int \frac{d^4 l}{(2\pi)^4} \frac{i}{l^2 - m_\pi^2 + i\epsilon} (2l^0 + q^0) \varepsilon_{cdh} (\tau_2)_h \\
&\quad \times \frac{i}{(l+q)^2 - m_\pi^2 + i\epsilon} (\tau_1)_d (-l-q)_k m_B^{-1} \frac{i}{-2l^0 + i\epsilon} (\tau_1)_c l_i \\
&= -i \frac{m_B^2}{8f_\pi^4} (\vec{\tau}_1 \cdot \vec{\tau}_2) g^2 \int \frac{d^4 l}{(2\pi)^4} \frac{l^0}{l^0 - i\epsilon} \frac{l_i (l+q)_k}{[(l+q)^2 - m_\pi^2 + i\epsilon][l^2 - m_\pi^2 + i\epsilon]}
\end{aligned}$$

We keep the explicit integral here because it enables some cancellation with the next diagram:

$$k = \begin{pmatrix} E_p - l^0 \\ \vec{p} - \vec{l} \end{pmatrix} \quad (5.2)$$

$$= i \left(-i \frac{g}{2f_\pi} m_B \right)^2 \left(\frac{1}{4f_\pi^2} m_B \right) \int \frac{d^4 l}{(2\pi)^4} \frac{i}{l^2 - m_\pi^2 + i\epsilon} (2l^0 + q^0) \varepsilon_{cdh} (\tau_2)_h$$

$$\times \frac{i}{(l+q)^2 - m_\pi^2 + i\epsilon} \varepsilon_{jkr} (-l-q)_r (\tau_1)_d m_B^{-1} \frac{i}{-2l^0 + i\epsilon} \varepsilon_{ijm} l_m (\tau_1)_c$$

Using $q^0 = 0$:

$$= -\frac{g^2 m_B^2}{16f_\pi^4} (\tau_2)_h (\tau_1)_d (\tau_1)_c \varepsilon_{cdh} \int \frac{d^4 l}{(2\pi)^4} \frac{l^0}{l^0 - i\epsilon} \frac{\varepsilon_{ijm} l_m \varepsilon_{jkr} (l+q)_r}{[(l+q)^2 - m_\pi^2 + i\epsilon][l^2 - m_\pi^2 + i\epsilon]}$$

Applying eq. (A.1) and $\varepsilon_{ijm} \varepsilon_{jkr} = -(\delta_{ik} \delta_{mr} - \delta_{ir} \delta_{mk})$:

$$= -i \frac{g^2 m_B^2}{8f_\pi^4} (\vec{\tau}_1 \cdot \vec{\tau}_2) \int \frac{d^4 l}{(2\pi)^4} \frac{l^0}{l^0 - i\epsilon} \frac{\delta_{ik} \vec{l} \cdot (\vec{l} + \vec{q}) - l_k (l+q)_i}{[(l+q)^2 - m_\pi^2 + i\epsilon][l^2 - m_\pi^2 + i\epsilon]}$$

Adding the previous integral and using eq. (A.7) gives:

$$\int \frac{d^4 l}{(2\pi)^4} \frac{l^0}{l^0 - i\epsilon} \frac{\delta_{ik} \vec{l} \cdot (\vec{l} + \vec{q}) - l_k (l+q)_i + l_i (l+q)_k}{[(l+q)^2 - m_\pi^2 + i\epsilon][l^2 - m_\pi^2 + i\epsilon]}$$

$$= \int \frac{d^4 l}{(2\pi)^4} \frac{l^0}{l^0 - i\epsilon} \frac{\delta_{ik} \vec{l} \cdot (\vec{l} + \vec{q})}{[(l+q)^2 - m_\pi^2 + i\epsilon][l^2 - m_\pi^2 + i\epsilon]} = \delta_{ik} \mathcal{I}_{\text{tr}} \quad (5.3)$$

Thus, summing up all three diagrams yields:

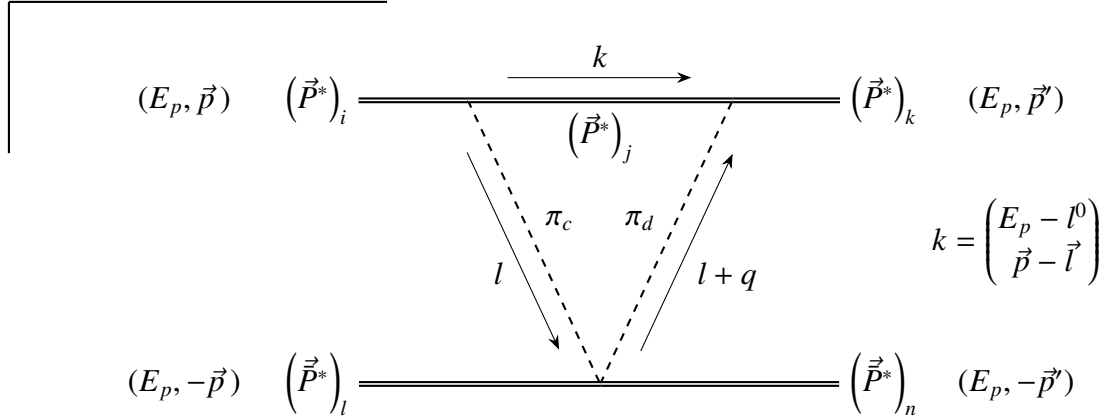
$$V_{\text{tr}}^{\text{eff}}(P^* \bar{P} \rightarrow P^* \bar{P}) = -i \frac{m_B^2}{4f_\pi^4} (\vec{\tau}_1 \cdot \vec{\tau}_2) \delta_{ik} (g^2 \mathcal{I}_{\text{tr}}) \quad (5.4)$$

$\mathbf{P}^* \bar{\mathbf{P}}^* \rightarrow \mathbf{P}^* \bar{\mathbf{P}}^*$

The $P^* \bar{P}^* \rightarrow P^* \bar{P}^*$ scattering includes four diagrams. However, we already encountered the potentials of these in the similar scattering of $P^* \bar{P} \rightarrow P^* \bar{P}$ and hence only state the results. Again, the integrals are kept explicit here because summing them enables some terms to cancel as shown in eq. (5.3).

$$\begin{aligned}
&= -i \frac{m_B^2}{8f_\pi^4} (\vec{\tau}_1 \cdot \vec{\tau}_2) g^2 \delta_{ik} \int \frac{d^4 l}{(2\pi)^4} \frac{l^0}{l^0 - i\epsilon} \frac{(l+q)_l l_n}{[(l+q)^2 - m_\pi^2 + i\epsilon][l^2 - m_\pi^2 + i\epsilon]} \\
&= -i \frac{m_B^2}{8f_\pi^4} (\vec{\tau}_1 \cdot \vec{\tau}_2) g^2 \delta_{ln} \int \frac{d^4 l}{(2\pi)^4} \frac{l^0}{l^0 - i\epsilon} \frac{l_i (l+q)_k}{[(l+q)^2 - m_\pi^2 + i\epsilon][l^2 - m_\pi^2 + i\epsilon]}
\end{aligned}$$

$$= -i \frac{m_B^2}{8f_\pi^4} (\vec{\tau}_1 \cdot \vec{\tau}_2) g^2 \delta_{ik} \int \frac{d^4 l}{(2\pi)^4} \frac{l^0}{l^0 - i\epsilon} \frac{\delta_{ln} \vec{l} \cdot (\vec{l} + \vec{q}) - l_n(l+q)_l}{[(l+q)^2 - m_\pi^2 + i\epsilon][l^2 - m_\pi^2 + i\epsilon]}$$

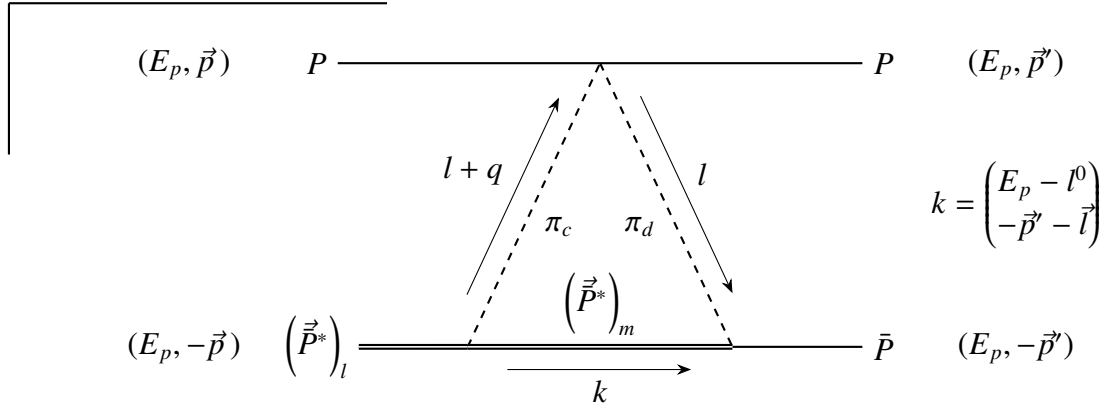


$$= -i \frac{m_B^2}{8f_\pi^4} (\vec{\tau}_1 \cdot \vec{\tau}_2) g^2 \delta_{ln} \int \frac{d^4 l}{(2\pi)^4} \frac{l^0}{l^0 - i\epsilon} \frac{\delta_{ik} \vec{l} \cdot (\vec{l} + \vec{q}) - l_k(l+q)_i}{[(l+q)^2 - m_\pi^2 + i\epsilon][l^2 - m_\pi^2 + i\epsilon]}$$

Summing over all diagrams yields:

$$\boxed{V_{\text{tr}}^{\text{eff}}(P^* \bar{P}^* \rightarrow P^* \bar{P}^*) = -i \frac{m_B^2}{4f_\pi^4} (\vec{\tau}_1 \cdot \vec{\tau}_2) \delta_{ik} \delta_{ln} (g^2 \mathcal{I}_{\text{tr}})} \quad (5.5)$$

$P \bar{P}^* \rightarrow P \bar{P}$



$$= i \left(i \frac{g}{2f_\pi} m_B \right) \left(-\frac{g}{2f_\pi} m_B \right) \left(\frac{1}{4f_\pi^2} m_B \right) \int \frac{d^4 l}{(2\pi)^4} \frac{i}{(l+q)^2 - m_\pi^2 + i\epsilon} \\ \times (2l^0 + q^0) \varepsilon_{cdh} (\tau_1)_h \frac{i}{l^2 - m_\pi^2 + i\epsilon} (\tau_2)_d (-l_m) m_B^{-1} \frac{i}{-2l^0 + i\epsilon} (\tau_2)_c \varepsilon_{lms} (l+q)_s$$

We use $q^0 = 0$:

$$= -i \frac{g^2 m_B^2}{16 f_\pi^4} (\tau_1)_h (\tau_2)_d (\tau_2)_c \varepsilon_{cdh} \int \frac{d^4 l}{(2\pi)^4} \frac{l^0}{l^0 - i\epsilon} \frac{\varepsilon_{lms} (l+q)_s l_m}{[(l+q)^2 - m_\pi^2 + i\epsilon][l^2 - m_\pi^2 + i\epsilon]}$$

Applying eq. (A.1):

$$= -\frac{g^2 m_B^2}{8 f_\pi^4} (\vec{\tau}_1 \cdot \vec{\tau}_2) \int \frac{d^4 l}{(2\pi)^4} \frac{l^0}{l^0 - i\epsilon} \frac{\varepsilon_{lms} (l+q)_s l_m}{[(l+q)^2 - m_\pi^2 + i\epsilon][l^2 - m_\pi^2 + i\epsilon]}$$

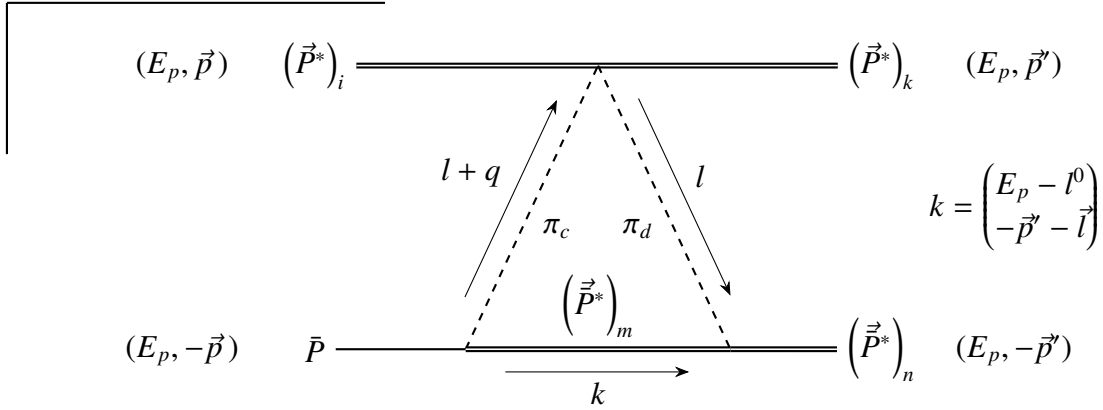
The integral vanishes due to symmetry. This can be easily shown by following the same calculation as outlined for \mathcal{I}_{tr} in sec. B.1:

$$\begin{aligned} & \int \frac{d^4 l}{(2\pi)^4} \frac{l^0}{l^0 - i\epsilon} \frac{\varepsilon_{lms} (l+q)_s l_m}{[(l+q)^2 - m_\pi^2 + i\epsilon][l^2 - m_\pi^2 + i\epsilon]} \\ &= \int_0^1 dx \int \frac{d^4 l}{(2\pi)^4} \frac{l^0}{l^0 - i\epsilon} \frac{\varepsilon_{lms} (l_m l_s - q_m q_s x(1-x))}{[l^2 - \vec{q}^2 x(1-x) - m_\pi^2 + i\epsilon]^2} \end{aligned} \quad (5.6)$$

Both $l_m l_s$ and $q_m q_s$ are symmetric under exchange of m, s , while ε_{lms} is anti-symmetric and thus:

$$\boxed{V_{\text{tr}}^{\text{eff}}(P\bar{P}^* \rightarrow P\bar{P}) = 0} \quad (5.7)$$

$\mathbf{P}^* \bar{\mathbf{P}} \rightarrow \mathbf{P}^* \bar{\mathbf{P}}$



$$\begin{aligned} &= i \left(-\frac{g}{2f_\pi} m_B \right) \left(i \frac{g}{2f_\pi} m_B \right) \left(\frac{1}{4f_\pi^2} m_B \right) \int \frac{d^4 l}{(2\pi)^4} \frac{i}{(l+q)^2 - m_\pi^2 + i\epsilon} \\ &\quad \times \delta_{ik} (2l^0 + q^0) \varepsilon_{cdh} (\tau_1)_h \frac{i}{l^2 - m_\pi^2 + i\epsilon} (\tau_2)_d (-\varepsilon_{mns} l_s) m_B^{-1} \frac{i}{-2l^0 + i\epsilon} (\tau_2)_c (l+q)_m \end{aligned}$$

Using $q^0 = 0$:

$$= -i \frac{g^2 m_B^2}{16 f_\pi^4} (\tau_1)_h (\tau_2)_d (\tau_2)_c \varepsilon_{cdh} \delta_{ik} \int \frac{d^4 l}{(2\pi)^4} \frac{l^0}{l^0 - i\epsilon} \frac{\varepsilon_{mns} (l+q)_m l_s}{[(l+q)^2 - m_\pi^2 + i\epsilon][l^2 - m_\pi^2 + i\epsilon]}$$

Applying eq. (A.1):

$$= -\frac{g^2 m_B^2}{8f_\pi^4} (\vec{\tau}_1 \cdot \vec{\tau}_2) \delta_{ik} \int \frac{d^4 l}{(2\pi)^4} \frac{l^0}{l^0 - i\epsilon} \frac{\varepsilon_{mns}(l+q)_m l_s}{[(l+q)^2 - m_\pi^2 + i\epsilon][l^2 - m_\pi^2 + i\epsilon]}$$

This integral vanishes due to symmetry as well (cf. eq. (5.6)).

$$\boxed{V_{\text{tr}}^{\text{eff}}(P^* \bar{P} \rightarrow P^* \bar{P}^*) = 0} \quad (5.8)$$

5.1.2 The football diagrams

The football diagrams consist solely out of 4-vertices. Since the Feynman rules in eq. (2.26) and (2.27) only differ by their polarization vectors, we can write down the $P\bar{P} \rightarrow P\bar{P}$ scattering explicitly and adjust for the other two possibilities.

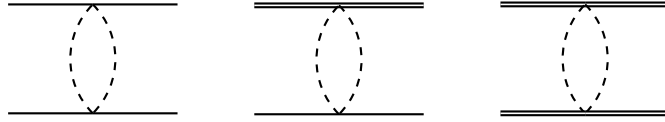
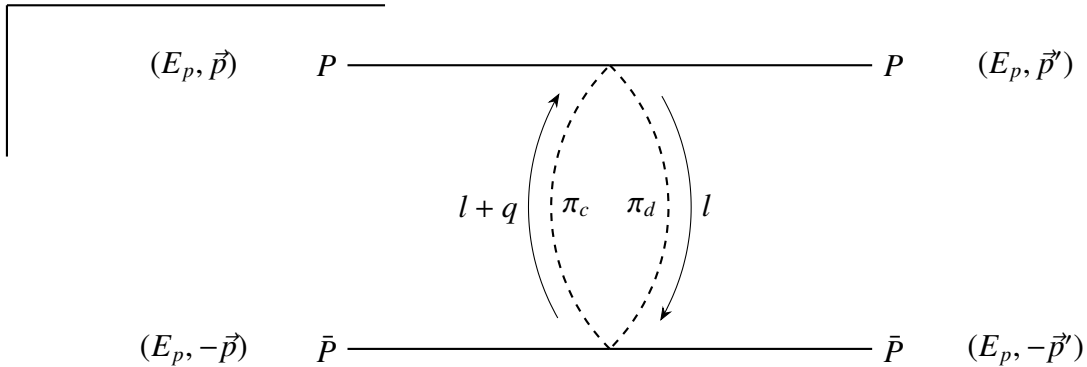


Fig. 5.6: Football-like diagrams



$$= i \frac{1}{2} \left(\frac{1}{4f_\pi^2} m_B \right)^2 \int \frac{d^4 l}{(2\pi)^4} (2l^0 + q^0) \varepsilon_{cde} (\tau_1)_e \frac{i}{(l+q)^2 - m_\pi^2 + i\epsilon} \frac{i}{l^2 - m_\pi^2 + i\epsilon} \\ \times \left(-(2l^0 + q^0) \right) \varepsilon_{cdf} (\tau_2)_f,$$

where we put in a combinatoric factor of 1/2 due to the symmetry of the loop. Using $q^0 = 0$ and $\varepsilon_{cde} \varepsilon_{cdf} = 2\delta_{ef}$ gives:

$$= i \frac{m_B^2}{4f_\pi^4} (\vec{\tau}_1 \cdot \vec{\tau}_2) \underbrace{\int \frac{d^4 l}{(2\pi)^4} \frac{(l^0)^2}{[(l+q)^2 - m_\pi^2 + i\epsilon][l^2 - m_\pi^2 + i\epsilon]}}_{=\mathcal{I}_{\text{fb}}}$$

Again, we abbreviated the integral with \mathcal{I}_{fb} . Its result is presented in sec. B.2. Therefore, the calculation of the football diagram for $P\bar{P} \rightarrow P\bar{P}$ scattering yields:

$$V_{\text{fb}}^{\text{eff}}(P\bar{P}) = i \frac{m_B^2}{4f_\pi^4} (\vec{\tau}_1 \cdot \vec{\tau}_2) \mathcal{I}_{\text{fb}} \quad (5.9)$$

Proceeding analogously for $P^*\bar{P} \rightarrow P^*\bar{P}$ and $P^*\bar{P}^* \rightarrow P^*\bar{P}^*$ scattering reads:

$$V_{\text{fb}}^{\text{eff}}(P^*\bar{P}) = i \frac{m_B^2}{4f_\pi^4} (\vec{\tau}_1 \cdot \vec{\tau}_2) \delta_{ik} \mathcal{I}_{\text{fb}} \quad (5.10)$$

$$V_{\text{fb}}^{\text{eff}}(P^*\bar{P}^*) = i \frac{m_B^2}{4f_\pi^4} (\vec{\tau}_1 \cdot \vec{\tau}_2) \delta_{ik} \delta_{ln} \mathcal{I}_{\text{fb}} \quad (5.11)$$

5.1.3 The box diagrams

The box diagrams consist exclusively out of 3-vertices, which either form a planar or a crossed box. In the planar box, only the irreducible part and not an iterated 1PE is part of the effective potential. When applying the residue theorem to the various integrals, we will see that the planar box splits: the first part can be identified as the iterated 1PE, the second one matches the crossed box integral (cf. sec. B.3). This is explicitly shown for $P\bar{P} \rightarrow P\bar{P}$ scattering but works identically for the other cases.



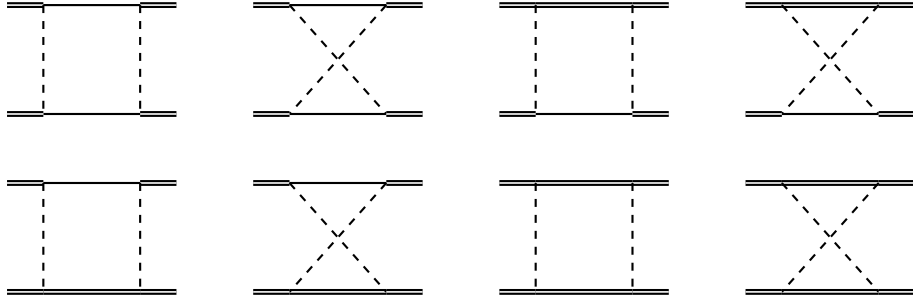
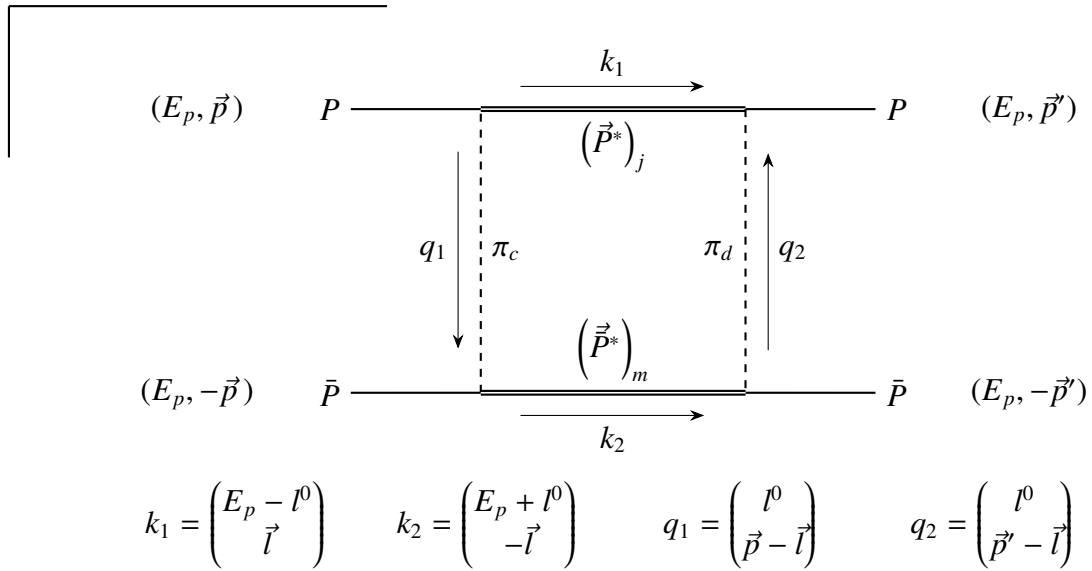
Fig. 5.7: Box-like diagrams for $P\bar{P} \rightarrow P\bar{P}$



Fig. 5.8: Box-like diagrams for $P^*\bar{P} \rightarrow P^*\bar{P}$



Fig. 5.9: Box-like diagrams for $P^*\bar{P} \rightarrow P^*\bar{P}^*$

Fig. 5.10: Box-like diagrams for $P^*\bar{P}^* \rightarrow P^*\bar{P}^*$ Fig. 5.11: Box-like diagrams for $P\bar{P} \rightarrow P^*\bar{P}^*$ Fig. 5.12: Box-like diagrams for $P\bar{P}^* \rightarrow P\bar{P}$ Fig. 5.13: Box-like diagrams for $P^*\bar{P} \rightarrow P^*\bar{P}^*$ **$P\bar{P} \rightarrow P\bar{P}$** 

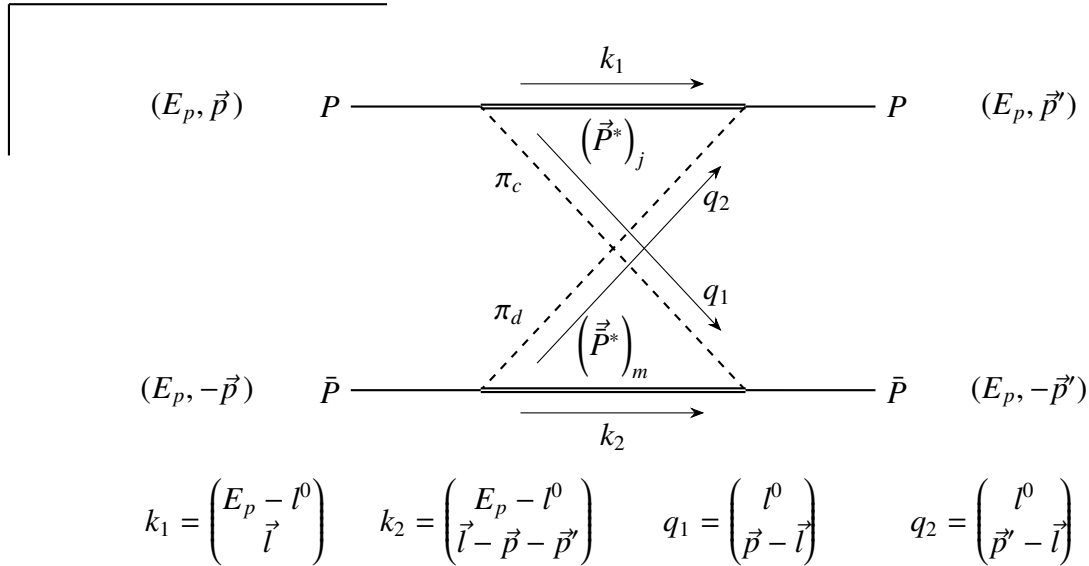
$$\begin{aligned}
&= i \left(-\frac{g}{2f_\pi} m_B \right)^4 \int \frac{d^4 l}{(2\pi)^4} (\tau_1)_d (-q_2)_j m_B^{-1} \frac{i}{-2l^0 + i\epsilon} (\tau_1)_c (q_1)_j \frac{i}{q_2^2 - m_\pi^2 + i\epsilon} \\
&\quad \times \frac{i}{q_1^2 - m_\pi^2 + i\epsilon} (\tau_2)_d (q_2)_m m_B^{-1} \frac{i}{2l^0 + i\epsilon} (\tau_2)_c (-q_1)_m \\
&= -i \frac{g^4 m_B^2}{64 f_\pi^4} (\tau_1)_d (\tau_1)_c (\tau_2)_d (\tau_2)_c \underbrace{\int \frac{d^4 l}{(2\pi)^4} \frac{(\vec{q}_2 \cdot \vec{q}_1)^2}{[l^0 + i\epsilon][l^0 - i\epsilon][q_2^2 - m_\pi^2 + i\epsilon][q_1^2 - m_\pi^2 + i\epsilon]}}_{=I_{\text{box}}^1}
\end{aligned}$$

Abbreviating the integral and using eq. (A.2): $(\tau_1)_d (\tau_1)_c (\tau_2)_d (\tau_2)_c = 3 - 2(\vec{\tau}_1 \cdot \vec{\tau}_2)$ gives:

$$= -i \frac{m_B^2}{64 f_\pi^4} (3 - 2(\vec{\tau}_1 \cdot \vec{\tau}_2)) g^4 I_{\text{box}}^1,$$

where we calculate I_{box}^1 in sec. B.3.

Turning towards the crossed box we obtain:



$$\begin{aligned}
&= i \left(-\frac{g}{2f_\pi} m_B \right)^4 \int \frac{d^4 l}{(2\pi)^4} (\tau_1)_d (-q_2)_j m_B^{-1} \frac{i}{-2l^0 + i\epsilon} (\tau_1)_c (q_1)_j \frac{i}{q_2^2 - m_\pi^2 + i\epsilon} \\
&\quad \times \frac{i}{q_1^2 - m_\pi^2 + i\epsilon} (\tau_2)_c (-q_1)_m m_B^{-1} \frac{i}{-2l^0 + i\epsilon} (\tau_2)_d (q_2)_m
\end{aligned}$$

Using eq. (A.3): $(\tau_1)_d (\tau_1)_c (\tau_2)_c (\tau_2)_d = 3 + 2(\vec{\tau}_1 \cdot \vec{\tau}_2)$ and abbreviating the integral gives:

$$= i \frac{g^4 m_B^2}{64 f_\pi^4} (\tau_1)_d (\tau_1)_c (\tau_2)_c (\tau_2)_d \underbrace{\int \frac{d^4 l}{(2\pi)^4} \frac{(\vec{q}_2 \cdot \vec{q}_1)^2}{[l^0 - i\epsilon]^2 [q_2^2 - m_\pi^2 + i\epsilon][q_1^2 - m_\pi^2 + i\epsilon]}}_{=I_{\text{box}}^2}$$

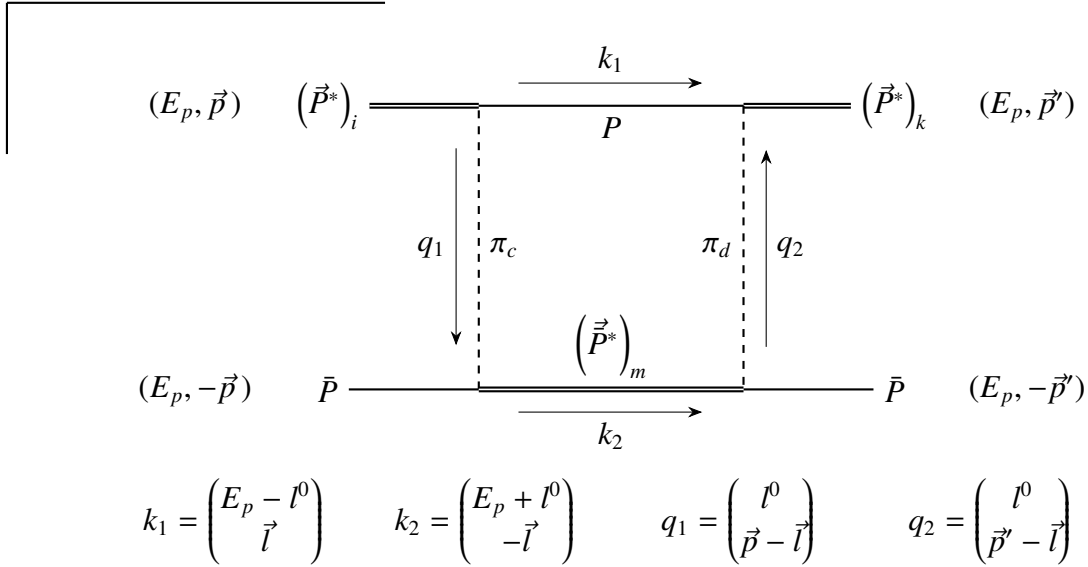
$$= i \frac{m_B^2}{64 f_\pi^4} (3 + 2(\vec{\tau}_1 \cdot \vec{\tau}_2)) g^4 \mathcal{I}_{\text{box}}^2$$

In sec. B.3, we show that the integrals $\mathcal{I}_{\text{box}}^1$ and $\mathcal{I}_{\text{box}}^2$ are not identical, but their irreducible contributions are. Since we are only interested in the irreducible part, which the crossed box exclusively is, we set $\mathcal{I}_{\text{box}}^1 \rightarrow \mathcal{I}_{\text{box}}^2$:

$$V_{\text{box}}^{\text{eff}}(P\bar{P} \rightarrow P\bar{P}) = i \frac{m_B^2}{16 f_\pi^4} (\vec{\tau}_1 \cdot \vec{\tau}_2) g^4 \mathcal{I}_{\text{box}}^2 \quad (5.12)$$

The diagrams in the scattering of $P^*\bar{P} \rightarrow P^*\bar{P}$ and $P^*\bar{P}^* \rightarrow P^*\bar{P}^*$ are similar to the ones in $P\bar{P} \rightarrow P\bar{P}$ and therefore often kept short.

$P^*\bar{P} \rightarrow P^*\bar{P}$

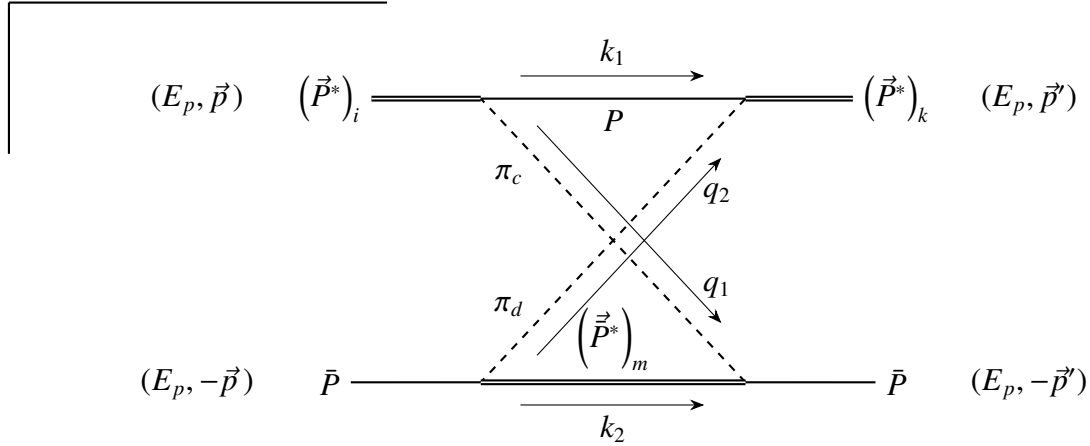


$$= i \left(-\frac{g}{2f_\pi} m_B \right)^4 \int \frac{d^4 l}{(2\pi)^4} (\tau_1)_d (-q_2)_k m_B^{-1} \frac{i}{-2l^0 + i\epsilon} (\tau_1)_c (q_1)_i \frac{i}{q_2^2 - m_\pi^2 + i\epsilon} \\ \times \frac{i}{q_1^2 - m_\pi^2 + i\epsilon} (\tau_2)_d (q_2)_m m_B^{-1} \frac{i}{2l^0 + i\epsilon} (\tau_2)_c (-q_1)_m$$

Applying eq. (A.2):

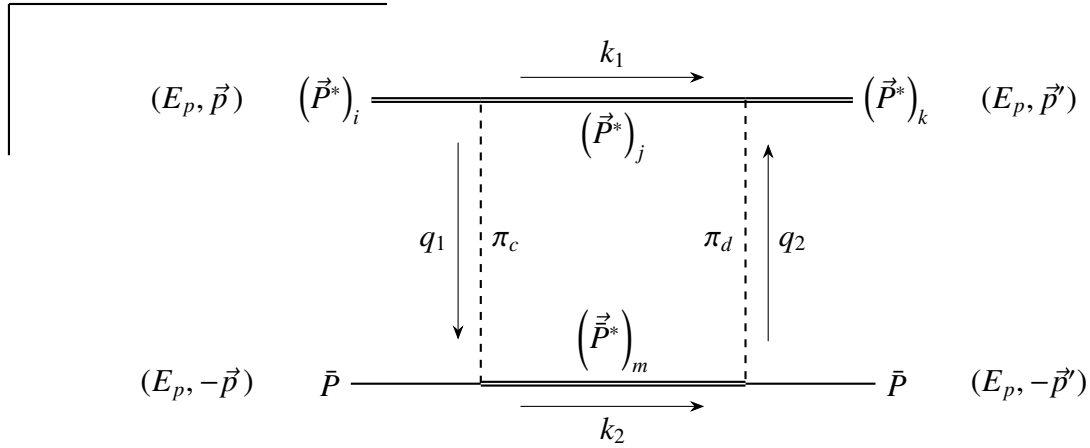
$$= -i \frac{g^4 m_B^2}{64 f_\pi^4} (3 - 2(\vec{\tau}_1 \cdot \vec{\tau}_2)) \int \frac{d^4 l}{(2\pi)^4} \frac{(q_2)_k (q_1)_i (\vec{q}_2 \cdot \vec{q}_1)}{[l^0 + i\epsilon][l^0 - i\epsilon][q_2^2 - m_\pi^2 + i\epsilon][q_1^2 - m_\pi^2 + i\epsilon]}$$

The integral of the crossed box changes correspondingly:



$$k_1 = \begin{pmatrix} E_p - l^0 \\ \vec{l} \end{pmatrix} \quad k_2 = \begin{pmatrix} E_p - l^0 \\ \vec{l} - \vec{p} - \vec{p}' \end{pmatrix} \quad q_1 = \begin{pmatrix} l^0 \\ \vec{p} - \vec{l} \end{pmatrix} \quad q_2 = \begin{pmatrix} l^0 \\ \vec{p}' - \vec{l} \end{pmatrix}$$

$$= i \frac{g^4 m_B^2}{64 f_\pi^4} (3 + 2(\vec{\tau}_1 \cdot \vec{\tau}_2)) \int \frac{d^4 l}{(2\pi)^4} \frac{(q_2)_k (q_1)_i (\vec{q}_2 \cdot \vec{q}_1)}{[l^0 - i\epsilon]^2 [q_2^2 - m_\pi^2 + i\epsilon] [q_1^2 - m_\pi^2 + i\epsilon]}$$



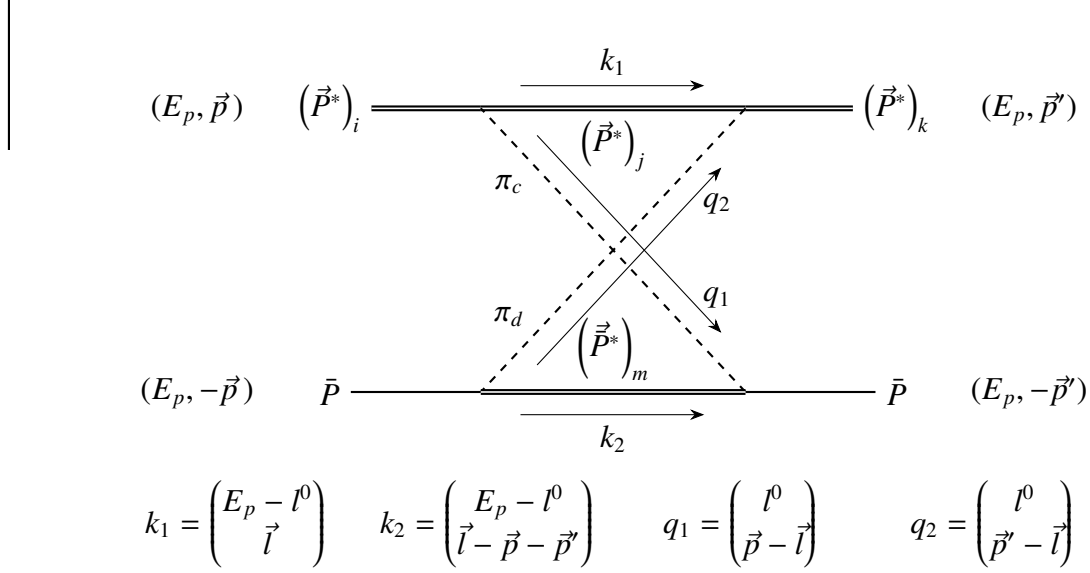
$$k_1 = \begin{pmatrix} E_p - l^0 \\ \vec{l} \end{pmatrix} \quad k_2 = \begin{pmatrix} E_p + l^0 \\ -\vec{l} \end{pmatrix} \quad q_1 = \begin{pmatrix} l^0 \\ \vec{p} - \vec{l} \end{pmatrix} \quad q_2 = \begin{pmatrix} l^0 \\ \vec{p}' - \vec{l} \end{pmatrix}$$

$$\begin{aligned} &= i \left(-\frac{g}{2f_\pi} m_B \right)^2 \left(-i \frac{g}{2f_\pi} m_B \right)^2 \int \frac{d^4 l}{(2\pi)^4} \varepsilon_{jkr} (-q_2)_r (\tau_1)_d m_B^{-1} \frac{i}{-2l^0 + i\epsilon} \varepsilon_{ijs} (q_1)_s (\tau_1)_c \\ &\quad \times \frac{i}{q_2^2 - m_\pi^2 + i\epsilon} \frac{i}{q_1^2 - m_\pi^2 + i\epsilon} (\tau_2)_d (q_2)_m m_B^{-1} \frac{i}{2l^0 + i\epsilon} (\tau_2)_c (-q_1)_m \\ &= i \frac{g^4 m_B^2}{64 f_\pi^4} (\tau_1)_d (\tau_1)_c (\tau_2)_d (\tau_2)_c \int \frac{d^4 l}{(2\pi)^4} \frac{\varepsilon_{jkr} \varepsilon_{ijs} (q_2)_r (q_1)_s (\vec{q}_2 \cdot \vec{q}_1)}{[l^0 + i\epsilon] [l^0 - i\epsilon] [q_2^2 - m_\pi^2 + i\epsilon] [q_1^2 - m_\pi^2 + i\epsilon]} \end{aligned}$$

Using $\varepsilon_{jkr}\varepsilon_{ijs} = -(\delta_{ki}\delta_{rs} - \delta_{ks}\delta_{ri})$ and eq. (A.2) gives:

$$= -i \frac{g^4 m_B^2}{64 f_\pi^4} (3 - 2(\vec{\tau}_1 \cdot \vec{\tau}_2)) \int \frac{d^4 l}{(2\pi)^4} \frac{\delta_{ik}(\vec{q}_2 \cdot \vec{q}_1)^2 - (q_2)_i (q_1)_k (\vec{q}_2 \cdot \vec{q}_1)}{[l^0 + i\epsilon][l^0 - i\epsilon][q_2^2 - m_\pi^2 + i\epsilon][q_1^2 - m_\pi^2 + i\epsilon]}$$

The corresponding crossed box behaves similarly:

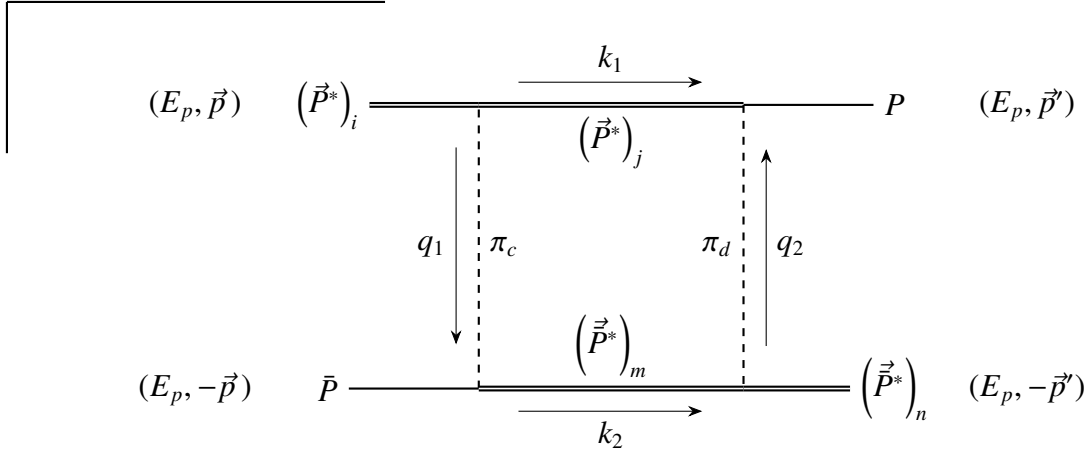


$$= i \frac{g^4 m_B^2}{64 f_\pi^4} (3 + 2(\vec{\tau}_1 \cdot \vec{\tau}_2)) \int \frac{d^4 l}{(2\pi)^4} \frac{\delta_{ik}(\vec{q}_2 \cdot \vec{q}_1)^2 - (q_2)_i (q_1)_k (\vec{q}_2 \cdot \vec{q}_1)}{[l^0 - i\epsilon]^2 [q_2^2 - m_\pi^2 + i\epsilon][q_1^2 - m_\pi^2 + i\epsilon]}$$

Summing up these contributions and using eq. (A.7) yields:

$$V_{\text{box}}^{\text{eff}}(P^* \bar{P} \rightarrow P^* \bar{P}) = i \frac{m_B^2}{16 f_\pi^4} (\vec{\tau}_1 \cdot \vec{\tau}_2) g^4 \delta_{ik} \mathcal{I}_{\text{box}}^2$$

(5.13)

$\mathbf{P}^* \bar{\mathbf{P}} \rightarrow \mathbf{P} \bar{\mathbf{P}}^*$ 

$$k_1 = \begin{pmatrix} E_p - l^0 \\ \vec{l} \end{pmatrix} \quad k_2 = \begin{pmatrix} E_p + l^0 \\ -\vec{l} \end{pmatrix} \quad q_1 = \begin{pmatrix} l^0 \\ \vec{p} - \vec{l} \end{pmatrix} \quad q_2 = \begin{pmatrix} l^0 \\ \vec{p}' - \vec{l} \end{pmatrix}$$

$$\begin{aligned} &= i \left(-\frac{g}{2f_\pi} m_B \right)^2 \left(-i \frac{g}{2f_\pi} m_B \right) \left(i \frac{g}{2f_\pi} m_B \right) \int \frac{d^4 l}{(2\pi)^4} (-q_2)_j (\tau_1)_d m_B^{-1} \frac{i}{-2l^0 + i\epsilon} \varepsilon_{ijs} (q_1)_s (\tau_1)_c \\ &\quad \times \frac{i}{q_2^2 - m_\pi^2 + i\epsilon} \frac{i}{q_1^2 - m_\pi^2 + i\epsilon} (\tau_2)_d \varepsilon_{mnr} (q_2)_r m_B^{-1} \frac{i}{2l^0 + i\epsilon} (\tau_2)_c (-q_1)_m \\ &= -i \frac{g^4 m_B^2}{64 f_\pi^4} (\tau_1)_d (\tau_1)_c (\tau_2)_d (\tau_2)_c \int \frac{d^4 l}{(2\pi)^4} \frac{\varepsilon_{ijs} \varepsilon_{mnr} (q_2)_r (q_1)_s (q_2)_j (q_1)_m}{[l^0 + i\epsilon][l^0 - i\epsilon][q_2^2 - m_\pi^2 + i\epsilon][q_1^2 - m_\pi^2 + i\epsilon]} \end{aligned}$$

Using eq. (A.2) gives:

$$= -i \frac{g^4 m_B^2}{64 f_\pi^4} (3 - 2(\vec{\tau}_1 \cdot \vec{\tau}_2)) \underbrace{\int \frac{d^4 l}{(2\pi)^4} \frac{\varepsilon_{ijs} \varepsilon_{nrm} (q_2)_j (q_1)_s (q_2)_r (q_1)_m}{[l^0 + i\epsilon][l^0 - i\epsilon][q_2^2 - m_\pi^2 + i\epsilon][q_1^2 - m_\pi^2 + i\epsilon]}}_{\rightarrow (\mathcal{I}_{\text{box}}^3)_{in}}$$

The expression underneath the curly brace denotes the omission of all reducible parts. Hence, we are allowed to directly use $\mathcal{I}_{\text{box}}^3$.

Turning towards the crossed box gives:

$$k_1 = \begin{pmatrix} E_p - l^0 \\ \vec{l} \end{pmatrix} \quad k_2 = \begin{pmatrix} E_p - l^0 \\ \vec{l} - \vec{p} - \vec{p}' \end{pmatrix} \quad q_1 = \begin{pmatrix} l^0 \\ \vec{p} - \vec{l} \end{pmatrix} \quad q_2 = \begin{pmatrix} l^0 \\ \vec{p}' - \vec{l} \end{pmatrix}$$

$$\begin{aligned}
&= i \left(-\frac{g}{2f_\pi} m_B \right)^2 \left(-i \frac{g}{2f_\pi} m_B \right) \left(i \frac{g}{2f_\pi} m_B \right) \int \frac{d^4 l}{(2\pi)^4} (-q_2)_j (\tau_1)_d m_B^{-1} \frac{i}{-2l^0 + i\epsilon} \varepsilon_{ijs} (q_1)_s (\tau_1)_c \\
&\quad \times \frac{i}{q_2^2 - m_\pi^2 + i\epsilon} \frac{i}{q_1^2 - m_\pi^2 + i\epsilon} (\tau_2)_c \varepsilon_{mnr} (-q_1)_r m_B^{-1} \frac{i}{-2l^0 + i\epsilon} (\tau_2)_d (q_2)_m \\
&= i \frac{g^4 m_B^2}{64 f_\pi^4} (\tau_1)_d (\tau_1)_c (\tau_2)_c (\tau_2)_d \int \frac{d^4 l}{(2\pi)^4} \frac{\varepsilon_{ijs} \varepsilon_{mnr} (q_1)_r (q_1)_s (q_2)_j (q_2)_m}{[l^0 - i\epsilon]^2 [q_2^2 - m_\pi^2 + i\epsilon] [q_1^2 - m_\pi^2 + i\epsilon]}
\end{aligned}$$

Using eq. (A.3) and relabeling $r \leftrightarrow m$:

$$= -i \frac{g^4 m_B^2}{64 f_\pi^4} (3 + 2(\vec{\tau}_1 \cdot \vec{\tau}_2)) \underbrace{\int \frac{d^4 l}{(2\pi)^4} \frac{\varepsilon_{ijs} \varepsilon_{nrm} (q_2)_j (q_1)_s (q_2)_r (q_1)_m}{[l^0 - i\epsilon]^2 [q_2^2 - m_\pi^2 + i\epsilon] [q_1^2 - m_\pi^2 + i\epsilon]}}_{= (\mathcal{I}_{\text{box}}^3)_{in}}$$

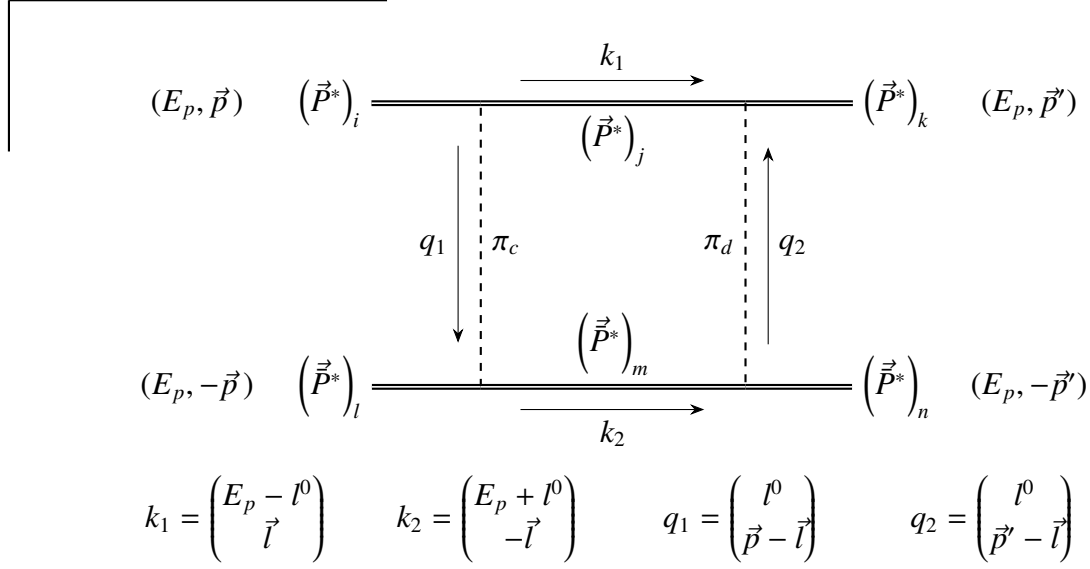
Together, we obtain:

$$V_{\text{box}}^{\text{eff}}(P^* \bar{P} \rightarrow P \bar{P}^*) = -i \frac{3m_B^2}{32f_\pi^4} g^4 (\mathcal{I}_{\text{box}}^3)_{in}$$

(5.14)

$P^* \bar{P}^* \rightarrow P^* \bar{P}^*$

For $P^* \bar{P}^* \rightarrow P^* \bar{P}^*$ scattering, we obtain eight diagrams of which the first six are similar to the ones presented in the scattering of $P \bar{P} \rightarrow P \bar{P}$ and $P^* \bar{P} \rightarrow P^* \bar{P}$. For the sake of brevity, their pictographic representations are omitted. Instead, we immediately consider the last two. Adding up all integrals of the eight contributions in eq. (5.15) allows again some cancellation as described in eq. (5.3).

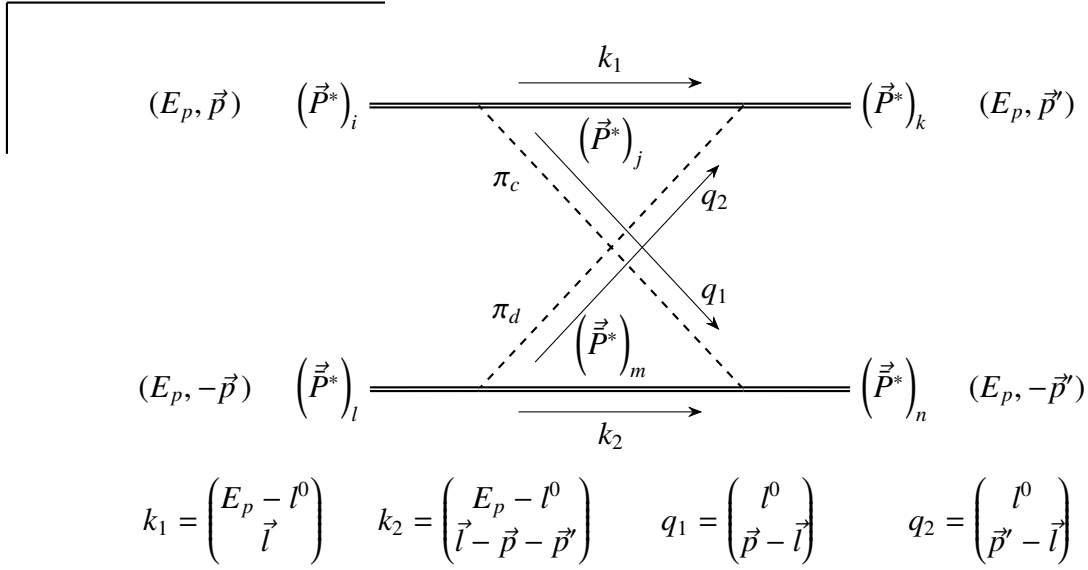


$$\begin{aligned}
&= i \left(-i \frac{g}{2f_\pi} m_B \right)^2 \left(i \frac{g}{2f_\pi} m_B \right)^2 \int \frac{d^4 l}{(2\pi)^4} \varepsilon_{jkr} (-q_2)_r (\tau_1)_d m_B^{-1} \frac{i}{-2l^0 + i\epsilon} \varepsilon_{ijs} (q_1)_s (\tau_1)_c \\
&\quad \times \frac{i}{q_2^2 - m_\pi^2 + i\epsilon} \frac{i}{q_1^2 - m_\pi^2 + i\epsilon} \varepsilon_{mnt} (q_2)_t (\tau_2)_d m_B^{-1} \frac{i}{2l^0 + i\epsilon} \varepsilon_{lmn} (-q_1)_u (\tau_2)_c \\
&= -i \frac{g^4 m_B^2}{64 f_\pi^4} (\tau_1)_d (\tau_1)_c (\tau_2)_d (\tau_2)_c \varepsilon_{jkr} \varepsilon_{ijs} \varepsilon_{mnt} \varepsilon_{lmn} \\
&\quad \times \int \frac{d^4 l}{(2\pi)^4} \frac{(q_2)_r (q_1)_s (q_2)_t (q_1)_u}{[l^0 + i\epsilon][l^0 - i\epsilon][q_2^2 - m_\pi^2 + i\epsilon][q_1^2 - m_\pi^2 + i\epsilon]}
\end{aligned}$$

Using eq. (A.2) and simplifying:

$$= -i \frac{g^4 m_B^2}{64 f_\pi^4} \left(3 - 2(\vec{\tau}_1 \cdot \vec{\tau}_2) \right) \int \frac{d^4 l}{(2\pi)^4} \frac{(\delta_{ik} \vec{q}_2 \cdot \vec{q}_1 - (q_2)_i (q_1)_k) (\delta_{ln} \vec{q}_2 \cdot \vec{q}_1 - (q_2)_l (q_1)_n)}{[l^0 + i\epsilon][l^0 - i\epsilon][q_2^2 - m_\pi^2 + i\epsilon][q_1^2 - m_\pi^2 + i\epsilon]}$$

Analogously, the crossed box reads:



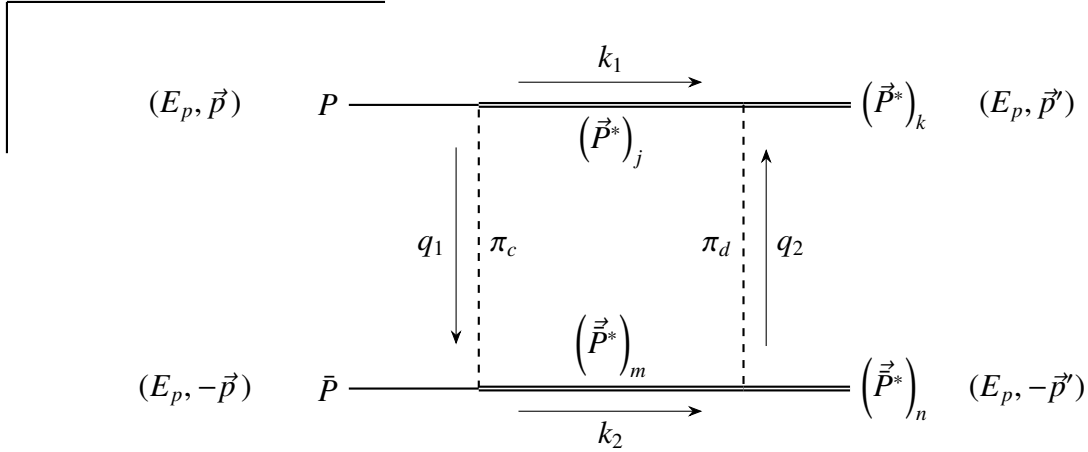
$$= i \frac{g^4 m_B^2}{64 f_\pi^4} (3 + 2(\vec{\tau}_1 \cdot \vec{\tau}_2)) \int \frac{d^4 l}{(2\pi)^4} \frac{(\delta_{ik} \vec{q}_2 \cdot \vec{q}_1 - (q_2)_i (q_1)_k) (\delta_{ln} \vec{q}_2 \cdot \vec{q}_1 - (q_2)_l (q_1)_n)}{[l^0 - i\epsilon]^2 [q_2^2 - m_\pi^2 + i\epsilon] [q_1^2 - m_\pi^2 + i\epsilon]}$$

Adding up all eight integrals and using eq. (A.7):

$$\begin{aligned} & \int \frac{d^4 l}{(2\pi)^4} \left(\frac{(\delta_{ik} \vec{q}_2 \cdot \vec{q}_1 - (q_2)_i (q_1)_k) (\delta_{ln} \vec{q}_2 \cdot \vec{q}_1 - (q_2)_l (q_1)_n)}{[l^0 - i\epsilon]^2 [q_2^2 - m_\pi^2 + i\epsilon] [q_1^2 - m_\pi^2 + i\epsilon]} + \frac{(q_2)_k (q_1)_i (q_2)_n (q_1)_l}{[l^0 - i\epsilon]^2 [q_2^2 - m_\pi^2 + i\epsilon] [q_1^2 - m_\pi^2 + i\epsilon]} \right. \\ & \quad \left. + \frac{\delta_{ik} (\vec{q}_2 \cdot \vec{q}_1) (q_2)_n (q_1)_l - (q_2)_i (q_1)_k (q_2)_n (q_1)_l}{[l^0 - i\epsilon]^2 [q_2^2 - m_\pi^2 + i\epsilon] [q_1^2 - m_\pi^2 + i\epsilon]} + \frac{\delta_{ln} (\vec{q}_2 \cdot \vec{q}_1) (q_2)_k (q_1)_i - (q_2)_l (q_1)_n (q_2)_k (q_1)_i}{[l^0 - i\epsilon]^2 [q_2^2 - m_\pi^2 + i\epsilon] [q_1^2 - m_\pi^2 + i\epsilon]} \right) \\ & = \delta_{ik} \delta_{ln} \int \frac{d^4 l}{(2\pi)^4} \frac{(\vec{q}_2 \cdot \vec{q}_1)^2}{[l^0 - i\epsilon]^2 [q_2^2 - m_\pi^2 + i\epsilon] [q_1^2 - m_\pi^2 + i\epsilon]} = \delta_{ik} \delta_{ln} \mathcal{I}_{\text{box}}^2 \end{aligned} \quad (5.15)$$

Summing up all these contributions yields:

$$V_{\text{box}}^{\text{eff}}(P^* \bar{P}^* \rightarrow P^* \bar{P}^*) = i \frac{m_B^2}{16 f_\pi^4} (\vec{\tau}_1 \cdot \vec{\tau}_2) g^4 \delta_{ik} \delta_{ln} \mathcal{I}_{\text{box}}^2 \quad (5.16)$$

$\mathbf{P}\bar{\mathbf{P}} \rightarrow \mathbf{P}^*\bar{\mathbf{P}}^*$ 

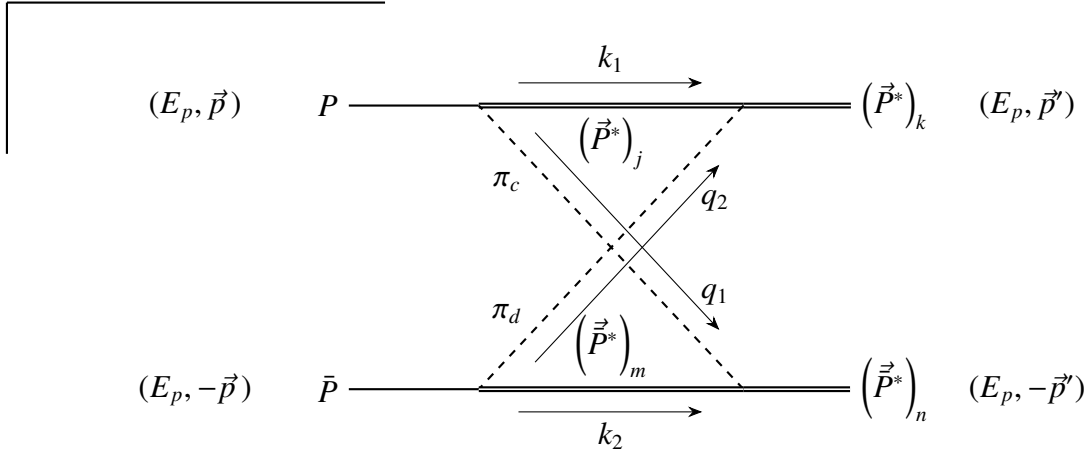
$$k_1 = \begin{pmatrix} E_p - l^0 \\ \vec{l} \end{pmatrix} \quad k_2 = \begin{pmatrix} E_p + l^0 \\ -\vec{l} \end{pmatrix} \quad q_1 = \begin{pmatrix} l^0 \\ \vec{p} - \vec{l} \end{pmatrix} \quad q_2 = \begin{pmatrix} l^0 \\ \vec{p}' - \vec{l} \end{pmatrix}$$

$$\begin{aligned} &= i \left(-\frac{g}{2f_\pi} m_B \right)^2 \left(-i \frac{g}{2f_\pi} m_B \right) \left(i \frac{g}{2f_\pi} m_B \right) \int \frac{d^4 l}{(2\pi)^4} \varepsilon_{jks} (-q_2)_s (\tau_1)_d m_B^{-1} \frac{i}{-2l^0 + i\epsilon} \\ &\quad \times (q_1)_j (\tau_1)_c \frac{i}{q_2^2 - m_\pi^2 + i\epsilon} \frac{i}{q_1^2 - m_\pi^2 + i\epsilon} (\tau_2)_d \varepsilon_{mnr} (q_2)_r m_B^{-1} \frac{i}{2l^0 + i\epsilon} (\tau_2)_c (-q_1)_m \\ &= -i \frac{g^4 m_B^2}{64 f_\pi^4} (\tau_1)_d (\tau_1)_c (\tau_2)_d (\tau_2)_c \\ &\quad \times \int \frac{d^4 l}{(2\pi)^4} \frac{\varepsilon_{jks} \varepsilon_{mnr} (q_2)_s (q_1)_j (q_2)_r (q_1)_m}{[l^0 + i\epsilon][l^0 - i\epsilon][q_2^2 - m_\pi^2 + i\epsilon][q_1^2 - m_\pi^2 + i\epsilon]} \end{aligned}$$

Using eq. (A.2) gives:

$$= -i \frac{g^4 m_B^2}{64 f_\pi^4} (3 - 2(\vec{\tau}_1 \cdot \vec{\tau}_2)) \underbrace{\int \frac{d^4 l}{(2\pi)^4} \frac{\varepsilon_{ksj} \varepsilon_{nrm} (q_2)_s (q_1)_j (q_2)_r (q_1)_m}{[l^0 + i\epsilon][l^0 - i\epsilon][q_2^2 - m_\pi^2 + i\epsilon][q_1^2 - m_\pi^2 + i\epsilon]}}_{\rightarrow (I_{\text{box}}^3)_{kn}}$$

The crossed box gives:



$$k_1 = \begin{pmatrix} E_p - l^0 \\ \vec{l} \end{pmatrix} \quad k_2 = \begin{pmatrix} E_p - l^0 \\ \vec{l} - \vec{p} - \vec{p}' \end{pmatrix} \quad q_1 = \begin{pmatrix} l^0 \\ \vec{p} - \vec{l} \end{pmatrix} \quad q_2 = \begin{pmatrix} l^0 \\ \vec{p}' - \vec{l} \end{pmatrix}$$

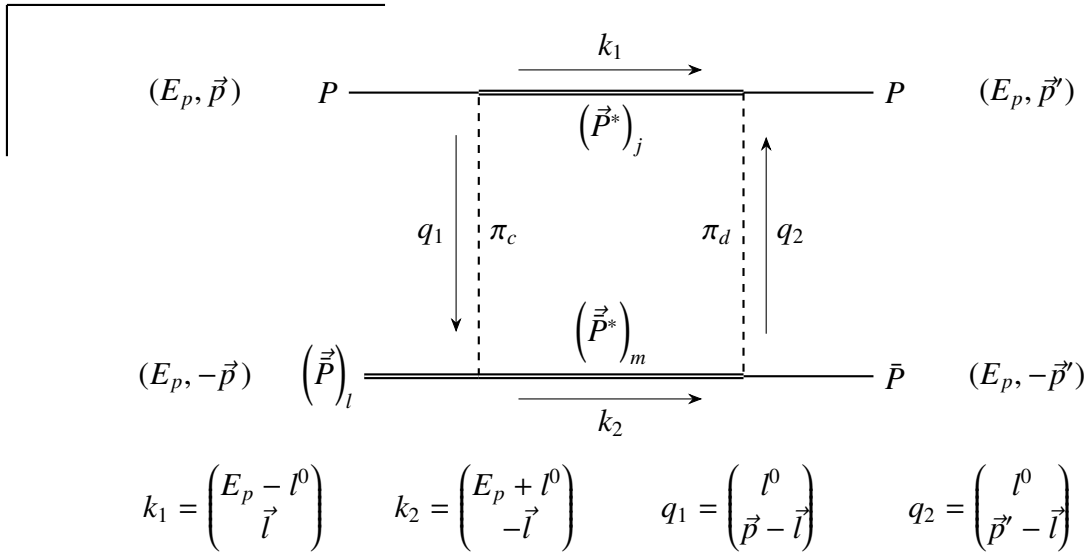
$$\begin{aligned} &= i \left(-\frac{g}{2f_\pi} m_B \right)^2 \left(-i \frac{g}{2f_\pi} m_B \right) \left(i \frac{g}{2f_\pi} m_B \right) \int \frac{d^4 l}{(2\pi)^4} \varepsilon_{jks} (-q_2)_s (\tau_1)_d m_B^{-1} \frac{i}{-2l^0 + i\epsilon} \\ &\quad \times (q_1)_j (\tau_1)_c \frac{i}{q_2^2 - m_\pi^2 + i\epsilon} \frac{i}{q_1^2 - m_\pi^2 + i\epsilon} (\tau_2)_c \varepsilon_{mnr} (-q_1)_r m_B^{-1} \frac{i}{-2l^0 + i\epsilon} (\tau_2)_d (q_2)_m \\ &= i \frac{g^4 m_B^2}{64 f_\pi^4} (\tau_1)_d (\tau_1)_c (\tau_2)_c (\tau_2)_d \int \frac{d^4 l}{(2\pi)^4} \frac{\varepsilon_{jks} \varepsilon_{mnr} (q_2)_s (q_1)_j (q_2)_m (q_1)_r}{[l^0 - i\epsilon]^2 [q_2^2 - m_\pi^2 + i\epsilon] [q_1^2 - m_\pi^2 + i\epsilon]} \end{aligned}$$

Using eq. (A.3):

$$= -i \frac{g^4 m_B^2}{64 f_\pi^4} (3 + 2(\vec{\tau}_1 \cdot \vec{\tau}_2)) \underbrace{\int \frac{d^4 l}{(2\pi)^4} \frac{\varepsilon_{ksj} \varepsilon_{nmr} (q_2)_s (q_1)_j (q_2)_m (q_1)_r}{[l^0 - i\epsilon]^2 [q_2^2 - m_\pi^2 + i\epsilon] [q_1^2 - m_\pi^2 + i\epsilon]}}_{=(I_{\text{box}}^3)_{kn}}$$

Adding both contributions gives:

$$V_{\text{box}}^{\text{eff}}(P\bar{P} \rightarrow P^* \bar{P}^*) = -i \frac{3m_B^2}{32f_\pi^4} g^4 (I_{\text{box}}^3)_{kn} \quad (5.17)$$

$\mathbf{P}\bar{\mathbf{P}}^* \rightarrow \mathbf{P}\bar{\mathbf{P}}$ 

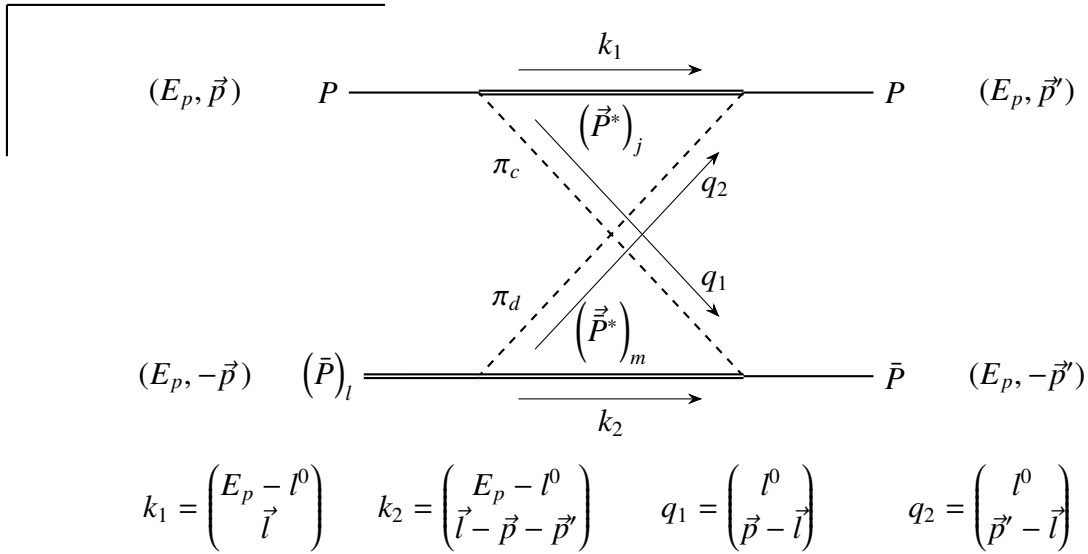
$$= i \left(-\frac{g}{2f_\pi} m_B \right)^3 \left(i \frac{g}{2f_\pi} m_B \right) \int \frac{d^4 l}{(2\pi)^4} (\tau_1)_d (-q_2)_j m_B^{-1} \frac{i}{-2l^0 + i\epsilon} (\tau_1)_c (q_1)_j$$

$$\times \frac{i}{q_2^2 - m_\pi^2 + i\epsilon} \frac{i}{q_1^2 - m_\pi^2 + i\epsilon} (\tau_2)_d (q_2)_m m_B^{-1} \frac{i}{2l^0 + i\epsilon} (\tau_2)_c \varepsilon_{lms} (-q_1)_s$$

Applying the usual steps:

$$= -\frac{g^4 m_B^2}{64 f_\pi^4} (3 - 2(\vec{\tau}_1 \cdot \vec{\tau}_2)) \int \frac{d^4 l}{(2\pi)^4} \frac{(\vec{q}_2 \cdot \vec{q}_1) \varepsilon_{lms} (q_2)_m (q_1)_s}{[l^0 + i\epsilon][l^0 - i\epsilon][q_2^2 - m_\pi^2 + i\epsilon][q_1^2 - m_\pi^2 + i\epsilon]}$$

This integral vanishes due to symmetry which can be seen by following the calculation of $\mathcal{I}_{\text{box}}^2$ in sec. B.3: after completing the square in the denominator all terms odd in l vanish. What remains will be proportional to either $\varepsilon_{lms} l_m l_s$ or $\varepsilon_{lms} q_m q_s$, which both give 0.



$$\begin{aligned}
&= i \left(-\frac{g}{2f_\pi} m_B \right)^3 \left(i \frac{g}{2f_\pi} m_B \right) \int \frac{d^4 l}{(2\pi)^4} (\tau_1)_d (-q_2)_j m_B^{-1} \frac{i}{-2l^0 + i\epsilon} (\tau_1)_c (q_1)_j \\
&\quad \times \frac{i}{q_2^2 - m_\pi^2 + i\epsilon} \frac{i}{q_1^2 - m_\pi^2 + i\epsilon} (\tau_2)_c (-q_1)_m m_B^{-1} \frac{i}{-2l^0 + i\epsilon} (\tau_2)_d \varepsilon_{lms} (q_2)_s
\end{aligned}$$

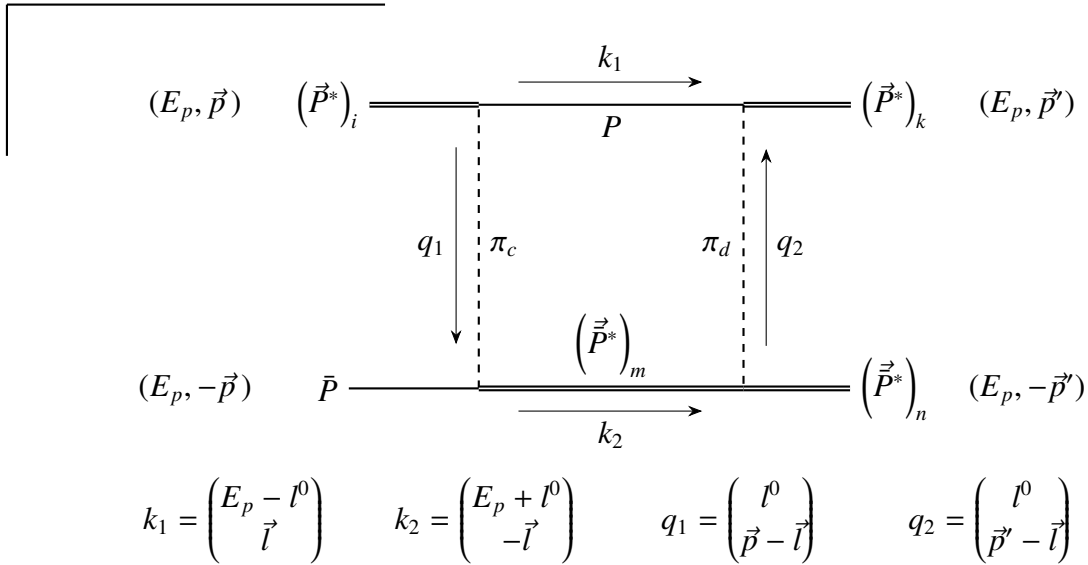
Using eq. (A.3):

$$= -\frac{g^4 m_B^2}{64 f_\pi^4} (3 + 2(\vec{\tau}_1 \cdot \vec{\tau}_2)) \int \frac{d^4 l}{(2\pi)^4} \frac{(\vec{q}_2 \cdot \vec{q}_1) \varepsilon_{lsm} (q_2)_s (q_1)_m}{[l^0 - i\epsilon]^2 [q_2^2 - m_\pi^2 + i\epsilon] [q_1^2 - m_\pi^2 + i\epsilon]}$$

For the same reason as mentioned before, this integral has to vanish. Thus:

$$\boxed{V_{\text{box}}^{\text{eff}}(P\bar{P}^* \rightarrow P\bar{P}) = 0} \quad (5.18)$$

$\mathbf{P}^* \bar{\mathbf{P}} \rightarrow \mathbf{P}^* \bar{\mathbf{P}}^*$

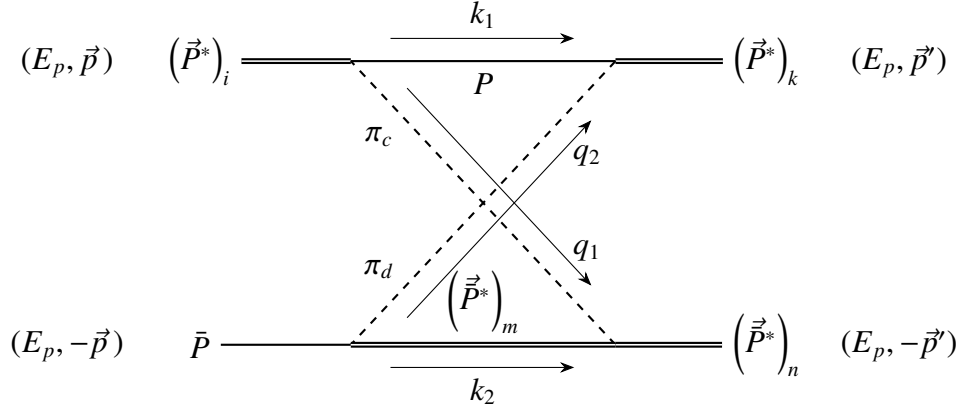


$$\begin{aligned}
&= i \left(-\frac{g}{2f_\pi} m_B \right)^3 \left(i \frac{g}{2f_\pi} m_B \right) \int \frac{d^4 l}{(2\pi)^4} (\tau_1)_d (-q_2)_k m_B^{-1} \frac{i}{-2l^0 + i\epsilon} (\tau_1)_c (q_1)_i \\
&\quad \times \frac{i}{q_2^2 - m_\pi^2 + i\epsilon} \frac{i}{q_1^2 - m_\pi^2 + i\epsilon} (\tau_2)_d \varepsilon_{mnu} (q_2)_u m_B^{-1} \frac{i}{2l^0 + i\epsilon} (\tau_2)_c (-q_1)_m
\end{aligned}$$

Applying eq. (A.2):

$$= -\frac{g^4 m_B^2}{64 f_\pi^4} (3 - 2(\vec{\tau}_1 \cdot \vec{\tau}_2)) \int \frac{d^4 l}{(2\pi)^4} \frac{\varepsilon_{num} (q_2)_u (q_1)_m (q_2)_k (q_1)_i}{[l^0 + i\epsilon][l^0 - i\epsilon][q_2^2 - m_\pi^2 + i\epsilon][q_1^2 - m_\pi^2 + i\epsilon]} \quad (5.19)$$

We keep the integral explicit here for subsequent summation. It will be added to the other planar box before the integral is treated in sec. B.



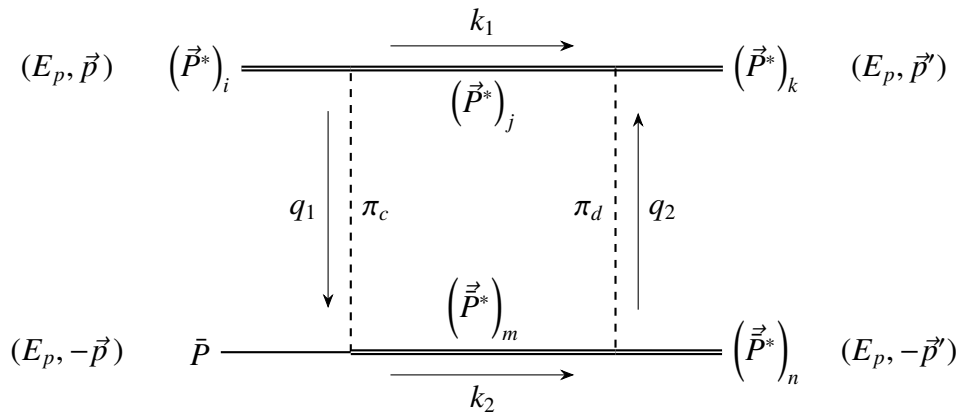
$$k_1 = \begin{pmatrix} E_p - l^0 \\ \vec{l} \end{pmatrix} \quad k_2 = \begin{pmatrix} E_p - l^0 \\ \vec{l} - \vec{p} - \vec{p}' \end{pmatrix} \quad q_1 = \begin{pmatrix} l^0 \\ \vec{p} - \vec{l} \end{pmatrix} \quad q_2 = \begin{pmatrix} l^0 \\ \vec{p}' - \vec{l} \end{pmatrix}$$

$$= i \left(-\frac{g}{2f_\pi} m_B \right)^3 \left(i \frac{g}{2f_\pi} m_B \right) \int \frac{d^4 l}{(2\pi)^4} (\tau_1)_d (-q_2)_k m_B^{-1} \frac{i}{-2l^0 + i\epsilon} (\tau_1)_c (q_1)_i \\ \times \frac{i}{q_2^2 - m_\pi^2 + i\epsilon} \frac{i}{q_1^2 - m_\pi^2 + i\epsilon} (\tau_2)_c \varepsilon_{mnu} (-q_1)_u m_B^{-1} \frac{i}{-2l^0 + i\epsilon} (\tau_2)_d (q_2)_m$$

Applying eq. (A.3):

$$= \frac{g^4 m_B^2}{64 f_\pi^4} (3 + 2(\vec{\tau}_1 \cdot \vec{\tau}_2)) \int \frac{d^4 l}{(2\pi)^4} \frac{\varepsilon_{num}(q_1)_u (q_2)_m (q_2)_k (q_1)_i}{[l^0 - i\epsilon]^2 [q_2^2 - m_\pi^2 + i\epsilon] [q_1^2 - m_\pi^2 + i\epsilon]} \\ = -\frac{g^4 m_B^2}{64 f_\pi^4} (3 + 2(\vec{\tau}_1 \cdot \vec{\tau}_2)) \int \frac{d^4 l}{(2\pi)^4} \frac{\varepsilon_{num}(q_2)_u (q_1)_m (q_2)_k (q_1)_i}{[l^0 - i\epsilon]^2 [q_2^2 - m_\pi^2 + i\epsilon] [q_1^2 - m_\pi^2 + i\epsilon]},$$

where we relabeled u and m in the last step. Again, we keep the integral explicit here for subsequent summation.



$$k_1 = \begin{pmatrix} E_p - l^0 \\ \vec{l} \end{pmatrix} \quad k_2 = \begin{pmatrix} E_p + l^0 \\ -\vec{l} \end{pmatrix} \quad q_1 = \begin{pmatrix} l^0 \\ \vec{p} - \vec{l} \end{pmatrix} \quad q_2 = \begin{pmatrix} l^0 \\ \vec{p}' - \vec{l} \end{pmatrix}$$

$$\begin{aligned}
&= i \left(-i \frac{g}{2f_\pi} m_B \right)^2 \left(i \frac{g}{2f_\pi} m_B \right) \left(-\frac{g}{2f_\pi} m_B \right) \int \frac{d^4 l}{(2\pi)^4} (\tau_1)_d \left(-\varepsilon_{jks}(q_2)_s \right) m_B^{-1} \frac{i}{-2l^0 + i\epsilon} \\
&\quad \times (\tau_1)_c \varepsilon_{ijr}(q_1)_r \frac{i}{q_2^2 - m_\pi^2 + i\epsilon} \frac{i}{q_1^2 - m_\pi^2 + i\epsilon} (\tau_2)_d \varepsilon_{mnu}(q_2)_u m_B^{-1} \frac{i}{2l^0 + i\epsilon} (\tau_2)_c (-(q_1)_m)
\end{aligned}$$

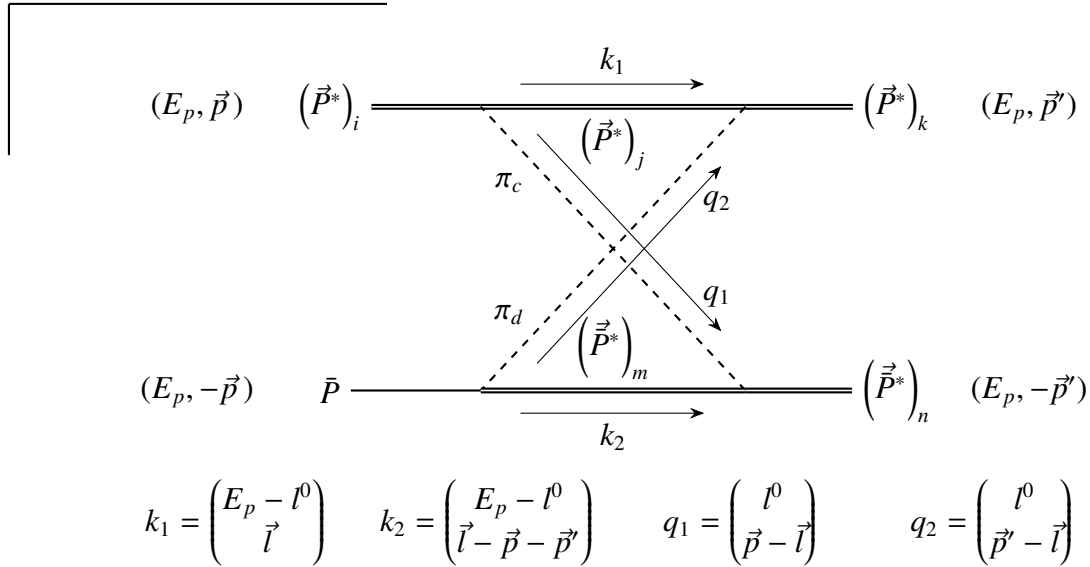
Applying eq. (A.2):

$$\begin{aligned}
&= \frac{g^4 m_B^2}{64 f_\pi^4} (3 - 2(\vec{\tau}_1 \cdot \vec{\tau}_2)) \int \frac{d^4 l}{(2\pi)^4} \frac{\varepsilon_{jks}(q_2)_s \varepsilon_{ijr}(q_1)_r \varepsilon_{mnu}(q_2)_u (q_1)_m}{[l^0 + i\epsilon][l^0 - i\epsilon][q_2^2 - m_\pi^2 + i\epsilon][q_1^2 - m_\pi^2 + i\epsilon]} \\
&= -\frac{g^4 m_B^2}{64 f_\pi^4} (3 - 2(\vec{\tau}_1 \cdot \vec{\tau}_2)) \int \frac{d^4 l}{(2\pi)^4} \frac{(\delta_{ik} \vec{q}_2 \cdot \vec{q}_1 - (q_2)_i (q_1)_k) \varepsilon_{num}(q_2)_u (q_1)_m}{[l^0 + i\epsilon][l^0 - i\epsilon][q_2^2 - m_\pi^2 + i\epsilon][q_1^2 - m_\pi^2 + i\epsilon]}
\end{aligned}$$

In the last line, the first term inside brackets reproduces an integral of the type that we saw earlier in $P\bar{P}^* \rightarrow P\bar{P}$ scattering (cf. eq. (5.18)), which hence vanishes. Adding up the second, remaining term and the integral of the planar box with one intermediate P -meson (eq. (5.19)), we obtain the purely irreducible integral for both planar boxes:

$$(\mathcal{I}_{\text{box}}^4)_{ikn} = \int \frac{d^4 l}{(2\pi)^4} \frac{((q_2)_k (q_1)_i - (q_2)_i (q_1)_k) \varepsilon_{num}(q_2)_u (q_1)_m}{[l^0 - i\epsilon]^2 [q_2^2 - m_\pi^2 + i\epsilon][q_1^2 - m_\pi^2 + i\epsilon]}$$

In a similar fashion, we obtain the corresponding crossed box:



$$\begin{aligned}
&= i \left(-i \frac{g}{2f_\pi} m_B \right)^2 \left(i \frac{g}{2f_\pi} m_B \right) \left(-\frac{g}{2f_\pi} m_B \right) \int \frac{d^4 l}{(2\pi)^4} (\tau_1)_d \left(-\varepsilon_{jks}(q_2)_s \right) m_B^{-1} \frac{i}{-2l^0 + i\epsilon} \\
&\quad \times (\tau_1)_c \varepsilon_{ijr}(q_1)_r \frac{i}{q_2^2 - m_\pi^2 + i\epsilon} \frac{i}{q_1^2 - m_\pi^2 + i\epsilon} (\tau_2)_c (-\varepsilon_{mnu}(q_1)_u) m_B^{-1} \frac{i}{-2l^0 + i\epsilon} (\tau_2)_d (q_2)_m
\end{aligned}$$

Applying eq. (A.3):

$$\begin{aligned}
&= -\frac{g^4 m_B^2}{64 f_\pi^4} (3 + 2(\vec{\tau}_1 \cdot \vec{\tau}_2)) \int \frac{d^4 l}{(2\pi)^4} \frac{\varepsilon_{jks}(q_2)_s \varepsilon_{ijr}(q_1)_r \varepsilon_{mnu}(q_1)_u (q_2)_m}{[l^0 - i\epsilon]^2 [q_2^2 - m_\pi^2 + i\epsilon] [q_1^2 - m_\pi^2 + i\epsilon]} \\
&= -\frac{g^4 m_B^2}{64 f_\pi^4} (3 + 2(\vec{\tau}_1 \cdot \vec{\tau}_2)) \int \frac{d^4 l}{(2\pi)^4} \frac{(\delta_{ik} \vec{q}_2 \cdot \vec{q}_1 - (q_2)_i (q_1)_k) \varepsilon_{num}(q_2)_u (q_1)_m}{[l^0 - i\epsilon]^2 [q_2^2 - m_\pi^2 + i\epsilon] [q_1^2 - m_\pi^2 + i\epsilon]},
\end{aligned}$$

where we relabeled u and m in the last step. Again, the first term in brackets reproduces a vanishing integral. Adding up both integrals of the crossed boxes, we obtain $\mathcal{I}_{\text{box}}^4$.

Upon C -conjugation of $V_{\text{box}}^{\text{eff}}(P^* \bar{P} \rightarrow P^* \bar{P}^*)$, we are expecting a sign flip stemming from the different sign in the Feynman rule in eq. (2.21). This suggests that the tensor structure of $V_{\text{box}}^{\text{eff}}(P^* \bar{P} \rightarrow P^* \bar{P}^*)$ is proportional to the Levi-Civita symbol, which also changes sign under interchange of indices. Checking $\mathcal{I}_{\text{box}}^4$ in sec. B.3 confirms this and hence:

$$V_{\text{box}}^{\text{eff}}(P^* \bar{P} \rightarrow P^* \bar{P}^*) = \mp \frac{3m_B^2}{32 f_\pi^4} g^4 (\mathcal{I}_{\text{box}}^4)_{ikn} \quad (5.20)$$

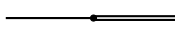
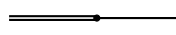
The lower sign denotes the corresponding anti-reaction of $P \bar{P}^* \rightarrow P^* \bar{P}$ with free polarization indices l, k, n instead of i, k, n , respectively. Keep in mind that this sign flip only comes from keeping the polarization indices explicit. Contracting the indices with their corresponding polarization vectors gives again a Hermitian result.

5.2 Corrections to leading order (CCI & C1PE)

The corrections to the LO diagrams can be split into the CCI in sec. 5.2.3, denoting the pion radiation diagrams, and the C1PE in sec. 5.2.2. Excluded are loops with exclusively heavy meson propagators, as they are suppressed when compared to loops with one pion propagator stemming from their large mass difference ($m_\pi \ll m_B$).

While we find an abundance of technically allowed diagrams (sec. D), many of them can be treated collectively. We differentiate between three cases:

1. A diagram or part of it proves to be either reducible, zero or nonphysical (sec. 5.2.1).
2. A part of a diagram contributes to corrections of propagators or 3-vertices and thus can be absorbed into the renormalization of the corresponding physical parameter m_π, m_B, g (sec. 5.2.2).
3. None of the above. The remaining diagrams are calculated explicitly (sec. 5.2.3). Note, however, that these CCI diagrams can also be interpreted as renormalization of D_1, E_1, D_2, E_2 .

Adding \mathcal{L}_λ gives rise to the Feynman rules  and , which exclusively apply to the longitudinal components of $P^{*\mu}$. Fixing the external legs to be on-shell allows one to adjust λ in such a manner that

$$\text{Diagram 1} + \text{Diagram 2} = 0 \quad (5.21)$$

$$\text{Diagram 3} + \text{Diagram 4} = 0 \quad (5.22)$$



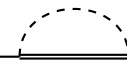

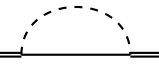
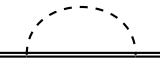

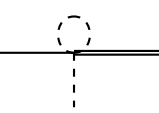
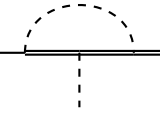
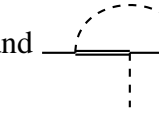

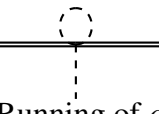
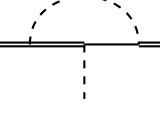
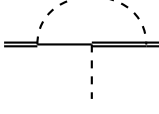
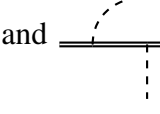

for $p^2 = m_B^2$.

5.2.2 Renormalization of m_π , m_B , g

Many more parts of diagrams contribute to corrections of propagators or 3-vertices. These self-energy/correction graphs also produce finite contributions. After treating the infinities with the $\overline{\text{MS}}$ subtraction scheme, these finite parts still contain some physical behavior of the masses and must be taken into account at NLO. Since the observable, physical mass is defined by the location of the propagator's pole, the renormalized mass is shifted to become the pole mass: $m_R \rightarrow \tilde{m}$.⁶⁴ To make the quantities of renormalization distinct, we denote the bare mass as m , the renormalized mass as m_R and the physical mass as \tilde{m} . This physical mass then reveals the running of the renormalized mass.

The same argument holds for the axial vector coupling g , which we determined by experiment (eq. (2.22)). However, g appears in two different Feynman rules (eqs. (2.19)/(2.20) and (2.21)). Both are corrected but through different diagrams (see below), giving us an elegant cross check: the running of both g should yield the same \tilde{g} .⁶⁵

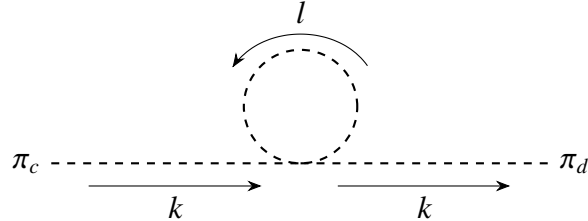
We encounter the following NLO corrections:

1.  corrects  (Running of m_π)
2.  corrects  (Running of m_B)
3.  and  correct  (Running of m_B)
4. ,  and  correct  (Running of g)
5. , ,  and  correct  (Running of g)

⁶⁴Schwartz, op. cit., pp.331ff.

⁶⁵Here, the tilde denotes "physical", not "pole".

Renormalizing m_π



$$\begin{aligned}
&= \frac{i\delta_{cd}}{f_\pi^2} \int \frac{d^4 l}{(2\pi)^4} m_\pi^2 \frac{i}{l^2 - m_\pi^2 + i\epsilon} \\
&= -\frac{\delta_{cd} m_\pi^2}{f_\pi^2} \underbrace{\int \frac{d^4 l}{(2\pi)^4} \frac{1}{l^2 - m_\pi^2 + i\epsilon}}_{=\mathcal{I}_{\text{corr}}^1}
\end{aligned}$$

Inserting $\mathcal{I}_{\text{corr}}^1$ from sec. B.4:

$$= i \frac{\delta_{cd} m_\pi^4}{16\pi^2 f_\pi^2} \left(R + 2 \ln \left(\frac{m_\pi}{\mu} \right) \right)$$

We absorb this one-particle irreducible graph into the pole mass of the pion as usual (cf. Schwartz⁶⁶) via the geometric series:

$$\begin{aligned}
\frac{i\delta_{cd}}{k^2 - m_\pi^2} &\longrightarrow \frac{i\delta_{cd}}{k^2 - m_\pi^2 + \frac{m_\pi^4}{16\pi^2 f_\pi^2} \left(R + 2 \ln \left(\frac{m_\pi}{\mu} \right) \right)} \\
&= \frac{i\delta_{cd}}{k^2 - m_{\pi,R}^2 + \frac{m_{\pi,R}^4}{8\pi^2 f_\pi^2} \ln \left(\frac{m_{\pi,R}}{\mu} \right)} \\
&= \frac{i\delta_{cd}}{k^2 - \widetilde{m}_\pi^2}
\end{aligned}$$

The above expression implies

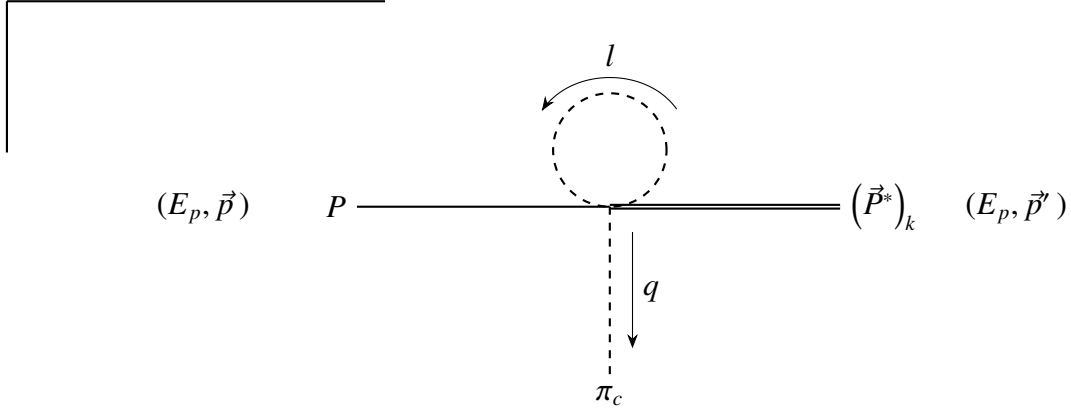
$$m_\pi^2 \longrightarrow \widetilde{m}_\pi^2 = m_{\pi,R}^2 \left(1 - \frac{m_{\pi,R}^2}{8\pi^2 f_\pi^2} \ln \left(\frac{m_{\pi,R}}{\mu} \right) \right),$$

which reveals the running of the pion mass.

⁶⁶Schwartz, op. cit., ch.18.

Renormalizing g

The corrections to the Feynman rule in eq. (2.19), $P \rightarrow P^*\pi$, are given by the following diagrams.



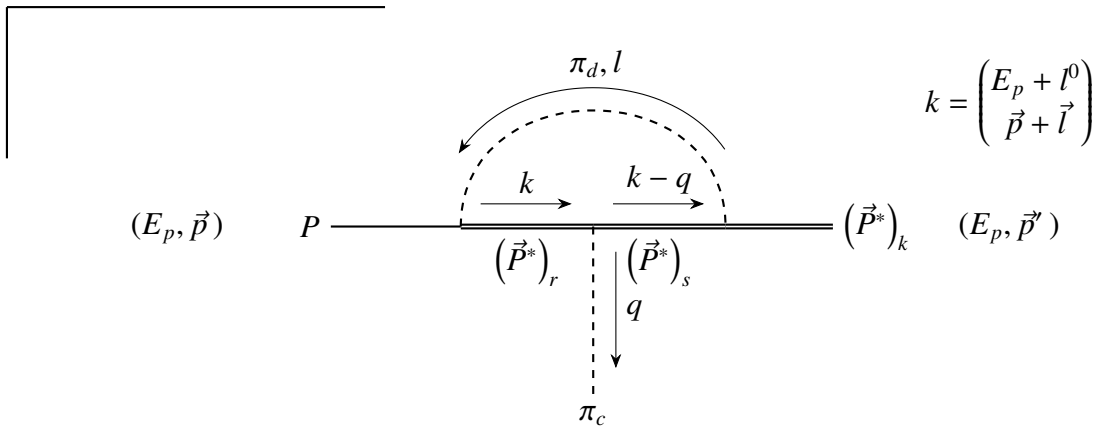
$$= \left(-\frac{g}{12f_\pi^3} m_B \right) (\tau_1)_c \int \frac{d^4 l}{(2\pi)^4} (-2q_k + 2l_k) \frac{i}{l^2 + m_\pi^2 + i\epsilon},$$

where we already executed the sum over the three internal components of the pions. However, odd powers of \vec{l} vanish and thus:

$$= i \frac{g}{6f_\pi^3} m_B (\tau_1)_c q_k \underbrace{\int \frac{d^4 l}{(2\pi)^4} \frac{1}{l^2 + m_\pi^2 + i\epsilon}}_{=\mathcal{I}_{\text{corr}}^1}$$

Inserting $\mathcal{I}_{\text{corr}}^1$ from sec. B.4:

$$= \frac{g}{2f_\pi} m_B q_k (\tau_1)_c \frac{m_\pi^2}{48\pi^2 f_\pi^2} \left(R + 2 \ln \left(\frac{m_\pi}{\mu} \right) \right)$$

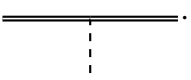


Inserting $\mathcal{I}_{\text{corr}}^3$ from sec. B.4:

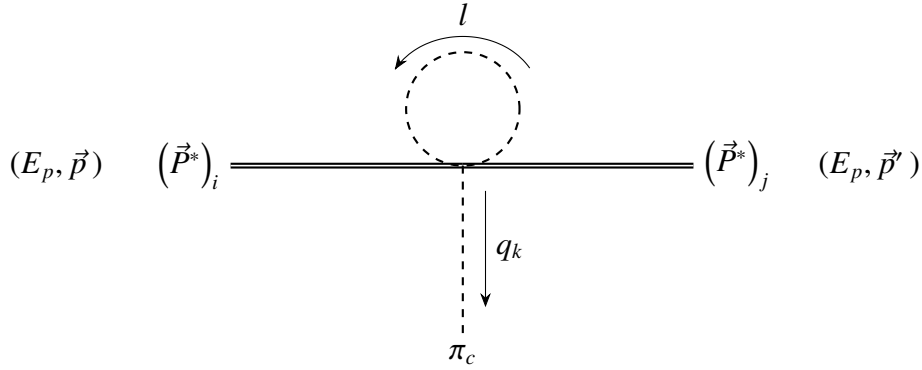
$$= -\frac{g}{2f_\pi} m_B q_k (\tau_1)_c \frac{g^2 m_\pi^2}{256\pi^2 f_\pi^2} \left(R + 2 \ln \left(\frac{m_\pi}{\mu} \right) \right)$$

g can be renormalized by simply adding all three diagrams to the existing Feynman rule:

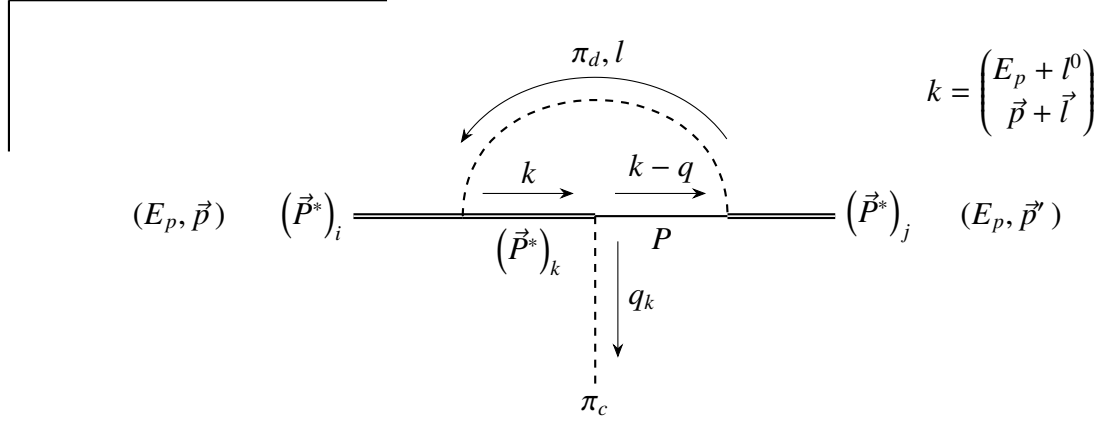
$$\begin{aligned} g &\longrightarrow g \left\{ 1 - \left(\frac{16}{3} + g^2 \right) \frac{m_\pi^2}{256\pi^2 f_\pi^2} \left(R + 2 \ln \left(\frac{m_\pi}{\mu} \right) \right) \right\} \\ &= g_R \left\{ 1 - \left(\frac{16}{3} + g_R^2 \right) \frac{m_\pi^2}{128\pi^2 f_\pi^2} \ln \left(\frac{m_\pi}{\mu} \right) \right\} \\ &= \widetilde{g} \end{aligned}$$

We expect the same resulting running of g through the correction of .

For the pion bubble vertex with two P^* -mesons, we get:



$$\begin{aligned} &= -\frac{g}{6f_\pi^3} m_B (\tau_1)_c \varepsilon_{ijk} q_k \underbrace{\int \frac{d^4 l}{(2\pi)^4} \frac{1}{l^2 + m_\pi^2 + i\epsilon}}_{=\mathcal{I}_{\text{corr}}^1} \\ &= i \frac{g}{2f_\pi} m_B (\tau_1)_c \varepsilon_{ijk} q_k \frac{m_\pi^2}{48\pi^2 f_\pi^2} \left(R + 2 \ln \left(\frac{m_\pi}{\mu} \right) \right) \end{aligned}$$



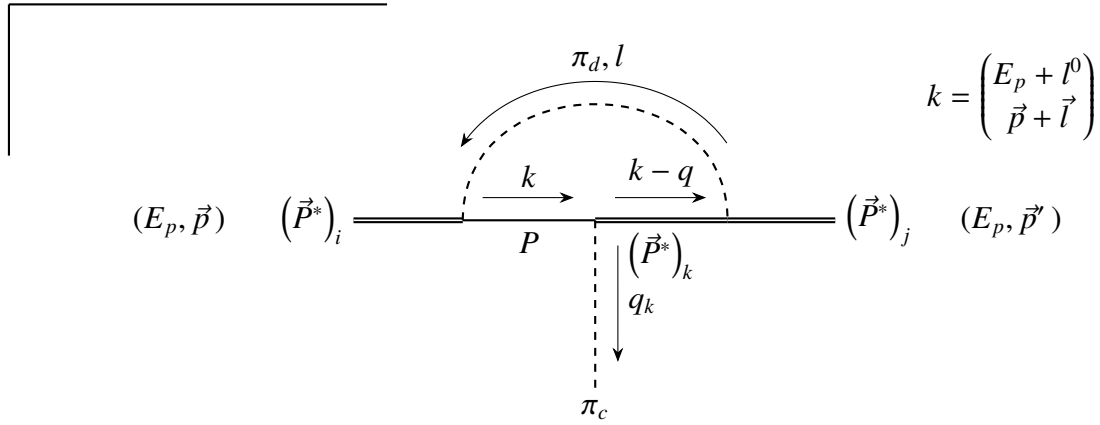
$$= \left(-\frac{g}{2f_\pi} m_B \right)^2 \left(-i \frac{g}{2f_\pi} m_B \right) \int \frac{d^4 l}{(2\pi)^4} \varepsilon_{iku} (-l_u) (\tau_1)_d m_B^{-1} \frac{i}{2l^0 + i\epsilon} q_k (\tau_1)_c$$

$$m_B^{-1} \frac{i}{2(l^0 - q^0) + i\epsilon} l_j (\tau_1)_d \frac{i}{l^2 - m_\pi^2 + i\epsilon}$$

Applying eq. (A.7):

$$= i \frac{g}{2f_\pi} m_B \varepsilon_{ijk} q_k (\tau_1)_c \left(i \frac{g^2}{16f_\pi^2} \right) \underbrace{\int \frac{d^4 l}{(2\pi)^4} \frac{\frac{l^2}{D-1}}{[l^0 + i\epsilon]^2 [l^2 - m_\pi^2 + i\epsilon]}}_{I_{\text{corr}}^3}$$

$$= i \frac{g}{2f_\pi} m_B \varepsilon_{ijk} q_k (\tau_1)_c \frac{g^2 m_\pi^2}{256\pi^2 f_\pi^2} \left(R + 2 \ln \left(\frac{m_\pi}{\mu} \right) \right)$$

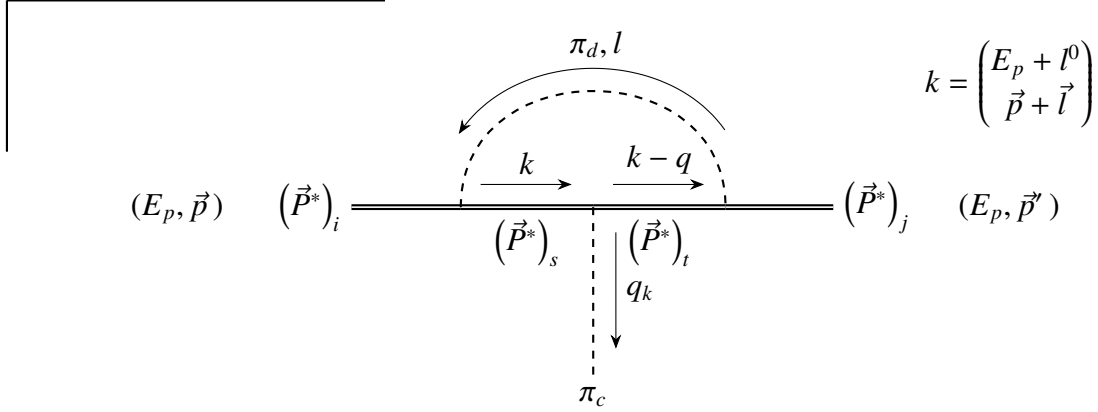


$$= \left(-\frac{g}{2f_\pi} m_B \right)^2 \left(-i \frac{g}{2f_\pi} m_B \right) \int \frac{d^4 l}{(2\pi)^4} (-l_i) (\tau_1)_d m_B^{-1} \frac{i}{2l^0 + i\epsilon} q_k (\tau_1)_c$$

$$m_B^{-1} \frac{i}{2(l^0 - q^0) + i\epsilon} \varepsilon_{kju} l_u (\tau_1)_d \frac{i}{l^2 - m_\pi^2 + i\epsilon}$$

Applying eq. (A.7):

$$\begin{aligned}
 &= i \frac{g}{2f_\pi} m_B \varepsilon_{ijk} q_k (\vec{\tau}_1)_c \left(i \frac{g^2}{16f_\pi^2} \right) \underbrace{\int \frac{d^4 l}{(2\pi)^4} \frac{\vec{l}^2}{[l^0 + i\epsilon]^2 [l^2 - m_\pi^2 + i\epsilon]}}_{I_{\text{corr}}^3} \\
 &= i \frac{g}{2f_\pi} m_B \varepsilon_{ijk} q_k (\vec{\tau}_1)_c \frac{g^2 m_\pi^2}{256\pi^2 f_\pi^2} \left(R + 2 \ln \left(\frac{m_\pi}{\mu} \right) \right)
 \end{aligned}$$



$$\begin{aligned}
 &= \left(-i \frac{g}{2f_\pi} m_B \right)^3 \int \frac{d^4 l}{(2\pi)^4} \varepsilon_{isu} (-l_u) (\tau_1)_d m_B^{-1} \frac{i}{2l^0 + i\epsilon} \varepsilon_{stk} q_k (\tau_1)_c \\
 &\quad m_B^{-1} \frac{i}{2(l^0 - q^0) + i\epsilon} \varepsilon_{tjv} l_v (\tau_1)_d \frac{i}{l^2 - m_\pi^2 + i\epsilon} \\
 &= -i \frac{g}{2f_\pi} m_B (\tau_1)_c \left(-i \frac{g^2}{16f_\pi^2} \varepsilon_{isu} \varepsilon_{stk} \varepsilon_{tjv} q_k \right) \int \frac{d^4 l}{(2\pi)^4} \frac{l_u l_v}{[l^0 + i\epsilon]^2 [l^2 - m_\pi^2 + i\epsilon]} \\
 &= -i \frac{g}{2f_\pi} m_B \varepsilon_{ijk} q_k (\tau_1)_c \left(i \frac{g^2}{16f_\pi^2} \right) \underbrace{\int \frac{d^4 l}{(2\pi)^4} \frac{\vec{l}^2}{[l^0 + i\epsilon]^2 [l^2 - m_\pi^2 + i\epsilon]}}_{I_{\text{corr}}^3} \\
 &= -i \frac{g}{2f_\pi} m_B \varepsilon_{ijk} q_k (\vec{\tau}_1)_c \frac{g^2 m_\pi^2}{256\pi^2 f_\pi^2} \left(R + 2 \ln \left(\frac{m_\pi}{\mu} \right) \right)
 \end{aligned}$$

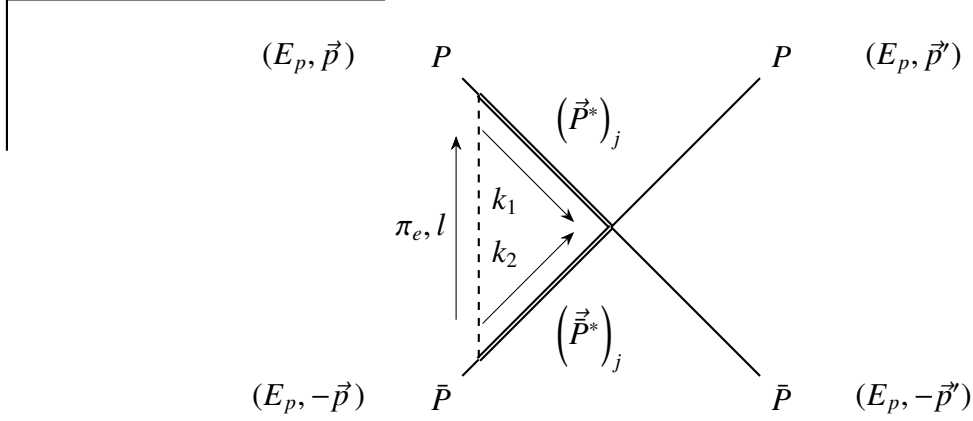
Adding all four diagrams reveals that g is renormalized in an identical fashion as previously:

$$\begin{aligned}
 g &\longrightarrow g \left\{ 1 - \left(\frac{16}{3} + g^2 \right) \frac{m_\pi^2}{256\pi^2 f_\pi^2} \left(R + 2 \ln \left(\frac{m_\pi}{\mu} \right) \right) \right\} \\
 &= g_R \left\{ 1 - \left(\frac{16}{3} + g_R^2 \right) \frac{m_\pi^2}{128\pi^2 f_\pi^2} \ln \left(\frac{m_\pi}{\mu} \right) \right\} \\
 &= \widetilde{g}
 \end{aligned}$$

5.2.3 The remaining diagrams

Cancellation

In the following, we show how many diagrams can be grouped in pairs that cancel each other. Identifying those diagrams helps us to drastically simplify the calculation.



$$k_1 = \begin{pmatrix} E_p + l^0 \\ \vec{p} + \vec{l} \end{pmatrix} \quad k_2 = \begin{pmatrix} E_p - l^0 \\ -\vec{p} - \vec{l} \end{pmatrix}$$

$$\begin{aligned} &= i \left(-\frac{g}{2f_\pi} m_B \right)^2 \int \frac{d^4 l}{(2\pi)^4} (\vec{\tau}_1)_e \left(-i(D_2 + (\vec{\tau}_1 \cdot \vec{\tau}_2) E_2) m_B^2 \right) (-l)_j (\vec{\tau}_2)_e l_j \delta_{st} \\ &\quad \times \frac{i}{l^2 - m_\pi^2 + i\epsilon} m_B^{-1} \frac{i}{-2l^0 + i\epsilon} m_B^{-1} \frac{i}{2l^0 + i\epsilon} \\ &= -i \frac{g^2 m_B^2}{16f_\pi^2} (\vec{\tau}_1)_e \left(D_2 + (\vec{\tau}_1 \cdot \vec{\tau}_2) E_2 \right) (\vec{\tau}_2)_e \underbrace{\int \frac{d^4 l}{(2\pi)^4} \frac{\vec{l}^2}{[l^0 - i\epsilon][l^0 + i\epsilon][l^2 - m_\pi^2 + i\epsilon]}}_{=\mathcal{I}_{\text{corr}}^4} \end{aligned}$$

Here, we expanded C_2 to make the dependence on the Pauli matrices explicit and abbreviated the integral for treatment in sec. B.4. Using eq. (A.3) again:

$$\begin{aligned} (\vec{\tau}_1)_e \left(D_i + (\vec{\tau}_1 \cdot \vec{\tau}_2) E_i \right) (\vec{\tau}_2)_e &= \left(D_i (\vec{\tau}_1 \cdot \vec{\tau}_2) + E_i (\vec{\tau}_1)_e (\vec{\tau}_1)_h (\vec{\tau}_2)_h (\vec{\tau}_2)_e \right) \\ &= \left(3E_i + (D_i + 2E_i) (\vec{\tau}_1 \cdot \vec{\tau}_2) \right) \end{aligned} \quad (5.23)$$

Thus, we obtain:

$$= -i \frac{g^2 m_B^2}{16f_\pi^2} \left(3E_2 + (D_2 + 2E_2) (\vec{\tau}_1 \cdot \vec{\tau}_2) \right) \mathcal{I}_{\text{corr}}^4$$

Since we are only interested in the irreducible contributions of a diagram, we substitute $\mathcal{I}_{\text{corr}}^4 \rightarrow \mathcal{I}_{\text{corr}}^5$ when omitting all reducible parts (cf. sec. B.4).

Examining the corresponding arc diagram gives:

$$(5.24)$$

$$k_1 = \begin{pmatrix} E_p + l^0 \\ \vec{p} + \vec{l} \end{pmatrix} \quad k_2 = \begin{pmatrix} E_p + l^0 \\ -\vec{p}' + \vec{l} \end{pmatrix}$$

$$\begin{aligned} &= i \left(-\frac{g}{2f_\pi} m_B \right)^2 \int \frac{d^4 l}{(2\pi)^4} (\vec{\tau}_1)_e \left(-i(D_2 + (\vec{\tau}_1 \cdot \vec{\tau}_2) E_2) m_B^2 \right) (-l_s) (\vec{\tau}_2)_e l_t \delta_{st} \\ &\quad \times \frac{i}{l^2 - m_\pi^2 + i\epsilon} m_B^{-1} \frac{i}{2l^0 + i\epsilon} m_B^{-1} \frac{i}{2l^0 + i\epsilon} \\ &= i \frac{g^2 m_B^2}{16f_\pi^2} (\vec{\tau}_1)_e \left(D_2 + (\vec{\tau}_1 \cdot \vec{\tau}_2) E_2 \right) (\vec{\tau}_2)_e \underbrace{\int \frac{d^4 l}{(2\pi)^4} \frac{\vec{l}^2}{[l^0 - i\epsilon]^2 [l^2 - m_\pi^2 + i\epsilon]}}_{=I_{\text{corr}}^5} \\ &= i \frac{g^2 m_B^2}{16f_\pi^2} \left(3E_2 + (D_2 + 2E_2)(\vec{\tau}_1 \cdot \vec{\tau}_2) \right) I_{\text{corr}}^5 \end{aligned}$$

This is almost identical when compared to the irreducible part of the corresponding pion radiation diagram above apart from the sign flip in one of the heavy meson propagators. Due to this, the diagrams always cancel each other exactly:

$$+ = 0$$

By extension, this applies to all pion radiation diagrams with an arc counterpart. Consulting sec. D shows that this holds for almost all of them except the ones in the scattering of $P^* \bar{P} \rightarrow P \bar{P}^*$ (fig. D.3), $P \bar{P} \rightarrow P^* \bar{P}^*$ (fig. D.5) and $P^* \bar{P} \rightarrow P^* \bar{P}^*$ (fig. D.7).

The canceling "partner" of a pion radiation diagram can be constructed by permuting the legs of the heavy anti-mesons (the diagram's bottom half) without separating any propagators.

Unfortunately, in diagrams with one external \bar{P} , \bar{P}^* each, the situation is not as apparent as in the other processes because permuting legs is not possible without changing the process. This finally brings us to the remaining contributing diagrams of the corrected LO.

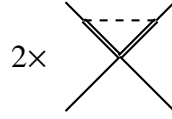


Fig. 5.14: Remaining corrections to contact diagrams for $P\bar{P} \rightarrow P\bar{P}$. The factor of 2 emphasizes that the triangle correction is to be applied to the opposite side, too.

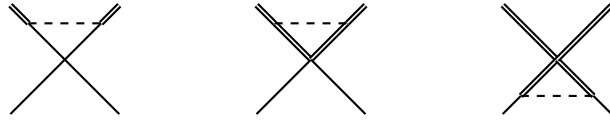


Fig. 5.15: Remaining corrections to contact diagrams for $P^*\bar{P} \rightarrow P^*\bar{P}$.

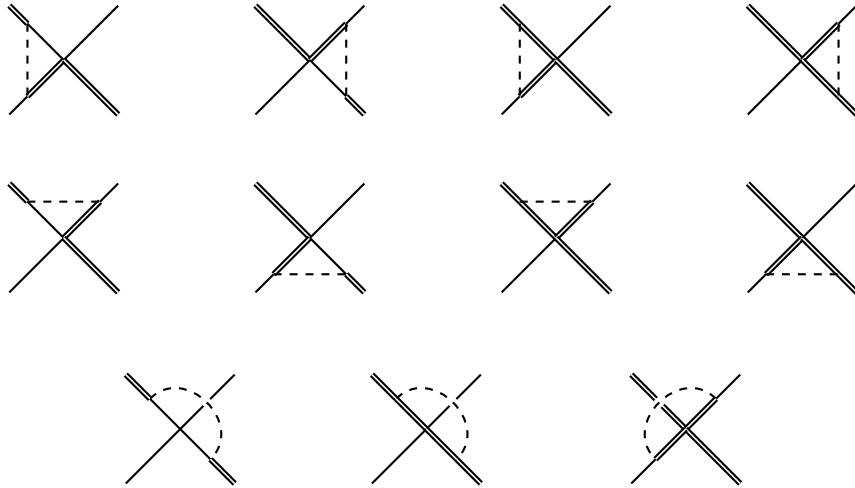


Fig. 5.16: Remaining corrections to contact diagrams for $P^*\bar{P} \rightarrow P\bar{P}^*$.

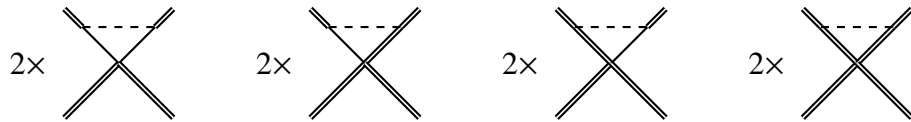


Fig. 5.17: Remaining corrections to contact diagrams for $P^*\bar{P}^* \rightarrow P^*\bar{P}^*$. The factors of 2 emphasize that the triangle correction is to be applied to the opposite side, too.

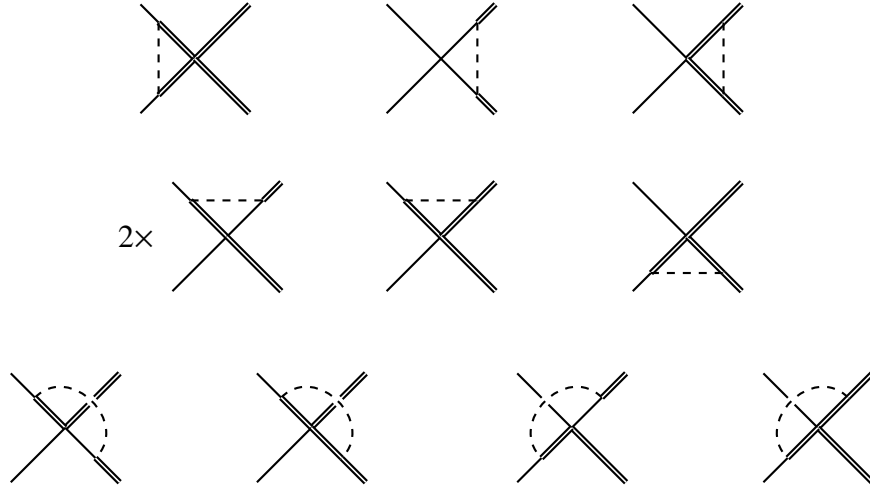


Fig. 5.18: Remaining corrections to contact diagrams for $P\bar{P} \rightarrow P^*\bar{P}^*$. The factor of 2 emphasizes that the propagator correction is to be applied to the opposite side, too.

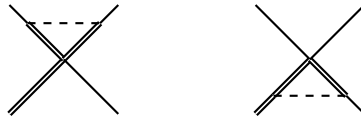


Fig. 5.19: Remaining corrections to contact diagrams for $P\bar{P}^* \rightarrow P\bar{P}$.

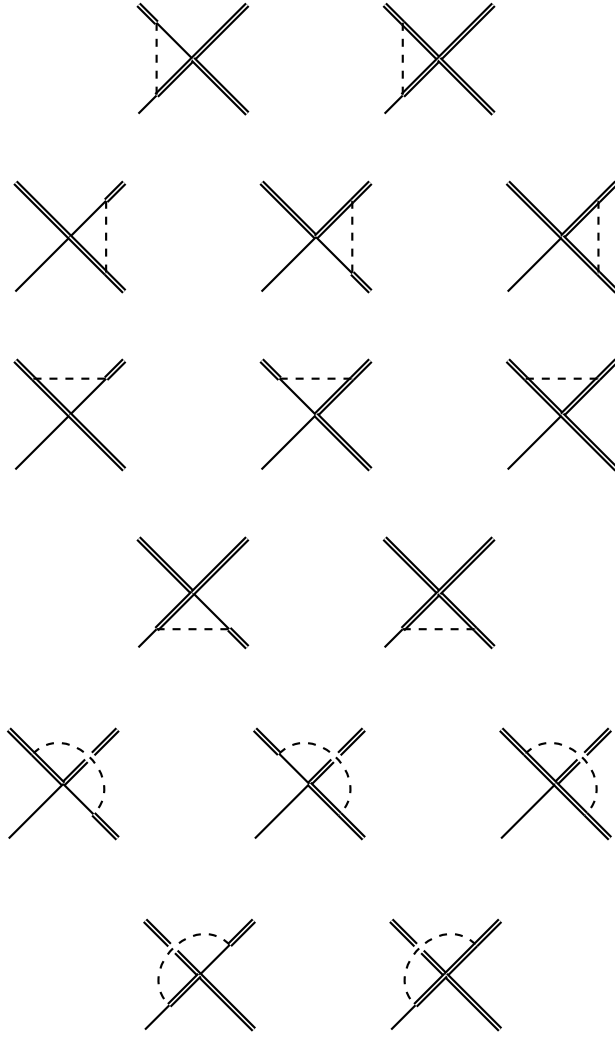


Fig. 5.20: Remaining corrections to contact diagrams for $P^* \bar{P} \rightarrow P^* \bar{P}^*$.

$P\bar{P} \rightarrow P\bar{P}$

(5.25)

$$k_1 = \begin{pmatrix} E_p + l^0 \\ \vec{p} + \vec{l} \end{pmatrix} \quad k_2 = \begin{pmatrix} E_p + l^0 \\ \vec{p}' + \vec{l} \end{pmatrix}$$

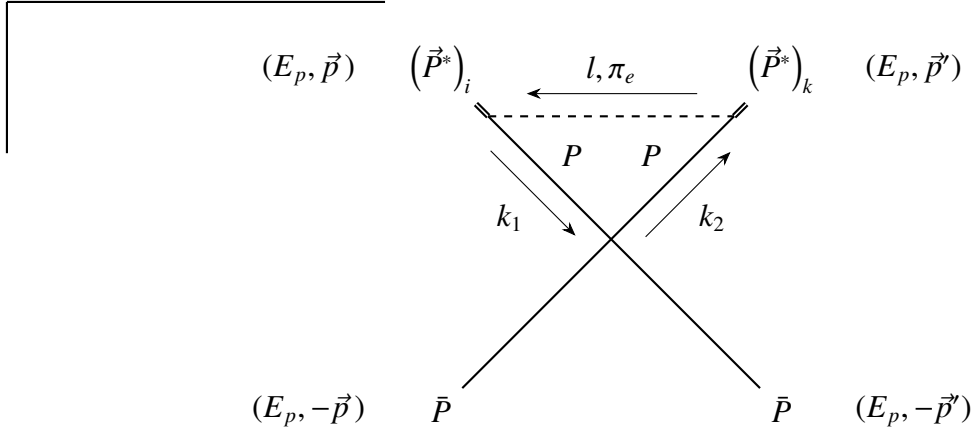
$$\begin{aligned}
&= i \left(-\frac{g}{2f_\pi} m_B \right)^2 \int \frac{d^4 l}{(2\pi)^4} (\vec{\tau}_1)_e \left(-i(D_1 + (\vec{\tau}_1 \cdot \vec{\tau}_2) E_1) m_B^2 \right) (-l_s) (\vec{\tau}_1)_e l_t \delta_{st} \\
&\quad \times \frac{i}{l^2 - m_\pi^2 + i\epsilon} m_B^{-1} \frac{i}{2l^0 + i\epsilon} m_B^{-1} \frac{i}{2l^0 + i\epsilon} \\
&= i \frac{g^2 m_B^2}{16f_\pi^2} (\vec{\tau}_1)_e \left(D_1 + (\vec{\tau}_1 \cdot \vec{\tau}_2) E_1 \right) (\vec{\tau}_1)_e \underbrace{\int \frac{d^4 l}{(2\pi)^4} \frac{\vec{l}^2}{[l^0 - i\epsilon]^2 [l^2 - m_\pi^2 + i\epsilon]}}_{= \mathcal{I}_{\text{corr}}^5}
\end{aligned}$$

Using eq. (A.4) lets us reinsert C_1 :

$$= i \frac{3g^2 m_B^2}{16f_\pi^2} C_1 \mathcal{I}_{\text{corr}}^5$$

Applying this loop correction to the opposite side gives a factor of 2 and thus:

$$\boxed{V_{\text{CC1}}^{\text{eff}}(P\bar{P} \rightarrow P\bar{P}) = i \frac{3g^2 m_B^2}{16f_\pi^2} C_1 (2\mathcal{I}_{\text{corr}}^5)} \quad (5.26)$$

$\mathbf{P}^* \bar{\mathbf{P}} \rightarrow \mathbf{P}^* \bar{\mathbf{P}}$ 

$$k_1 = \begin{pmatrix} E_p + l^0 \\ \vec{p} + \vec{l} \end{pmatrix} \quad k_2 = \begin{pmatrix} E_p + l^0 \\ \vec{p}' + \vec{l} \end{pmatrix}$$

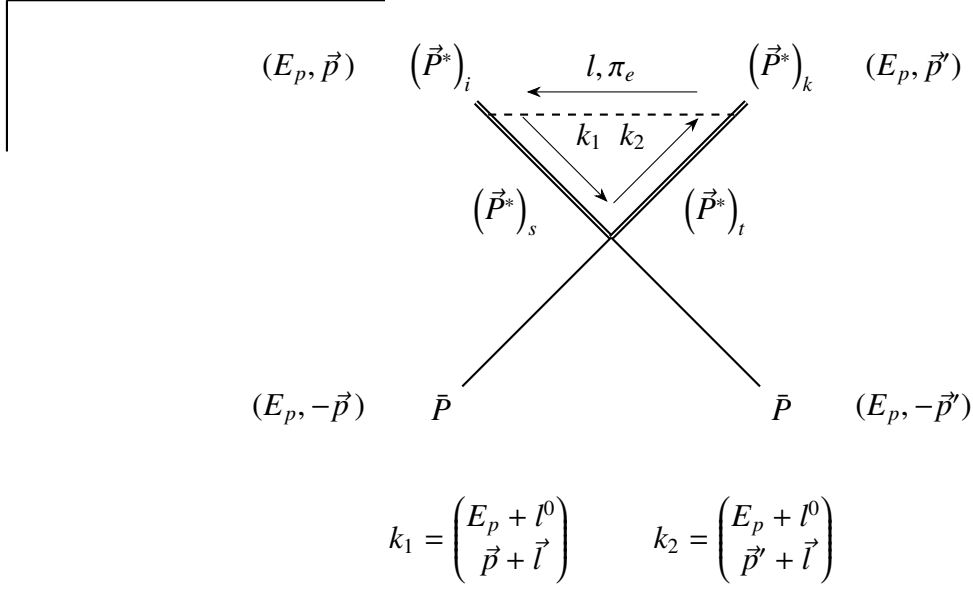
$$\begin{aligned} &= i \left(-\frac{g}{2f_\pi} m_B \right)^2 \int \frac{d^4 l}{(2\pi)^4} (\tau_1)_e \left(-i(D_1 + (\vec{\tau}_1 \cdot \vec{\tau}_2) E_1) m_B^2 \right) (-l_i) (\tau_1)_e l_k \\ &\quad \times \frac{i}{l^2 - m_\pi^2 + i\epsilon} m_B^{-1} \frac{i}{2l^0 + i\epsilon} m_B^{-1} \frac{i}{2l^0 + i\epsilon} \\ &= i \frac{g^2 m_B^2}{16f_\pi^2} (\tau_1)_e \left(D_1 + (\vec{\tau}_1 \cdot \vec{\tau}_2) E_1 \right) (\tau_1)_e \frac{\delta_{ik}}{D-1} \underbrace{\int \frac{d^4 l}{(2\pi)^4} \frac{l^2}{[l^0 - i\epsilon]^2 [l^2 - m_\pi^2 + i\epsilon]}}_{=\mathcal{I}_{\text{corr}}^5} \end{aligned}$$

Using eqs. (A.4) and (A.7), the expression simplifies to:

$$= i \frac{3g^2 m_B^2}{16f_\pi^2} C_1 \frac{\delta_{ik}}{D-1} \mathcal{I}_{\text{corr}}^5$$

We are well aware that the factor of $1/(D-1)$ needs to be included into the calculation of $\mathcal{I}_{\text{corr}}^5$. However, we show in sec. B.4 that $\mathcal{I}_{\text{corr}}^5/(D-1) = \mathcal{I}_{\text{corr}}^1$ and thus:

$$= i \frac{3g^2 m_B^2}{16f_\pi^2} C_1 \delta_{ik} \mathcal{I}_{\text{corr}}^1$$



$$= i \left(-i \frac{g}{2f_\pi} m_B \right)^2 \int \frac{d^4 l}{(2\pi)^4} (\tau_1)_e \left(-i(D_1 + (\vec{\tau}_1 \cdot \vec{\tau}_2) E_1) m_B^2 \right) (-\varepsilon_{ijs} l_j) \delta_{st} (\tau_1)_e \varepsilon_{ikm} l_m$$

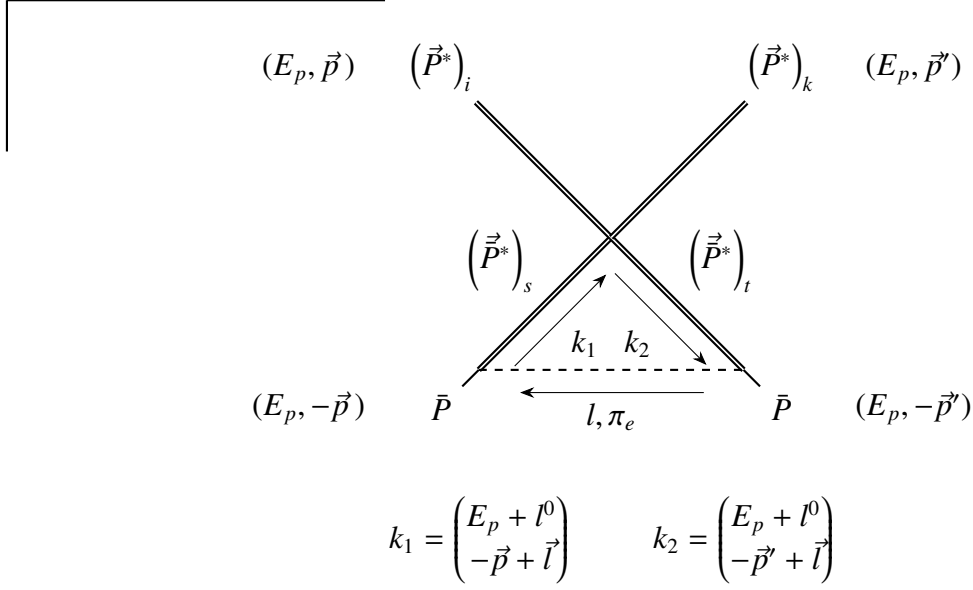
$$\times \frac{i}{l^2 - m_\pi^2 + i\epsilon} m_B^{-1} \frac{i}{2l^0 + i\epsilon} m_B^{-1} \frac{i}{2l^0 + i\epsilon}$$

Using eqs. (A.4) and (A.7) further simplifies:

$$= -i \frac{3g^2 m_B^2}{16f_\pi^2} C_1 \varepsilon_{ijs} \varepsilon_{ikm} \delta_{st} \int \frac{d^4 l}{(2\pi)^4} \frac{l_j l_m}{[l^0 - i\epsilon]^2 [l^2 - m_\pi^2 + i\epsilon]}$$

$$= i \frac{3g^2 m_B^2}{16f_\pi^2} C_1 \frac{2\delta_{ik}}{D-1} \mathcal{I}_{\text{corr}}^5$$

$$= i \frac{6g^2 m_B^2}{16f_\pi^2} C_1 \delta_{ik} \mathcal{I}_{\text{corr}}^1$$



$$= i \left(-\frac{g}{2f_\pi} m_B \right)^2 \int \frac{d^4 l}{(2\pi)^4} (\tau_2)_e \left(-i (C_1 \delta_{ik} \delta_{st} + C_2 \delta_{is} \delta_{kt} - C_2 \delta_{it} \delta_{sk}) m_B^2 \right) (\tau_2)_e (-l_s) \frac{i}{l^2 - m_\pi^2 + i\epsilon} l_t \\ \times m_B^{-1} \frac{i}{2l^0 + i\epsilon} m_B^{-1} \frac{i}{2l^0 + i\epsilon}$$

Using eq. (A.4) simplifies:

$$= i \frac{3g^2 m_B^2}{16f_\pi^2} (C_1 \delta_{ik} \delta_{st} + C_2 \delta_{is} \delta_{kt} - C_2 \delta_{it} \delta_{sk}) \int \frac{d^4 l}{(2\pi)^4} \frac{l_s l_t}{[l^0 - i\epsilon]^2 [l^2 - m_\pi^2 + i\epsilon]} \\ = i \frac{3g^2 m_B^2}{16f_\pi^2} C_1 \delta_{ik} \mathcal{I}_{\text{corr}}^5$$

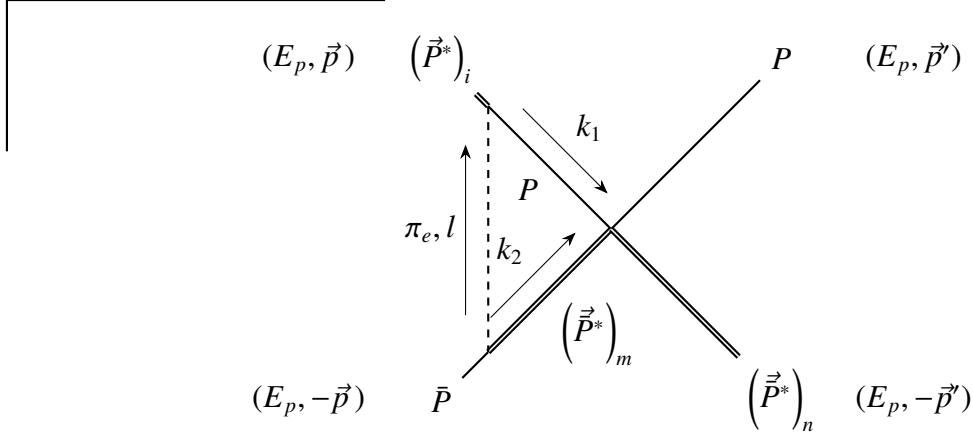
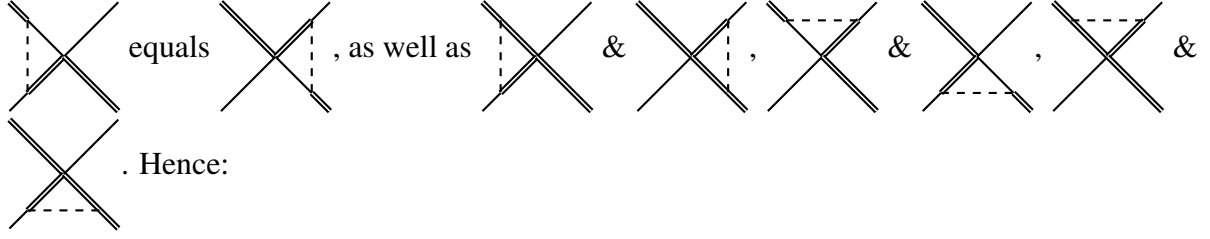
Adding up all three diagrams gives:

$$V_{\text{CCI}}^{\text{eff}}(P^* \bar{P} \rightarrow P^* \bar{P}) = i \frac{3g^2 m_B^2}{16f_\pi^2} C_1 \delta_{ik} \left(\mathcal{I}_{\text{corr}}^5 + 3\mathcal{I}_{\text{corr}}^1 \right) \quad (5.27)$$

This contribution breaks HQSS explicitly when compared to eq. (5.26) (cf. full potentials in sec. 6). By using dimensional regularization, a factor of $(D - 1)$ enters $\mathcal{I}_{\text{corr}}^5$ (cf. eq. (B.17)) in comparison to $\mathcal{I}_{\text{corr}}^1$ (cf. eq. (B.13)). Since this factor is not just 3 but $3 - \epsilon$, this gives a contribution when multiplied with $2/\epsilon$ in the R -term. Only in the limit of precisely $D = 4$, HQSS would be recovered.

$\mathbf{P}^*\bar{\mathbf{P}} \rightarrow \mathbf{P}\bar{\mathbf{P}}^*$

For $P^*\bar{P} \rightarrow P\bar{P}^*$ scattering, there are eleven diagrams we need to take into account. However, the first eight are very similar to one another. It is easy to show by explicit calculation that



$$k_1 = \begin{pmatrix} E_p + l^0 \\ \vec{p} + \vec{l} \end{pmatrix} \quad k_2 = \begin{pmatrix} E_p - l^0 \\ -\vec{p} - \vec{l} \end{pmatrix}$$

$$\begin{aligned} &= i \left(-\frac{g}{2f_\pi} m_B \right)^2 \int \frac{d^4 l}{(2\pi)^4} (\tau_1)_e \left(-i(D_1 + (\vec{\tau}_1 \cdot \vec{\tau}_2) E_1) m_B^2 \right) \delta_{mn} (-l_i) (\tau_2)_e l_m \\ &\quad \times \frac{i}{l^2 - m_\pi^2 + i\epsilon} m_B^{-1} \frac{i}{-2l^0 + i\epsilon} m_B^{-1} \frac{i}{2l^0 + i\epsilon} \\ &= -i \frac{g^2 m_B^2}{16f_\pi^2} (\tau_1)_e \left(D_1 + (\vec{\tau}_1 \cdot \vec{\tau}_2) E_1 \right) (\tau_2)_e \frac{\delta_{in}}{D-1} \underbrace{\int \frac{d^4 l}{(2\pi)^4} \frac{\vec{l}^2}{[l^0 - i\epsilon][l^0 + i\epsilon][l^2 - m_\pi^2 + i\epsilon]}}_{\rightarrow \mathcal{I}_{\text{corr}}^5}, \end{aligned}$$

where we dropped all reducible pieces in the last step and immediately used $\mathcal{I}_{\text{corr}}^5$. Applying eq. (5.23):

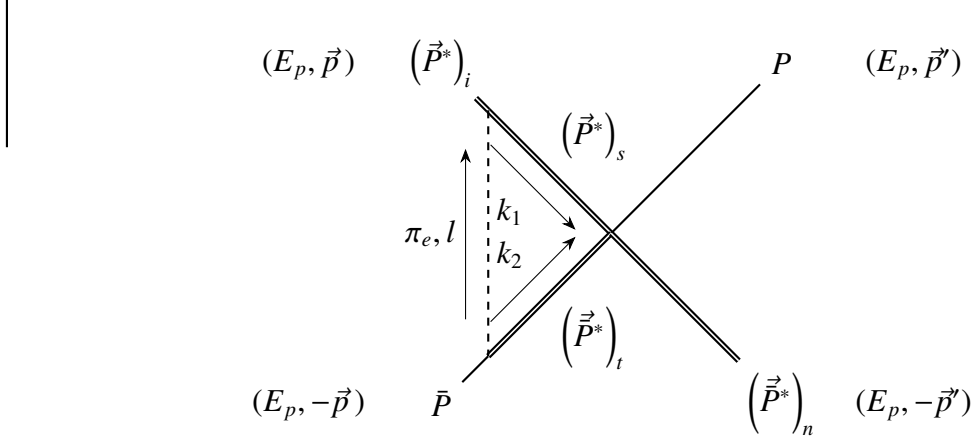
$$= -i \frac{3g^2 m_B^2}{16f_\pi^2} Z_1 \delta_{in} \frac{\mathcal{I}_{\text{corr}}^5}{D-1},$$

where we abbreviated the SU(2)-isospin structure:

$$Z_i := E_i + \frac{D_i + 2E_i}{3} (\vec{\tau}_1 \cdot \vec{\tau}_2) \quad (5.28)$$

Substituting $\mathcal{I}_{\text{corr}}^5/(D-1) = \mathcal{I}_{\text{corr}}^1$:

$$= -i \frac{3g^2 m_B^2}{16f_\pi^2} Z_1 \delta_{in} \mathcal{I}_{\text{corr}}^1$$



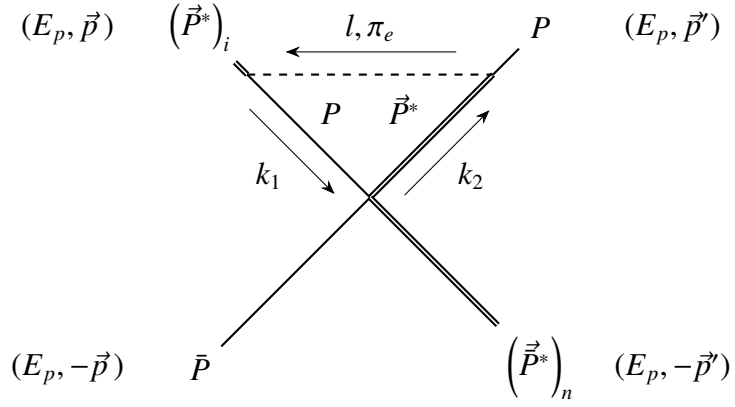
$$k_1 = \begin{pmatrix} E_p + l^0 \\ \vec{p} + \vec{l} \end{pmatrix} \quad k_2 = \begin{pmatrix} E_p - l^0 \\ -\vec{p} - \vec{l} \end{pmatrix}$$

$$\begin{aligned} &= i \left(-\frac{g}{2f_\pi} m_B \right) \left(-i \frac{g}{2f_\pi} m_B \right) \int \frac{d^4 l}{(2\pi)^4} (\tau_1)_e \left(-\varepsilon_{ms} (D_2 + (\vec{\tau}_1 \cdot \vec{\tau}_2) E_2) m_B^2 \right) \\ &\quad \times (-\varepsilon_{isr} l_r) (\tau_2)_e l_t \frac{i}{l^2 - m_\pi^2 + i\epsilon} m_B^{-1} \frac{i}{-2l^0 + i\epsilon} m_B^{-1} \frac{i}{2l^0 + i\epsilon} \\ &= -i \frac{g^2 m_B^2}{16f_\pi^2} (\tau_1)_e \left(D_2 + (\vec{\tau}_1 \cdot \vec{\tau}_2) E_2 \right) (\tau_2)_e \varepsilon_{ms} \varepsilon_{isr} \delta_{ut} \int \frac{d^4 l}{(2\pi)^4} \frac{l_u l_r}{[l^0 - i\epsilon][l^0 + i\epsilon][l^2 - m_\pi^2 + i\epsilon]} \\ &= -i \frac{3g^2 m_B^2}{16f_\pi^2} Z_2 \underbrace{\int \frac{d^4 l}{(2\pi)^4} \frac{\delta_{in} \vec{l}^2 - l_i l_n}{[l^0 - i\epsilon][l^0 + i\epsilon][l^2 - m_\pi^2 + i\epsilon]}}_{\rightarrow \mathcal{I}_{\text{corr}}^5 - \mathcal{I}_{\text{corr}}^1}, \end{aligned}$$

where we used Z_2 as defined in eq. (5.28). Furthermore, we can replace $\mathcal{I}_{\text{corr}}^5/(D-1) = \mathcal{I}_{\text{corr}}^1$ and thus:

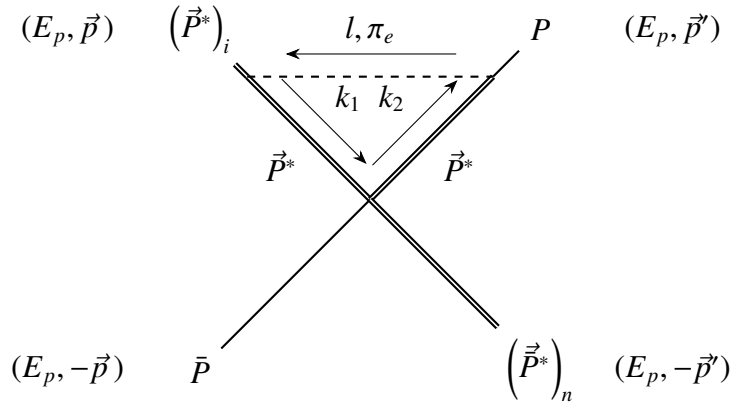
$$= -i \frac{3g^2 m_B^2}{16f_\pi^2} Z_2 \delta_{in} \left(\mathcal{I}_{\text{corr}}^5 - \mathcal{I}_{\text{corr}}^1 \right)$$

Only the SU(2)-isospin structure changes when considering the completely irreducible versions of the two previous diagrams. This can also be calculated easily but is omitted for the sake of brevity.



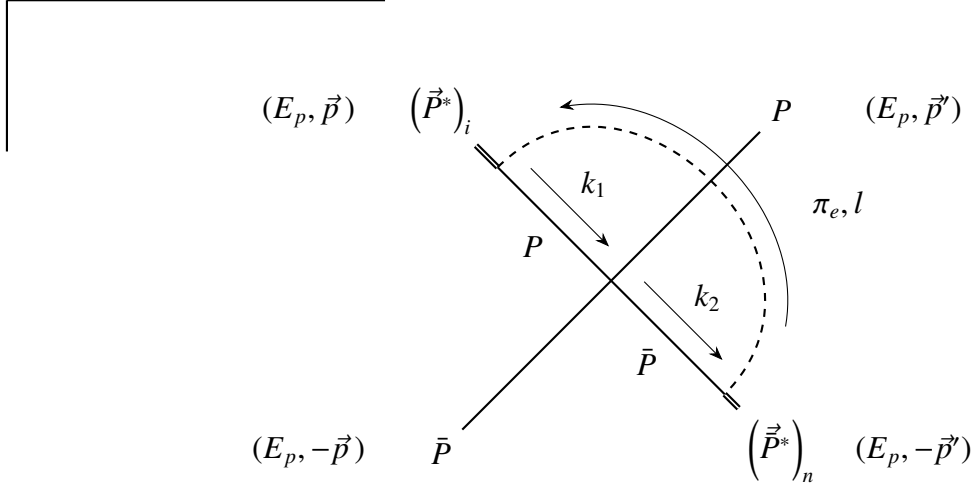
$$k_1 = \begin{pmatrix} E_p + l^0 \\ \vec{p} + \vec{l} \end{pmatrix} \quad k_2 = \begin{pmatrix} E_p + l^0 \\ \vec{p}' + \vec{l} \end{pmatrix}$$

$$= i \frac{3g^2 m_B^2}{16f_\pi^2} C_2 \delta_{in} \mathcal{I}_{\text{corr}}^1$$



$$k_1 = \begin{pmatrix} E_p + l^0 \\ \vec{p} + \vec{l} \end{pmatrix} \quad k_2 = \begin{pmatrix} E_p + l^0 \\ \vec{p}' + \vec{l} \end{pmatrix}$$

$$= -i \frac{3g^2 m_B^2}{16f_\pi^2} C_2 \delta_{in} (\mathcal{I}_{\text{corr}}^5 - \mathcal{I}_{\text{corr}}^1)$$

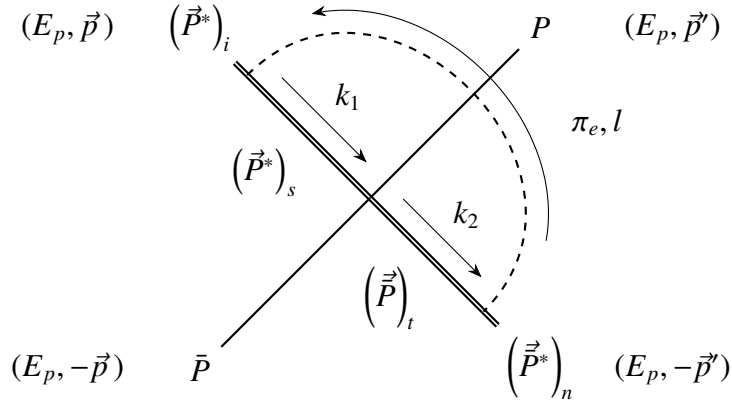


$$k_1 = \begin{pmatrix} E_p + l^0 \\ \vec{p} + \vec{l} \end{pmatrix} \quad k_2 = \begin{pmatrix} E_p + l^0 \\ -\vec{p}' + \vec{l} \end{pmatrix}$$

$$\begin{aligned} &= i \left(-\frac{g}{2f_\pi} m_B \right)^2 \int \frac{d^4 l}{(2\pi)^4} (\tau_1)_e \left(-i(D_1 + (\vec{\tau}_1 \cdot \vec{\tau}_2) E_1) m_B^2 \right) (-l_i) (\tau_2)_e l_n \\ &\quad \times \frac{i}{l^2 - m_\pi^2 + i\epsilon} m_B^{-1} \frac{i}{2l^0 + i\epsilon} m_B^{-1} \frac{i}{2l^0 + i\epsilon} \\ &= i \frac{g^2 m_B^2}{16f_\pi^2} (\tau_1)_e \left(D_1 + (\vec{\tau}_1 \cdot \vec{\tau}_2) E_1 \right) (\tau_2)_e \frac{\delta_{in}}{D-1} \underbrace{\int \frac{d^4 l}{(2\pi)^4} \frac{\vec{l}^2}{[l^0 - i\epsilon]^2 [l^2 - m_\pi^2 + i\epsilon]}}_{=\mathcal{I}_{\text{corr}}^5} \end{aligned}$$

Replacing $\mathcal{I}_{\text{corr}}^5/(D-1)$ and using Z_1 from eq. (5.28):

$$= i \frac{3g^2 m_B^2}{16f_\pi^2} Z_1 \delta_{in} \mathcal{I}_{\text{corr}}^1$$

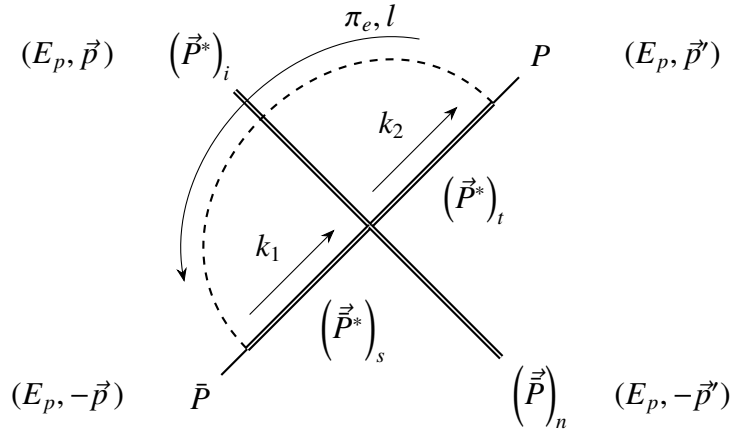


$$k_1 = \begin{pmatrix} E_p + l^0 \\ \vec{p} + \vec{l} \end{pmatrix} \quad k_2 = \begin{pmatrix} E_p + l^0 \\ -\vec{p}' + \vec{l} \end{pmatrix}$$

$$= i \left(-i \frac{g}{2f_\pi} m_B \right) \left(i \frac{g}{2f_\pi} m_B \right) \int \frac{d^4 l}{(2\pi)^4} (\tau_1)_e \left(-i(D_2 + (\vec{\tau}_1 \cdot \vec{\tau}_2) E_2) m_B^2 \right) \\ \times (-\varepsilon_{isr} l_r) (\tau_2)_e \varepsilon_{imu} l_u \delta_{ts} \frac{i}{l^2 - m_\pi^2 + i\epsilon} m_B^{-1} \frac{i}{2l^0 + i\epsilon} m_B^{-1} \frac{i}{2l^0 + i\epsilon}$$

Using eq. (A.7) and Z_2 as defined in eq. (5.28) and replacing $\mathcal{I}_{\text{corr}}^5/(D-1) = \mathcal{I}_{\text{corr}}^1$ gives:

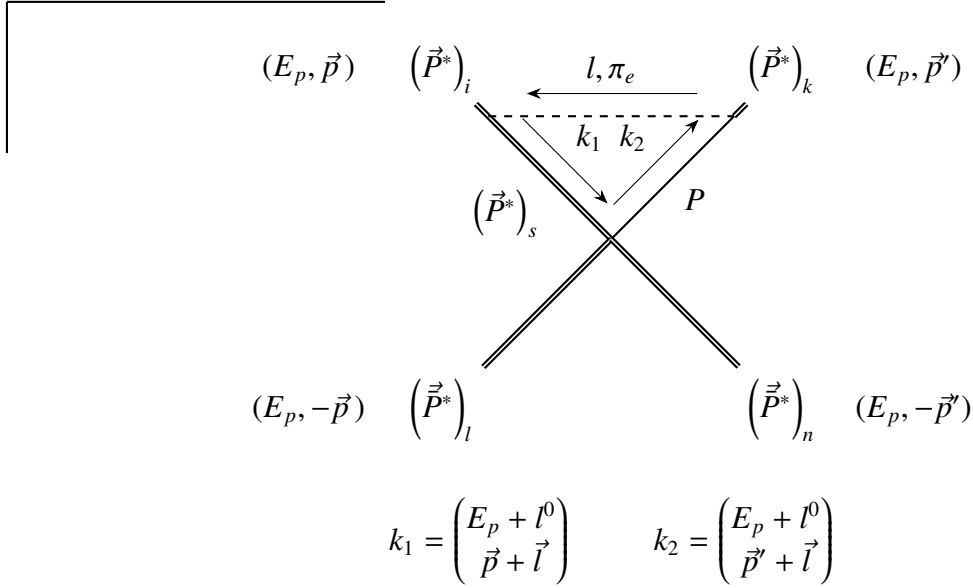
$$= -i \frac{3g^2 m_B^2}{16f_\pi^2} Z_2 \delta_{in} (\mathcal{I}_{\text{corr}}^5 - \mathcal{I}_{\text{corr}}^1)$$



$$k_1 = \begin{pmatrix} E_p + l^0 \\ -\vec{p} + \vec{l} \end{pmatrix} \quad k_2 = \begin{pmatrix} E_p + l^0 \\ \vec{p}' + \vec{l} \end{pmatrix}$$

$$\begin{aligned}
&= i \left(-\frac{g}{2f_\pi} m_B \right)^2 \int \frac{d^4 l}{(2\pi)^4} (\tau_1)_e \left(-i(D_1 + (\vec{\tau}_1 \cdot \vec{\tau}_2) E_1) m_B^2 \right) \delta_{ln}(-l_i) (\tau_1)_e l_k \\
&\quad \times \frac{i}{l^2 - m_\pi^2 + i\epsilon} m_B^{-1} \frac{i}{2l^0 + i\epsilon} m_B^{-1} \frac{i}{2l^0 + i\epsilon} \\
&= i \frac{g^2 m_B^2}{16f_\pi^2} (\tau_1)_e \left(D_1 + (\vec{\tau}_1 \cdot \vec{\tau}_2) E_1 \right) (\tau_1)_e \frac{\delta_{ik} \delta_{ln}}{D-1} \underbrace{\int \frac{d^4 l}{(2\pi)^4} \frac{\vec{l}^2}{[l^0 - i\epsilon]^2 [l^2 - m_\pi^2 + i\epsilon]}}_{=\mathcal{I}_{\text{corr}}^5} \\
&= i \frac{3g^2 m_B^2}{16f_\pi^2} C_1 \delta_{ik} \delta_{ln} \mathcal{I}_{\text{corr}}^1,
\end{aligned}$$

where we used eqs. (A.4) and (A.7).

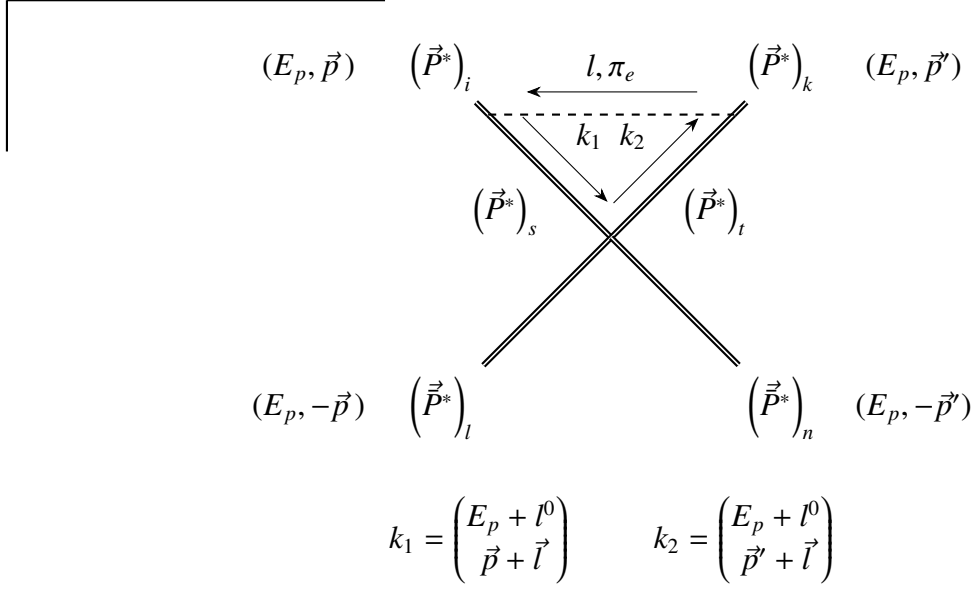


$$\begin{aligned}
&= i \left(-i \frac{g}{2f_\pi} m_B \right) \left(-\frac{g}{2f_\pi} m_B \right) \int \frac{d^4 l}{(2\pi)^4} (\tau_1)_e \left(-\varepsilon_{lns} (D_2 + (\vec{\tau}_1 \cdot \vec{\tau}_2) E_2) m_B^2 \right) (\tau_1)_e \\
&\quad \times (-\varepsilon_{isr} l_r) l_k \frac{i}{l^2 - m_\pi^2 + i\epsilon} m_B^{-1} \frac{i}{2l^0 + i\epsilon} m_B^{-1} \frac{i}{2l^0 + i\epsilon}
\end{aligned}$$

Using eq. (A.7):

$$= i \frac{3g^2 m_B^2}{16f_\pi^2} C_2 \left(\frac{\varepsilon_{iks} \varepsilon_{lns}}{D-1} \right) \mathcal{I}_{\text{corr}}^5 = i \frac{3g^2 m_B^2}{16f_\pi^2} C_2 \varepsilon_{iks} \varepsilon_{lns} \mathcal{I}_{\text{corr}}^1$$

The other three diagrams, which include vertex (2.31), give the same contribution.



$$= i \left(-i \frac{g}{2f_\pi} m_B \right)^2 \int \frac{d^4 l}{(2\pi)^4} (\tau_1)_e \left(-i (C_1 \delta_{st} \delta_{ln} + C_2 \delta_{st} \delta_{nt} - C_2 \delta_{sn} \delta_{tl}) m_B^2 \right) (\tau_1)_e (-\varepsilon_{isr} l_r) \varepsilon_{tku} l_u$$

$$\times \frac{i}{l^2 - m_\pi^2 + i\epsilon} m_B^{-1} \frac{i}{2l^0 + i\epsilon} m_B^{-1} \frac{i}{2l^0 + i\epsilon}$$

Using eq. (A.7):

$$= i \frac{3g^2 m_B^2}{16f_\pi^2} \frac{2C_1 \delta_{ik} \delta_{ln} - C_2 \delta_{in} \delta_{lk} + C_2 \delta_{il} \delta_{nk}}{D-1} \mathcal{I}_{\text{corr}}^5$$

Replacing $\mathcal{I}_{\text{corr}}^5/(D-1) = \mathcal{I}_{\text{corr}}^1$:

$$= i \frac{3g^2 m_B^2}{16f_\pi^2} (2C_1 \delta_{ik} \delta_{ln} + C_2 \delta_{il} \delta_{nk} - C_2 \delta_{in} \delta_{lk}) \mathcal{I}_{\text{corr}}^1$$

Adding up all eight diagrams gives:

$$\boxed{V_{\text{CCI}}^{\text{eff}}(P^* \bar{P}^* \rightarrow P^* \bar{P}^*) = i \frac{3g^2 m_B^2}{16f_\pi^2} (C_1 \delta_{ik} \delta_{ln} + C_2 \delta_{il} \delta_{nk} - C_2 \delta_{in} \delta_{lk}) (6\mathcal{I}_{\text{corr}}^1)} \quad (5.30)$$

$\mathbf{P}\bar{\mathbf{P}} \rightarrow \mathbf{P}^*\bar{\mathbf{P}}^*$

For clarity's sake, the detailed Feynman diagrams are omitted in the following. Only the respective contributions are assigned to their diagram for simplified summation afterwards. These calculations frequently use eqs. (A.2) to (A.4) and $\mathcal{I}_{\text{corr}}^5/(D-1) = \mathcal{I}_{\text{corr}}^1$.

$$\begin{aligned}
& \text{Diagram 1} = -i \frac{3g^2 m_B^2}{16f_\pi^2} \delta_{kn} (Z_1 - 2Z_2) (\mathcal{I}_{\text{corr}}^1) \\
& \text{Diagram 2} = -i \frac{3g^2 m_B^2}{16f_\pi^2} Z_1 \delta_{kn} (\mathcal{I}_{\text{corr}}^1) \\
& \text{Diagram 3} = -i \frac{3g^2 m_B^2}{16f_\pi^2} Z_2 \delta_{kn} (2\mathcal{I}_{\text{corr}}^1) \\
& 2 \times \text{Diagram 4} = i \frac{3g^2 m_B^2}{16f_\pi^2} C_2 \delta_{kn} (2\mathcal{I}_{\text{corr}}^1) \\
& \text{Diagram 5} = -i \frac{3g^2 m_B^2}{16f_\pi^2} C_2 \delta_{kn} (\mathcal{I}_{\text{corr}}^5 - \mathcal{I}_{\text{corr}}^1) \\
& \text{Diagram 6} = -i \frac{3g^2 m_B^2}{16f_\pi^2} C_2 \delta_{kn} (\mathcal{I}_{\text{corr}}^5 - \mathcal{I}_{\text{corr}}^1) \\
& \text{Diagram 7} = i \frac{3g^2 m_B^2}{16f_\pi^2} Z_1 \delta_{kn} (\mathcal{I}_{\text{corr}}^1) \\
& \text{Diagram 8} = -i \frac{3g^2 m_B^2}{16f_\pi^2} Z_2 \delta_{kn} (\mathcal{I}_{\text{corr}}^5 - \mathcal{I}_{\text{corr}}^1) \\
& \text{Diagram 9} = i \frac{3g^2 m_B^2}{16f_\pi^2} Z_1 \delta_{kn} (\mathcal{I}_{\text{corr}}^1) \\
& \text{Diagram 10} = -i \frac{3g^2 m_B^2}{16f_\pi^2} Z_2 \delta_{kn} (\mathcal{I}_{\text{corr}}^5 - \mathcal{I}_{\text{corr}}^1)
\end{aligned}$$

$$V_{\text{CCI}}^{\text{eff}}(P\bar{P} \rightarrow P^*\bar{P}^*) = i \frac{3g^2 m_B^2}{16f_\pi^2} \delta_{kn} \left((2Z_2 + 4C_2) \mathcal{I}_{\text{corr}}^1 - (2C_2 + 2Z_2) \mathcal{I}_{\text{corr}}^5 \right)$$

(5.31)

$\mathbf{P}\bar{\mathbf{P}}^* \rightarrow \mathbf{P}\bar{\mathbf{P}}$

$$\begin{array}{c} \diagup \quad \diagdown \\ \diagdown \quad \diagup \end{array} = \begin{array}{c} \diagup \quad \diagdown \\ \diagup \quad \diagdown \end{array} = 0$$

Because the indices of the Levi-Civita tensor are always contracted with one another, these diagrams vanish.

$\mathbf{P}^*\bar{\mathbf{P}} \rightarrow \mathbf{P}^*\bar{\mathbf{P}}^*$

$$\begin{array}{l} \begin{array}{c} \diagup \quad \diagdown \\ \diagdown \quad \diagup \end{array} = \frac{3g^2 m_B^2}{16f_\pi^2} Z_2 \epsilon_{ikn} (\mathcal{I}_{\text{corr}}^1) \\ \begin{array}{c} \diagup \quad \diagdown \\ \diagup \quad \diagdown \end{array} = \frac{3g^2 m_B^2}{16f_\pi^2} (Z_1 + Z_2) \epsilon_{ikn} (\mathcal{I}_{\text{corr}}^1) \\ \begin{array}{c} \diagup \quad \diagdown \\ \diagdown \quad \diagup \end{array} = \frac{3g^2 m_B^2}{16f_\pi^2} Z_2 \epsilon_{ikn} (\mathcal{I}_{\text{corr}}^1) \\ \begin{array}{c} \diagup \quad \diagdown \\ \diagup \quad \diagdown \end{array} = \frac{3g^2 m_B^2}{16f_\pi^2} Z_1 \epsilon_{ikn} (\mathcal{I}_{\text{corr}}^1) \\ \begin{array}{c} \diagup \quad \diagdown \\ \diagdown \quad \diagup \end{array} = \frac{3g^2 m_B^2}{16f_\pi^2} Z_2 \epsilon_{ikn} (\mathcal{I}_{\text{corr}}^1) \\ \\ \begin{array}{c} \diagup \quad \diagdown \\ \diagdown \quad \diagup \end{array} = \frac{3g^2 m_B^2}{16f_\pi^2} C_2 \epsilon_{ikn} (\mathcal{I}_{\text{corr}}^1) \\ \begin{array}{c} \diagup \quad \diagdown \\ \diagdown \quad \diagup \end{array} = \frac{3g^2 m_B^2}{16f_\pi^2} C_2 \epsilon_{ikn} (\mathcal{I}_{\text{corr}}^1) \\ \begin{array}{c} \diagup \quad \diagdown \\ \diagdown \quad \diagup \end{array} = -\frac{3g^2 m_B^2}{16f_\pi^2} C_2 \epsilon_{ikn} (\mathcal{I}_{\text{corr}}^1) \\ \begin{array}{c} \diagup \quad \diagdown \\ \diagdown \quad \diagup \end{array} = -\frac{3g^2 m_B^2}{16f_\pi^2} C_2 \epsilon_{ikn} (\mathcal{I}_{\text{corr}}^1) \\ \begin{array}{c} \diagup \quad \diagdown \\ \diagdown \quad \diagup \end{array} = \frac{3g^2 m_B^2}{16f_\pi^2} C_2 \epsilon_{ikn} (2\mathcal{I}_{\text{corr}}^1) \end{array}$$

$$\begin{aligned}
\text{Diagram 1} &= -\frac{3g^2 m_B^2}{16f_\pi^2} Z_1 \epsilon_{ikn} (\mathcal{I}_{\text{corr}}^1) \\
\text{Diagram 2} &= \frac{3g^2 m_B^2}{16f_\pi^2} Z_2 \epsilon_{ikn} (\mathcal{I}_{\text{corr}}^1) \\
\text{Diagram 3} &= \frac{3g^2 m_B^2}{16f_\pi^2} Z_2 \epsilon_{ikn} (\mathcal{I}_{\text{corr}}^1) \\
\text{Diagram 4} &= \frac{3g^2 m_B^2}{16f_\pi^2} Z_2 \epsilon_{ikn} (\mathcal{I}_{\text{corr}}^1) \\
\text{Diagram 5} &= -\frac{3g^2 m_B^2}{16f_\pi^2} (Z_1 - Z_2) \epsilon_{ikn} (\mathcal{I}_{\text{corr}}^1)
\end{aligned}$$

$$V_{\text{CCI}}^{\text{eff}}(P^* \bar{P} \rightarrow P^* \bar{P}^*) = \pm \frac{3g^2 m_B^2}{16f_\pi^2} \epsilon_{ikn} (8Z_2 + 2C_2) \mathcal{I}_{\text{corr}}^1 \quad (5.32)$$

The lower sign denotes the corresponding anti-reaction of $P\bar{P}^* \rightarrow P^*\bar{P}$ with free polarization indices l, k, n instead of i, k, n , respectively.

6 The effective potentials

Below, we collect all contributions to $P^{(*)}\bar{P}^{(*)} \rightarrow P^{(*)}\bar{P}^{(*)}$ scattering, both at LO and at NLO. Summing up the triangles, the football and the boxes finally gives the total 2PE potential. The contributions from $\mathcal{L}_{4H}^{(2)}$ are not explicitly stated (cf. sec. 2.2).

The R -terms, which handle the infinities (cf. sec. B), are omitted. $L(q)$ is defined in eq. (A.14). The polarization vectors $\epsilon_{1,i}$, $\epsilon_{1',k}^*$, $\epsilon_{2,l}^*$ and $\epsilon_{2',n}$ can be attached to truncate the remaining indices i, k, l and n . From now on, they will carry an index to denote which particle they belong to as this allows us to apply the partial wave projectors. D_1, E_1, D_2, E_2 remain to be extracted from experimental data.

$P\bar{P} \rightarrow P\bar{P}$

$$V_{\text{CI}}^{\text{eff}}(P\bar{P} \rightarrow P\bar{P}) = C_1 m_B^2 = (D_1 + (\vec{\tau}_1 \cdot \vec{\tau}_2) E_1) m_B^2$$

$$V_{\text{1PE}}^{\text{eff}}(P\bar{P} \rightarrow P\bar{P}) = 0$$

$$\begin{aligned} V_{\text{2PE}}^{\text{eff}}(P\bar{P} \rightarrow P\bar{P}) &= i \frac{m_B^2}{4f_\pi^4} (\vec{\tau}_1 \cdot \vec{\tau}_2) \left(-g^2 I_{\text{tr}} + I_{\text{fb}} + \frac{g^4}{4} I_{\text{box}}^2 \right) \\ &= -\frac{m_B^2}{384\pi^2 f_\pi^4} (\vec{\tau}_1 \cdot \vec{\tau}_2) \left\{ \vec{q}^2 \left(\frac{5}{24} g^4 + \frac{13}{6} g^2 + \frac{5}{6} \right) + m_\pi^2 (4g^4 + 2g^2 + 4) \right. \\ &\quad \left. + \ln\left(\frac{m_\pi}{\mu}\right) \left[\vec{q}^2 \left(\frac{23}{4} g^4 - 5g^2 - 1 \right) + m_\pi^2 \left(\frac{45}{2} g^4 - 18g^2 - 6 \right) \right] \right. \\ &\quad \left. + L(q) \left[\vec{q}^2 \left(\frac{23}{4} g^4 - 5g^2 - 1 \right) + m_\pi^2 (5g^4 - 8g^2 - 4) + \frac{12g^4 m_\pi^4}{4m_\pi^2 + \vec{q}^2} \right] \right\} \end{aligned}$$

$$\begin{aligned} V_{\text{CCI}}^{\text{eff}}(P\bar{P} \rightarrow P\bar{P}) &= i \frac{3g^2 m_B^2}{16f_\pi^2} C_1 (2I_{\text{corr}}^5) \\ &= \frac{3g^2 m_B^2 m_\pi^2}{64\pi^2 f_\pi^2} (D_1 + (\vec{\tau}_1 \cdot \vec{\tau}_2) E_1) \left(3 \ln\left(\frac{m_\pi}{\mu}\right) + 1 \right) \end{aligned}$$

$\mathbf{P}^* \bar{\mathbf{P}} \rightarrow \mathbf{P}^* \bar{\mathbf{P}}$

$$\begin{aligned}
V_{\text{CI}}^{\text{eff}}(P^* \bar{P} \rightarrow P^* \bar{P}) &= C_1 m_B^2 \delta_{ik} = (D_1 + (\vec{\tau}_1 \cdot \vec{\tau}_2) E_1) m_B^2 \delta_{ik} \\
V_{\text{1PE}}^{\text{eff}}(P^* \bar{P} \rightarrow P^* \bar{P}) &= 0 \\
V_{\text{2PE}}^{\text{eff}}(P^* \bar{P} \rightarrow P^* \bar{P}) &= i \frac{m_B^2}{4f_\pi^4} (\vec{\tau}_1 \cdot \vec{\tau}_2) \delta_{ik} \left(-g^2 \mathcal{I}_{\text{tr}} + \mathcal{I}_{\text{fb}} + \frac{g^4}{4} \mathcal{I}_{\text{box}}^2 \right) \\
&= \delta_{ik} V_{\text{2PE}}^{\text{eff}}(P \bar{P} \rightarrow P \bar{P}) \\
V_{\text{CCI}}^{\text{eff}}(P^* \bar{P} \rightarrow P^* \bar{P}) &= i \frac{3g^2 m_B^2}{16f_\pi^2} C_1 \delta_{ik} (\mathcal{I}_{\text{corr}}^5 + 3\mathcal{I}_{\text{corr}}^1) \\
&= \frac{3g^2 m_B^2 m_\pi^2}{64\pi^2 f_\pi^2} (D_1 + (\vec{\tau}_1 \cdot \vec{\tau}_2) E_1) \delta_{ik} \left(3 \ln \left(\frac{m_\pi}{\mu} \right) + \frac{1}{2} \right)
\end{aligned}$$

 $\mathbf{P}^* \bar{\mathbf{P}} \rightarrow \mathbf{P} \bar{\mathbf{P}}^*$

$$\begin{aligned}
V_{\text{CI}}^{\text{eff}}(P^* \bar{P} \rightarrow P \bar{P}^*) &= C_2 m_B^2 \delta_{in} = (D_2 + (\vec{\tau}_1 \cdot \vec{\tau}_2) E_2) m_B^2 \delta_{in} \\
V_{\text{1PE}}^{\text{eff}}(P^* \bar{P} \rightarrow P \bar{P}^*) &= -\frac{g^2 m_B^2}{4f_\pi^2} (\vec{\tau}_1 \cdot \vec{\tau}_2) \frac{q_i q_n}{\vec{q}^2 + m_\pi^2} \\
V_{\text{2PE}}^{\text{eff}}(P^* \bar{P} \rightarrow P \bar{P}^*) &= -i \frac{3m_B^2}{32f_\pi^4} g^4 (\mathcal{I}_{\text{box}}^3)_{in} \\
&= \frac{m_B^2}{384\pi^2 f_\pi^4} g^4 (\delta_{in} \vec{q}^2 - q_i q_n) \left(\frac{9}{4} - \frac{9}{2} L(q) - \frac{9}{2} \ln \left(\frac{m_\pi}{\mu} \right) \right) \\
V_{\text{CCI}}^{\text{eff}}(P^* \bar{P} \rightarrow P \bar{P}^*) &= i \frac{3g^2 m_B^2}{16f_\pi^2} \delta_{in} ((4C_2 + 2Z_2) \mathcal{I}_{\text{corr}}^1 - (2C_2 + 2Z_2) \mathcal{I}_{\text{corr}}^5) \\
&= -\frac{3g^2 m_B^2 m_\pi^2}{64\pi^2 f_\pi^2} \delta_{in} \left\{ \left((D_2 + 2E_2) + (\vec{\tau}_1 \cdot \vec{\tau}_2) \frac{2D_2 + 7E_2}{3} \right) \ln \left(\frac{m_\pi}{\mu} \right) \right. \\
&\quad \left. + D_2 + E_2 + (\vec{\tau}_1 \cdot \vec{\tau}_2) \frac{D_2 + 5E_2}{3} \right\}
\end{aligned}$$

$\mathbf{P}^* \bar{\mathbf{P}}^* \rightarrow \mathbf{P}^* \bar{\mathbf{P}}^*$

$$\begin{aligned}
V_{\text{CI}}^{\text{eff}}(P^* \bar{P}^* \rightarrow P^* \bar{P}^*) &= (C_1 \delta_{ik} \delta_{ln} + C_2 \delta_{il} \delta_{kn} - C_2 \delta_{in} \delta_{kl}) m_B^2 \\
&= ((D_1 \delta_{ik} \delta_{ln} + D_2 \delta_{il} \delta_{kn} - D_2 \delta_{in} \delta_{kl}) \\
&\quad + (\vec{\tau}_1 \cdot \vec{\tau}_2) (E_1 \delta_{ik} \delta_{ln} + E_2 \delta_{il} \delta_{kn} - E_2 \delta_{in} \delta_{kl})) m_B^2 \\
V_{\text{1PE}}^{\text{eff}}(P^* \bar{P}^* \rightarrow P^* \bar{P}^*) &= -\frac{g^2 m_B^2}{4f_\pi^2} (\vec{\tau}_1 \cdot \vec{\tau}_2) \varepsilon_{ikr} \varepsilon_{lns} \frac{q_r q_s}{\vec{q}^2 + m_\pi^2} \\
V_{\text{2PE}}^{\text{eff}}(P^* \bar{P}^* \rightarrow P^* \bar{P}^*) &= i \frac{m_B^2}{4f_\pi^4} (\vec{\tau}_1 \cdot \vec{\tau}_2) \delta_{ik} \delta_{ln} \left(-g^2 \mathcal{I}_{\text{tr}} + \mathcal{I}_{\text{fb}} + \frac{g^4}{4} \mathcal{I}_{\text{box}}^2 \right) \\
&= \delta_{ik} \delta_{ln} V_{\text{2PE}}^{\text{eff}}(P\bar{P} \rightarrow P\bar{P}) \\
V_{\text{CCI}}^{\text{eff}}(P^* \bar{P}^* \rightarrow P^* \bar{P}^*) &= i \frac{3g^2 m_B^2}{16f_\pi^2} (C_1 \delta_{ik} \delta_{ln} + C_2 \delta_{il} \delta_{nk} - C_2 \delta_{in} \delta_{lk}) (6\mathcal{I}_{\text{corr}}^1) \\
&= \frac{9g^2 m_B^2 m_\pi^2}{64\pi^2 f_\pi^2} \left\{ (D_1 \delta_{ik} \delta_{ln} + D_2 \delta_{il} \delta_{nk} - D_2 \delta_{in} \delta_{lk}) \right. \\
&\quad \left. + (\vec{\tau}_1 \cdot \vec{\tau}_2) (E_1 \delta_{ik} \delta_{ln} + E_2 \delta_{il} \delta_{nk} - E_2 \delta_{in} \delta_{lk}) \right\} \ln\left(\frac{m_\pi}{\mu}\right)
\end{aligned}$$

 $\mathbf{P}\bar{\mathbf{P}} \rightarrow \mathbf{P}^* \bar{\mathbf{P}}^*$

$$\begin{aligned}
V_{\text{CI}}^{\text{eff}}(P\bar{P} \rightarrow P^* \bar{P}^*) &= C_2 m_B^2 \delta_{kn} = (D_2 + (\vec{\tau}_1 \cdot \vec{\tau}_2) E_2) m_B^2 \delta_{kn} \\
V_{\text{1PE}}^{\text{eff}}(P\bar{P} \rightarrow P^* \bar{P}^*) &= -\frac{g^2 m_B^2}{4f_\pi^2} (\vec{\tau}_1 \cdot \vec{\tau}_2) \frac{q_k q_n}{\vec{q}^2 + m_\pi^2} \\
V_{\text{2PE}}^{\text{eff}}(P\bar{P} \rightarrow P^* \bar{P}^*) &= -i \frac{3m_B^2}{32f_\pi^4} g^4 (\mathcal{I}_{\text{box}}^3)_{kn} \\
&= \frac{m_B^2}{384\pi^2 f_\pi^4} g^4 (\delta_{kn} \vec{q}^2 - q_k q_n) \left(\frac{9}{4} - \frac{9}{2} L(q) - \frac{9}{2} \ln\left(\frac{m_\pi}{\mu}\right) \right) \\
V_{\text{CCI}}^{\text{eff}}(P\bar{P} \rightarrow P^* \bar{P}^*) &= i \frac{3g^2 m_B^2}{16f_\pi^2} \delta_{kn} ((2Z_2 + 4C_2) \mathcal{I}_{\text{corr}}^1 - (2C_2 + 2Z_2) \mathcal{I}_{\text{corr}}^5) \\
&= -\frac{3g^2 m_B^2 m_\pi^2}{64\pi^2 f_\pi^2} \delta_{kn} \left\{ \left((D_2 + 2E_2) + (\vec{\tau}_1 \cdot \vec{\tau}_2) \frac{2D_2 + 7E_2}{3} \right) \ln\left(\frac{m_\pi}{\mu}\right) \right. \\
&\quad \left. + D_2 + E_2 + (\vec{\tau}_1 \cdot \vec{\tau}_2) \frac{D_2 + 5E_2}{3} \right\}
\end{aligned}$$

$P\bar{P}^* \rightarrow P\bar{P}$

$$\begin{aligned}
 V_{\text{CI}}^{\text{eff}}(P\bar{P}^* \rightarrow P\bar{P}) &= V_{\text{1PE}}^{\text{eff}}(P\bar{P}^* \rightarrow P\bar{P}) \\
 &= V_{\text{2PE}}^{\text{eff}}(P\bar{P}^* \rightarrow P\bar{P}) = V_{\text{CCI}}^{\text{eff}}(P\bar{P}^* \rightarrow P\bar{P}) \\
 &= 0
 \end{aligned}$$

$P^*\bar{P} \rightarrow P^*\bar{P}$

$$\begin{aligned}
 V_{\text{CI}}^{\text{eff}}(P^*\bar{P} \rightarrow P^*\bar{P}) &= \pm i C_2 \varepsilon_{ikn} m_B^2 = \pm i (D_2 + (\vec{\tau}_1 \cdot \vec{\tau}_2) E_2) \varepsilon_{ikn} m_B^2 \\
 V_{\text{1PE}}^{\text{eff}}(P^*\bar{P} \rightarrow P^*\bar{P}) &= \mp i \frac{g^2 m_B^2}{4 f_\pi^2} (\vec{\tau}_1 \cdot \vec{\tau}_2) \frac{\varepsilon_{ikr} q_r q_n}{\vec{q}^2 + m_\pi^2} \\
 V_{\text{2PE}}^{\text{eff}}(P^*\bar{P} \rightarrow P^*\bar{P}) &= \mp \frac{3 m_B^2}{32 f_\pi^4} g^4 (I_{\text{box}}^4)_{ikn} \\
 &= \mp i \frac{m_B^2}{384 \pi^2 f_\pi^4} g^4 (\varepsilon_{nku} q_u q_i - \varepsilon_{niu} q_u q_k) \left(\frac{9}{4} - \frac{9}{2} L(q) - \frac{9}{2} \ln \left(\frac{m_\pi}{\mu} \right) \right) \\
 V_{\text{CCI}}^{\text{eff}}(P^*\bar{P} \rightarrow P^*\bar{P}) &= \pm \frac{3 g^2 m_B^2}{16 f_\pi^2} \varepsilon_{ikn} (8Z_2 + 2C_2) I_{\text{corr}}^1 \\
 &= \mp i \frac{3 g^2 m_B^2 m_\pi^2}{64 \pi^2 f_\pi^2} \varepsilon_{ikn} \left((2D_2 + 8E_2) + (\vec{\tau}_1 \cdot \vec{\tau}_2) \frac{8D_2 + 22E_2}{3} \right) \ln \left(\frac{m_\pi}{\mu} \right)
 \end{aligned}$$

The lower sign denotes the corresponding anti-vertex with two \bar{P}^* -mesons and polarization indices l, k, n instead of i, k, n , respectively.

7 Partial wave decomposition

For the coupled-channel LSE (eq. (3.1)), we need the effective potentials from sec. 6 decomposed into the four channels $J^{PC} = 0^{++}, 1^{++}, 1^{+-}, 2^{++}$ and their respective basis (cf. sec. 3). For this, we use:⁶⁷

$$V_{\alpha\beta}^{\text{eff}}(J^{PC}) = \frac{1}{2J+1} \int \frac{d\Omega_n}{4\pi} \frac{d\Omega_{n'}}{4\pi} \text{Tr} \left[P^\dagger(\alpha, \vec{n}') V^{\text{eff}} P(\beta, \vec{n}) \right], \quad (7.1)$$

with $\vec{n} = \vec{p}/|\vec{p}|$ and $\vec{n}' = \vec{p}'/|\vec{p}'|$. Due to the spacial symmetry of this $2 \rightarrow 2$ reaction, only the angle between incoming and outgoing momenta will be important: $\Theta = \angle(\vec{p}, \vec{p}')$. Thus, we can rewrite:

$$V_{\alpha\beta}^{\text{eff}}(J^{PC}) = \frac{1}{2J+1} \int_{-1}^{+1} \frac{dx}{2} \text{Tr} \left[P^\dagger(\alpha, \vec{n}') V^{\text{eff}} P(\beta, \vec{n}) \right], \quad (7.2)$$

with $x = \cos(\Theta)$. We take the trace over the indices of total angular momentum since J is conserved.

The partial wave projectors can be found in a paper by Nefediev et al.⁶⁸ (the explicit arguments \vec{n}, \vec{n}' are omitted for brevity's sake):

$$\begin{aligned} P(B\bar{B}({}^1S_0)) &= 1 & P^\dagger(B\bar{B}({}^1S_0)) &= 1 \\ P(B^*\bar{B}^*({}^1S_0)) &= \frac{1}{\sqrt{3}} (\vec{\epsilon}_1^* \cdot \vec{\epsilon}_2) & P^\dagger(B^*\bar{B}^*({}^1S_0)) &= \frac{1}{\sqrt{3}} (\vec{\epsilon}_2^* \cdot \vec{\epsilon}_1) \\ P(B^*\bar{B}^*({}^5D_0)) &= -\sqrt{\frac{3}{8}} S_{xy} v_{xy} & P^\dagger(B^*\bar{B}^*({}^5D_0)) &= -\sqrt{\frac{3}{8}} S'_{st} v'_{st} \\ \\ P(B\bar{B}^*({}^3S_1))_x &= \epsilon_{2,x} & P^\dagger(B\bar{B}^*({}^3S_1))_s &= \epsilon_{2',s}^* \\ P(B^*\bar{B}({}^3S_1))_h &= \epsilon_{1,h}^* & P^\dagger(B^*\bar{B}({}^3S_1))_g &= \epsilon_{1',g} \\ P(B\bar{B}^*({}^3D_1))_x &= -\frac{3}{\sqrt{2}} \epsilon_{2,y} v_{xy} & P^\dagger(B\bar{B}^*({}^3D_1))_s &= -\frac{3}{\sqrt{2}} \epsilon_{2',t}^* v'_{st} \\ P(B^*\bar{B}({}^3D_1))_x &= -\frac{3}{\sqrt{2}} \epsilon_{1,y}^* v_{xy} & P^\dagger(B^*\bar{B}({}^3D_1))_s &= -\frac{3}{\sqrt{2}} \epsilon_{1',t}^* v'_{st} \\ P(B^*\bar{B}^*({}^5D_1))_h &= -\frac{3}{\sqrt{2}} i \epsilon_{h x j} S_{xy} v_{jy} & P^\dagger(B^*\bar{B}^*({}^5D_1))_g &= +\frac{3}{\sqrt{2}} i \epsilon_{g s j} S'_{st} v'_{jt} \end{aligned}$$

⁶⁷Nefediev et al., op. cit., pp.8,23f.

⁶⁸Ibid.

$$\begin{aligned}
P(B^* \bar{B}^*(^3S_1))_x &= A_x & P^\dagger(B^* \bar{B}^*(^3S_1))_s &= A'_s \\
P(B^* \bar{B}^*(^3D_1))_h &= -\frac{3}{\sqrt{2}} A_x v_{hx} & P^\dagger(B^* \bar{B}^*(^3D_1))_g &= -\frac{3}{\sqrt{2}} A'_s v'_{gs} \\
P(B \bar{B}(^1D_2))_{xy} &= -\sqrt{\frac{15}{2}} v_{xy} & P^\dagger(B \bar{B}(^1D_2))_{st} &= -\sqrt{\frac{15}{2}} v'_{st} \\
P(B \bar{B}(^3D_2))_{zy} &= -\frac{\sqrt{5}}{2} i \epsilon_{2,h} (\epsilon_{zhx} v_{xy} + \epsilon_{yhx} v_{xz}) & P^\dagger(B \bar{B}(^3D_2))_{tj} &= +\frac{\sqrt{5}}{2} i \epsilon_{2',g}^* (\epsilon_{jgs} v'_{st} + \epsilon_{tgs} v'_{sj}) \\
P(B^* \bar{B}^*(^5S_2))_{xy} &= \frac{1}{2} S_{xy} & P^\dagger(B^* \bar{B}^*(^5S_2))_{st} &= \frac{1}{2} S'_{st} \\
P(B^* \bar{B}^*(^1D_2))_{xy} &= -\sqrt{\frac{5}{2}} (\vec{\epsilon}_1^* \cdot \vec{\epsilon}_2) v_{xy} & P^\dagger(B^* \bar{B}^*(^1D_2))_{st} &= -\sqrt{\frac{5}{2}} (\vec{\epsilon}_{2'}^* \cdot \vec{\epsilon}_{1'}) v'_{st} \\
P(B^* \bar{B}^*(^5D_2))_{zy} &= -\sqrt{\frac{45}{56}} (S_{zx} v_{xy} + S_{yx} v_{xz} - \frac{2}{3} \delta_{zy} S_{lx} v_{lx}) \\
P^\dagger(B^* \bar{B}^*(^5D_2))_{jt} &= -\sqrt{\frac{45}{56}} (S'_{js} v'_{st} + S'_{ts} v'_{sj} - \frac{2}{3} \delta_{jt} S'_{ls} v'_{ls}) \\
P(B^* \bar{B}^*(^5G_2))_{zw} &= \sqrt{\frac{175}{32}} S_{xy} v_{xyzw} & P^\dagger(B^* \bar{B}^*(^5G_2))_{uw} &= \sqrt{\frac{175}{32}} S'_{st} v'_{stuw} \\
v_{xy} &= n_x n_y - \frac{1}{3} \delta_{xy} & v'_{st} &= n'_s n'_t - \frac{1}{3} \delta_{st} \\
S_{xy} &= \epsilon_{1,x}^* \epsilon_{2,y} + \epsilon_{1,y}^* \epsilon_{2,x} - \frac{2}{3} \delta_{xy} (\vec{\epsilon}_1^* \cdot \vec{\epsilon}_2) & S'_{st} &= \epsilon_{2',s}^* \epsilon_{1',t} + \epsilon_{2',t}^* \epsilon_{1',s} - \frac{2}{3} \delta_{st} (\vec{\epsilon}_{2'}^* \cdot \vec{\epsilon}_{1'}) \\
A_x &= \frac{i}{\sqrt{2}} \epsilon_{xyz} \epsilon_{1,y}^* \epsilon_{2,z} & A'_s &= \frac{i}{\sqrt{2}} \epsilon_{stu} \epsilon_{1',t} \epsilon_{2',u}^* \\
v_{xyzw} &= n_x n_y n_z n_w - \frac{1}{7} (n_x n_y \delta_{zw} + n_x n_z \delta_{yw} + n_x n_w \delta_{yz} + n_y n_z \delta_{xw} + n_y n_w \delta_{xz} + n_z n_w \delta_{xy}) \\
&\quad + \frac{1}{35} (\delta_{xy} \delta_{zw} + \delta_{xz} \delta_{yw} + \delta_{xw} \delta_{yz}) \\
v'_{stuw} &= n'_s n'_t n'_u n'_v - \frac{1}{7} (n'_s n'_t \delta_{uw} + n'_s n'_u \delta_{tv} + n'_s n'_v \delta_{tu} + n'_t n'_u \delta_{sv} + n'_t n'_v \delta_{su} + n'_u n'_v \delta_{st}) \\
&\quad + \frac{1}{35} (\delta_{st} \delta_{uw} + \delta_{su} \delta_{tv} + \delta_{sv} \delta_{tu})
\end{aligned}$$

To obtain the projected states of $J^P = 1^+$ for C -parity \pm , we need two different projectors for the two different initial states, e.g.:

$$\begin{aligned}
|B \bar{B}^*, \pm\rangle &= \frac{1}{\sqrt{2}} (|B \bar{B}^*\rangle \pm |B^* \bar{B}\rangle) \\
\Rightarrow P(B \bar{B}(^3S_1, \pm)) |B \bar{B}^*, \pm\rangle &= \frac{1}{\sqrt{2}} (P(B \bar{B}(^3S_1)) |B \bar{B}^*\rangle \pm P(B^* \bar{B}(^3S_1)) |B^* \bar{B}\rangle)
\end{aligned}$$

The projectors are normalized as:

$$\int \frac{d\Omega_n}{4\pi} P^\dagger(\alpha, \vec{n}) P(\alpha, \vec{n}) = 2J + 1$$

Some exemplary calculations for the partial wave projected effective potentials are given below. We take the spin sums (denoted with \sum and without explicit spin labels) of matching polarization vectors as described in eq. (2.15):

$$\begin{aligned} (V_{\text{CI}}^{\text{eff}})_{22}(0^{++}) &= \frac{1}{2 \cdot 0 + 1} \int_{-1}^{+1} \frac{dx}{2} P^\dagger(B^* \bar{B}^* (^1S_0)) V_{\text{CI}}^{\text{eff}}(B^* \bar{B}^* \rightarrow B^* \bar{B}^*) P(B^* \bar{B}^* (^1S_0)) \\ &= \int_{-1}^{+1} \frac{dx}{2} \frac{1}{\sqrt{3}} (\vec{\epsilon}_{2'}^* \cdot \vec{\epsilon}_{1'}) m_B^2 (C_1 (\vec{\epsilon}_1 \cdot \vec{\epsilon}_1^*) (\vec{\epsilon}_2^* \cdot \vec{\epsilon}_{2'}) \\ &\quad + C_2 (\vec{\epsilon}_1 \times \vec{\epsilon}_1^*) (\vec{\epsilon}_2^* \times \vec{\epsilon}_{2'})) \frac{1}{\sqrt{3}} (\vec{\epsilon}_1^* \cdot \vec{\epsilon}_2) \\ &= \frac{m_B^2}{3} \int_{-1}^{+1} \frac{dx}{2} \left(C_1 \left(\sum \epsilon_{2',i}^* \epsilon_{2',k} \right) \left(\sum \epsilon_{1',j}^* \epsilon_{1',i} \right) \left(\sum \epsilon_{2,k}^* \epsilon_{2,n} \right) \left(\sum \epsilon_{1,n}^* \epsilon_{1,j} \right) \right. \\ &\quad \left. + C_2 \left(\sum \epsilon_{2',i}^* \epsilon_{2',y} \right) \left(\sum \epsilon_{1',s}^* \epsilon_{1',i} \right) \left(\sum \epsilon_{2,x}^* \epsilon_{2,n} \right) \left(\sum \epsilon_{1,n}^* \epsilon_{1,r} \right) \epsilon_{rst} \epsilon_{xyt} \right) \\ &= \frac{m_B^2}{3} \int_{-1}^{+1} \frac{dx}{2} (C_1 \delta_{ik} \delta_{ji} \delta_{kn} \delta_{nj} + C_2 \delta_{iy} \delta_{si} \delta_{xn} \delta_{nr} \epsilon_{rst} \epsilon_{xyt}) \\ &= m_B^2 (C_1 + 2C_2) \end{aligned}$$

In the case $J = 0$, we are in no need of a trace since P, P^\dagger are scalars.

$$\begin{aligned}
(V_{\text{CI}}^{\text{eff}})_{11}(1^{+\pm}) &= \frac{1}{2 \cdot 1 + 1} \int_{-1}^{+1} \frac{dx}{2} \text{Tr} \left[P^\dagger(B\bar{B}^*(^3S_1, \pm)) V_{\text{CI}}^{\text{eff}} P(B\bar{B}^*(^3S_1, \pm)) \right] \\
&= \frac{1}{3} \int_{-1}^{+1} \frac{dx}{2} \text{Tr} \left[\frac{1}{\sqrt{2}} (P^\dagger(B\bar{B}^*(^3S_1)) \pm P^\dagger(B^*\bar{B}(^3S_1))) \right. \\
&\quad \left. \times V_{\text{CI}}^{\text{eff}} \frac{1}{\sqrt{2}} (P(B\bar{B}^*(^3S_1)) \pm P(B^*\bar{B}(^3S_1))) \right] \\
&= \frac{m_B^2}{6} \int_{-1}^{+1} \frac{dx}{2} \text{Tr} \left[C_1 \epsilon_{2',s}^* (\vec{\epsilon}_2^* \cdot \vec{\epsilon}_{2'}) \epsilon_{2,x} \pm C_2 \epsilon_{1',g}^* (\vec{\epsilon}_2^* \cdot \vec{\epsilon}_{1'}) \epsilon_{2,x} \right. \\
&\quad \left. \pm C_2 \epsilon_{2',s}^* (\vec{\epsilon}_1 \cdot \vec{\epsilon}_{2'}) \epsilon_{1,h}^* + C_1 \epsilon_{1',g}^* (\vec{\epsilon}_{1'}^* \cdot \vec{\epsilon}_1) \epsilon_{1,h}^* \right] \\
&= \frac{m_B^2}{6} \int_{-1}^{+1} \frac{dx}{2} C_1 \text{Tr} \left[\left(\sum \epsilon_{2',s}^* \epsilon_{2',j} \right) \left(\sum \epsilon_{2,j}^* \epsilon_{2,x} \right) + \left(\sum \epsilon_{1',k}^* \epsilon_{1',g} \right) \left(\sum \epsilon_{1,h}^* \epsilon_{1,k} \right) \right] \\
&\quad \pm C_2 \text{Tr} \left[\left(\sum \epsilon_{1',m}^* \epsilon_{1',g} \right) \left(\sum \epsilon_{2,m}^* \epsilon_{2,x} \right) + \left(\sum \epsilon_{2',s}^* \epsilon_{2',r} \right) \left(\sum \epsilon_{1,h}^* \epsilon_{1,r} \right) \right] \\
&= \frac{m_B^2}{6} \int_{-1}^{+1} \frac{dx}{2} C_1 \text{Tr} [\delta_{sj} \delta_{jx} + \delta_{kg} \delta_{hk}] \pm C_2 \text{Tr} [\delta_{mg} \delta_{mx} + \delta_{sr} \delta_{hr}] \\
&= \frac{m_B^2}{6} \int_{-1}^{+1} \frac{dx}{2} 6C_1 \pm 6C_2 \\
&= m_B^2 (C_1 \pm C_2)
\end{aligned}$$

The partial wave projected potentials are collected below. The pertinent integrals of the decomposition are often abbreviated as $Q(p', p)$, $R(p', p)$, $S(p', p)$. Their explicit expressions are given in appendix E. We denote $|\vec{p}'| = p'$ and $|\vec{p}| = p$. $C_i = D_i + (\vec{\tau}_1 \cdot \vec{\tau}_2) E_i$ is used. Because the 2PE is of special interest, its full potentials will be repeated after the partial wave decomposed potentials for easy comparability.

7.1 $\mathbf{J}^{\text{PC}} = \mathbf{0}^{++}$

$$0^{++} : \quad \alpha, \beta = \{B\bar{B}({}^1S_0), B^*\bar{B}^*({}^1S_0), B^*\bar{B}^*({}^5D_0)\} = \{1, 2, 3\}$$

$$V_{\text{CI}}^{\text{eff}}(0^{++}) = m_B^2 \begin{pmatrix} C_1 & \sqrt{3}C_2 & 0 \\ \sqrt{3}C_2 & C_1 + 2C_2 & 0 \\ 0 & 0 & 0 \end{pmatrix}$$

$$V_{\text{IPE}}^{\text{eff}}(0^{++}) = -\frac{g^2 m_B^2}{4f_\pi^2}(\vec{\tau}_1 \cdot \vec{\tau}_2) \begin{pmatrix} 0 & \frac{1}{\sqrt{3}}Q_2 & \frac{1}{\sqrt{6}}(Q_2 - 3Q_n) \\ \frac{1}{\sqrt{3}}Q_2 & \frac{2}{3}Q_2 & \frac{1}{\sqrt{8}}Q_n \\ \frac{1}{\sqrt{6}}(Q_2 - 3Q_{n'}) & \frac{1}{\sqrt{8}}Q_{n'} & \frac{3}{4}(-Q_2 + Q_n + Q_{n'}) \end{pmatrix}$$

$$V_{\text{CCI}}^{\text{eff}}(0^{++}) = \frac{3g^2 m_B^2 m_\pi^2}{64\pi^2 f_\pi^2} \begin{pmatrix} C_1 \left(3 \ln\left(\frac{m_\pi}{\mu}\right) + 1\right) & -\sqrt{3}\{\dots\} & 0 \\ -\sqrt{3}\{\dots\} & 3(C_1 + 2C_2) \ln\left(\frac{m_\pi}{\mu}\right) & 0 \\ 0 & 0 & 0 \end{pmatrix}$$

$$\text{with } \{\dots\} = \left((D_2 + 2E_2) + (\vec{\tau}_1 \cdot \vec{\tau}_2) \frac{2D_2 + 7E_2}{3} \right) \ln\left(\frac{m_\pi}{\mu}\right) + D_2 + E_2 + (\vec{\tau}_1 \cdot \vec{\tau}_2) \frac{D_2 + 5E_2}{3}$$

$$V_{\text{2PE}}^{\text{eff}}(0^{++}) = -\frac{m_B^2}{384\pi^2 f_\pi^4}(\vec{\tau}_1 \cdot \vec{\tau}_2) \begin{pmatrix} S_0 & \sqrt{27}g^4\{\dots\} & -\sqrt{\frac{27}{2}}g^4[\dots] \\ \sqrt{27}g^4\{\dots\} & S_0 & 0 \\ -\sqrt{\frac{27}{2}}g^4[\dots]' & 0 & S_2 \end{pmatrix}$$

$$\text{with } \{\dots\} = (p'^2 + p^2) \left(\frac{1}{2} - \ln\left(\frac{m_\pi}{\mu}\right) \right) - R_2$$

$$\text{and } [\dots] = 2p^2 \left(\frac{1}{2} - \ln\left(\frac{m_\pi}{\mu}\right) \right) + R_2 - 3R_n$$

$$\text{and } [\dots]' = 2p'^2 \left(\frac{1}{2} - \ln\left(\frac{m_\pi}{\mu}\right) \right) + R_2 - 3R_{n'}$$

The full 2PE potentials for the four cases read:

$$\begin{aligned}
V_{2\text{PE}}^{\text{eff}}(B\bar{B} \rightarrow B\bar{B}) &= -\frac{m_B^2}{384\pi^2 f_\pi^4} (\vec{\tau}_1 \cdot \vec{\tau}_2) \left\{ \vec{q}^2 \left(\frac{5}{24}g^4 + \frac{13}{6}g^2 + \frac{5}{6} \right) + m_\pi^2 (4g^4 + 2g^2 + 4) \right. \\
&\quad \left. + \ln\left(\frac{m_\pi}{\mu}\right) \left[\vec{q}^2 \left(\frac{23}{4}g^4 - 5g^2 - 1 \right) + m_\pi^2 \left(\frac{45}{2}g^4 - 18g^2 - 6 \right) \right] \right. \\
&\quad \left. + L(q) \left[\vec{q}^2 \left(\frac{23}{4}g^4 - 5g^2 - 1 \right) + m_\pi^2 (5g^4 - 8g^2 - 4) + \frac{12g^4 m_\pi^4}{4m_\pi^2 + \vec{q}^2} \right] \right\} \\
V_{2\text{PE}}^{\text{eff}}(B\bar{B} \rightarrow B^* \bar{B}^*) &= \frac{m_B^2}{384\pi^2 f_\pi^4} g^4 \left((\vec{\epsilon}_{1'}^* \cdot \vec{\epsilon}_{2'}) \vec{q}^2 - (\vec{\epsilon}_{1'}^* \cdot \vec{q})(\vec{\epsilon}_{2'} \cdot \vec{q}) \right) \left(\frac{9}{4} - \frac{9}{2}L(q) - \frac{9}{2} \ln\left(\frac{m_\pi}{\mu}\right) \right) \\
V_{2\text{PE}}^{\text{eff}}(B^* \bar{B}^* \rightarrow B\bar{B}) &= \frac{m_B^2}{384\pi^2 f_\pi^4} g^4 \left((\vec{\epsilon}_2^* \cdot \vec{\epsilon}_1) \vec{q}^2 - (\vec{\epsilon}_2^* \cdot \vec{q})(\vec{\epsilon}_1 \cdot \vec{q}) \right) \left(\frac{9}{4} - \frac{9}{2}L(q) - \frac{9}{2} \ln\left(\frac{m_\pi}{\mu}\right) \right) \\
V_{2\text{PE}}^{\text{eff}}(B^* \bar{B}^* \rightarrow B^* \bar{B}^*) &= (\vec{\epsilon}_{1'}^* \cdot \vec{\epsilon}_1^*)(\vec{\epsilon}_2^* \cdot \vec{\epsilon}_{2'}) V_{2\text{PE}}^{\text{eff}}(B\bar{B} \rightarrow B\bar{B})
\end{aligned}$$

7.2 $\mathbf{J}^{\text{PC}} = \mathbf{1}^{++}$

$$1^{++} : \quad \alpha, \beta = \{B\bar{B}^*(^3S_1, +), B\bar{B}^*(^3D_1, +), B^*\bar{B}^*(^5D_1)\} = \{1, 2, 3\}$$

$$V_{\text{CI}}^{\text{eff}}(1^{++}) = m_B^2 \begin{pmatrix} C_1 + C_2 & 0 & 0 \\ 0 & 0 & 0 \\ 0 & 0 & 6(C_1 - C_2) \end{pmatrix}$$

$$V_{\text{IPE}}^{\text{eff}}(1^{++}) = -\frac{g^2 m_B^2}{4f_\pi^2}(\vec{\tau}_1 \cdot \vec{\tau}_2) \begin{pmatrix} \frac{1}{3}Q_2 & -\frac{1}{\sqrt{2}}(Q_n - Q_2) & 0 \\ -\frac{1}{\sqrt{2}}(Q_{n'} - Q_2) & -\frac{1}{6}\{\dots\} & 0 \\ 0 & 0 & 3(Q_{x^2} + Q_x) \end{pmatrix}$$

$$\text{with } \{\dots\} = 3Q_n + 3Q_{n'} - 9Q_x - Q_2$$

$$V_{\text{CCI}}^{\text{eff}}(1^{++}) = \frac{3g^2 m_B^2 m_\pi^2}{64\pi^2 f_\pi^2} \begin{pmatrix} \{\dots\} & 0 & 0 \\ 0 & 0 & 0 \\ 0 & 0 & 18(C_1 - C_2) \ln\left(\frac{m_\pi}{\mu}\right) \end{pmatrix}$$

$$\text{with } \{\dots\} = \left(D_1 - D_2 - 2E_2 + (\vec{\tau}_1 \cdot \vec{\tau}_2) \frac{3E_1 - 2D_2 - 7E_2}{3}\right) \ln\left(\frac{m_\pi}{\mu}\right) \\ + \frac{D_1}{2} - D_2 - E_2 + (\vec{\tau}_1 \cdot \vec{\tau}_2) \frac{3E_1 - 2D_2 - 10E_2}{6}$$

$$V_{\text{2PE}}^{\text{eff}}(1^{++}) = -\frac{m_B^2}{384\pi^2 f_\pi^4}(\vec{\tau}_1 \cdot \vec{\tau}_2) \begin{pmatrix} S_0 - 3g^4\{\dots\} & -\frac{3}{\sqrt{8}}g^4[\dots] & 0 \\ -\frac{3}{\sqrt{8}}g^4[\dots]' & S_2 + \frac{3}{4}g^4((\dots) + R_{x^2} - 3R_2) & 0 \\ 0 & 0 & 6S_2 \end{pmatrix}$$

$$\text{with } \{\dots\} = (p'^2 + p^2) \left(\frac{1}{2} - \ln\left(\frac{m_\pi}{\mu}\right)\right) - R_2$$

$$\text{and } [\dots] = 2p^2 \left(\frac{1}{2} - \ln\left(\frac{m_\pi}{\mu}\right)\right) + R_2 - 3R_n$$

$$\text{and } [\dots]' = 2p'^2 \left(\frac{1}{2} - \ln\left(\frac{m_\pi}{\mu}\right)\right) + R_2 - 3R_{n'}$$

$$\text{and } (\dots) = -9R_x + 3R_n + 3R_{n'} - R_2$$

The full 2PE potentials for the seven cases read:

$$\begin{aligned}
V_{2\text{PE}}^{\text{eff}}(B^* \bar{B} \rightarrow B \bar{B}^*) &= \frac{m_B^2}{384\pi^2 f_\pi^4} g^4 \left((\vec{\epsilon}_1 \cdot \vec{\epsilon}_2) \vec{q}^2 - (\vec{\epsilon}_1 \cdot \vec{q})(\vec{\epsilon}_2 \cdot \vec{q}) \right) \left(\frac{9}{4} - \frac{9}{2} L(q) - \frac{9}{2} \ln \left(\frac{m_\pi}{\mu} \right) \right) \\
V_{2\text{PE}}^{\text{eff}}(B \bar{B}^* \rightarrow B^* \bar{B}) &= \frac{m_B^2}{384\pi^2 f_\pi^4} g^4 \left((\vec{\epsilon}_1^* \cdot \vec{\epsilon}_2^*) \vec{q}^2 - (\vec{\epsilon}_1^* \cdot \vec{q})(\vec{\epsilon}_2^* \cdot \vec{q}) \right) \left(\frac{9}{4} - \frac{9}{2} L(q) - \frac{9}{2} \ln \left(\frac{m_\pi}{\mu} \right) \right) \\
V_{2\text{PE}}^{\text{eff}}(B^* \bar{B} \rightarrow B^* \bar{B}) &= -\frac{m_B^2}{384\pi^2 f_\pi^4} (\vec{\tau}_1 \cdot \vec{\tau}_2) (\vec{\epsilon}_1^* \cdot \vec{\epsilon}_1) \\
&\quad \times \left\{ \vec{q}^2 \left(\frac{5}{24} g^4 + \frac{13}{6} g^2 + \frac{5}{6} \right) + m_\pi^2 (4g^4 + 2g^2 + 4) \right. \\
&\quad \left. + \ln \left(\frac{m_\pi}{\mu} \right) \left[\vec{q}^2 \left(\frac{23}{4} g^4 - 5g^2 - 1 \right) + m_\pi^2 \left(\frac{45}{2} g^4 - 18g^2 - 6 \right) \right] \right. \\
&\quad \left. + L(q) \left[\vec{q}^2 \left(\frac{23}{4} g^4 - 5g^2 - 1 \right) + m_\pi^2 (5g^4 - 8g^2 - 4) + \frac{12g^4 m_\pi^4}{4m_\pi^2 + \vec{q}^2} \right] \right\} \\
V_{2\text{PE}}^{\text{eff}}(B \bar{B}^* \rightarrow B \bar{B}^*) &= -\frac{m_B^2}{384\pi^2 f_\pi^4} (\vec{\tau}_1 \cdot \vec{\tau}_2) (\vec{\epsilon}_2^* \cdot \vec{\epsilon}_2) \left\{ \dots \right\} \\
V_{2\text{PE}}^{\text{eff}}(B^* \bar{B} \rightarrow B^* \bar{B}^*) &= -i \frac{m_B^2}{384\pi^2 f_\pi^4} g^4 \epsilon_{1,i} \epsilon_{2',n} \epsilon_{1',k}^* (\epsilon_{nku} q_u q_i - \epsilon_{niu} q_u q_k) \left(\frac{9}{4} - \frac{9}{2} L(q) - \frac{9}{2} \ln \left(\frac{m_\pi}{\mu} \right) \right) \\
V_{2\text{PE}}^{\text{eff}}(B \bar{B}^* \rightarrow B^* \bar{B}^*) &= i \frac{m_B^2}{384\pi^2 f_\pi^4} g^4 \epsilon_{2,l}^* \epsilon_{2',n} \epsilon_{1',k}^* (\epsilon_{nku} q_u q_l - \epsilon_{nlu} q_u q_k) \left(\frac{9}{4} - \frac{9}{2} L(q) - \frac{9}{2} \ln \left(\frac{m_\pi}{\mu} \right) \right) \\
V_{2\text{PE}}^{\text{eff}}(B^* \bar{B}^* \rightarrow B^* \bar{B}^*) &= -\frac{m_B^2}{384\pi^2 f_\pi^4} (\vec{\tau}_1 \cdot \vec{\tau}_2) (\vec{\epsilon}_1^* \cdot \vec{\epsilon}_1) (\vec{\epsilon}_2^* \cdot \vec{\epsilon}_2) \left\{ \dots \right\}
\end{aligned}$$

7.3 $J^{PC} = 1^{+-}$

$$1^{+-} : \quad \alpha, \beta = \{B\bar{B}^*(^3S_1, -), B\bar{B}^*(^3D_1, -), B^*\bar{B}^*(^3S_1), B^*\bar{B}^*(^3D_1)\} = \{1, 2, 3, 4\}$$

$$V_{CI}^{\text{eff}}(1^{+-}) = m_B^2 \begin{pmatrix} C_1 - C_2 & 0 & 2C_2 & 0 \\ 0 & 0 & 0 & 0 \\ 2C_2 & 0 & -(C_1 + C_2) & 0 \\ 0 & 0 & 0 & 0 \end{pmatrix}$$

$$V_{IPE}^{\text{eff}}(1^{+-}) = -\frac{g^2 m_B^2}{4f_\pi^2} (\vec{\tau}_1 \cdot \vec{\tau}_2) \times \begin{pmatrix} -\frac{1}{3}Q_2 & \frac{1}{\sqrt{2}}(Q_n - Q_2) & \frac{2}{3}Q_2 & \frac{1}{\sqrt{18}}(3Q_n - Q_2) \\ \frac{1}{\sqrt{2}}(Q_{n'} - Q_2) & \frac{1}{6}\{\dots\} & \frac{1}{\sqrt{18}}(3Q_{n'} - Q_2) & \frac{1}{6}\{\dots\} + \frac{3}{2}Q_x^2 - \frac{1}{2}Q_2 \\ \frac{2}{3}Q_2 & \frac{1}{\sqrt{18}}(3Q_n - Q_2) & -\frac{1}{3}Q_2 & \frac{1}{\sqrt{18}}(3Q_n - Q_2) \\ \frac{1}{\sqrt{18}}(3Q_{n'} - Q_2) & \frac{1}{6}\{\dots\} + \frac{3}{2}Q_x^2 - \frac{1}{2}Q_2 & \frac{1}{\sqrt{18}}(3Q_{n'} - Q_2) & \frac{1}{6}\{\dots\} \end{pmatrix}$$

with $\{\dots\} = 3Q_n + 3Q_{n'} - 9Q_x - Q_2$

$$V_{CCI}^{\text{eff}}(1^{+-}) = \frac{3g^2 m_B^2 m_\pi^2}{64\pi^2 f_\pi^2} \begin{pmatrix} \{\dots\} & 0 & 2[\dots] \ln\left(\frac{m_\pi}{\mu}\right) & 0 \\ 0 & 0 & 0 & 0 \\ 2[\dots] \ln\left(\frac{m_\pi}{\mu}\right) & 0 & -3(C_1 + C_2) \ln\left(\frac{m_\pi}{\mu}\right) & 0 \\ 0 & 0 & 0 & 0 \end{pmatrix}$$

$$\begin{aligned} \text{with } \{\dots\} &= \left(D_1 + D_2 + 2E_2 + (\vec{\tau}_1 \cdot \vec{\tau}_2) \frac{3E_1 + 2D_2 + 7E_2}{3} \right) \ln\left(\frac{m_\pi}{\mu}\right) \\ &\quad + \frac{D_1}{2} + D_2 + E_2 + (\vec{\tau}_1 \cdot \vec{\tau}_2) \frac{3E_1 + 2D_2 + 10E_2}{6} \\ [\dots] &= 2D_2 + 8E_2 + (\vec{\tau}_1 \cdot \vec{\tau}_2) \frac{8D_2 + 22E_2}{3} \end{aligned}$$

$$V_{2\text{PE}}^{\text{eff}}(1^{+-}) = -\frac{m_B^2}{384\pi^2 f_\pi^4}(\vec{\tau}_1 \cdot \vec{\tau}_2) \times \begin{pmatrix} S_0 + 3g^4\{\dots\} & \frac{3}{\sqrt{8}}g^4[\dots] & -6g^4\{\dots\} & \frac{3}{\sqrt{8}}g^4[\dots] \\ \frac{3}{\sqrt{8}}g^4[\dots]' & S_2 - \frac{3}{4}g^4((\dots) + R_{x^2} - 3R_2) & \frac{3}{\sqrt{8}}g^4[\dots]' & -\frac{3}{4}g^4((\dots) - R_{x^2}) \\ -6g^4\{\dots\} & \frac{3}{\sqrt{8}}g^4[\dots] & -S_0 & 0 \\ \frac{3}{\sqrt{8}}g^4[\dots]' & -\frac{3}{4}g^4((\dots) - R_{x^2}) & 0 & -S_2 \end{pmatrix}$$

$$\text{with } \{\dots\} = (p'^2 + p^2) \left(\frac{1}{2} - \ln \left(\frac{m_\pi}{\mu} \right) \right) - R_2$$

$$\text{and } [\dots] = 2p^2 \left(\frac{1}{2} - \ln \left(\frac{m_\pi}{\mu} \right) \right) + R_2 - 3R_n$$

$$\text{and } [\dots]' = 2p'^2 \left(\frac{1}{2} - \ln \left(\frac{m_\pi}{\mu} \right) \right) + R_2 - 3R_{n'}$$

$$\text{and } (\dots) = -9R_x + 3R_n + 3R_{n'} - R_2$$

The full 2PE potentials for the seven cases read:

$$\begin{aligned}
V_{2\text{PE}}^{\text{eff}}(B^* \bar{B} \rightarrow B \bar{B}^*) &= \frac{m_B^2}{384\pi^2 f_\pi^4} g^4 \left((\vec{\epsilon}_1 \cdot \vec{\epsilon}_2) \vec{q}^2 - (\vec{\epsilon}_1 \cdot \vec{q})(\vec{\epsilon}_2 \cdot \vec{q}) \right) \left(\frac{9}{4} - \frac{9}{2} L(q) - \frac{9}{2} \ln \left(\frac{m_\pi}{\mu} \right) \right) \\
V_{2\text{PE}}^{\text{eff}}(B \bar{B}^* \rightarrow B^* \bar{B}) &= \frac{m_B^2}{384\pi^2 f_\pi^4} g^4 \left((\vec{\epsilon}_1^* \cdot \vec{\epsilon}_2^*) \vec{q}^2 - (\vec{\epsilon}_1^* \cdot \vec{q})(\vec{\epsilon}_2^* \cdot \vec{q}) \right) \left(\frac{9}{4} - \frac{9}{2} L(q) - \frac{9}{2} \ln \left(\frac{m_\pi}{\mu} \right) \right) \\
V_{2\text{PE}}^{\text{eff}}(B^* \bar{B} \rightarrow B^* \bar{B}) &= - \frac{m_B^2}{384\pi^2 f_\pi^4} (\vec{\tau}_1 \cdot \vec{\tau}_2) (\vec{\epsilon}_1^* \cdot \vec{\epsilon}_1) \\
&\quad \times \left\{ \vec{q}^2 \left(\frac{5}{24} g^4 + \frac{13}{6} g^2 + \frac{5}{6} \right) + m_\pi^2 (4g^4 + 2g^2 + 4) \right. \\
&\quad \left. + \ln \left(\frac{m_\pi}{\mu} \right) \left[\vec{q}^2 \left(\frac{23}{4} g^4 - 5g^2 - 1 \right) + m_\pi^2 \left(\frac{45}{2} g^4 - 18g^2 - 6 \right) \right] \right. \\
&\quad \left. + L(q) \left[\vec{q}^2 \left(\frac{23}{4} g^4 - 5g^2 - 1 \right) + m_\pi^2 (5g^4 - 8g^2 - 4) + \frac{12g^4 m_\pi^4}{4m_\pi^2 + \vec{q}^2} \right] \right\} \\
V_{2\text{PE}}^{\text{eff}}(B \bar{B}^* \rightarrow B \bar{B}^*) &= - \frac{m_B^2}{384\pi^2 f_\pi^4} (\vec{\tau}_1 \cdot \vec{\tau}_2) (\vec{\epsilon}_2^* \cdot \vec{\epsilon}_2) \left\{ \dots \right\} \\
V_{2\text{PE}}^{\text{eff}}(B^* \bar{B} \rightarrow B^* \bar{B}^*) &= -i \frac{m_B^2}{384\pi^2 f_\pi^4} g^4 \epsilon_{1,i} \epsilon_{2',n} \epsilon_{1',k}^* (\epsilon_{nku} q_u q_i - \epsilon_{niu} q_u q_k) \left(\frac{9}{4} - \frac{9}{2} L(q) - \frac{9}{2} \ln \left(\frac{m_\pi}{\mu} \right) \right) \\
V_{2\text{PE}}^{\text{eff}}(B \bar{B}^* \rightarrow B^* \bar{B}^*) &= i \frac{m_B^2}{384\pi^2 f_\pi^4} g^4 \epsilon_{2,l}^* \epsilon_{2',n} \epsilon_{1',k}^* (\epsilon_{nku} q_u q_l - \epsilon_{nlu} q_u q_k) \left(\frac{9}{4} - \frac{9}{2} L(q) - \frac{9}{2} \ln \left(\frac{m_\pi}{\mu} \right) \right) \\
V_{2\text{PE}}^{\text{eff}}(B^* \bar{B}^* \rightarrow B^* \bar{B}^*) &= - \frac{m_B^2}{384\pi^2 f_\pi^4} (\vec{\tau}_1 \cdot \vec{\tau}_2) (\vec{\epsilon}_1^* \cdot \vec{\epsilon}_1) (\vec{\epsilon}_2^* \cdot \vec{\epsilon}_2) \left\{ \dots \right\}
\end{aligned}$$

7.4 $J^{PC} = 2^{++}$

$$2^{++} : \quad \alpha, \beta = \left\{ B\bar{B}({}^1D_2), B\bar{B}^*({}^3D_2), B^*\bar{B}^*({}^5S_2), B^*\bar{B}^*({}^1D_2), B^*\bar{B}^*({}^5D_2), B^*\bar{B}^*({}^5G_2) \right\} \\ = \{1, 2, 3, 4, 5, 6\}$$

$$(V_{\text{CI}}^{\text{eff}})_{\alpha\beta}(2^{++}) = \begin{cases} m_B^2(C_1 - C_2), & \text{if } \alpha = \beta = 3 \\ 0 & \text{else} \end{cases}$$

$$V_{\text{IPE}}^{\text{eff}}(2^{++}) = -\frac{g^2 m_B^2}{4f_\pi^2}(\vec{\tau}_1 \cdot \vec{\tau}_2) \\ \times \begin{pmatrix} 0 & 0 & -\frac{1}{\sqrt{30}}(3Q_{n'} - Q_2) & \frac{1}{\sqrt{12}}(3Q_{x^2} - Q_2) & -\frac{1}{\sqrt{21}}K_{15} & -\sqrt{\frac{3}{560}}K_{16} \\ 0 & 0 & \frac{1}{\sqrt{20}}(3Q_{n'} - Q_2) & 0 & \frac{1}{\sqrt{504}}K_{25} & -\frac{1}{\sqrt{1400}}K_{26} \\ -\frac{1}{\sqrt{30}}(3Q_n - Q_2) & \frac{1}{\sqrt{20}}(3Q_n - Q_2) & -\frac{1}{12}Q_2 & \frac{1}{\sqrt{90}}(3Q_n - Q_2) & -\sqrt{\frac{7}{90}}(3Q_n - Q_2) & 0 \\ \frac{1}{\sqrt{12}}(3Q_{x^2} - Q_2) & 0 & \frac{1}{\sqrt{90}}(3Q_{n'} - Q_2) & \frac{1}{6}(3Q_{x^2} - Q_2) & \frac{1}{\sqrt{63}}K_{45} & \frac{1}{8\sqrt{35}}K_{46} \\ -\frac{1}{\sqrt{21}}K_{51} & \frac{1}{\sqrt{504}}K_{52} & -\sqrt{\frac{7}{90}}(3Q_{n'} - Q_2) & \frac{1}{\sqrt{63}}K_{54} & \frac{3}{14}K_{55} & -\frac{1}{56\sqrt{5}}K_{56} \\ -\sqrt{\frac{3}{560}}K_{61} & -\frac{1}{\sqrt{1400}}K_{62} & 0 & \frac{1}{8\sqrt{35}}K_{64} & -\frac{1}{56\sqrt{5}}K_{65} & \frac{1}{28}K_{66} \end{pmatrix}$$

$$\text{with } K_{51} = K_{15} = 3Q_{x^2} - 9Q_x + 3Q_n + 3Q_{n'} - 2Q_2$$

$$K_{61} = 35Q_{n'x^2} - Q_{x^2} + 20Q_x - 5Q_{n'} + 2Q_n + Q_2$$

$$K_{16} = 35Q_{nx^2} - Q_{x^2} + 20Q_x - 5Q_n + 2Q_{n'} + Q_2$$

$$K_{52} = K_{25} = 18Q_{x^2} - 18Q_x + 6Q_{n'} + 6Q_n + 8Q_2$$

$$K_{62} = 35Q_{n'x^2} - 5Q_{x^2} - 20Q_x - 5Q_{n'} + 2Q_n + Q_2$$

$$K_{26} = 35Q_{nx^2} - 5Q_{x^2} - 20Q_x - 5Q_n + 2Q_{n'} + Q_2$$

$$K_{54} = K_{45} = 3Q_{x^2} - Q_x + 3Q_{n'} + 3Q_n - 2Q_2$$

$$K_{64} = 35Q_{n'x^2} - 35Q_{x^2} - 140Q_x - 5Q_{n'} + 2Q_n + Q_2$$

$$K_{46} = 35Q_{nx^2} - 35Q_{x^2} - 140Q_x - 5Q_n + 2Q_{n'} + Q_2$$

$$K_{55} = -8Q_{x^2} + 11Q_x - 6(Q_{n'} + Q_n) + 7Q_2$$

$$K_{65} = 35Q_{n'x^2} - 5Q_{x^2} + 20Q_x - 5Q_{n'} + 2Q_n + Q_2$$

$$K_{56} = 35Q_{nx^2} - 5Q_{x^2} + 20Q_x - 5Q_n + 2Q_{n'} + Q_2$$

$$K_{66} = 245Q_{x^3} - 105(Q_{n'x^2} + Q_{nx^2}) + 15Q_{x^2} + 15(Q_{n'} + Q_n) + 5Q_x - 3Q_2$$

$$(V_{\text{CCI}}^{\text{eff}})_{\alpha\beta}(2^{++}) = \begin{cases} \frac{9g^2 m_B^2 m_\pi^2}{64\pi^2 f_\pi^2}(C_1 - C_2) \ln\left(\frac{m_\pi}{\mu}\right) & \text{if } \alpha = \beta = 3 \\ 0 & \text{else} \end{cases}$$

$$V_{2\text{PE}}^{\text{eff}}(2^{++}) = -\frac{m_B^2}{384\pi^2 f_\pi^4}(\vec{\tau}_1 \cdot \vec{\tau}_2) \times \begin{pmatrix} 0 & 0 & \sqrt{\frac{27}{40}}K_{13} & 0 & \sqrt{\frac{243}{28}}K_{15} & \sqrt{\frac{3}{35}}K_{16} \\ 0 & 0 & 0 & 0 & -\frac{9}{\sqrt{224}}(3R_{x^2} - R_2) & \frac{9}{\sqrt{1120}}K_{26} \\ \sqrt{\frac{27}{40}}K_{31} & 0 & S_0 & 0 & 0 & 0 \\ 0 & 0 & 0 & 0 & 0 & 0 \\ \sqrt{\frac{243}{28}}K_{51} & -\frac{9}{\sqrt{224}}(3R_{x^2} - R_2) & 0 & 0 & 0 & 0 \\ \sqrt{\frac{3}{35}}K_{61} & \frac{9}{\sqrt{1120}}K_{62} & 0 & 0 & 0 & 0 \end{pmatrix}$$

$$\text{with } K_{31} = 2p^2 \left(\frac{1}{2} - \ln \left(\frac{m_\pi}{\mu} \right) \right) - 3R_n + R_2$$

$$K_{13} = 2p'^2 \left(\frac{1}{2} - \ln \left(\frac{m_\pi}{\mu} \right) \right) - 3R_{n'} + R_2$$

$$K_{51} = K_{15} = -2R_{x^2} + 3R_x - R_{n'} - R_n + R_2$$

$$K_{61} = 15p'^2 \left(\frac{1}{2} - \ln \left(\frac{m_\pi}{\mu} \right) \right) + \frac{9}{8}(-30R_{x^2} + 20R_x + 5R_{n'} - 2R_n - R_2)$$

$$K_{16} = 15p^2 \left(\frac{1}{2} - \ln \left(\frac{m_\pi}{\mu} \right) \right) + \frac{9}{8}(-30R_{x^2} + 20R_x + 5R_n - 2R_{n'} - R_2)$$

$$K_{62} = \frac{50}{3}(p'^2 + p^2) \left(\frac{1}{2} - \ln \left(\frac{m_\pi}{\mu} \right) \right) - 35R_{n'x^2} - R_{x^2} - 20R_x + 5R_{n'} - 2R_n - R_2$$

$$K_{26} = \frac{50}{3}(p'^2 + p^2) \left(\frac{1}{2} - \ln \left(\frac{m_\pi}{\mu} \right) \right) - 35R_{nx^2} - R_{x^2} - 20R_x + 5R_n - 2R_{n'} - R_2$$

The full 2PE potentials for the nine cases read:

$$\begin{aligned}
V_{2\text{PE}}^{\text{eff}}(B\bar{B} \rightarrow B\bar{B}) &= -\frac{m_B^2}{384\pi^2 f_\pi^4} (\vec{\tau}_1 \cdot \vec{\tau}_2) \left\{ \vec{q}^2 \left(\frac{5}{24} g^4 + \frac{13}{6} g^2 + \frac{5}{6} \right) + m_\pi^2 (4g^4 + 2g^2 + 4) \right. \\
&\quad \left. + \ln\left(\frac{m_\pi}{\mu}\right) \left[\vec{q}^2 \left(\frac{23}{4} g^4 - 5g^2 - 1 \right) + m_\pi^2 \left(\frac{45}{2} g^4 - 18g^2 - 6 \right) \right] \right. \\
&\quad \left. + L(q) \left[\vec{q}^2 \left(\frac{23}{4} g^4 - 5g^2 - 1 \right) + m_\pi^2 (5g^4 - 8g^2 - 4) + \frac{12g^4 m_\pi^4}{4m_\pi^2 + \vec{q}^2} \right] \right\} \\
V_{2\text{PE}}^{\text{eff}}(B\bar{B}^* \rightarrow B\bar{B}) &= V_{2\text{PE}}^{\text{eff}}(B\bar{B} \rightarrow B\bar{B}^*) = 0 \\
V_{2\text{PE}}^{\text{eff}}(B\bar{B}^* \rightarrow B\bar{B}^*) &= (\vec{\epsilon}_2^* \cdot \vec{\epsilon}_{2'}) V_{2\text{PE}}^{\text{eff}}(B\bar{B} \rightarrow B\bar{B}) \\
V_{2\text{PE}}^{\text{eff}}(B\bar{B} \rightarrow B^* \bar{B}^*) &= \frac{m_B^2}{384\pi^2 f_\pi^4} g^4 \left((\vec{\epsilon}_1^* \cdot \vec{\epsilon}_{2'}) \vec{q}^2 - (\vec{\epsilon}_1^* \cdot \vec{q})(\vec{\epsilon}_{2'} \cdot \vec{q}) \right) \left(\frac{9}{4} - \frac{9}{2} L(q) - \frac{9}{2} \ln\left(\frac{m_\pi}{\mu}\right) \right) \\
V_{2\text{PE}}^{\text{eff}}(B^* \bar{B}^* \rightarrow B\bar{B}) &= \frac{m_B^2}{384\pi^2 f_\pi^4} g^4 \left((\vec{\epsilon}_2^* \cdot \vec{\epsilon}_1) \vec{q}^2 - (\vec{\epsilon}_2^* \cdot \vec{q})(\vec{q} \cdot \vec{\epsilon}_1) \right) \left(\frac{9}{4} - \frac{9}{2} L(q) - \frac{9}{2} \ln\left(\frac{m_\pi}{\mu}\right) \right) \\
V_{2\text{PE}}^{\text{eff}}(B\bar{B}^* \rightarrow B^* \bar{B}^*) &= \frac{m_B^2}{384\pi^2 f_\pi^4} g^4 i \epsilon_{2,l}^* \epsilon_{1',k} \epsilon_{2',n} (\epsilon_{nku} q_u q_l - \epsilon_{nlu} q_u q_k) \left(\frac{9}{4} - \frac{9}{2} L(q) - \frac{9}{2} \ln\left(\frac{m_\pi}{\mu}\right) \right) \\
V_{2\text{PE}}^{\text{eff}}(B^* \bar{B}^* \rightarrow B\bar{B}^*) &= \frac{m_B^2}{384\pi^2 f_\pi^4} g^4 i \epsilon_{1,i} \epsilon_{2,l}^* \epsilon_{2',n} (\epsilon_{nku} q_u q_i - \epsilon_{niu} q_u q_k) \left(\frac{9}{4} - \frac{9}{2} L(q) - \frac{9}{2} \ln\left(\frac{m_\pi}{\mu}\right) \right) \\
V_{2\text{PE}}^{\text{eff}}(B^* \bar{B}^* \rightarrow B^* \bar{B}^*) &= (\vec{\epsilon}_1^* \cdot \vec{\epsilon}_1) (\vec{\epsilon}_2^* \cdot \vec{\epsilon}_{2'}) V_{2\text{PE}}^{\text{eff}}(B\bar{B} \rightarrow B\bar{B})
\end{aligned}$$

7.5 External comparison

Let us now select four of the above mentioned results for the 1PE and compare them to the ones calculated by Wang et al..⁶⁹ From their paper, one obtains for $J^{PC} = 1^{+-}$ and S -wave to S -wave (all function's arguments are omitted for brevity):

$$V_{SS}^{\pi\lambda\lambda'} = \frac{g^2}{24f_\pi^2} \begin{pmatrix} 1 & -2 \\ -2 & 1 \end{pmatrix}^{\lambda\lambda'} (2p'p \Delta_1^{\pi\lambda\lambda'} - (p'^2 + p^2) \Delta_0^{\pi\lambda\lambda'}),$$

where $\lambda, \lambda' = \{1, 2\} = \{B\bar{B}^*, B^*\bar{B}^*\}$ denotes the incoming and outgoing channel, respectively. The Δ -functions are given as:

$$\begin{aligned} \Delta_k^{\pi\lambda\lambda'} &= \int_{-1}^{+1} \frac{dx}{2} x^k \frac{D_a^{\pi\lambda\lambda'} + D_b^{\pi\lambda\lambda'}}{\sqrt{\vec{q}^2 + m_\pi^2}}, \\ D_a^{\pi\lambda\lambda'} &= \left(\sqrt{\vec{q}^2 + m_\pi^2} + m_1^{\lambda\lambda'} + m_2^{\lambda\lambda'} + p'^2/2m_1^{\lambda\lambda'} + p^2/2m_2^{\lambda\lambda'} - M \right)^{-1}, \\ D_b^{\pi\lambda\lambda'} &= \left(\sqrt{\vec{q}^2 + m_\pi^2} + m_1^{\lambda\lambda'} + m_2^{\lambda\lambda'} + p'^2/2m_1^{\lambda\lambda'} + p^2/2m_2^{\lambda\lambda'} - M \right)^{-1}, \end{aligned}$$

with M being the system's total energy.

However, since we neglect the mass difference between B and B^* , $m_1 = m_2 = m_{1'} = m_{2'} = m_B$. Additionally, when considering M to second order in \vec{l} , D_a and D_b are reduced to

$$\begin{aligned} D_a^{\pi\lambda\lambda'} &= D_b^{\pi\lambda\lambda'} = (\vec{q}^2 + m_\pi^2)^{-1/2} \\ \Rightarrow \Delta_k^\pi &= \int_{-1}^{+1} \frac{dx}{2} \frac{2x^k}{\vec{q}^2 + m_\pi^2} \\ \Rightarrow V_{SS}^{\pi\lambda\lambda'} &= \frac{g^2}{12f_\pi^2} \begin{pmatrix} 1 & -2 \\ -2 & 1 \end{pmatrix}^{\lambda\lambda'} \int_{-1}^{+1} \frac{dx}{2} \frac{2p'px - (p'^2 + p^2)}{\vec{q}^2 + m_\pi^2} \\ &= -\frac{g^2}{12f_\pi^2} \begin{pmatrix} 1 & -2 \\ -2 & 1 \end{pmatrix}^{\lambda\lambda'} Q_2. \end{aligned}$$

The corresponding partial waves in this calculation are found in $V_{1PE}^{\text{eff}}(1^{+-})$:

$$\begin{pmatrix} (V_{1PE}^{\text{eff}})_{11}(1^{+-}) & (V_{1PE}^{\text{eff}})_{13}(1^{+-}) \\ (V_{1PE}^{\text{eff}})_{31}(1^{+-}) & (V_{1PE}^{\text{eff}})_{33}(1^{+-}) \end{pmatrix} = \frac{g^2 m_B^2}{12f_\pi^2} (\vec{\tau}_1 \cdot \vec{\tau}_2) \begin{pmatrix} 1 & -2 \\ -2 & 1 \end{pmatrix} Q_2$$

We have an additional factor of m_B^2 from the normalization of the heavy meson fields and the factor of $(\vec{\tau}_1 \cdot \vec{\tau}_2)$ that will be evaluated as -1 for $I = 0$ (cf. eq. (A.5)).

The results match one another as expected since we used the same conventions in the definition of U (eq. (2.6)), the Lagrangians (eqs. (2.10), (2.16), (2.17)) and the partial wave decomposition (eq. (7.1)). Hence, there is no factor necessary for a direct comparison of both results.

The results for CI also match the results from Baru et al..⁷⁰

⁶⁹Wang et al., op. cit., p.5f, eqs. (22) - (28).

⁷⁰Baru et al., loc. cit.

8 Summary and discussion

The full potential of the $B^{(*)}-\bar{B}^{(*)}$ system up to NLO was calculated and decomposed into the partial waves with quantum numbers $J^{PC} = 0^{++}, 1^{++}, 1^{+-}, 2^{++}$. The motivation to move beyond the LO in the chiral expansion was given by the relatively slow convergence of the chiral expansion with $\chi \sim 0.5$ and the promotion of a S - to D -wave CI to LO in works done by Wang et al.⁷¹ and Nefediev et al..⁷² Additionally, observations of exotic multiquark states from the $c\bar{c}$ -sector together with HQFS suggest the existence of several, still to be discovered spin partners W_{bJ} to the $Z_b^\pm(10610)$ and $Z_b^\pm(10650)$. This is the reason for the partial wave analysis beyond their quantum numbers $J^{PC} = 1^{+-}$.

Using Weinberg's formalism,⁷³ we were able to restore naive power counting by excluding reducible contributions from the effective potentials. Expanding this completely irreducible potential perturbatively to NLO and then summing via the LSE yields the T -matrix. The partial wave projected potentials in secs. 7.1 to 7.4 are ready for this computation.

For the calculation of the effective potential V^{eff} , we employed χ PT & HM χ PT, both expanded in $\chi = p_{\text{typ}}/\Lambda_h$, and a non-relativistic approximation of the heavy meson fields, expanded in p_{typ}/m_H . We limited ourselves to the SU(2) isospin subgroup of the full chiral symmetry. The effective potential was calculated at LO, $\mathcal{O}(1)$, comprising the CI and the 1PE, and at NLO, $\mathcal{O}(\chi^2)$, comprising one-loop corrections to LO (CCI and C1PE) and the 2PE. Both C1PE and CCI can be absorbed into the renormalization of m_π , m_B , g and the contact constants D_1 , E_1 , D_2 , E_2 , respectively. Although the CCI is given explicitly, the renormalization of these constants can be easily read off by comparison of $V_{\text{CI}}^{\text{eff}}$ with $V_{\text{CCI}}^{\text{eff}}$. Finally, $V_{2\text{PE}}^{\text{eff}}$ comprises terms proportional to $L(q)$, defined in eq. (A.14), which correspond to the interesting long-range behavior; all terms constant or quadratic in q can be absorbed into the CI at LO, $\mathcal{L}_{4H}^{(0)}$, or NLO, $\mathcal{L}_{4H}^{(2)}$ and hence only add to the counter terms.

The relative error of the perturbative calculation can be estimated from the size of the first subleading terms in the chiral expansion, $\mathcal{O}(\chi^3)$, and the non-relativistic expansion of $|H(p_{\text{typ}})\rangle$, $\mathcal{O}(p_{\text{typ}}/m_H)$. Using $p_{\text{typ}} \approx 0.5 \text{ GeV}$, $\Lambda_h \approx 1 \text{ GeV}$ and $m_H = m_B \approx 5.3 \text{ GeV}$, we obtain:

$$\mathcal{O}(\chi^3) \sim 0.13 \quad \mathcal{O}(p_{\text{typ}}/m_H) \sim 0.09$$

Still, the constants D_1 , E_1 , D_2 , E_2 need to be extracted from fitting line shapes to available data. However, the 2PE does not introduce additional parameters improving the fit's accuracy.

⁷¹Wang et al., op. cit.

⁷²Nefediev et al., op. cit.

⁷³Weinberg, op. cit.

9 Acknowledgments

First and foremost, I want to thank Prof. Dr. Christoph Hanhart for entrusting me with such a fascinating topic within the scope of a master's thesis and the supervision I experienced thereby. I am also grateful for having been able to participate in the Moscow International School of Physics in March 2020.

Secondly, my thanks go to PD Dr. Bastian Kubis for adopting me into his group's weekly seminars and the resulting unofficial supervision through valuable feedback.

I experienced brilliant support by Dr. Alexey Nefediev and Dr. Vadim Baru. Your obliging attitude and scientific diligence shall be my example.

I want to thank my dear friends Maurus Geiger and Hannah Schäfer for countless discussions and insightful help, and Stefan Ropertz, Tobias Isken, Max & Ingrid Dax, Dominik Stamen, Frederic Noël and Leon von Detten for being the valuable companions that they are.

Finally, gratitude goes to my girlfriend, Anika Kortegast, for her loving support beyond all scientific explanations; to my brother Max and my parents for their care and encouragement; to the many colleagues, friends and fellow students who accompanied and endured me.

A Relations

In the following, the Pauli matrices are denoted $\vec{\tau}$.⁷⁴ The relations below can be shown using $(\tau)_c(\tau)_d = \delta_{cd}\mathbb{1} + i\epsilon_{cdh}(\tau)_h$.

$$(\tau_i)_h(\tau_j)_d(\tau_j)_c\epsilon_{cdh} = -2i(\vec{\tau}_i \cdot \vec{\tau}_j) \quad (\text{A.1})$$

$$(\tau_i)_d(\tau_i)_c(\tau_j)_d(\tau_j)_c = 3 - 2(\vec{\tau}_i \cdot \vec{\tau}_j) \quad (\text{A.2})$$

$$(\tau_i)_d(\tau_i)_c(\tau_j)_c(\tau_j)_d = 3 + 2(\vec{\tau}_i \cdot \vec{\tau}_j) \quad (\text{A.3})$$

$$(\tau_i)_d(\tau_i)_c(\tau_j)_c(\tau_i)_d = 3(\vec{\tau}_i \cdot \vec{\tau}_j) \quad (\text{A.4})$$

When selecting a total isospin I of the initial (and thereby final) two-particle state, one can use:⁷⁵

$$\vec{\tau}_1 \cdot \vec{\tau}_2^c = 3 - 2I(I+1) = \begin{cases} +3 & \text{if } I = 0, \\ -1 & \text{if } I = 1. \end{cases} \quad (\text{A.5})$$

However, recall that we used $\vec{\tau}_2^c \equiv \vec{\tau}_2$ throughout the calculation, where c denotes the charge conjugation.

When facing integrals in dimensional regularization, we often employ Feynman parameters:⁷⁶

$$\frac{1}{AB} = \int_0^1 \frac{dx}{[(A-B)x + B]^2} \quad (\text{A.6})$$

Symmetry inside loop integrals allows one to make the followin replacements:^{77,78}

$$\begin{aligned} l^\mu l^\nu &\longrightarrow \frac{1}{D} l^2 g^{\mu\nu} \\ \Rightarrow l^i l^j &\longrightarrow \frac{1}{D-1} \vec{l}^2 \delta^{ij} \end{aligned} \quad (\text{A.7})$$

We can reduce our loop integrals to a radial integration in Euclidean space:⁷⁹

$$\int_0^\infty dl_E \frac{l_E^a}{[l_E^2 + \Xi]^b} = \Xi^{\frac{a+1}{2}-b} \frac{\Gamma\left(\frac{a+1}{2}\right) \Gamma\left(b - \frac{a+1}{2}\right)}{2\Gamma(b)} \quad (\text{A.8})$$

⁷⁴Machleidt and Entem, op. cit., pp.63,65,74.

⁷⁵Baru et al., op. cit., p.7.

⁷⁶Michael E. Peskin and Daniel V. Schroeder. *An Introduction to quantum field theory*. Reading, USA: Addison-Wesley, 1995. ISBN: 9780201503975, 0201503972. URL: <http://www.slac.stanford.edu/~mpeskin/QFT.html>, p.806.

⁷⁷Ibid., p.807.

⁷⁸Machleidt and Entem, op. cit., p.75.

⁷⁹Schwartz, op. cit., p.826f.

The angular integration in $(D - 1)$ -dimensional space is performed using

$$\int d\Omega_{D-1} = \frac{2\pi^{(D-1)/2}}{\Gamma\left(\frac{D-1}{2}\right)}. \quad (\text{A.9})$$

Performing the limit $\epsilon \rightarrow 0$ for $D = 4 - \epsilon$ dimensions makes us use the following properties of the gamma function:⁸⁰

$$\Gamma\left(\frac{4-D}{2}\right) = \Gamma\left(\frac{\epsilon}{2}\right) = \frac{2}{\epsilon} - \gamma_E + \mathcal{O}(\epsilon), \quad (\text{A.10})$$

$$\Gamma\left(\frac{2-D}{2}\right) = \frac{\Gamma\left(\frac{\epsilon}{2}\right)}{\frac{\epsilon}{2} - 1} = -\frac{2}{\epsilon} + \gamma_E - 1 + \mathcal{O}(\epsilon), \quad (\text{A.11})$$

where $\gamma_E = 0.5772\dots$ is the Euler-Mascheroni constant. Most x -integrations are solved by using

$$\int_0^1 dx m_\pi^2 \ln\left(\frac{q^2 x(1-x) + m_\pi^2}{\mu^2}\right) = 2m_\pi^2 \left(-1 + L(q) + \ln\left(\frac{m_\pi}{\mu}\right)\right), \quad (\text{A.12})$$

$$\int_0^1 dx q^2 x(1-x) \ln\left(\frac{q^2 x(1-x) + m_\pi^2}{\mu^2}\right) = -\frac{5}{18}q^2 + \frac{2}{3}m_\pi^2 + \frac{q^2}{3} \ln\left(\frac{m_\pi}{\mu}\right) + \left(\frac{q^2}{3} - \frac{2}{3}m_\pi^2\right)L(q), \quad (\text{A.13})$$

$$L(q) = \frac{\sqrt{4m_\pi^2 + q^2}}{q} \ln\left(\frac{\sqrt{4m_\pi^2 + q^2} + q}{2m_\pi}\right), \quad (\text{A.14})$$

with $q = |\vec{q}|$.

⁸⁰Machleidt and Entem, op. cit., p.67f.

B Integrals of dimensional regularization

To regulate the divergent integrals, we employ dimensional regularization with the scale parameter μ . In general, we solve the integrals by, firstly, using Feynman parameters (eq. (A.6)), secondly, shifting the denominator to even powers of l , thirdly, applying the residue theorem to execute the l^0 -integration and finally, going to $D - 1$ dimensions and utilizing eqs. (A.8) and (A.9).

B.1 The triangle integral

$$\mathcal{I}_{\text{tr}} = \int \frac{d^4 l}{(2\pi)^4} \frac{l^0}{l^0 - i\epsilon} \frac{(\vec{l} + \vec{q}) \cdot \vec{l}}{[(l + q)^2 - m_\pi^2 + i\epsilon][l^2 - m_\pi^2 + i\epsilon]}$$

Introducing Feynman parameters:

$$= \int \frac{d^4 l}{(2\pi)^4} \int_0^1 dx \frac{l^0}{l^0 - i\epsilon} \frac{\vec{l}^2 + \vec{l} \cdot \vec{q}}{[l^2 + (2l \cdot q + q^2)x - m_\pi^2 + i\epsilon]^2}$$

Shifting $l \rightarrow l - qx$, using $q^0 = 0$ and dropping all odd powers of l due to symmetry:

$$\begin{aligned} &= \int_0^1 dx \int \frac{d^4 l}{(2\pi)^4} \frac{l^0}{l^0 - i\epsilon} \frac{\vec{l}^2 - \vec{q}^2 x(1-x)}{[l^2 - \vec{q}^2 x(1-x) - m_\pi^2 + i\epsilon]^2} \\ &= \int_0^1 dx \int \frac{d^3 \vec{l}}{(2\pi)^3} \int \frac{dl^0}{2\pi} \frac{l^0}{l^0 - i\epsilon} \frac{\vec{l}^2 - \vec{q}^2 x(1-x)}{[(l^0)^2 - \vec{l}^2 - \vec{q}^2 x(1-x) - m_\pi^2 + i\epsilon]^2} \end{aligned}$$

Executing the l^0 -integration with the residue theorem and setting $\epsilon \rightarrow 0$:

$$= \frac{i}{4} \int_0^1 dx \int \frac{d^3 \vec{l}}{(2\pi)^3} \frac{\vec{l}^2 - \vec{q}^2 x(1-x)}{[\vec{l}^2 + \vec{q}^2 x(1-x) + m_\pi^2]^{3/2}}$$

Going to $D - 1$ dimensions and inserting μ lets us rewrite:

$$= \frac{i}{4} \mu^{4-D} \int_0^1 dx \int \frac{d^{D-1} \vec{l}}{(2\pi)^{D-1}} \frac{\vec{l}^2 - \vec{q}^2 x(1-x)}{[\vec{l}^2 + \vec{q}^2 x(1-x) + m_\pi^2]^{3/2}}$$

Transforming to $(D-1)$ -dimensional spherical coordinates ($d^{D-1}\vec{l} = l^{D-2}dl d\Omega_{D-1}$ with $|\vec{l}| = l$) and using eq. (A.9):

$$= \frac{i\sqrt{\pi}}{(4\pi)^{D/2}} \frac{\mu^{4-D}}{\Gamma\left(\frac{D-1}{2}\right)} \int_0^1 dx \int_0^\infty dl \frac{l^D - l^{D-2}\vec{q}^2 x(1-x)}{[l^2 + \vec{q}^2 x(1-x) + m_\pi^2]^{3/2}}$$

At last availing ourselves of eq. (A.8) gives, after some simplification and use of $\Gamma(x+1) = x \cdot \Gamma(x)$ and $\Gamma(3/2) = \sqrt{\pi}/2$:

$$= \frac{i}{(4\pi)^{D/2}} \mu^{4-D} \int_0^1 dx \left\{ \frac{\left(\frac{D-1}{2}\right)}{(\vec{q}^2 x(1-x) + m_\pi^2)^{(2-D)/2}} \Gamma\left(\frac{2-D}{2}\right) - \frac{\vec{q}^2 x(1-x)}{(\vec{q}^2 x(1-x) + m_\pi^2)^{(4-D)/2}} \Gamma\left(\frac{4-D}{2}\right) \right\}$$

Now, we are ready to insert $D = 4 - \epsilon$ in the limit of $\epsilon \rightarrow 0$, where we use eqs. (A.10) and (A.11). In addition, we substitute $a^\epsilon = \exp(\epsilon \cdot \ln(a)) = 1 + \epsilon \cdot \ln(a) + \mathcal{O}(\epsilon^2)$ for $\epsilon \rightarrow 0$.

$$= \frac{i}{16\pi^2} \int_0^1 dx \left\{ \left(\frac{5}{2} \vec{q}^2 x(1-x) + \frac{3}{2} m_\pi^2 \right) \left(-\frac{2}{\epsilon} + \gamma_E - 1 - \ln(4\pi) + \ln\left(\frac{\vec{q}^2 x(1-x) + m_\pi^2}{\mu^2} \right) \right) + 2\vec{q}^2 x(1-x) + m_\pi^2 \right\}$$

Executing the x -integration (eqs. (A.12) and (A.13)):

$$\boxed{\mathcal{I}_{\text{tr}} = \frac{i}{16\pi^2} \left\{ \left(\frac{5}{12} \vec{q}^2 + \frac{3}{2} m_\pi^2 \right) R - \frac{13}{36} \vec{q}^2 - \frac{m_\pi^2}{3} + \left(\frac{5}{6} \vec{q}^2 + 3m_\pi^2 \right) \ln\left(\frac{m_\pi}{\mu} \right) + \left(\frac{5}{6} \vec{q}^2 + \frac{4}{3} m_\pi^2 \right) L(q) \right\}} \quad (\text{B.1})$$

$$\text{with } R := -\frac{2}{\epsilon} + \gamma_E - 1 - \ln(4\pi) \quad (\text{B.2})$$

Working in a modified minimal subtraction scheme (\overline{MS}) means absorbing the term proportional to R into the counterterms at next-to-next-to-leading order.

B.2 The football integral

$$\mathcal{I}_{\text{fb}} = \int \frac{d^4 l}{(2\pi)^4} \frac{(l^0)^2}{[(l+q)^2 - m_\pi^2 + i\epsilon][l^2 - m_\pi^2 + i\epsilon]}$$

Introducing Feynman parameters, shifting $l \rightarrow l - qx$, using $q^0 = 0$ and dropping all odd powers of l :

$$\begin{aligned} &= \int_0^1 dx \int \frac{d^4 l}{(2\pi)^4} \frac{(l^0)^2}{[l^2 - \vec{q}^2 x(1-x) - m_\pi^2 + i\epsilon]^2} \\ &= \int_0^1 dx \int \frac{d^3 \vec{l}}{(2\pi)^3} \int \frac{dl^0}{2\pi} \frac{(l^0)^2}{[(l^0)^2 - \vec{l}^2 - \vec{q}^2 x(1-x) - m_\pi^2 + i\epsilon]^2} \end{aligned}$$

Executing the l^0 -integration with the residue theorem and setting $\epsilon \rightarrow 0$:

$$= -\frac{i}{4} \int_0^1 dx \int \frac{d^3 \vec{l}}{(2\pi)^3} \frac{1}{[\vec{l}^2 + \vec{q}^2 x(1-x) + m_\pi^2]^{1/2}}$$

Going to $D-1$ dimensions, transforming to spherical coordinates and performing the angular integration with eq. (A.9):

$$= -\frac{i\sqrt{\pi}}{(4\pi)^{D/2}} \frac{\mu^{4-D}}{\Gamma(\frac{D-1}{2})} \int_0^1 dx \int_0^\infty dl \frac{l^{D-2}}{[l^2 + \vec{q}^2 x(1-x) + m_\pi^2]^{1/2}}$$

Applying eq. (A.8) and using $\Gamma(1/2) = \sqrt{\pi}$:

$$= -\frac{1}{2} \frac{i}{(4\pi)^{D/2}} \mu^{4-D} \int_0^1 dx \frac{\Gamma(\frac{D-1}{2})}{(\vec{q}^2 x(1-x) + m_\pi^2)^{(2-D)/2}}$$

Inserting $D = 4 - \epsilon$:

$$= -\frac{i}{32\pi^2} \int_0^1 dx (\vec{q}^2 x(1-x) + m_\pi^2) \left(-\frac{2}{\epsilon} + \gamma_E - 1 - \ln(4\pi) + \ln\left(\frac{\vec{q}^2 x(1-x) + m_\pi^2}{\mu^2}\right) \right)$$

Executing the x -integration (eqs. A.12 and A.13):

$$\boxed{\mathcal{I}_{\text{fb}} = \frac{i}{16\pi^2} \left\{ -\left(\frac{\vec{q}^2}{12} + \frac{m_\pi^2}{2}\right) R + \frac{5}{36} \vec{q}^2 + \frac{2}{3} m_\pi^2 - \left(\frac{\vec{q}^2}{6} + m_\pi^2\right) \ln\left(\frac{m_\pi}{\mu}\right) - \left(\frac{\vec{q}^2}{6} + \frac{4}{6} m_\pi^2\right) L(q) \right\}} \quad (\text{B.3})$$

R is defined in eq. (B.2).

B.3 The box integrals

The first integral is not explicitly calculated since it splits into the repeated 1PE and the irreducible 2PE contribution. Because the LSE already takes care of iterated diagrams, we show that we can omit this doubled 1PE and thus use $\mathcal{I}_{\text{box}}^1 \rightarrow \mathcal{I}_{\text{box}}^2$ (cf. Machleidt & Entem⁸¹).

$$\mathcal{I}_{\text{box}}^1 = \int \frac{d^4 l}{(2\pi)^4} \frac{(\vec{q}_2 \cdot \vec{q}_1)^2}{[l^0 + i\epsilon][l^0 - i\epsilon][q_2^2 - m_\pi^2 + i\epsilon][q_1^2 - m_\pi^2 + i\epsilon]}$$

Expanding $q_1^2 = (l^0)^2 - \vec{q}_1^2$ and $q_2^2 = (l^0)^2 - \vec{q}_2^2$ and introducing Feynman parameters:

$$\begin{aligned} &= \int \frac{d^4 l}{(2\pi)^4} \int_0^1 dx \frac{(\vec{q}_2 \cdot \vec{q}_1)^2}{[l^0 + i\epsilon][l^0 - i\epsilon][(l^0)^2 + (\vec{q}_1^2 - \vec{q}_2^2)x - \vec{q}_1^2 - m_\pi^2 + i\epsilon]^2} \\ &= \int_0^1 dx \int \frac{d^3 \vec{l}}{(2\pi)^3} (\vec{q}_2 \cdot \vec{q}_1)^2 \int \frac{dl^0}{2\pi} \frac{1}{[l^0 + i\epsilon][l^0 - i\epsilon][(l^0)^2 - a^2 + i\epsilon]^2} \end{aligned} \quad (\text{B.4})$$

Here, $a^2 = (\vec{q}_2^2 - \vec{q}_1^2)x + \vec{q}_1^2 + m_\pi^2$.

The l^0 -integration diverges as $\epsilon \rightarrow 0$ and our approximation of the heavy meson propagator produces nonphysical poles. To avoid this pinch singularity,⁸² we use a formalism discussed by Weinberg:⁸³ the heavy meson propagator is approximated. Thus, including a term of second order shifts the location of the pole and evades the singularity:

$$i\epsilon \rightarrow i\zeta = \frac{\vec{p}^2}{2m_B} - \frac{\vec{l}^2}{2m_B} + i\epsilon$$

Consider eq. (B.4) with $i\epsilon \rightarrow i\zeta$:

$$= \int_0^1 dx \int \frac{d^3 \vec{l}}{(2\pi)^3} (\vec{q}_2 \cdot \vec{q}_1)^2 \int \frac{dl^0}{2\pi} \frac{1}{[l^0 + i\zeta][l^0 - i\zeta][(l^0)^2 - a^2 + i\epsilon]^2}$$

Applying the residue theorem and setting $\epsilon \rightarrow 0$:

$$= \int_0^1 dx \int \frac{d^3 \vec{l}}{(2\pi)^3} (\vec{q}_2 \cdot \vec{q}_1)^2 \frac{i}{4} \frac{2a - i\zeta}{i\zeta a^3 (a - i\zeta)^2}$$

Expanding the fraction for $a \gg i\zeta$ and dropping everything of order $\mathcal{O}(\zeta)$:

$$= \int_0^1 dx \int \frac{d^3 \vec{l}}{(2\pi)^3} (\vec{q}_2 \cdot \vec{q}_1)^2 \frac{i}{4} \left(\frac{3}{a^5} + \frac{2}{i\zeta a^4} + \mathcal{O}(\zeta) \right) \quad (\text{B.5})$$

The first term of this expansion reproduces the integral encountered in the crossed box (cf. eq. (B.7)). The second term comes from the poles moving towards one another and is the repeated

⁸¹Ibid., p.74.

⁸²"pinch", because the singularity would be squeezed between $+i\epsilon$ and $-i\epsilon$

⁸³Weinberg, op. cit., p.7.

1PE, which we will show below. The dropped terms scale at leading order with $i\zeta/a^6$. Since $i\zeta \sim p_{typ}^2/m_B$ and $a^2 \sim p_{typ}^2$, these neglected terms are of order $O(m_B^{-1} p_{typ}^{-4})$.

Inserting $i\zeta = \vec{p}^2/(2m_B) - \vec{l}^2(2m_B)$:

$$\mathcal{I}_{\text{box}}^1 = \mathcal{I}_{\text{box}}^2 + i m_B \int_0^1 dx \int \frac{d^3 \vec{l}}{(2\pi)^3} \frac{(\vec{q}_2 \cdot \vec{q}_1)^2}{[\vec{p}^2 - \vec{l}^2][(\vec{q}_2^2 - \vec{q}_1^2)x + \vec{q}_1^2 + m_\pi^2]^2}$$

Undoing the Feynman parameters:

$$\mathcal{I}_{\text{box}}^1 - \mathcal{I}_{\text{box}}^2 = i m_B \int \frac{d^3 \vec{l}}{(2\pi)^3} \frac{(\vec{q}_2 \cdot \vec{q}_1)^2}{[\vec{p}^2 - \vec{l}^2][\vec{q}_2^2 + m_\pi^2][\vec{q}_1^2 + m_\pi^2]},$$

which is the non-relativistic version of the reducible 2PE as stated by Kaiser⁸⁴ without the adequate prefactor of $-ig^4 m_B^2/16f_\pi^4$. Its chiral dimension is $O(m_B p_{typ}/\Lambda_h^2)$.

$$V_{2\text{PE, it}}^{\text{eff}}(\vec{p}', \vec{p}) = m_B \int \frac{d^3 \vec{l}}{(2\pi)^3} \frac{V_{1\text{PE}}^{\text{eff}}(\vec{p}', \vec{l}) V_{1\text{PE}}^{\text{eff}}(\vec{l}, \vec{p})}{\vec{p}^2 - \vec{l}^2 + i\epsilon} \quad (\text{B.6})$$

We do not need to worry about the SU(2) isospin structure as below in integral $\mathcal{I}_{\text{corr}}^4$ (sec. B.4) because it is identical both in the iterated 1PE and the planar box.

Since we are only interested in the irreducible contributions at NLO, we drop this reducible term and use $\mathcal{I}_{\text{box}}^2$ instead. This is the same as omitting the heavy meson poles (generated by $[l^0 + i\epsilon][l^0 - i\epsilon]$). In conclusion, the treatment of the planar box comes down to a sign flip $+i\epsilon \rightarrow -i\epsilon$ in one of the heavy meson propagators.

$$\mathcal{I}_{\text{box}}^2 = \int \frac{d^4 l}{(2\pi)^4} \frac{(\vec{q}_2 \cdot \vec{q}_1)^2}{[l^0 - i\epsilon]^2 [q_2^2 - m_\pi^2 + i\epsilon][q_1^2 - m_\pi^2 + i\epsilon]}$$

Following the same steps as outlined for $\mathcal{I}_{\text{box}}^1$ above yields:

$$= \int_0^1 dx \int \frac{d^3 \vec{l}}{(2\pi)^3} (\vec{q}_2 \cdot \vec{q}_1)^2 \int \frac{dl^0}{2\pi} \frac{1}{[l^0 - i\epsilon]^2 [(l^0)^2 - (\vec{q}_2^2 - \vec{q}_1^2)x - \vec{q}_1^2 - m_\pi^2 + i\epsilon]^2}$$

Executing the l^0 -integration with the residue theorem and setting $\epsilon \rightarrow 0$:

$$= i \frac{3}{4} \int_0^1 dx \int \frac{d^3 \vec{l}}{(2\pi)^3} \frac{(\vec{q}_2 \cdot \vec{q}_1)^2}{[(\vec{q}_2^2 - \vec{q}_1^2)x + \vec{q}_1^2 + m_\pi^2]^{5/2}} \quad (\text{B.7})$$

Shift $\vec{l} \rightarrow \vec{l} + \vec{p}$ such that $\vec{q}_1 = \vec{p} - \vec{l} \rightarrow -\vec{l}$ and $\vec{q}_2 = \vec{p}' - \vec{l} \rightarrow -\vec{l} + \vec{q}$ with $\vec{q} = \vec{p}' - \vec{p}$:

$$= i \frac{3}{4} \int_0^1 dx \int \frac{d^3 \vec{l}}{(2\pi)^3} \frac{(\vec{l} \cdot (\vec{l} - \vec{q}))^2}{[\vec{l}^2 + (-2\vec{l} \cdot \vec{q} + \vec{q}^2)x + m_\pi^2]^{5/2}}$$

⁸⁴Norbert Kaiser, R. Brockmann, and W. Weise. “Peripheral nucleon-nucleon phase shifts and chiral symmetry”. In: *Nucl. Phys. A* 625 (1997), pp. 758–788. doi: 10.1016/S0375-9474(97)00586-1. eprint: nucl-th/9706045.

Completing the square in the denominator through $\vec{l} \rightarrow \vec{l} + \vec{q}x$ and dropping terms odd in \vec{l} :

$$= i \frac{3}{4} \int_0^1 dx \int \frac{d^3 \vec{l}}{(2\pi)^3} \frac{\vec{l}^4 - 2\vec{l}^2 \vec{q}^2 x(1-x) + (\vec{l} \cdot \vec{q})^2 (2x-1)^2 + (\vec{q}^2 x(1-x))^2}{[\vec{l}^2 + \vec{q}^2 x(1-x) + m_\pi^2]^{5/2}}$$

Going to $D-1$ dimensions, inserting μ and using eq. (A.7):

$$= i \frac{3}{4} \mu^{4-D} \int_0^1 dx \int \frac{d^{D-1} \vec{l}}{(2\pi)^{D-1}} \frac{\vec{l}^4 + \vec{l}^2 \vec{q}^2 (2\frac{D+1}{D-1}x^2 - 2\frac{D+1}{D-1}x + 1) + (\vec{q}^2 x(1-x))^2}{[\vec{l}^2 + \vec{q}^2 x(1-x) + m_\pi^2]^{5/2}}$$

Going to $(D-1)$ -dimensional spherical coordinates and using eq. (A.9):

$$= i \frac{3\sqrt{\pi}}{(4\pi)^{D/2}} \frac{\mu^{4-D}}{\Gamma\left(\frac{D-1}{2}\right)} \int_0^1 dx \int_0^\infty dl \frac{l^{D+2} + l^D \vec{q}^2 (2\frac{D+1}{D-1}x^2 - 2\frac{D+1}{D-1}x + 1) + l^{D-2} (\vec{q}^2 x(1-x))^2}{[l^2 + \vec{q}^2 x(1-x) + m_\pi^2]^{5/2}}$$

Solving the l -integration with eq. (A.8) and using $\Gamma(5/2) = 3\sqrt{\pi}/4$:

$$= i \frac{2}{(4\pi)^{D/2}} \mu^{4-D} \int_0^1 dx \left(\frac{\left(\frac{D+1}{2}\right)\left(\frac{D-1}{2}\right)}{[\vec{q}^2 x(1-x) + m_\pi^2]^{(2-D)/2}} \Gamma\left(\frac{2-D}{2}\right) \right. \\ \left. + \frac{\left(\frac{D-1}{2}\right) \vec{q}^2 \left(2\frac{D+1}{D-1}x^2 - 2\frac{D+1}{D-1}x + \frac{1}{D-1}\right)}{[\vec{q}^2 x(1-x) + m_\pi^2]^{(4-D)/2}} \Gamma\left(\frac{4-D}{2}\right) \right. \\ \left. + \frac{(\vec{q}^2 x(1-x))^2}{[\vec{q}^2 x(1-x) + m_\pi^2]^{(6-D)/2}} \Gamma\left(\frac{6-D}{2}\right) \right)$$

Inserting $D = 4 - \epsilon$:

$$= \frac{i}{16\pi^2} \int_0^1 dx \left\{ \left(-\frac{35}{2}x^2 + \frac{35}{2}x - 1 \right) \vec{q}^2 + \frac{15}{2}m_\pi^2 \right\} R \\ + (-22x^2 + 22x - 1) \vec{q}^2 + 8m_\pi^2 + \frac{2\vec{q}^4 x^2 (1-x)^2}{m_\pi^2 + \vec{q}^2 x(1-x)} \\ + \left\{ \left(-\frac{35}{2}x^2 + \frac{35}{2}x - 1 \right) \vec{q}^2 + \frac{15}{2}m_\pi^2 \right\} \ln(\vec{q}^2 x(1-x) + m_\pi^2) \right\} \quad (\text{B.8})$$

Executing the x -integration (eqs. (A.12) and (A.13)):

$$\boxed{\mathcal{I}_{\text{box}}^2 = \frac{i}{16\pi^2} \left\{ \left(\frac{23}{12} \vec{q}^2 + \frac{15}{2} m_\pi^2 \right) R + \frac{5}{36} \vec{q}^2 + \frac{8}{3} m_\pi^2 \right.} \\ \left. + \left(\frac{23}{6} \vec{q}^2 + 15 m_\pi^2 \right) \ln\left(\frac{m_\pi}{\mu}\right) + \left(\frac{23}{6} \vec{q}^2 + \frac{10}{3} m_\pi^2 + \frac{8m_\pi^4}{4m_\pi^2 + \vec{q}^2} \right) L(q) \right\}} \quad (\text{B.9})$$

R is defined in eq. (B.2). We used

$$\int_0^1 dx \frac{2\vec{q}^4 x^2 (1-x)^2}{m_\pi^2 + \vec{q}^2 x (1-x)} = -m_\pi^2 + \frac{\vec{q}^2}{6} + \frac{4m_\pi^4}{4m_\pi^2 + \vec{q}^2} L(q). \quad (\text{B.10})$$

$$\left(\mathcal{I}_{\text{box}}^3 \right)_{in} = \int \frac{d^4 l}{(2\pi)^4} \frac{\varepsilon_{ijs} \varepsilon_{nrm} (q_2)_j (q_1)_s (q_2)_r (q_1)_m}{[l^0 - i\epsilon]^2 [q_2^2 - m_\pi^2 + i\epsilon] [q_1^2 - m_\pi^2 + i\epsilon]}$$

Introducing Feynman parameters and applying the residue theorem as outlined for $\mathcal{I}_{\text{box}}^1$:

$$= i \frac{3}{4} \int_0^1 dx \int \frac{d^3 \vec{l}}{(2\pi)^3} \frac{\varepsilon_{ijs} \varepsilon_{nrm} (q_2)_j (q_1)_s (q_2)_r (q_1)_m}{[(\vec{q}_2^2 - \vec{q}_1^2)x + \vec{q}_1^2 + m_\pi^2]^{5/2}}$$

Shift $\vec{l} \rightarrow \vec{l} + \vec{p}$ such that $\vec{q}_1 = \vec{p} - \vec{l} \rightarrow -\vec{l}$ and $\vec{q}_2 = \vec{p}' - \vec{l} \rightarrow -\vec{l} + \vec{q}$ with $\vec{q} = \vec{p}' - \vec{p}$:

$$= i \frac{3}{4} \int_0^1 dx \int \frac{d^3 \vec{l}}{(2\pi)^3} \frac{\varepsilon_{ijs} \varepsilon_{nrm} (l-q)_j l_s (l-q)_r l_m}{[\vec{l}^2 + (-2\vec{l} \cdot \vec{q} + \vec{q}^2)x + m_\pi^2]^{5/2}}$$

Going to $D-1$ dimensions, inserting μ , completing the square via $\vec{l} \rightarrow \vec{l} + \vec{q}x$:

$$= i \frac{3}{4} \mu^{4-D} \int_0^1 dx \int \frac{d^{D-1} \vec{l}}{(2\pi)^{D-1}} \frac{\varepsilon_{ijs} \varepsilon_{nrm} (l_j + q_j(x-1))(l_s + q_s x)(l_r + q_r(x-1))(l_m + q_m x)}{[\vec{l}^2 + \vec{q}^2 x(1-x) + m_\pi^2]^{5/2}}$$

Due to the anti-symmetry of the Levi-Civita tensor, most of the numerator vanishes since $\varepsilon_{ijs}(l_j + q_j x)(l_s + q_s x) = 0$, and thus:

$$\begin{aligned} &= i \frac{3}{4} \mu^{4-D} \int_0^1 dx \int \frac{d^{D-1} \vec{l}}{(2\pi)^{D-1}} \frac{\varepsilon_{ijs} \varepsilon_{nrm} (-l_s q_j)(-l_m q_r)}{[\vec{l}^2 + \vec{q}^2 x(1-x) + m_\pi^2]^{5/2}} \\ &= i \frac{3}{4} \mu^{4-D} \int_0^1 dx (\delta_{in} \vec{q}^2 - q_i q_n) \int \frac{d^{D-1} \vec{l}}{(2\pi)^{D-1}} \frac{\frac{\vec{l}^2}{D-1}}{[\vec{l}^2 + \vec{q}^2 x(1-x) + m_\pi^2]^{5/2}}, \end{aligned}$$

where we used eq. (A.7).

Going to $(D-1)$ -dimensional spherical coordinates and using eq. (A.9):

$$= i \frac{3\sqrt{\pi}}{(4\pi)^{D/2}} \frac{\mu^{4-D}}{\Gamma\left(\frac{D-1}{2}\right)} \int_0^1 dx (\delta_{in} \vec{q}^2 - q_i q_n) \int_0^\infty dl \frac{\frac{l^D}{D-1}}{[l^2 + \vec{q}^2 x(1-x) + m_\pi^2]^{5/2}}$$

Solving the l -integration with eq. (A.8) and using $\Gamma(5/2) = 3\sqrt{\pi}/4$:

$$\begin{aligned} &= i \frac{2}{(4\pi)^{D/2}} \frac{\mu^{4-D}}{\Gamma\left(\frac{D-1}{2}\right)} \int_0^1 dx \frac{\delta_{in} \vec{q}^2 - q_i q_n}{D-1} \frac{\Gamma\left(\frac{4-D}{2}\right) \Gamma\left(\frac{D+1}{2}\right)}{[\vec{q}^2 x(1-x) + m_\pi^2]^{(4-D)/2}} \\ &= \frac{i}{(4\pi)^{D/2}} \mu^{4-D} \int_0^1 dx (\delta_{in} \vec{q}^2 - q_i q_n) \frac{\Gamma\left(\frac{4-D}{2}\right)}{[\vec{q}^2 x(1-x) + m_\pi^2]^{(4-D)/2}} \end{aligned}$$

Inserting $D = 4 - \epsilon$:

$$= -\frac{i}{16\pi^2} \int_0^1 dx \left(\delta_{in} \vec{q}^2 - q_i q_n \right) \left(R + 1 + \ln \left(\frac{\vec{q}^2 x(1-x) + m_\pi^2}{\mu^2} \right) \right)$$

Executing the x -integration (eq. (A.12)):

$$\boxed{(\mathcal{I}_{\text{box}}^3)_{in} = \frac{i}{16\pi^2} (\delta_{in} \vec{q}^2 - q_i q_n) \left\{ -R + 1 - 2L(q) - 2 \ln \left(\frac{m_\pi}{\mu} \right) \right\}} \quad (\text{B.11})$$

$$(\mathcal{I}_{\text{box}}^4)_{ikn} = \int \frac{d^4 l}{(2\pi)^4} \frac{((q_2)_k (q_1)_i - (q_2)_i (q_1)_k) \varepsilon_{num}(q_2)_u (q_1)_m}{[l^0 - i\epsilon]^2 [q_2^2 - m_\pi^2 + i\epsilon] [q_1^2 - m_\pi^2 + i\epsilon]}$$

Introducing Feynman parameters and applying the residue theorem as outlined for $\mathcal{I}_{\text{box}}^1$:

$$= i \frac{3}{4} \int_0^1 dx \int \frac{d^3 \vec{l}}{(2\pi)^3} \frac{((q_2)_k (q_1)_i - (q_2)_i (q_1)_k) \varepsilon_{num}(q_2)_u (q_1)_m}{[(\vec{q}_2^2 - \vec{q}_1^2)x + \vec{q}_1^2 + m_\pi^2]^{5/2}}$$

Shift $\vec{l} \rightarrow \vec{l} + \vec{p}$ such that $\vec{q}_1 = \vec{p} - \vec{l} \rightarrow -\vec{l}$ and $\vec{q}_2 = \vec{p}' - \vec{l} \rightarrow -\vec{l} + \vec{q}$ with $\vec{q} = \vec{p}' - \vec{p}$:

$$= i \frac{3}{4} \int_0^1 dx \int \frac{d^3 \vec{l}}{(2\pi)^3} \frac{((l-q)_k l_i - (l-q)_i l_k) \varepsilon_{num}(l-q)_u l_m}{[\vec{l}^2 + (-2\vec{l} \cdot \vec{q} + \vec{q}^2)x + m_\pi^2]^{5/2}}$$

Going to $D-1$ dimensions, inserting μ , completing the square via $\vec{l} \rightarrow \vec{l} + \vec{q}x$:

$$= i \frac{3}{4} \mu^{4-D} \int_0^1 dx \int \frac{d^{D-1} \vec{l}}{(2\pi)^{D-1}} \frac{((l+q(x-1))_k (l+qx)_i - (l+q(x-1))_i (l+qx)_k)}{[\vec{l}^2 + \vec{q}^2 x(1-x) + m_\pi^2]^{5/2}} \\ \times \varepsilon_{num}(l+q(x-1))_u (l+qx)_m$$

Everything proportional to $\varepsilon_{num} l_u l_m$ or $\varepsilon_{num} q_u q_m$ and every term of odd power in l vanishes due to symmetry:

$$= i \frac{3}{4} \mu^{4-D} \int_0^1 dx \int \frac{d^{D-1} \vec{l}}{(2\pi)^{D-1}} \frac{(l_k q_i - l_i q_k) \varepsilon_{num} (l_u q_m x + l_m q_u (x-1))}{[\vec{l}^2 + \vec{q}^2 x(1-x) + m_\pi^2]^{5/2}} \\ = i \frac{3}{4} \mu^{4-D} \int_0^1 dx (\varepsilon_{nku} q_u q_i - \varepsilon_{niu} q_u q_k) \int \frac{d^{D-1} \vec{l}}{(2\pi)^{D-1}} \frac{\frac{\vec{l}^2}{D-1}}{[\vec{l}^2 + \vec{q}^2 x(1-x) + m_\pi^2]^{5/2}}$$

Solving the remaining integral follows exactly the same calculation as in $\mathcal{I}_{\text{box}}^3$ above and thus:

$$\boxed{(\mathcal{I}_{\text{box}}^4)_{ikn} = \frac{i}{16\pi^2} (\varepsilon_{nku} q_u q_i - \varepsilon_{niu} q_u q_k) \left\{ -R + 1 - 2L(q) - 2 \ln \left(\frac{m_\pi}{\mu} \right) \right\}} \quad (\text{B.12})$$

B.4 Integrals from CCI or C1PE

The iterated CI is completely reducible: no matter which of the Feynman rules are chosen, they are only constants. Thus, any iterated CI without the factors of mass and $-iC_i$ gives:

$$V_{\text{CI, it}}^{\text{eff}} \propto -i \int \frac{d^4 l}{(2\pi)^4} \frac{1}{[l^0 + i\epsilon][l^0 - i\epsilon]}$$

To avoid the nonphysical pinch singularity as $\epsilon \rightarrow 0$, we include a term of second order that shifts the location of the pole.

$$i\epsilon \rightarrow i\zeta = \frac{\vec{p}^2}{2m_B} - \frac{\vec{l}^2}{2m_B} + i\epsilon$$

This yields:

$$V_{\text{CI, it}}^{\text{eff}} \propto m_B \int \frac{d^3 \vec{l}}{(2\pi)^3} \frac{1}{\vec{p}^2 - \vec{l}^2 + i\epsilon}$$

Comparison to eq. (B.6) reveals that the iterated CI is completely reducible and thus will be reproduced by the LSE. The diagram's chiral dimension is $\mathcal{O}(m_B p_{\text{typ}}/\Lambda_h^2)$.

$$\begin{aligned} \mathcal{I}_{\text{corr}}^1 &= \int \frac{d^4 l}{(2\pi)^4} \frac{1}{l^2 - m_\pi^2 + i\epsilon} \\ &= \int \frac{d^3 \vec{l}}{(2\pi)^3} \int \frac{dl^0}{2\pi} \frac{1}{(l^0)^2 - \vec{l}^2 - m_\pi^2 + i\epsilon} \end{aligned}$$

Executing the l^0 -integration with the residue theorem and setting $\epsilon \rightarrow 0$:

$$= -\frac{i}{2} \int \frac{d^3 \vec{l}}{(2\pi)^3} \frac{1}{[\vec{l}^2 + m_\pi^2]^{1/2}}$$

Going to $D - 1$ dimensions and inserting μ lets us rewrite:

$$= -\frac{i}{2} \mu^{4-D} \int \frac{d^{D-1} \vec{l}}{(2\pi)^{D-1}} \frac{1}{\vec{l}^2 + m_\pi^2}$$

Transforming to $(D - 1)$ -dimensional spherical coordinates ($d^{D-1} \vec{l} = l^{D-2} dl d\Omega_{D-1}$ with $|\vec{l}| = l$) and using eq. (A.9):

$$= -\frac{i}{2} \frac{2\sqrt{\pi}}{(4\pi)^{D/2}} \frac{\mu^{4-D}}{\Gamma\left(\frac{D-1}{2}\right)} \int_0^\infty dl \frac{l^{D-2}}{l^2 + m_\pi^2}$$

Using eq. (A.8) and simplifying:

$$= -\frac{i}{(4\pi)^{D/2}} \mu^{4-D} \frac{\Gamma\left(\frac{2-D}{2}\right)}{m_\pi^{2-D}} \quad (\text{B.13})$$

Inserting $D = 4 - \epsilon$:

$$= -\frac{i}{16\pi^2} m_\pi^2 \left(\frac{4\pi\mu^2}{m_\pi^2} \right)^{\epsilon/2} \left(-\frac{2}{\epsilon} + \gamma_E - 1 \right)$$

Setting $\epsilon \rightarrow 0$ and using R from eq. (B.2):

$$= -\frac{i}{16\pi^2} m_\pi^2 \left(R + 2 \ln \left(\frac{m_\pi}{\mu} \right) \right)$$

$$\begin{aligned} \mathcal{I}_{\text{corr}}^2 &= \int \frac{d^4 l}{(2\pi)^4} \frac{\vec{l}^2}{[l^0 + i\epsilon][l^2 - m_\pi^2 + i\epsilon]} \\ &= \int \frac{d^3 \vec{l}}{(2\pi)^3} \int \frac{dl^0}{2\pi} \frac{\vec{l}^2}{[l^0 + i\epsilon][(l^0)^2 - \vec{l}^2 - m_\pi^2 + i\epsilon]} \end{aligned}$$

Executing the l^0 -integration with the residue theorem and setting $\epsilon \rightarrow 0$:

$$= \frac{i}{2} \int \frac{d^3 \vec{l}}{(2\pi)^3} \frac{\vec{l}^2}{\vec{l}^2 + m_\pi^2}$$

Going to $D - 1$ dimensions and inserting μ lets us rewrite:

$$= \frac{i}{2} \mu^{4-D} \int \frac{d^{D-1} \vec{l}}{(2\pi)^{D-1}} \frac{\vec{l}^2}{\vec{l}^2 + m_\pi^2}$$

Transforming to $(D - 1)$ -dimensional spherical coordinates ($d^{D-1} \vec{l} = l^{D-2} dl d\Omega_{D-1}$ with $|\vec{l}| = l$) and using eq. (A.9):

$$= i \frac{2\sqrt{\pi}}{(4\pi)^{D/2}} \frac{\mu^{4-D}}{\Gamma\left(\frac{D-1}{2}\right)} \int_0^\infty dl \frac{l^D}{l^2 + m_\pi^2} \quad (\text{B.14})$$

Using eq. (A.8) and simplifying:

$$= -i \frac{\sqrt{\pi}}{(4\pi)^{D/2}} \mu^{4-D} \frac{\Gamma\left(\frac{3-D}{2}\right)}{m_\pi^{(1-D)}} \quad (\text{B.15})$$

Inserting $D = 4 - \epsilon$ and immediately putting $\epsilon \rightarrow 0$:

$$= -i \frac{\sqrt{\pi}}{16\pi^2} m_\pi^3 \Gamma\left(-\frac{1}{2}\right) = \frac{i}{8\pi} m_\pi^3$$

This result comes somewhat surprising since there appear to be no infinities left. However, it reveals a feature of dimensional regularization: polynomial divergent integrals are set to zero

because they need a regulator mass scale (like m_π) that is absent in dimensional regularization. Thus, they have to vanish. This means that the infinities are not dropped (the integral clearly diverges) but are regulator-*independent* (cf. Leibbrandt⁸⁵). We can show this by treating the integral in eq. (B.14) in a different manner (assume even D):

$$\begin{aligned} \int_0^\infty dl \frac{l^D}{l^2 + m_\pi^2} &= \int_0^\infty dl \frac{l^2 l^{D-2}}{l^2 + m_\pi^2} \\ &= \int_0^\infty dl \frac{l^2 + m_\pi^2}{l^2 + m_\pi^2} l^{D-2} - m_\pi^2 \int_0^\infty dl \frac{l^{D-2}}{l^2 + m_\pi^2} \end{aligned}$$

Repeating this $D/2$ times gives:

$$\begin{aligned} &= (-m_\pi^2)^{D/2} \int_0^\infty \frac{dl}{l^2 + m_\pi^2} + \text{polynomial divergencies} \\ &= (-m_\pi^2)^{D/2} \frac{\pi}{2m_\pi} + \text{polynomial divergencies} \end{aligned}$$

The divergencies are handled through renormalization as before. Reinserting into eq. (B.14):

$$\mathcal{I}_{\text{corr}}^2 = i \frac{2\sqrt{\pi}}{(4\pi)^{D/2}} \frac{\mu^{4-D}}{\Gamma\left(\frac{D-1}{2}\right)} \frac{\pi}{2m_\pi} (-m_\pi^2)^{D/2} \xrightarrow{D=4-\epsilon} i \frac{m_\pi^3}{16\sqrt{\pi}} \frac{1}{\Gamma\left(\frac{3-\epsilon}{2}\right)} \left(-\frac{4\pi\mu^2}{m_\pi^2}\right)^{\epsilon/2}$$

When taking the limit $\epsilon \rightarrow 0$ the term converges:

$$= \frac{i}{8\pi} m_\pi^3 + \text{polynomial divergencies},$$

which matches our previous result.

In sec. 5.2.2, we consider the integral $\mathcal{I}_{\text{corr}}^2/(D-1)$. This is calculated in a similar way as $\mathcal{I}_{\text{corr}}^2$ itself. However, entering the calculation after the use of eq. (A.8) (cf. eq. (B.15)):

$$\begin{aligned} &= -i \frac{\sqrt{\pi}}{(4\pi)^{D/2}} \frac{\mu^{4-D}}{D-1} \frac{\Gamma\left(\frac{3-D}{2}\right)}{m^{(1-D)}} \\ &= i \frac{\sqrt{\pi}}{(4\pi)^{D/2}} \frac{\mu^{4-D}}{2} \frac{\Gamma\left(\frac{1-D}{2}\right)}{m^{(1-D)}} \end{aligned}$$

Inserting $D = 4 - \epsilon$ and putting $\epsilon \rightarrow 0$:

$$= i \frac{\sqrt{\pi}}{32\pi^2} m_\pi^3 \Gamma\left(-\frac{3}{2}\right) = \frac{1}{3} \frac{i}{8\pi} m_\pi^3$$

⁸⁵George Leibbrandt. “Introduction to the technique of dimensional regularization”. In: *Rev. Mod. Phys.* 47 (4 Oct. 1975), pp. 849–876. doi: 10.1103/RevModPhys.47.849. URL: <https://link.aps.org/doi/10.1103/RevModPhys.47.849>, p.864.

$$\begin{aligned} \mathcal{I}_{\text{corr}}^3 &= \int \frac{d^4 l}{(2\pi)^4} \frac{\frac{\vec{l}^2}{D-1}}{[l^0 + i\epsilon]^2 [l^2 - m_\pi^2 + i\epsilon]} \\ &= \int \frac{d^3 \vec{l}}{(2\pi)^3} \int \frac{dl^0}{2\pi} \frac{\frac{\vec{l}^2}{D-1}}{[l^0 + i\epsilon]^2 [(l^0)^2 - \vec{l}^2 - m_\pi^2 + i\epsilon]} \end{aligned}$$

Executing the l^0 -integration with the residue theorem and setting $\epsilon \rightarrow 0$:

$$= -\frac{i}{2} \int \frac{d^3 \vec{l}}{(2\pi)^3} \frac{\frac{\vec{l}^2}{D-1}}{[\vec{l}^2 + m_\pi^2]^{3/2}}$$

Going to $D-1$ dimensions and inserting μ lets us rewrite:

$$= -\frac{i}{2} \frac{\mu^{4-D}}{D-1} \int \frac{d^{D-1} \vec{l}}{(2\pi)^{D-1}} \frac{\vec{l}^2}{[\vec{l}^2 + m_\pi^2]^{3/2}}$$

Transforming to $(D-1)$ -dimensional spherical coordinates ($d^{D-1} \vec{l} = l^{D-2} dl d\Omega_{D-1}$ with $|\vec{l}| = l$) and using eq. (A.9):

$$= -\frac{2i\sqrt{\pi}}{(4\pi)^{D/2}} \frac{\mu^{4-D}}{\Gamma\left(\frac{D-1}{2}\right)} \frac{1}{D-1} \int_0^\infty dl \frac{l^D}{[l^2 + m_\pi^2]^{3/2}}$$

Using eq. (A.8) and simplifying:

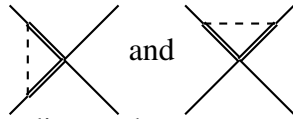
$$= -\frac{i}{(4\pi)^{D/2}} \mu^{4-D} \frac{\Gamma\left(\frac{2-D}{2}\right)}{m_\pi^{2-D}}$$

Inserting $D = 4 - \epsilon$:

$$= -\frac{i}{16\pi^2} m_\pi^2 \left(R + 2 \ln \left(\frac{m_\pi}{\mu} \right) \right)$$

$\mathcal{I}_{\text{corr}}^4$ is not calculated explicitly because it splits into the 1PE plus CI, which are already included, and the irreducible CCI contribution. Because the LSE already takes care of iterated diagrams, we show that we can omit this 1PE plus CI and thus use $\mathcal{I}_{\text{corr}}^4 \rightarrow \mathcal{I}_{\text{corr}}^5$, similar to integral $\mathcal{I}_{\text{box}}^1$ in sec. B.3. In this case, we need to be careful when dealing with the SU(2)

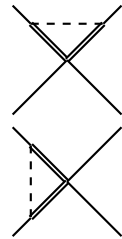
isospin indices, which vary between, e.g.



and

considering that, firstly, the

involved 3-vertices do not lie on the legs leading to the same external states:

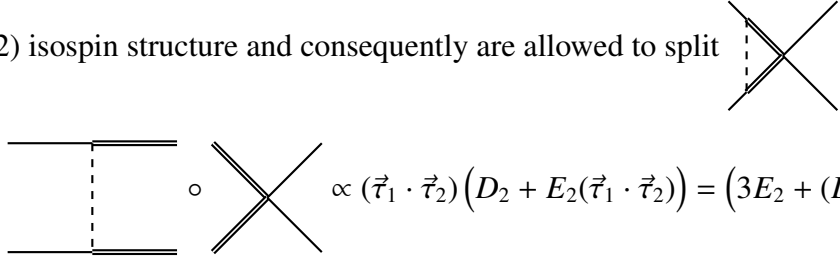


$$\propto (3D_1 + 3E_1(\vec{\tau}_1 \cdot \vec{\tau}_2)) = 3C_1$$

$$\propto (3E_2 + (D_2 + 2E_2)(\vec{\tau}_1 \cdot \vec{\tau}_2)) = 3Z_2$$

Secondly, the order in which the Pauli matrices appear inside V^{eff} changes between the consecutive 1PE plus CI and the CCI. The planar box (sec. B.3) was never affected by these issues because the order is unchanged.

However, when considering the consecutive potentials of 1PE and CI, we still get the same SU(2) isospin structure and consequently are allowed to split



$$\propto (\vec{\tau}_1 \cdot \vec{\tau}_2) (D_2 + E_2(\vec{\tau}_1 \cdot \vec{\tau}_2)) = (3E_2 + (D_2 + 2E_2)(\vec{\tau}_1 \cdot \vec{\tau}_2))$$

With this small preamble, we can now treat $\mathcal{I}_{\text{corr}}^4$:

$$\begin{aligned} \mathcal{I}_{\text{corr}}^4 &= \int \frac{d^4 l}{(2\pi)^4} \frac{\vec{l}^2}{[l^0 + i\epsilon][l^0 - i\epsilon][l^2 - m_\pi^2 + i\epsilon]} \\ &= \int \frac{d^3 \vec{l}}{(2\pi)^3} \int \frac{dl^0}{2\pi} \frac{\vec{l}^2}{[l^0 + i\epsilon][l^0 - i\epsilon][(l^0)^2 - \vec{l}^2 - m_\pi^2 + i\epsilon]} \end{aligned}$$

The l^0 -integration diverges as $\epsilon \rightarrow 0$. To avoid the nonphysical pinch singularity, we employ Weinberg's formalism⁸⁶ and shift the location of the pole via a term of second order:

$$i\epsilon \rightarrow i\zeta = \frac{\vec{p}^2}{2m_B} - \frac{(\vec{p} + \vec{l})^2}{2m_B} + i\epsilon$$

$$\mathcal{I}_{\text{corr}}^4 = \int \frac{d^3 \vec{l}}{(2\pi)^3} \int \frac{dl^0}{2\pi} \frac{\vec{l}^2}{[l^0 + i\zeta][l^0 - i\zeta][(l^0)^2 - \vec{l}^2 - m_\pi^2 + i\epsilon]}$$

Executing the l^0 -integration with the residue theorem and setting $\epsilon \rightarrow 0$:

$$= \int \frac{d^3 \vec{l}}{(2\pi)^3} \left(-\frac{i}{2}\right) \frac{1}{i\zeta[\vec{l}^2 + m_\pi^2] - (i\zeta)^2[\vec{l}^2 + m_\pi^2]^{1/2}}$$

Expanding the fraction for $[\vec{l}^2 + m_\pi^2]^{1/2} \gg i\zeta$ and dropping everything of order $\mathcal{O}(\zeta)$:

$$= \int \frac{d^3 \vec{l}}{(2\pi)^3} \left(-\frac{i}{2}\right) \left(\frac{1}{[\vec{l}^2 + m_\pi^2]^{3/2}} + \frac{1}{i\zeta[\vec{l}^2 + m_\pi^2]} + \mathcal{O}(\zeta) \right)$$

The first term of this expansion reproduces the integral encountered in the corresponding arc diagram (cf. eq. (B.16)). The second term is 1PE plus CI, which we will show by reinserting $i\zeta = \vec{p}^2/(2m_B) - (\vec{p} + \vec{l})^2/(2m_B)$:

$$\mathcal{I}_{\text{corr}}^4 = \mathcal{I}_{\text{corr}}^5 - i m_B \int \frac{d^3 \vec{l}}{(2\pi)^3} \frac{\vec{l}^2}{[\vec{p}^2 - (\vec{p} + \vec{l})^2][\vec{l}^2 + m_\pi^2]}$$

⁸⁶Weinberg, loc. cit.

Shifting the integration variable $\vec{l} \rightarrow \vec{l} - \vec{p}$:

$$\mathcal{I}_{\text{corr}}^4 = \mathcal{I}_{\text{corr}}^5 - i m_B \int \frac{d^3 \vec{l}}{(2\pi)^3} \frac{(\vec{l} - \vec{p})^2}{[\vec{p}^2 - \vec{l}^2][(\vec{l} - \vec{p})^2 + m_\pi^2]}$$

Reinserting the adequate prefactor of $ig^2 m_B^2 [3E_2 + (D_2 + 2E_2)(\vec{\tau}_1 \cdot \vec{\tau}_2)]/4f_\pi^2$, we can identify the latter term via eq. (B.6) as the non-relativistic version of the reducible 1PE plus CI. Its chiral dimension is $\mathcal{O}(m_B p_{\text{typ}}/\Lambda_h^2)$. Since we are only interested in the irreducible contributions at NLO, we drop this term and use $\mathcal{I}_{\text{corr}}^5$ instead. As mentioned above, this is the same as omitting the heavy meson poles (generated by $[l^0 + i\epsilon][l^0 - i\epsilon]$).

$$\begin{aligned} \mathcal{I}_{\text{corr}}^5 &= \int \frac{d^4 l}{(2\pi)^4} \frac{\vec{l}^2}{[l^0 - i\epsilon]^2 [l^2 - m_\pi^2 + i\epsilon]} \\ &= \int \frac{d^3 \vec{l}}{(2\pi)^3} \int \frac{dl^0}{2\pi} \frac{\vec{l}^2}{[l^0 - i\epsilon]^2 [(l^0)^2 - \vec{l}^2 - m_\pi^2 + i\epsilon]} \end{aligned} \quad (\text{B.16})$$

Executing the l^0 -integration with the residue theorem and setting $\epsilon \rightarrow 0$:

$$= -\frac{i}{2} \int \frac{d^3 \vec{l}}{(2\pi)^3} \frac{\vec{l}^2}{[\vec{l}^2 + m_\pi^2]^{3/2}}$$

Going to $D - 1$ dimensions and inserting μ lets us rewrite:

$$= -\frac{i}{2} \mu^{4-D} \int \frac{d^{D-1} \vec{l}}{(2\pi)^{D-1}} \frac{\vec{l}^2}{[\vec{l}^2 + m_\pi^2]^{3/2}}$$

Transforming to $(D-1)$ -dimensional spherical coordinates ($d^{D-1} \vec{l} = l^{D-2} dl d\Omega_{D-1}$ with $|\vec{l}| = l$) and using eq. (A.9):

$$= -\frac{2i\sqrt{\pi}}{(4\pi)^{D/2}} \frac{\mu^{4-D}}{\Gamma\left(\frac{D-1}{2}\right)} \int_0^\infty dl \frac{l^D}{[l^2 + m_\pi^2]^{3/2}}$$

Using eq. (A.8) and simplifying:

$$= -\frac{i}{(4\pi)^{D/2}} \mu^{4-D} (D-1) \frac{\Gamma\left(\frac{2-D}{2}\right)}{m_\pi^{2-D}} \quad (\text{B.17})$$

Inserting $D = 4 - \epsilon$:

$$= -\frac{i}{16\pi^2} m_\pi^2 \left(3R + 6 \ln\left(\frac{m_\pi}{\mu}\right) + 2 \right)$$

In sec. 5.2.3, we encountered integrals of type $\mathcal{I}_{\text{corr}}^5/(D-1)$. They are calculated in a similar way as $\mathcal{I}_{\text{corr}}^5$ itself. However, entering the calculation after the use of eq. (A.8) (cf. eq. (B.17)):

$$\frac{\mathcal{I}_{\text{corr}}^5}{D-1} = -\frac{i}{(4\pi)^{D/2}} \mu^{4-D} \frac{\Gamma\left(\frac{2-D}{2}\right)}{m_\pi^{2-D}} = -\frac{i}{16\pi^2} m_\pi^2 \left(R + 2 \ln\left(\frac{m_\pi}{\mu}\right) \right)$$

We already know this integral as $\mathcal{I}_{\text{corr}}^1$. Thus:

$$\frac{\mathcal{I}_{\text{corr}}^5}{D-1} = \mathcal{I}_{\text{corr}}^1$$

C Diagrams of 2PE

Presented below is a full collection of 2PE diagrams sorted by scattering channel:

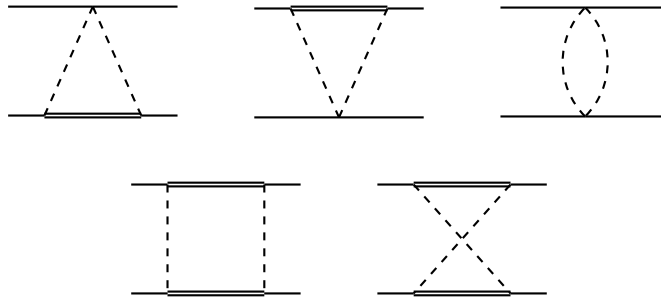


Fig. C.1: 2PE contributions to the scattering of $P\bar{P} \rightarrow P\bar{P}$.

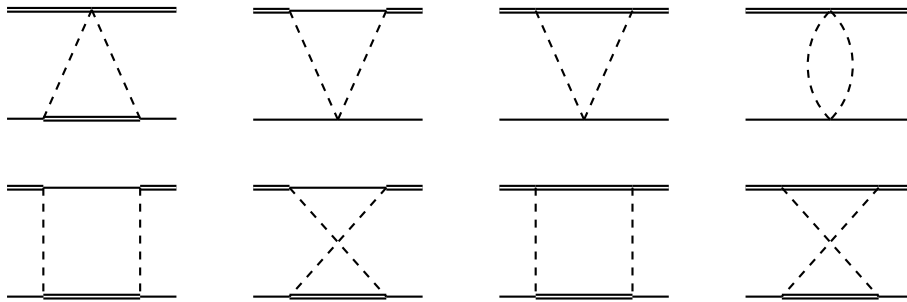
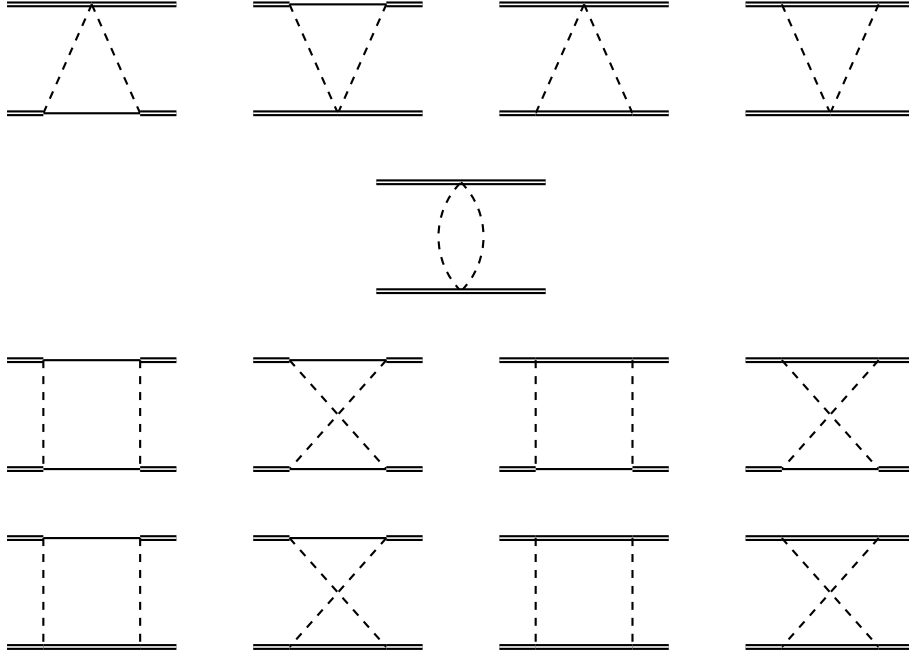
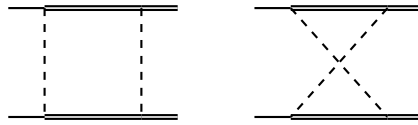
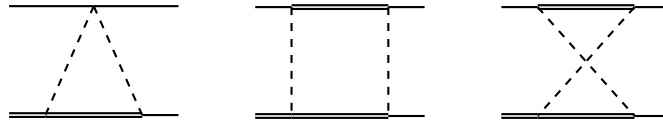
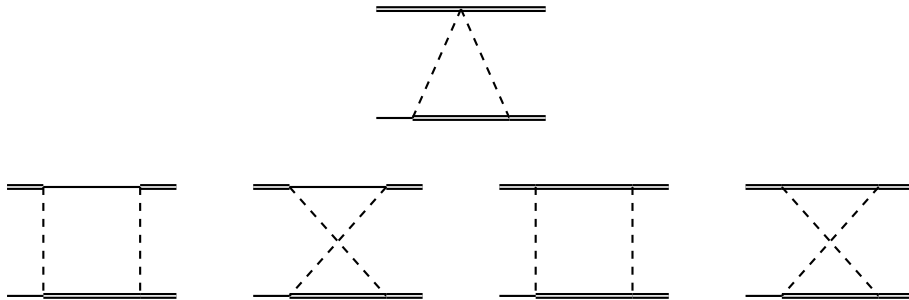


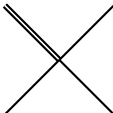
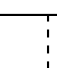
Fig. C.2: 2PE contributions to the scattering of $P^*\bar{P} \rightarrow P^*\bar{P}$.



Fig. C.3: 2PE contributions to the scattering of $P^*\bar{P} \rightarrow P\bar{P}^*$.

Fig. C.4: 2PE contributions to the scattering of $P^*\bar{P}^* \rightarrow P^*\bar{P}^*$.Fig. C.5: 2PE contributions to the scattering of $P^*\bar{P} \rightarrow P^*\bar{P}^*$.Fig. C.6: 2PE contributions to the scattering of $P\bar{P}^* \rightarrow P\bar{P}$.Fig. C.7: 2PE contributions to the scattering of $P^*\bar{P} \rightarrow P^*\bar{P}^*$.

D Diagrams of CCI and C1PE

Presented below are all the CCI and C1PE diagrams, that are allowed through the Feynman rules (the iterated CI is excluded as discussed in sec. 5.2.1). Some scattering reactions seem to be missing due to the nonexistence of the vertices  and  in the Lagrangian.

This section solely provides a list of combinations which are possible, not which actually contribute. The diagrams of C1PE from the scattering reactions of $P\bar{P} \rightarrow P^*\bar{P}^*$, $P\bar{P}^* \rightarrow P\bar{P}$ and $P\bar{P}^* \rightarrow P^*\bar{P}^*$ are omitted for the sake of brevity because they purely consist out of vertex corrections and thus are contained within the renormalization of m_π , g and m_P (cf. sec. 5.2.2). However, the respective CCI diagrams are included because no explicit renormalization of D_1 , E_1 , D_2 , E_2 is pursued.

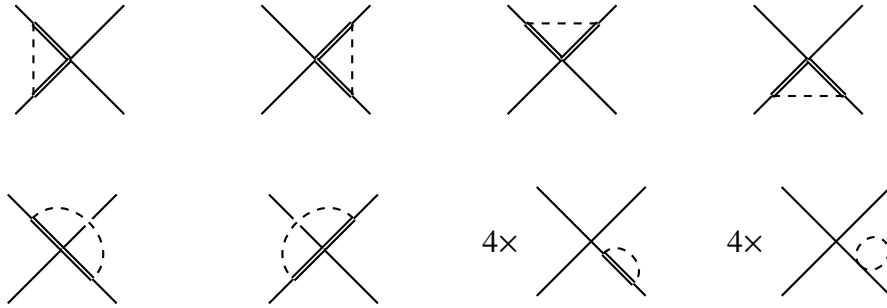


Fig. D.1: Corrections to contact diagrams for $P\bar{P} \rightarrow P\bar{P}$. The factors of 4 emphasize that the propagator correction is to be applied to every leg.

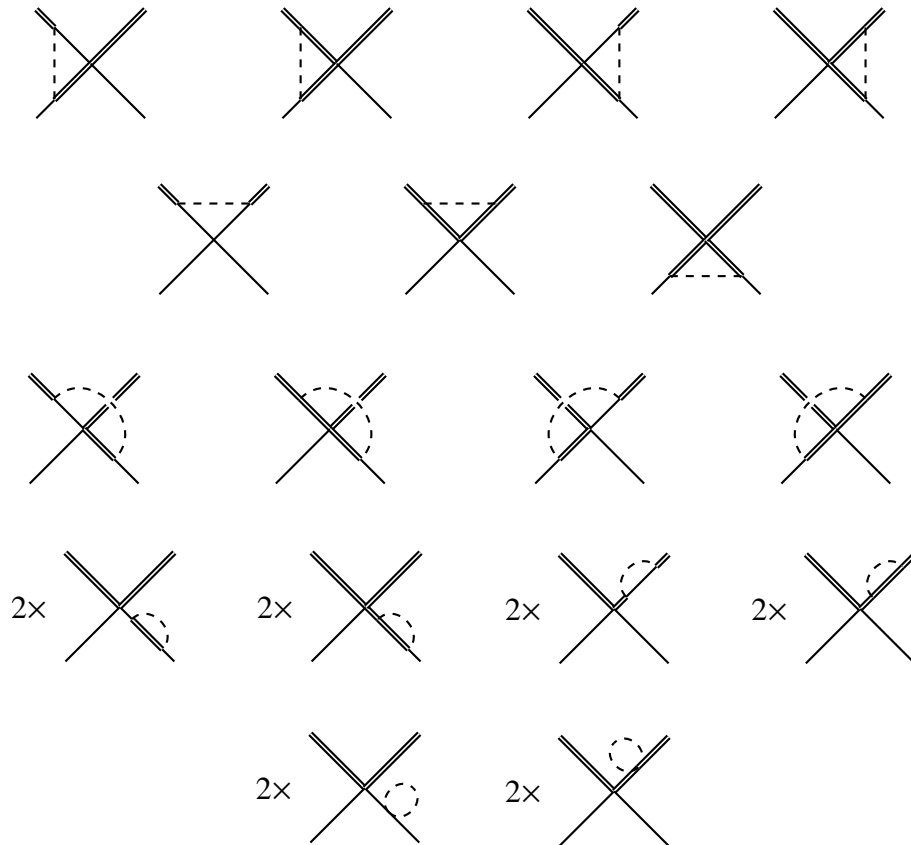


Fig. D.2: Corrections to contact diagrams for $P^* \bar{P} \rightarrow P^* \bar{P}$. The factors of 2 emphasize that the propagator correction is to be applied to the leg of the respective incoming particle, too.

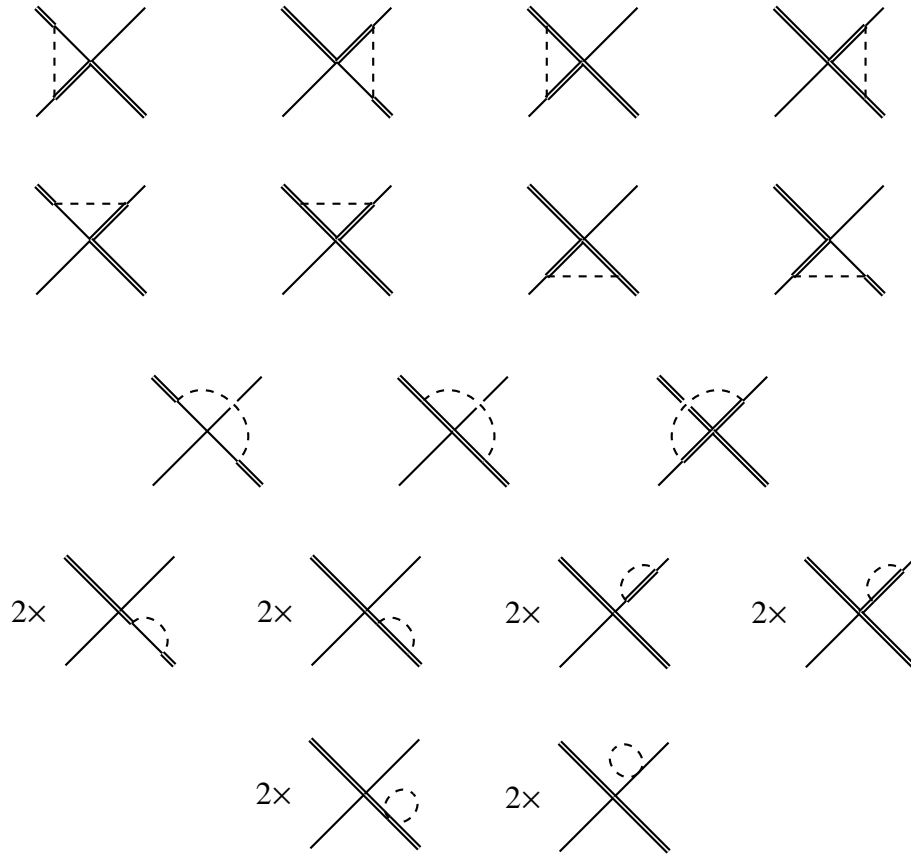


Fig. D.3: Corrections to contact diagrams for $P^* \bar{P} \rightarrow P \bar{P}^*$. The factors of 2 emphasize that the propagator correction is to be applied to the leg of the incoming, opposite particle, too.

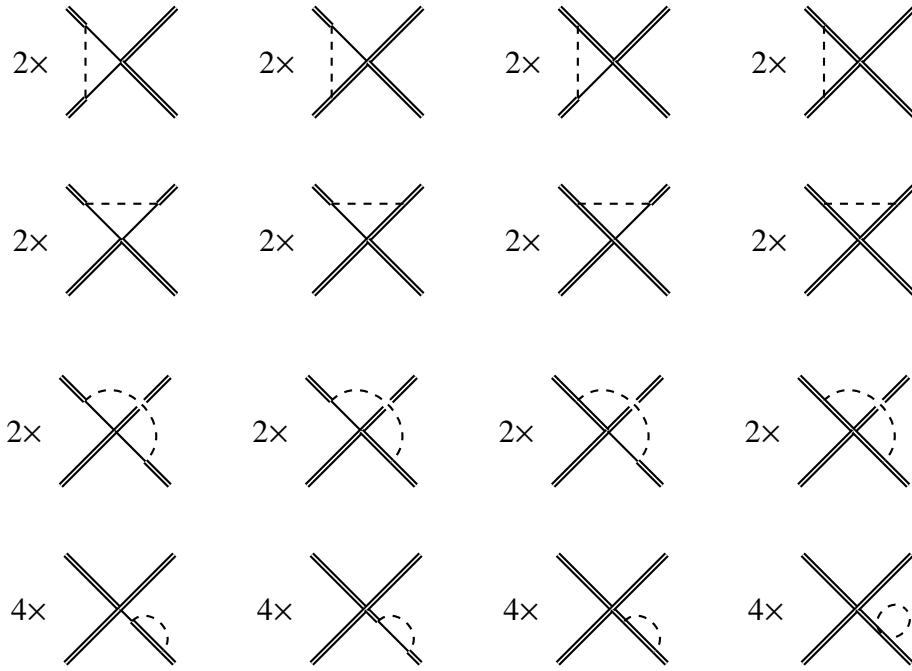


Fig. D.4: Corrections to contact diagrams for $P^*\bar{P}^* \rightarrow P^*\bar{P}^*$. The factors of 4 emphasize that the propagator correction is to be applied to every leg. The factors of 2 emphasize that the triangle/arc correction is to be applied to the opposite side, too.

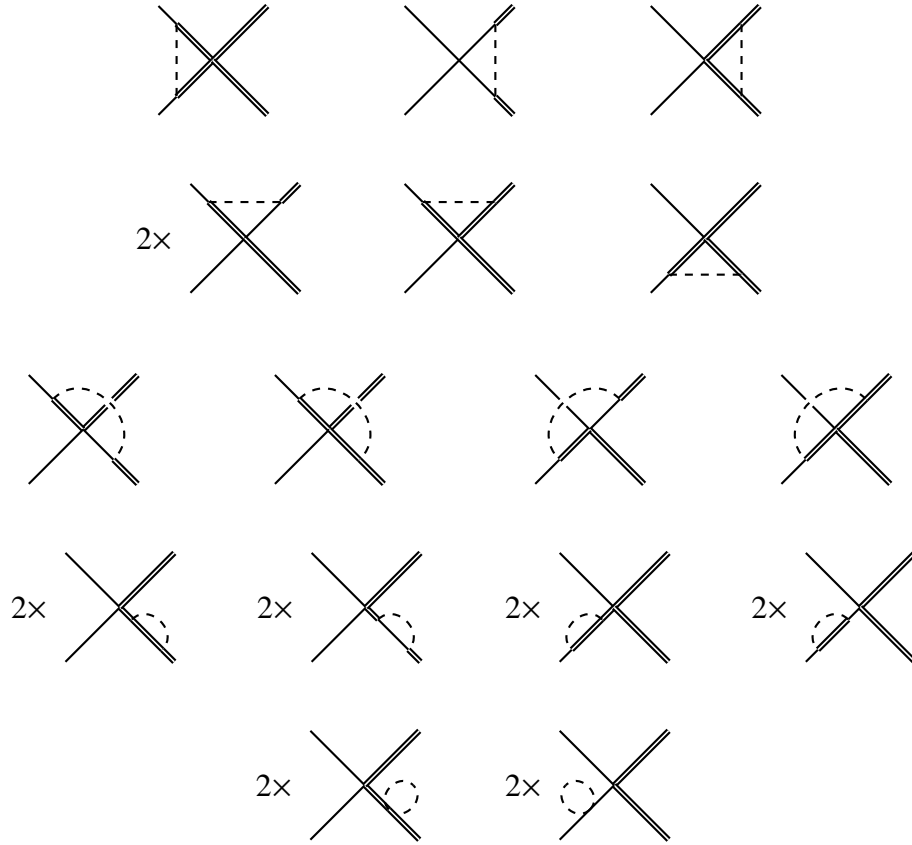


Fig. D.5: Corrections to contact diagrams for $P\bar{P} \rightarrow P^*\bar{P}^*$. The factors of 2 emphasize that the propagator corrections are to be applied to the opposite side, too.

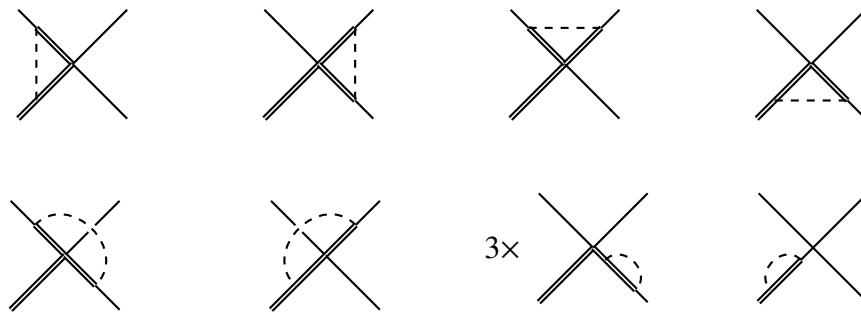


Fig. D.6: Corrections to contact diagrams for $P\bar{P}^* \rightarrow P\bar{P}$. The factor of 3 emphasizes that the propagator correction is to be applied to the two remaining P -meson legs, too.

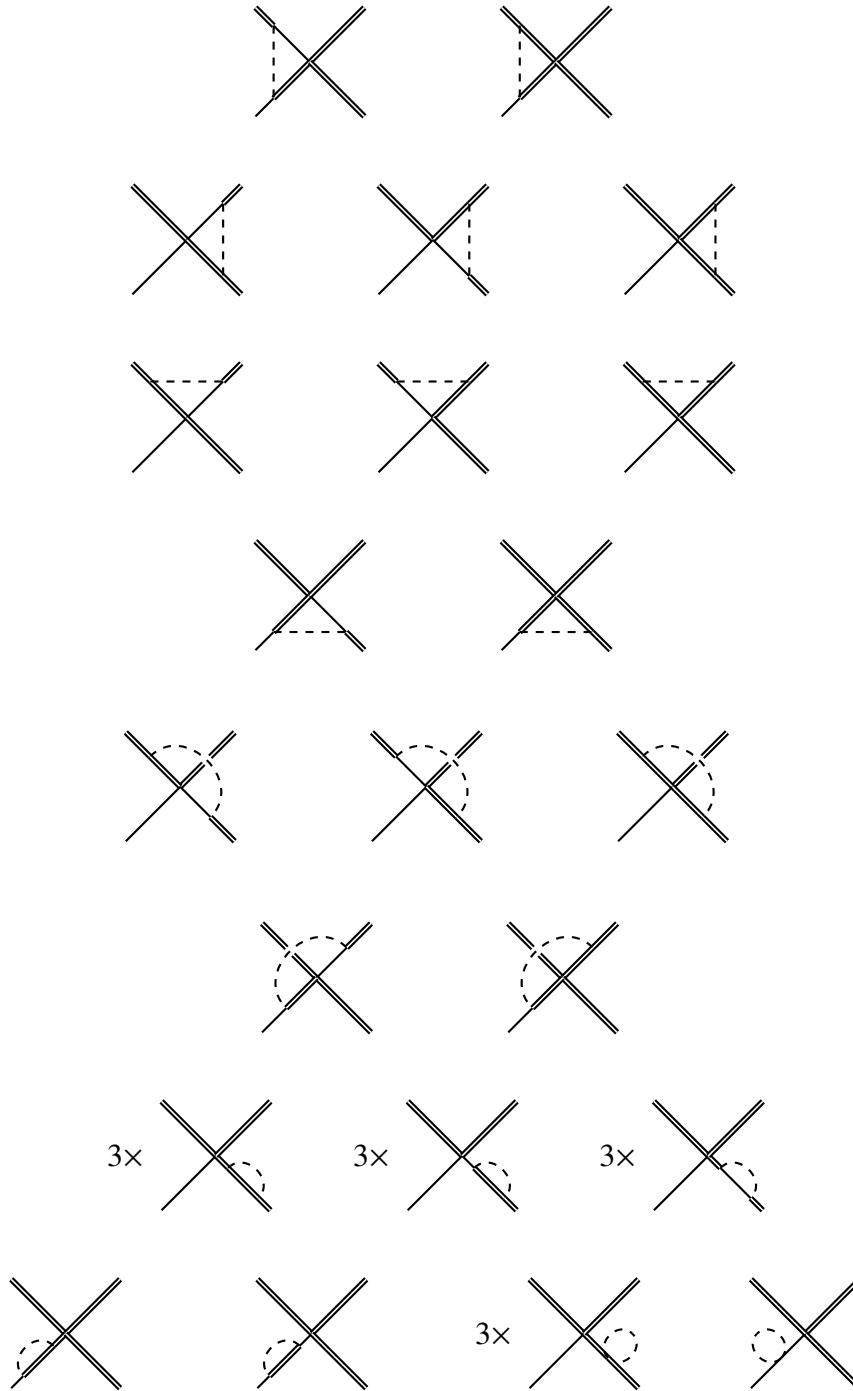


Fig. D.7: Corrections to contact diagrams for $P^* \bar{P} \rightarrow P^* \bar{P}^*$. The factors of 3 emphasize that the propagator corrections are to be applied to the two remaining P^* -meson legs, too.

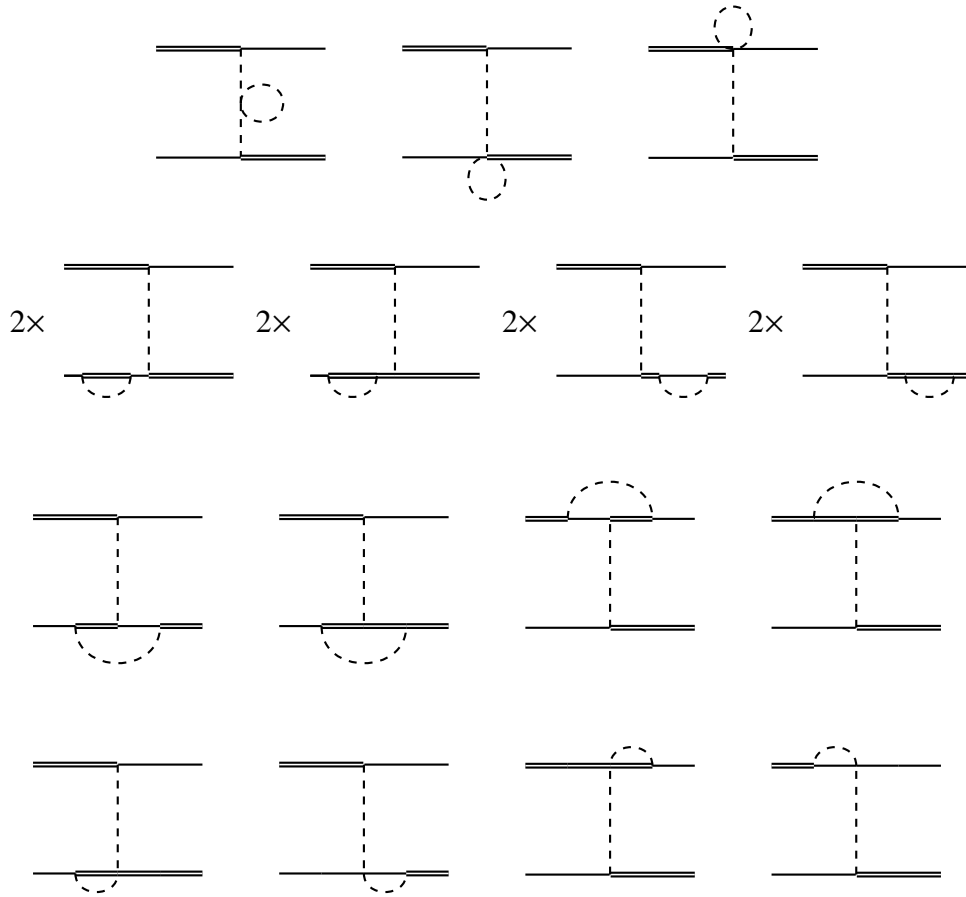


Fig. D.8: Corrections to 1PE diagrams for $P^*\bar{P} \rightarrow P\bar{P}^*$. The factors of 2 emphasize that the propagator correction is to be applied to the respective leg diagonally opposite, too.

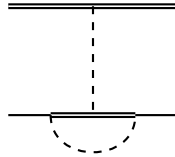


Fig. D.9: NLO contribution to 1PE for $P^*\bar{P} \rightarrow P^*\bar{P}$.

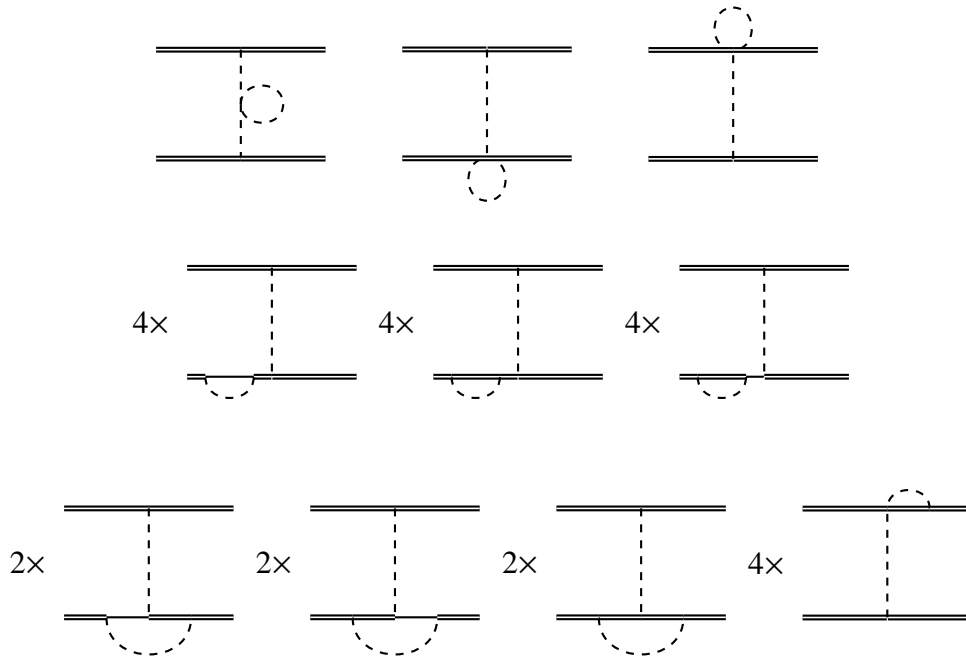


Fig. D.10: Corrections to 1PE diagrams for $P^*\bar{P}^* \rightarrow P^*\bar{P}^*$. The factors of 4 emphasize that the propagator/vertex correction is to be applied to every leg. The factors of 2 emphasize that the 3-vertex correction is to be applied to the opposite vertex, too.

E Integrals of partial wave decomposition

Presented below are the abbreviated integrals of the partial wave decomposition in sec. 7. These are the integrations of $\cos(\Theta) = x$ over $q^2/(q^2 + m_\pi^2)$, $L(q)$ or the terms inside curly braces encountered in e.g. $V_{2\text{PE}}^{\text{eff}}(P\bar{P} \rightarrow P\bar{P})$ in sec.6. We denote $|\vec{p}'| = p'$, $|\vec{p}| = p$, $|\vec{q}| = q$, $\vec{n} = \vec{p}/p$, $\vec{n}' = \vec{p}'/p'$. In addition, $\vec{q}^2 = p'^2 + p^2 - 2p'px$ and $\vec{n}' \cdot \vec{n} = x$ and

$$\begin{aligned}\vec{n} \cdot \vec{q} &= p'x - p = \frac{p'^2 - p^2 - q^2}{2p}, \\ \vec{n}' \cdot \vec{q} &= p' - px = \frac{p'^2 - p^2 + q^2}{2p'}.\end{aligned}$$

$$\begin{aligned}Q_2(p', p) &= \int_{-1}^{+1} \frac{dx}{2} \frac{\vec{q}^2}{\vec{q}^2 + m_\pi^2} \\ &= 1 - \frac{m_\pi^2}{2p'p} \operatorname{artanh}\left(\frac{2p'p}{p'^2 + p^2 + m_\pi^2}\right)\end{aligned}$$

$$\begin{aligned}Q_n(p', p) &= \int_{-1}^{+1} \frac{dx}{2} \frac{(\vec{n} \cdot \vec{q})^2}{\vec{q}^2 + m_\pi^2} \\ &= 1 - \frac{p'^2 + p^2 + m_\pi^2}{4p^2} + \frac{(p'^2 - p^2 + m_\pi^2)^2}{8p'p^3} \operatorname{artanh}\left(\frac{2p'p}{p'^2 + p^2 + m_\pi^2}\right)\end{aligned}$$

$$\begin{aligned}Q_{n'}(p', p) &= \int_{-1}^{+1} \frac{dx}{2} \frac{(\vec{n}' \cdot \vec{q})^2}{\vec{q}^2 + m_\pi^2} \\ &= 1 - \frac{p'^2 + p^2 + m_\pi^2}{4p'^2} + \frac{(-p'^2 + p^2 + m_\pi^2)^2}{8p'^3p} \operatorname{artanh}\left(\frac{2p'p}{p'^2 + p^2 + m_\pi^2}\right)\end{aligned}$$

$$\begin{aligned}Q_x(p', p) &= \int_{-1}^{+1} \frac{dx}{2} \frac{(\vec{n}' \cdot \vec{q})(\vec{n} \cdot \vec{q})x}{\vec{q}^2 + m_\pi^2} \\ &= \frac{5}{12} - \frac{p'^4 + p^4 - m_\pi^4}{8p'^2p^2} + \frac{((p'^2 - p^2)^2 - m_\pi^4)(p'^2 + p^2 + m_\pi^2)}{16p'^3p^3} \operatorname{artanh}\left(\frac{2p'p}{p'^2 + p^2 + m_\pi^2}\right)\end{aligned}$$

$$\begin{aligned}Q_{x^2}(p', p) &= \int_{-1}^{+1} \frac{dx}{2} \frac{\vec{q}^2 x^2}{\vec{q}^2 + m_\pi^2} \\ &= \frac{1}{3} + \frac{m_\pi^2(p'^2 + p^2 + m_\pi^2)}{4p'^2p^2} - \frac{m_\pi^2(p'^2 + p^2 + m_\pi^2)^2}{8p'^3p^3} \operatorname{artanh}\left(\frac{2p'p}{p'^2 + p^2 + m_\pi^2}\right)\end{aligned}$$

$$\begin{aligned}
Q_{nx^2}(p', p) &= \int_{-1}^{+1} \frac{dx}{2} \frac{(\vec{n} \cdot \vec{q})^2 x^2}{\vec{q}^2 + m_\pi^2} \\
&= \frac{-p^6 + p^4(5p'^2 + m_\pi^2) + p^2(m_\pi^2 - \frac{p'^4}{3} + \frac{2m_\pi^2 p^2}{3}) - (p'^2 + m_\pi^2)^3}{16p^4 p'^2} \\
&\quad + \frac{(p^4 - (p'^2 + m_\pi^2)^2)^2}{32p^5 p'^3} \operatorname{artanh}\left(\frac{2p'p}{p'^2 + p^2 + m_\pi^2}\right) \\
Q_{n'x^2}(p', p) &= \int_{-1}^{+1} \frac{dx}{2} \frac{(\vec{n}' \cdot \vec{q})^2 x^2}{\vec{q}^2 + m_\pi^2} \\
&= \frac{-p'^6 + p'^4(5p^2 + m_\pi^2) + p'^2(m_\pi^2 - \frac{p^4}{3} + \frac{2m_\pi^2 p^2}{3}) - (p^2 + m_\pi^2)^3}{16p'^4 p^2} \\
&\quad + \frac{(p'^4 - (p^2 + m_\pi^2)^2)^2}{32p'^5 p^3} \operatorname{artanh}\left(\frac{2p'p}{p'^2 + p^2 + m_\pi^2}\right) \\
Q_{x^3}(p', p) &= \int_{-1}^{+1} \frac{dx}{2} \frac{(\vec{n}' \cdot \vec{q})(\vec{n} \cdot \vec{q}) x^3}{\vec{q}^2 + m_\pi^2} \\
&= \frac{-p'^8 - p'^6(2m_\pi^2 + \frac{4p^4}{3}) + p'^4(2m_\pi^2 p^2 + \frac{118p^4}{15}) + p'^2(2m_\pi^6 + \frac{16m_\pi^4 p^2}{3} + 2m_\pi^2 p^4 - \frac{4p^6}{3})}{32p'^4 p^4} \\
&\quad + \frac{(m_\pi^2 - p^2)(p^2 + m_\pi^2)^3}{32p'^4 p^4} \\
&\quad + \frac{((p'^2 - p^2)^2 - m_\pi^4)(p'^2 + p^2 + m_\pi^2)^3}{64p'^5 p^5} \operatorname{artanh}\left(\frac{2p'p}{p'^2 + p^2 + m_\pi^2}\right)
\end{aligned}$$

Since $q^2 = p'^2 + p^2 - 2p'px$, we can substitute x inside the R -integrals:

$$\frac{dx}{2} = -\frac{q}{2p'p} dq$$

In the following, we relabel q as ρ to avoid ambiguity between the transferred momentum and an integration variable. The limits of integration are:

$$\begin{aligned} x_b = +1 &\longrightarrow \rho_b = p' - p \\ x_a = -1 &\longrightarrow \rho_a = p' + p \end{aligned}$$

And thus, we can solve the R -integrals analytically:

$$\begin{aligned} R_0(p', p) &= \int_{-1}^{+1} \frac{dx}{2} L(q) = \frac{1}{2p'p} \int_{p'-p}^{p'+p} d\rho \rho \cdot L(\rho) \\ &= -\frac{1}{2} + \frac{1}{2p'p} \left[\frac{m_\pi^2 \rho^2}{4m_\pi^2 + \rho^2} L^2(\rho) - \frac{\rho^2}{2} L(\rho) \right]_{p'-p}^{p'+p} \\ R_2(p', p) &= \int_{-1}^{+1} \frac{dx}{2} \vec{q}^2 L(q) = \frac{1}{2p'p} \int_{p'-p}^{p'+p} d\rho \rho^3 \cdot L(\rho) \\ &= -\frac{1}{2p'p} \left[\frac{\rho^2}{16} (4m_\pi^2 + \rho^2) + \frac{m_\pi^4 \rho^2}{4m_\pi^2 + \rho^2} L^2(\rho) + \frac{\rho^2}{4} (2m_\pi^2 + \rho^2) L(\rho) \right]_{p'-p}^{p'+p} \\ R_4(p', p) &= \int_{-1}^{+1} \frac{dx}{2} \vec{q}^4 L(q) = \frac{1}{2p'p} \int_{p'-p}^{p'+p} d\rho \rho^5 \cdot L(\rho) \\ &= \frac{1}{4p'p} \left[-\frac{\rho^6}{18} - \frac{m_\pi^2 \rho^4}{12} + m_\pi^4 \rho^2 + \frac{m_\pi^6}{4} \frac{\rho^2}{4m_\pi^2 + \rho^2} L^2(\rho) + \left(-2m_\pi^4 + \frac{m_\pi^2 \rho^2}{3} + \frac{\rho^4}{3} \right) \rho^2 L(\rho) \right]_{p'-p}^{p'+p} \\ R_6(p', p) &= \int_{-1}^{+1} \frac{dx}{2} \vec{q}^6 L(q) = \frac{1}{2p'p} \int_{p'-p}^{p'+p} d\rho \rho^7 \cdot L(\rho) \\ &= -\frac{1}{16p'p} \left[\frac{\rho^8}{8} + \frac{m_\pi^2 \rho^6}{9} - \frac{5m_\pi^4 \rho^4}{6} + 10m_\pi^6 \rho^2 + 40m_\pi^8 \frac{\rho^2}{4m_\pi^2 + \rho^2} L^2(\rho) \right. \\ &\quad \left. - \rho^2 L(\rho) \left(\rho^6 + \frac{2m_\pi^2 \rho^4}{3} - \frac{10m_\pi^4 \rho^2}{3} - 20m_\pi^6 \right) \right]_{p'-p}^{p'+p} \\ R_8(p', p) &= \int_{-1}^{+1} \frac{dx}{2} \vec{q}^8 L(q) = \frac{1}{2p'p} \int_{p'-p}^{p'+p} d\rho \rho^9 \cdot L(\rho) \\ &= \frac{1}{8p'p} \left[-\frac{\rho^{10}}{25} - \frac{m_\pi^2 \rho^8}{40} + \frac{7m_\pi^4 \rho^6}{45} - \frac{7m_\pi^6 \rho^4}{6} + 14m_\pi^8 \rho^2 + 112m_\pi^{10} \frac{\rho^2}{4m_\pi^2 + \rho^2} L^2(\rho) \right. \\ &\quad \left. - \rho^2 L(\rho) \left(\frac{2\rho^8}{5} + \frac{m_\pi^2 \rho^6}{5} - \frac{14m_\pi^4 \rho^4}{15} + \frac{14m_\pi^6 \rho^2}{3} - 28m_\pi^8 \right) \right]_{p'-p}^{p'+p} \end{aligned}$$

$$\begin{aligned}
R_n(p', p) &= \int_{-1}^{+1} \frac{dx}{2} (\vec{n} \cdot \vec{q})^2 L(q) = -\frac{1}{2p'p^3} \int_{p'-p}^{p'+p} d\rho \left(\rho^4 - 2\rho^2(p'^2 - p^2) + (p'^2 - p^2)^2 \right) \rho \cdot L(\rho) \\
&= -\frac{1}{p^2} \left(R_4(p', p) - 2(p'^2 - p^2)R_2(p', p) + (p'^2 - p^2)^2 R_0(p', p) \right) \\
R_{n'}(p', p) &= \int_{-1}^{+1} \frac{dx}{2} (\vec{n}' \cdot \vec{q})^2 L(q) = R_n(p, p') \\
R_x(p', p) &= \int_{-1}^{+1} \frac{dx}{2} (\vec{n}' \cdot \vec{q})(\vec{n} \cdot \vec{q}) x L(q) \\
&= \frac{1}{16p'^3 p^3} \int_{p'-p}^{p'+p} d\rho \left(\rho^6 - (p'^2 + p^2)\rho^4 - (p'^2 - p^2)^2 \rho^2 + (p'^2 - p^2)^2 (p'^2 + p^2) \right) \rho \cdot L(\rho) \\
&= \frac{1}{8p'^2 p^2} \left(R_6(p', p) - (p'^2 + p^2)R_4(p', p) - (p'^2 - p^2)^2 R_2(p', p) + (p'^2 - p^2)^2 (p'^2 + p^2) R_0(p', p) \right) \\
R_{x^2}(p', p) &= \int_{-1}^{+1} \frac{dx}{2} \vec{q}^2 x^2 L(q) \\
&= \frac{1}{8p'^3 p^3} \int_{p'-p}^{p'+p} d\rho \left(\rho^4 - 2(p'^2 + p^2)\rho^2 + (p'^2 + p^2)^2 \right) \rho^3 \cdot L(\rho) \\
&= \frac{1}{4p'^2 p^2} \left(R_6(p', p) - 2(p'^2 + p^2)R_4(p', p) + (p'^2 + p^2)^2 R_2(p', p) \right) \\
R_{nx^2}(p', p) &= \int_{-1}^{+1} \frac{dx}{2} (\vec{n} \cdot \vec{q})^2 x^2 L(q) \\
&= \frac{1}{32p'^5 p^3} \int_{p'-p}^{p'+p} d\rho \left(-\rho^8 - 4p'^2 \rho^6 + (6p'^4 - 2p^4)\rho^4 + 4p'^2 (p'^4 - p^4)\rho^2 + (p'^4 - p^4)^2 \right) \rho \cdot L(\rho) \\
&= \frac{1}{16p'^4 p'^2} \left(-R_8 - 4p'^2 R_6 + (6p'^4 - 2p^4)R_4 + 4p'^2 (p'^4 - p^4)R_2 + (p'^4 - p^4)^2 R_0 \right) \\
R_{n'x^2}(p', p) &= \int_{-1}^{+1} \frac{dx}{2} (\vec{n}' \cdot \vec{q})^2 x^2 L(q) \\
&= \frac{1}{32p'^5 p^3} \int_{p'-p}^{p'+p} d\rho \left(-\rho^8 - 4p^2 \rho^6 + (6p^4 - 2p'^4)\rho^4 + 4p^2 (p^4 - p'^4)\rho^2 + (p^4 - p'^4)^2 \right) \rho \cdot L(\rho) \\
&= \frac{1}{16p'^4 p^2} \left(-R_8 - 4p^2 R_6 + (6p^4 - 2p'^4)R_4 + 4p^2 (p^4 - p'^4)R_2 + (p^4 - p'^4)^2 R_0 \right)
\end{aligned}$$

$L(\rho)$ is given as

$$L(\rho) = \frac{\sqrt{4m_\pi^2 + \rho^2}}{\rho} \ln \left(\frac{\sqrt{4m_\pi^2 + \rho^2} + \rho}{2m_\pi} \right).$$

$$S_k(p', p) = \int_{-1}^{+1} \frac{dx}{2} P_k(x) \left\{ \vec{q}^2 \left(\frac{5}{24} g^4 + \frac{13}{6} g^2 + \frac{5}{6} \right) + m_\pi^2 (4g^4 + 2g^2 + 4) \right. \\ \left. + \ln \left(\frac{m_\pi}{\mu} \right) \left[\vec{q}^2 \left(\frac{23}{4} g^4 - 5g^2 - 1 \right) + m_\pi^2 \left(\frac{45}{2} g^4 - 18g^2 - 6 \right) \right] \right. \\ \left. + L(q) \left[\vec{q}^2 \left(\frac{23}{4} g^4 - 5g^2 - 1 \right) + m_\pi^2 (5g^4 - 8g^2 - 4) + \frac{12g^4 m_\pi^4}{4m_\pi^2 + \vec{q}^2} \right] \right\},$$

where $P_k(x)$ denotes the k -th Legendre polynomial. For selected k , we obtain (the R -functions arguments are omitted for brevity's sake):

$$S_0(p', p) = (p'^2 + p^2) \left(\frac{5}{24} g^4 + \frac{13}{6} g^2 + \frac{5}{6} \right) + m_\pi^2 (4g^4 + 2g^2 + 4) \\ + \ln \left(\frac{m_\pi}{\mu} \right) \left((p'^2 + p^2) \left(\frac{23}{4} g^4 - 5g^2 - 1 \right) + m_\pi^2 \left(\frac{45}{2} g^4 - 18g^2 - 6 \right) \right) \\ + R_2 \left(\frac{23}{4} g^4 - 5g^2 - 1 \right) + m_\pi^2 R_0 (5g^4 - 8g^2 - 4) \\ - \frac{3g^4 m_\pi^4}{p' p} \left[\frac{\rho^2}{4m_\pi^2 + \rho^2} L^2(\rho) \right]_{p'-p}^{p'+p}$$

$$S_2(p', p) = \int_{-1}^{+1} \frac{dx}{2} \frac{3x^2 - 1}{2} L(q) \left(\vec{q}^2 \left(\frac{23}{4} g^4 - 5g^2 - 1 \right) + m_\pi^2 (5g^4 - 8g^2 - 4) + \frac{12g^4 m_\pi^4}{4m_\pi^2 + \vec{q}^2} \right) \\ = \frac{1}{16p'^3 p^3} \int_{p'-p}^{p'+p} d\rho (3\rho^4 - 6(p'^2 + p^2)\rho^2 + 3(p'^2 + p^2)^2 - 4p'^2 p^2) \rho \cdot L(\rho) \\ \times \left(\rho^2 \left(\frac{23}{4} g^4 - 5g^2 - 1 \right) + m_\pi^2 (5g^4 - 8g^2 - 4) + \frac{12g^4 m_\pi^4}{4m_\pi^2 + \rho^2} \right) \\ = \frac{1}{8p'^2 p^2} \left((3R_6 - 6(p'^2 + p^2)R_4 + (3(p'^2 + p^2)^2 - 4p'^2 p^2)R_2) \left(\frac{23}{4} g^4 - 5g^2 - 1 \right) \right. \\ \left. + (3R_4 - 6(p'^2 + p^2)R_2 + (3(p'^2 + p^2)^2 - 4p'^2 p^2)R_0) m_\pi^2 (5g^4 - 8g^2 - 4) \right. \\ \left. + 9g^4 m_\pi^4 \left[3m_\pi^2 \rho^2 - \frac{\rho^4}{4} + \rho^2 (-6m_\pi^2 + \rho^2) L(\rho) + \frac{12m_\pi^4 \rho^2}{4m_\pi^2 + \rho^2} L^2(\rho) \right]_{p'-p}^{p'+p} \right. \\ \left. + 72g^4 m_\pi^4 (p'^2 + p^2) \left[\frac{\rho^2}{4} - \frac{\rho^2}{2} L(\rho) + \frac{m_\pi^2 \rho^2}{4m_\pi^2 + \rho^2} L^2(\rho) \right]_{p'-p}^{p'+p} \right. \\ \left. + 6g^4 m_\pi^4 \left[\frac{\rho^2}{4m_\pi^2 + \rho^2} L^2(\rho) \right]_{p'-p}^{p'+p} \right)$$

Bibliography

- Ablikim, M. et al. “Observation of a Charged Charmoniumlike Structure $Z_c(4020)$ and Search for the $Z_c(3900)$ in $e^+e^- \rightarrow \pi^+\pi^-h_c$ ”. In: *Phys. Rev. Lett.* 111 (24 Dec. 2013), p. 242001. doi: 10.1103/PhysRevLett.111.242001. URL: <https://link.aps.org/doi/10.1103/PhysRevLett.111.242001>.
- Ablikim, M. et al. “Observation of a Charged Charmoniumlike Structure in $e^+e^- \rightarrow \pi^+\pi^-J/\psi$ at $\sqrt{s}=4.26$ GeV”. In: *Phys. Rev. Lett.* 110 (25 June 2013), p. 252001. doi: 10.1103/PhysRevLett.110.252001. URL: <https://link.aps.org/doi/10.1103/PhysRevLett.110.252001>.
- Acosta, D. et al. “Observation of the Narrow State $X(3872) \rightarrow J/\psi\pi^+\pi^-$ in $\bar{p}p$ Collisions at $\sqrt{s} = 1.96$ TeV”. In: *Phys. Rev. Lett.* 93 (7 Aug. 2004), p. 072001. doi: 10.1103/PhysRevLett.93.072001. URL: <https://link.aps.org/doi/10.1103/PhysRevLett.93.072001>.
- Ali, Ahmed, Christian Hambrock, and Wei Wang. “Tetraquark interpretation of the charged bottomonium-like states $Z_b^\pm(10610)$ and $Z_b^\pm(10650)$ and implications”. In: *Phys. Rev. D* 85 (5 Mar. 2012), p. 054011. doi: 10.1103/PhysRevD.85.054011. URL: <https://link.aps.org/doi/10.1103/PhysRevD.85.054011>.
- Baru, V., E. Epelbaum, A. A. Filin, C. Hanhart, and A. V. Nefediev. “Spin partners of the $Z_b(10610)$ and $Z_b(10650)$ revisited”. In: *JHEP* 06 (2017), p. 158. doi: 10.1007/JHEP06(2017)158. arXiv: 1704.07332 [hep-ph].
- Bernard, V., N. Kaiser, and Ulf-G. Meissner. “Chiral Dynamics in Nucleons and Nuclei”. In: *International Journal of Modern Physics E* 04.02 (June 1995), pp. 193–344. ISSN: 1793-6608. doi: 10.1142/s0218301395000092. URL: <http://dx.doi.org/10.1142/s0218301395000092>.
- Bondar, A. et al. “Observation of Two Charged Bottomoniumlike Resonances in $\Upsilon(5S)$ Decays”. In: *Phys. Rev. Lett.* 108 (12 Mar. 2012), p. 122001. doi: 10.1103/PhysRevLett.108.122001. URL: <https://link.aps.org/doi/10.1103/PhysRevLett.108.122001>.
- Brambilla, Nora, Simon Eidelman, Christoph Hanhart, Alexey Nefediev, Cheng-Ping Shen, Christopher E. Thomas, Antonio Vairo, and Chang-Zheng Yuan. *The XYZ states: experimental and theoretical status and perspectives*. 2019. arXiv: 1907.07583 [hep-ex].
- Casalbuoni, R., A. Deandrea, N. Di Bartolomeo, R. Gatto, F. Feruglio, and G. Nardulli. “Phenomenology of heavy meson chiral lagrangians”. In: *Physics Reports* 281.3 (Mar. 1997), pp. 145–238. ISSN: 0370-1573. doi: 10.1016/s0370-1573(96)00027-0. URL: [http://dx.doi.org/10.1016/S0370-1573\(96\)00027-0](http://dx.doi.org/10.1016/S0370-1573(96)00027-0).
- Choi, S.-K. et al. “Observation of a Narrow Charmoniumlike State in Exclusive $B^\pm \rightarrow K^\pm\pi^+\pi^-J/\psi$ Decays”. In: *Phys. Rev. Lett.* 91 (26 Dec. 2003), p. 262001. doi: 10.1103/PhysRevLett.91.262001. URL: <https://link.aps.org/doi/10.1103/PhysRevLett.91.262001>.

- Cleven, Martin, Harald W. Griesshammer, Feng-Kun Guo, Christoph Hanhart, and Ulf-G. Meissner. “Strong and radiative decays of the $D_{s0}^*(2317)$ and $D_{s1}(2460)$ ”. In: *The European Physical Journal A* 50.9 (Sept. 2014). ISSN: 1434-601X. DOI: 10.1140/epja/i2014-14149-y. URL: <http://dx.doi.org/10.1140/epja/i2014-14149-y>.
- Gamermann, D., L. R. Dai, and E. Oset. “Radiative decay of the dynamically generated open and hidden charm scalar meson resonances $D_{s0}^*(2317)$ and $X(3700)$ ”. In: *Physical Review C* 76.5 (Nov. 2007). ISSN: 1089-490X. DOI: 10.1103/physrevc.76.055205. URL: <http://dx.doi.org/10.1103/PhysRevC.76.055205>.
- Garmash, A. et al. “Observation of $Z_b(10610)$ and $Z_b(10650)$ Decaying to B Mesons”. In: *Phys. Rev. Lett.* 116 (21 May 2016), p. 212001. DOI: 10.1103/PhysRevLett.116.212001. URL: <https://link.aps.org/doi/10.1103/PhysRevLett.116.212001>.
- Gasser, J. and H. Leutwyler. “Chiral Perturbation Theory to One Loop”. In: *Annals Phys.* 158 (1984), p. 142. DOI: 10.1016/0003-4916(84)90242-2.
- Hanhart, C. *Theory of hadronic molecules applied to the XYZ states*. 2017. arXiv: 1709.09920 [hep-ph].
- Hanhart, Christoph. “Meson production in nucleon-nucleon collisions close to the threshold”. In: *Physics Reports* 397.3-4 (July 2004), pp. 155–256. ISSN: 0370-1573. DOI: 10.1016/j.physrep.2004.03.007. URL: <http://dx.doi.org/10.1016/j.physrep.2004.03.007>.
- Kaiser, Norbert, R. Brockmann, and W. Weise. “Peripheral nucleon-nucleon phase shifts and chiral symmetry”. In: *Nucl. Phys.* A625 (1997), pp. 758–788. DOI: 10.1016/S0375-9474(97)00586-1. eprint: nucl-th/9706045.
- Leibbrandt, George. “Introduction to the technique of dimensional regularization”. In: *Rev. Mod. Phys.* 47 (4 Oct. 1975), pp. 849–876. DOI: 10.1103/RevModPhys.47.849. URL: <https://link.aps.org/doi/10.1103/RevModPhys.47.849>.
- Liu, Zhan-Wei, Bo Wang, and Xiang Liu. “ $\bar{B}^{(*)}\bar{B}^{(*)}$ interactions in chiral effective field theory”. In: *Physical Review D* 99.3 (Feb. 2019). ISSN: 2470-0029. DOI: 10.1103/physrevd.99.036007. URL: <http://dx.doi.org/10.1103/PhysRevD.99.036007>.
- Machleidt, R. and D.R. Entem. “Chiral effective field theory and nuclear forces”. In: *Physics Reports* 503.1 (2011), pp. 1–75. ISSN: 0370-1573. DOI: <https://doi.org/10.1016/j.physrep.2011.02.001>. URL: <http://www.sciencedirect.com/science/article/pii/S0370157311000457>.
- Manohar, Aneesh V. and Mark B. Wise. *Heavy Quark Physics*. Cambridge Monographs on Particle Physics, Nuclear Physics and Cosmology. Cambridge University Press, 2000. DOI: 10.1017/CB09780511529351.006.
- Nefediev, A. V., V. Baru, E. Epelbaum, A. A. Filin, C. Hanhart, and Q. Wang. “Spin partners W_{bJ} from the line shapes of the $Z_b(10610)$ and $Z_b(10650)$ ”. In: *Physical Review D* 99.9 (May 2019). ISSN: 2470-0029. DOI: 10.1103/physrevd.99.094013. URL: <http://dx.doi.org/10.1103/PhysRevD.99.094013>.
- Pavón Valderrama, M. “Power counting and perturbative one pion exchange in heavy meson molecules”. In: *Physical Review D* 85.11 (June 2012). ISSN: 1550-2368. DOI: 10.1103/physrevd.85.114037. URL: <http://dx.doi.org/10.1103/PhysRevD.85.114037>.

- Peskin, Michael E. and Daniel V. Schroeder. *An Introduction to quantum field theory*. Reading, USA: Addison-Wesley, 1995. ISBN: 9780201503975, 0201503972. URL: <http://www.slac.stanford.edu/~mpeskin/QFT.html>.
- Scherer, Stefan and Matthias R. Schindler. *A Chiral Perturbation Theory Primer*. 2005. arXiv: [hep-ph/0505265](https://arxiv.org/abs/hep-ph/0505265) [hep-ph].
- Schwartz, Matthew D. *Quantum Field Theory and the Standard Model*. Cambridge University Press, 2014. ISBN: 1107034736, 9781107034730. URL: <http://www.cambridge.org/us/academic/subjects/physics/theoretical-physics-and-mathematical-physics/quantum-field-theory-and-standard-model>.
- Tanabashi, M. et al. “Review of Particle Physics”. In: *Phys. Rev. D* 98 (3 Aug. 2018), p. 030001. doi: [10.1103/PhysRevD.98.030001](https://doi.org/10.1103/PhysRevD.98.030001). URL: <https://link.aps.org/doi/10.1103/PhysRevD.98.030001>.
- Wang, Q., V. Baru, A. A. Filin, C. Hanhart, A. V. Nefediev, and J.-L. Winyen. “The line shapes of the $Z_b(10610)$ and $Z_b(10650)$ in the elastic and inelastic channels revisited”. In: *Phys. Rev. D* 98 (7 Oct. 2018), p. 074023. doi: [10.1103/PhysRevD.98.074023](https://doi.org/10.1103/PhysRevD.98.074023). URL: <https://link.aps.org/doi/10.1103/PhysRevD.98.074023>.
- Weinberg, Steven. “Effective chiral lagrangians for nucleon-pion interactions and nuclear forces”. In: *Nuclear Physics B* 363.1 (1991), pp. 3–18. ISSN: 0550-3213. doi: [https://doi.org/10.1016/0550-3213\(91\)90231-L](https://doi.org/10.1016/0550-3213(91)90231-L). URL: <http://www.sciencedirect.com/science/article/pii/055032139190231L>.
- Wise, Mark B. “Chiral perturbation theory for hadrons containing a heavy quark”. In: *Phys. Rev. D* 45 (7 Apr. 1992), R2188–R2191. doi: [10.1103/PhysRevD.45.R2188](https://doi.org/10.1103/PhysRevD.45.R2188). URL: <https://link.aps.org/doi/10.1103/PhysRevD.45.R2188>.

List of Figures

1.1	Charmonium-like states with completely determined quantum numbers and without hidden strangeness (as of July 2019).	3
1.2	Bottomium-like states with completely determined quantum numbers and without hidden strangeness (as of July 2019).	4
1.3	Line shapes for the invariant mass distribution at $\sqrt{s} \sim M(B\bar{B}^*)$ (a) and $\sqrt{s} \sim M(B^*\bar{B}^*)$ (b) in three different schemes.	5
2.1	Box diagrams of $P^*\bar{P} \rightarrow P^*\bar{P}$ at NLO in time-ordered perturbation theory. . .	15
2.2	Exemplary diagrams of $P^*\bar{P} \rightarrow P^*\bar{P}$ at NLO which violate naive power counting. . .	15
5.1	Triangle-like diagrams for $P\bar{P} \rightarrow P\bar{P}$	30
5.2	Triangle-like diagrams for $P^*\bar{P} \rightarrow P^*\bar{P}$	31
5.3	Triangle-like diagrams for $P^*\bar{P}^* \rightarrow P^*\bar{P}^*$	31
5.4	Triangle-like diagram for $P\bar{P}^* \rightarrow P\bar{P}$	31
5.5	Triangle-like diagram for $P^*\bar{P} \rightarrow P^*\bar{P}^*$	31
5.6	Football-like diagrams	38
5.7	Box-like diagrams for $P\bar{P} \rightarrow P\bar{P}$	39
5.8	Box-like diagrams for $P^*\bar{P} \rightarrow P^*\bar{P}$	39
5.9	Box-like diagrams for $P^*\bar{P} \rightarrow P\bar{P}^*$	39
5.10	Box-like diagrams for $P^*\bar{P}^* \rightarrow P^*\bar{P}^*$	40
5.11	Box-like diagrams for $P\bar{P} \rightarrow P^*\bar{P}^*$	40
5.12	Box-like diagrams for $P\bar{P}^* \rightarrow P\bar{P}$	40
5.13	Box-like diagrams for $P^*\bar{P} \rightarrow P^*\bar{P}^*$	40
5.14	Remaining corrections to contact diagrams for $P\bar{P} \rightarrow P\bar{P}$. The factor of 2 emphasizes that the triangle correction is to be applied to the opposite side, too.	68
5.15	Remaining corrections to contact diagrams for $P^*\bar{P} \rightarrow P^*\bar{P}$	68
5.16	Remaining corrections to contact diagrams for $P^*\bar{P} \rightarrow P\bar{P}^*$	68
5.17	Remaining corrections to contact diagrams for $P^*\bar{P}^* \rightarrow P^*\bar{P}^*$. The factors of 2 emphasize that the triangle correction is to be applied to the opposite side, too.	68
5.18	Remaining corrections to contact diagrams for $P\bar{P} \rightarrow P^*\bar{P}^*$. The factor of 2 emphasizes that the propagator correction is to be applied to the opposite side, too.	69
5.19	Remaining corrections to contact diagrams for $P\bar{P}^* \rightarrow P\bar{P}$	69
5.20	Remaining corrections to contact diagrams for $P^*\bar{P} \rightarrow P^*\bar{P}^*$	70
C.1	2PE contributions to the scattering of $P\bar{P} \rightarrow P\bar{P}$	124
C.2	2PE contributions to the scattering of $P^*\bar{P} \rightarrow P^*\bar{P}$	124

C.3	2PE contributions to the scattering of $P^*\bar{P} \rightarrow P\bar{P}^*$	124
C.4	2PE contributions to the scattering of $P^*\bar{P}^* \rightarrow P^*\bar{P}^*$	125
C.5	2PE contributions to the scattering of $P\bar{P} \rightarrow P^*\bar{P}^*$	125
C.6	2PE contributions to the scattering of $P\bar{P}^* \rightarrow P\bar{P}$	125
C.7	2PE contributions to the scattering of $P^*\bar{P} \rightarrow P^*\bar{P}^*$	125
D.1	Corrections to contact diagrams for $P\bar{P} \rightarrow P\bar{P}$. The factors of 4 emphasize that the propagator correction is to be applied to every leg.	126
D.2	Corrections to contact diagrams for $P^*\bar{P} \rightarrow P^*\bar{P}$. The factors of 2 emphasize that the propagator correction is to be applied to the leg of the respective incoming particle, too.	127
D.3	Corrections to contact diagrams for $P^*\bar{P} \rightarrow P\bar{P}^*$. The factors of 2 emphasize that the propagator correction is to be applied to the leg of the incoming, opposite particle, too.	128
D.4	Corrections to contact diagrams for $P^*\bar{P}^* \rightarrow P^*\bar{P}^*$. The factors of 4 emphasize that the propagator correction is to be applied to every leg. The factors of 2 emphasize that the triangle/arc correction is to be applied to the opposite side, too.	129
D.5	Corrections to contact diagrams for $P\bar{P} \rightarrow P^*\bar{P}^*$. The factors of 2 emphasize that the propagator corrections are to be applied to the opposite side, too. . . .	130
D.6	Corrections to contact diagrams for $P\bar{P}^* \rightarrow P\bar{P}$. The factor of 3 emphasizes that the propagator correction is to be applied to the two remaining P -meson legs, too.	130
D.7	Corrections to contact diagrams for $P^*\bar{P} \rightarrow P^*\bar{P}^*$. The factors of 3 emphasize that the propagator corrections are to be applied to the two remaining P^* -meson legs, too.	131
D.8	Corrections to 1PE diagrams for $P^*\bar{P} \rightarrow P\bar{P}^*$. The factors of 2 emphasize that the propagator correction is to be applied to the respective leg diagonally opposite, too.	132
D.9	NLO contribution to 1PE for $P^*\bar{P} \rightarrow P^*\bar{P}$	132
D.10	Corrections to 1PE diagrams for $P^*\bar{P}^* \rightarrow P^*\bar{P}^*$. The factors of 4 emphasize that the propagator/vertex correction is to be applied to every leg. The factors of 2 emphasize that the 3-vertex correction is to be applied to the opposite vertex, too.	133